Western&Graduate&PostdoctoralStudies

Electronic Thesis and Dissertation Repository

8-8-2024 3:00 PM

Spatially explicit assignment of harvested waterfowl using stable isotopes

Jackson W. Kusack, *Western University*

Supervisor: Hobson, Keith A., *The University of Western Ontario*
A thesis submitted in partial fulfillment of the requirements for the Doctor of Philosophy degree in Biology
© Jackson W. Kusack 2024

Follow this and additional works at: https://ir.lib.uwo.ca/etd

Part of the Biodiversity Commons, Biology Commons, and the Ecology and Evolutionary Biology Commons

Recommended Citation

Abstract

Naturally occurring stable isotopes within animal tissues can provide intrinsic markers for predictable assignment to origin of migratory animals, without additional tracking devices. The use of feather stable-hydrogen isotopes (δ^2H_f) in waterfowl research has been limited until recently and the opportunity to use stable isotopes in general to inform waterfowl management, particularly when assessing source origins and connectivity, is unrealized. Many of the current waterfowl monitoring programs (e.g., preseason banding) are spatially limited due to accessibility, but intrinsic markers provide a complementary method to estimate harvest source areas and evaluate biases. In my Ph.D. dissertation, across four data chapters, I used δ^2H_f measurements to inform direct connections between harvest and source areas for harvested waterfowl in eastern North America, assessing and improving on the current methods. First, I used δ^2H_f and stable-carbon isotope ($\delta^{13}C$) measurements to evaluate differences in the origin of harvested American Black Duck (*Anas rubripes*) across its range (Chapter 2). I found evidence supporting the flyover hypothesis, where American Black Duck harvested in Atlantic Canada showed predominantly southern (local) origins, while those harvested elsewhere originated farther north in the boreal. Second, I critically evaluated the current methods used to predict origins based on stable isotopes in waterfowl feathers (Chapter 3). Here I aggregated known-origin calibration data (δ^2H_f vs. δ^2H_p) and informed the best practices for assignment methods moving forward. Lastly, focusing specifically on leg-band returns and how they can be directly integrated into likelihood-based assignment, I explored spatiotemporal patterns in the natal source areas of waterfowl in eastern North America (Chapter 4) and critically evaluated the use of band returns as a prior probability of origin, directly comparing source areas derived from band returns and δ^2H_f measurements (Chapter 5). I found evidence of flyway-specific natal sources with northward shifts later in the harvest period. When used as a prior probability of origin, band returns greatly refined derived source areas, despite their spatial bias. Together, these contributions address key conservation questions for species of conservation concern, inform best practices when using stable isotopes, and demonstrate the value of stable isotopes as a tool for waterfowl management.

Keywords

Summary for Lay Audience

Naturally occurring chemical markers stored within animal tissues can help us determine where migratory animals spend different parts of their life. For migratory ducks, these markers are useful when determining connections between areas where ducks breed or were raised and where they are hunted. These naturally occurring markers are beneficial because they do not require any initial capture or marking to gain information on a duck's origin. Most often these connections are determined using metal leg bands. Banding only occurs in the south of Canada and across the continental United States because it is difficult to reach far northern areas, which may lead to errors when creating connections with breeding areas. In my research, I studied how we can use naturally occurring chemical markers in feathers to determine important breeding areas for hunted ducks. In Chapter 2, I investigated connections between breeding and hunting areas for a species of conservation concern, the American Black Duck. I found that American Black Duck hunted in Atlantic Canada bred in local areas. In all other hunting areas, ducks showed breeding areas in the northern forests of eastern Canada. In Chapter 3, I used feathers from ducklings raised in known lakes across North America and Europe to evaluate and improve the methods used to predict the chemical markers in duck feathers across the continent. In Chapter 4, I used leg bands to investigate how variable the connections between breeding and hunting areas are and how they change over the hunting season. I found that breeding areas matched hunting areas in the same flyway but hunted ducks had more northern breeding areas later in the hunting season. In Chapter 5, I used metal leg bands together with chemical markers to combine the two data sources and improve methods used to create connections between hunting and breeding areas for several duck species in eastern North America. I found that combining band returns with chemical markers to determine breeding origins allowed for more precise estimates. My research helps us understand and protect waterfowl by improving our ability to track their origins.

Co-Authorship Statement

This dissertation contains modified versions of peer-reviewed publications (Chapters 2 and 3) and two manuscripts in preparation for submission for publication (Chapters 4 and 5), for which I am the lead author. The abstracts of the published manuscripts are incorporated into the general introduction (Chapter 1) and the main body of the manuscripts have been incorporated into the data chapters. Most supplementary materials from these publications can be found in the appendices, with the following exceptions: (1) Figures S3–38 from Chapter 2 (Kusack et al. 2022) were omitted to avoid unnecessary page use and (2) Table S1 from Chapter 3 (Kusack et al. 2023) was modified for this dissertation and included in the general introduction as Table 1.1 (the unmodified version is linked as Table B1). The manuscript formatting, including changes to a first-person narrator, has been modified to reflect that of the entire dissertation.

A version of Chapter 2 is published in the Journal of Wildlife Management [citation: Kusack, J. W., D. C. Tozer, M. L. Schummer, and K. A. Hobson. 2022. Origins of harvested American black ducks: stable isotopes support the flyover hypothesis. The Journal of Wildlife Management 87:e22324]. JWK, DCT, and KAH conceptualized the study. JWK performed lab work, analyzed the data, drafted the manuscript, and is the corresponding author. DCT, KAH, and MLS provided funding. MLS provided data. All coauthors provided feedback on the manuscript.

A version of Chapter 3 is published in PLOS One [citation: Kusack, J. W., D. C. Tozer, K. M. Harvey, M. L. Schummer, and K. A. Hobson. 2023. Assigning harvested waterfowl to geographic origin using feather δ^2H isoscapes: What is the best analytical approach? PLOS One 18:e0288262]. JWK conceptualized the study with DCT and KAH, performed lab work, analyzed the data, drafted the manuscript, and is the corresponding author. DCT, MLS, and KAH provided funding. KMH and MLS coordinated sample collection in the USA. All coauthors provided feedback on the manuscript, with extensive contributions from KAH.

Chapter 4 is in preparation for submission to a peer-reviewed journal with D. C. Tozer and K. A. Hobson as co-authors. JWK conceived and designed the study, analyzed the data, and drafted the manuscript. DCT and KAH provided feedback on the manuscript, with extensive contributions from KAH.

Chapter 5 is in preparation for submission to a peer-reviewed journal with D. C. Tozer, D. Wojtaszek, M. L. Schummer, D. N. Fowler, and K. A. Hobson as co-authors. JWK conceived and designed the study, analyzed the data, and drafted the manuscript. DCT, MLS, DNF, and KAH provided feedback on the manuscript, with extensive contributions from KAH. MLS coordinated sample collection in the USA. DW performed lab work.

Acknowledgements

Special thanks to my family, whose support allowed me to pursue graduate school on the other side of the country. To my parents, Mark Kusack and Megan West, thank you for nurturing my love of the natural world. To my grandparents Lynn and Keith Kusack and Judith and Kenneth Russell, I am eternally grateful for your endless love. I would not be here without all your support and encouragement.

Most of all, thank you to my loving partner, Orin Turner, who has been with me throughout this rollercoaster ride of a degree. Thank you for always encouraging me to celebrate my successes and reminding me to enjoy every day. Your patience and unconditional love got me through many stressful times, even though many were self-imposed. Thank you from the bottom of my heart.

Table of Contents

List of Tables

List of Figures

List of Appendices

List of Abbreviations and Symbols

Provinces and states:

IL	Illinois
IN	Indiana
MI	Michigan
MN	Minesota
NB	New Brunswick
NS	Nova Scotia
NY	New York
OH	Ohio
ON	Ontario
PA	Pennsylvania
PEI	Prince Edward Island
QC	Quebec
WI	Wisconsin

Black duck management regions:

INT	interior United States
NATL	north Atlantic United States
NEC	northeastern Canada
NWC	northwestern Canada
SATL	south Atlantic United States
SEC	southeastern Canada
SEC$_{ATL}$	southeastern Canada, Atlantic region
SEC$_{QC}$	southeastern Canada, Quebec
SWC	southwestern Canada

Species:

ABDU	American Black Duck
AGWT	American Green-winged Teal
AMWI	American Wigeon
BUFF	Bufflehead
BWTE	Blue-winged Teal
CANV	Canvasback
CITE	Cinnamon Teal
COEI	Common Eider
COGO	Common Goldeneye
COME	Common Merganser
GADW	Gadwall
GRSC	Greater Scaup
HOME	Hooded Merganser
LESC	Lesser Scaup
LTDU	Long-tailed Duck
MALL	Mallard
MODU	Mottled Duck
NOPI	Northern Pintail
NSHO	Northern Shoveller
REDH	Redhead
RNDU	Ring-necked Duck
RUDU	Ruddy Duck

WODU	Wood Duck
WWSC	White-winged Scoter

General:

°	degrees
‰	parts per thousand (permille)
~	approximately
AHM	adaptive harvest management
b	total number of hatch-year birds banded (preseason banding effort)
B_a, B_j	age ratio based on banding data for adults (a) and juveniles (j)
BBS	Breeding Bird Survey
BCR	Bird Conservation Region
BWB	bowhead whale baleen
β	parameter estimate
$C/^{12}C/^{13}C$	carbon
$\delta^{13}C$	stable-carbon isotope ratio
°C	degrees Celsius
CA	Canada
CBS	caribou hoof standard
CDT	Canyon Diablo Troilite (standard)
CF-IRMS	continuous-flow isotope-ratio mass spectrometer
CFS	chicken feather standard
CHS	cow hoof standard
CI	confidence interval
COIL	Cornel Isotope Laboratory
d	number of dimensions in Kernel Density Estimation
δ	delta notation
ECCC	Environment and Climate Change Canada
e.g.	for example
EPSG	European Petroleum Survey Group
et. al.	and others
f	relative harvest rate
F	F-test statistic
GNIP	Global Network of Isotopes in Precipitation
GPS	Global Positioning System
h	bandwidth in Kernel Density Estimation
$H/^1H$	hydrogen
^2H	deuterium
δ^2H	stable-hydrogen isotopes ratio
δ^2H_f	stable-hydrogen isotopes ratio in feathers
δ^2H_p	stable-hydrogen isotopes ratio in precipitation
δ^2H_{tissue}	stable-hydrogen isotopes ratio in tissue
δ^2H_{VSMOW}	stable-hydrogen isotopes ratio, relative to VSMOW
Ha	hectares
IAEA	International Atomic Energy Agency
i.e.	that is
Jan–Dec	months, January–December
KDE	Kernel Density Estimation
KHS	kudu horn standard
km	kilometer
κ	concentration parameter (multivariate circular mixing models)

Lat.	latitude
LMM	linear mixed-effect model
LSIS-AFAR	Laboratory for Stable Isotope Science-Advanced Facility for Avian Research
mg	milligramme
MA	amount-weighted mean annual precipitation
MCMC	Markov Chain Monte Carlo
MGS	amount-weighted mean growing-season precipitation
MM	amount-weighted mean monthly precipitation
μ	mean
μ_c	isoscape cell specific mean
n	sample size
N	North
N/^{14}C/^{15}C	nitrogen
δ^{15}N	stable-nitrogen isotope ratio
NAD	North American Datum
O/^{16}O/^{17}O/^{18}O	oxygen
p	p-value
P1	first primary feather
PIT	passive integrated transponder
pmix	mixing proportion (multivariate circular mixing models)
prop.	proportion
RCWIP2	Regionalized Cluster-Based Water Isotope Prediction Version 2 model
r	number of direct recoveries
R	fall age ratio
R^2, $R^2_{conditional}$, $R^2_{marginal}$	coefficient of determination
S/^{32}S/^{33}S/^{34}S/^{36}S sulphur	
SD	standard deviation
SD_{resid}	standard deviation of residuals
SE	standard error
δ^{87}Sr	stable-strontium isotopes ratio
std.	standardized
σ	standard deviation
σ^2	variance
σ_{cal}, SD_{resid}	standard deviation of calibration residuals (calibration error)
σ_{iso}	isoscape cell specific standard error
t	t-test statistic
Ψ	movement probability
USA	United States of America
USGS	United States Geological Survey
USFWS	United States Fish and Wildlife Service
VHF	very high frequency
VPDB	Vienna Peedee Belemnite (standard)
vs.	versus
VSMOW	Vienna Standard Mean Ocean Water
WGS	World Geodetic System
W	West
W_a, W_j	age ratio based on harvest (wings) data for adult (a) and juveniles (j)
^{H}X	heavy isotope of element X
^{L}X	light isotope of element X

Chapter 1

1 General Introduction

1.1 Seasonal migration in waterfowl

More than half of North American bird species migrate between northern breeding areas in the summer to southern non-breeding areas to overwinter, but no group is a more recognizable symbol of these movements than waterfowl. For many these 'V' formations of Canada Geese (*Branta canadensis*) passing overhead are the harbingers of migration. Each Autumn, tens of millions of waterfowl migrate to avoid adverse conditions, mainly cold temperatures and ice-up, on the breeding grounds. These migrations differ in distance with some species exhibiting intercontinental migration like Blue-winged Teal (*Spatula discors*) which migrates as far as Colombia and Venezuela and others showing short-distance migrations like the Harlequin Duck (*Histrionicus histrionicus*) which breeds in subalpine rivers and moves to relatively close coastal areas to overwinter. While these movements may not rival the circumglobal long-distance migrations seen in some waterbirds (e.g., Arctic Tern *Sterna paradisaea*; Egevang et al. 2010), the sheer biomass of these movements is impressive.

Seasonal migration is not ubiquitous across waterfowl, as several species exhibit differential migration (i.e., cohorts within the population migrate differently), partial migration (i.e., cohorts within the population are non-migratory) or are non-migratory. For example, some Wood Ducks (*Aix sponsa*) remain on the breeding grounds in the north and endure cold temperatures to be the first individuals back in the spring (Bellrose and Holm 1994). Mallard (*Anas platyrhynchos*) in particular overwinter as far north as open water allows (Baldassarre 2014). In other species, migratory movements have been completely lost in subpopulations (e.g., Trumpeter Swan *Cygnus buccinator* reintroduced in Ontario; Handrigan et al. 2016). Other species, particularly those that breed in the south, are mostly non-migratory, but still often make regional movements within their range (e.g., Masked Duck *Nomonyx Dominicus*, Mottled Duck *Anas fulvigula*, Muscovy Duck *Cairina moschata*).

Migration, in the context of this thesis, is described as seasonal directional movements between breeding grounds and non-breeding areas, but other migratory movements such as moult migration are common. Moult is energetically costly in waterfowl and exposes individuals to predation, as synchronous replacement of flight feathers leaves them unable to fly. Many waterfowl undergo a moult migration to favourable areas where individuals replace flight feathers in refugia away from predators (Salomonsen 1968). Moult of flight feathers mainly occurs at the breeding site, during brood-rearing, but moult migration has been documented for unpaired immature birds and adults with failed broods (Sheaffer et al. 2007) and adult males in species that exhibit no biparental care (e.g., Wood Duck, Bellrose and Holm 1994). Most often these moult migratory movements occur as post-breeding northward movements towards isolated and relatively safe coastal areas (Davis et al. 1985, Abraham et al. 1999, Sheaffer et al. 2007, Luukkonen et al. 2008), but some moult migrations for ducks have been observed at large inland marshes and lakes (e.g., Delta Marsh in Manitoba and Camas Reserve in Idaho, Salomonsen 1968).

1.2   Connectivity

Migratory connectivity is the measure of geographic cohesion, in a species or population, between at least two points in the annual cycle (e.g., breeding, stopover, non-breeding) (Boulet and Norris 2006). In most cases, these connections have been established between the breeding and non-breeding areas (Greenberg and Marra 2005), as these regions encompass the majority of the annual cycle for migratory individuals. Connectivity can be 'weak' or 'strong', where strong connectivity indicates that individuals from a given region move to a single area with fewer individuals migrating to other areas. For example, Canada Geese show moderately strong connectivity, as three migratory subspecies breed and overwinter in regionally separated areas with little overlap (Mowbray et al. 2020). Weak connectivity indicates that individuals from a breeding region spread out among many different non-breeding areas, with little to no concentration of movements (Webster et al. 2002). This spectrum demonstrates extreme examples of connectivity, but most species have intermediate levels and tend towards weaker connectivity (Finch et al. 2017).

Connectivity is important because conditions experienced at discrete periods of the annual cycle can have carry-over (or cross-seasonal) effects that influence subsequent periods (Sedinger and Alisauskas 2014). In American Redstarts (*Setophaga ruticilla*), carry-over effects of poor territory quality in the non-breeding grounds affect the timing of migration and body condition at arrival on the breeding grounds on an individual level (Marra et al. 1998). The same mechanisms could be working in waterfowl, as many species allocate endogenous reserves gained during the non-breeding period to egg production (Sharp et al. 2013), but this mechanistic relationship has not been explored as extensively in ducks. At the population level, poor habitat quality on the non-breeding grounds (e.g., wet vs dry years) can have carry-over effects on productivity in the following year (Heitmeyer and Fredrickson 1981, Raveling and Heitmeyer 1989). At the individual level, similar effects of non-breeding habitat quality (e.g., greater food availability) positively influence the likelihood of breeding (Sedinger et al. 2011).

For waterfowl management, understanding connectivity is key because it can provide information on zones of production leading to the recruitment of individuals into the fall harvest (Munro and Kimball 1982, Szymanski and Dubovsky 2013). However, connectivity between areas of productivity and the harvest endpoint clearly differs from mainstream concepts linking breeding and wintering origins described above. Instead, these connections pair breeding source areas to harvest areas as a measure of 'harvest connectivity' (i.e., the strength of connections between breeding areas and harvest areas). While this is often referred to as migratory connectivity (e.g., Roberts et al. 2022) and these connections still likely correlate to the overall population connectivity, I make the distinction here to acknowledge that these connections are only representative of the harvested cohort. Further, harvest connectivity can be directly related to harvest pressures, although this assumes additive effects of harvest mortality on populations (see Sedinger and Herzog 2012).

Harvest connectivity can be described formally using a harvest derivation, which, after correcting for regional harvest rates and population size, describes the proportion of individuals sourced from different breeding areas for a given harvest area (Munro and Kimball 1982). These derivations have historically been performed by defining harvest

areas as geopolitical or management boundaries, including important management regions (Munro and Kimball 1982, Powell and Klaasen 1998) or states and provinces (Szymanski and Dubovsky 2013, De Sobrino et al. 2017), and have been done on species-by-species basis with an emphasis on those with many band returns (e.g., American Black Duck *Anas rubripes*, Geis et al. 1971; Canada Goose, Klimstra and Padding 2012; Canvasback *Aythya valisineria*, Stewart et al. 1958, Geis 1974; Mallard, Geis 1971, 1972, Munro and Kimball 1982, Powell and Klaasen 1998, Zuwerink 2001; Wood Duck, Bowers and Hamilton 1977; Blue-winged Teal, Szymanski and Dubovsky 2013). More recently, regional derivations defined for individual flyways have been performed, such as De Sobrino et al. (2017) who analyzed the harvest derivations for nine dabbling duck species harvested in the Pacific Flyway. Although range-wide estimates of connectivity have been formally established for some waterfowl, we do not have this information for most species.

Establishing connectivity is challenging and has been measured largely through extrinsic (e.g., VHF radio-telemetry tags, Taylor et al. 2017; geolocator tags, Stutchbury et al. 2009; GPS tags, Zhu et al. 2020) and intrinsic (e.g., stable isotopes, Asante et al. 2017; genetics, Ruegg et al. 2017; trace elements, Kaimal et al. 2009) markers that provide estimates for geographic locations of occupancy at different points of the annual cycle. External trackers provide tracking of movements post-tagging (i.e., after the point of capture) while intrinsic markers provide information about that individual's history pre-sampling. Stable isotopes of several elements are particularly useful as intrinsic markers, as they allow us to gain vital information on previous geographic locations for an individual without initial capture (Hobson and Wassenaar 2019). Only one sampling point is required to gain insights into the life history of an individual, which is especially important in the context of harvest. This is not possible with other extrinsic tracking methods which necessitate initial capture and subsequent recapture (e.g., archival geolocators, band returns), and cannot provide retroactive information for the origin of an individual. Further, with the advent of interpolated surfaces showing geospatial changes in isotope values in foodwebs ('isoscapes', Bowen and West 2019), connections can be made without establishing species-specific baselines across a geographic range necessary for other intrinsic markers such as genetics (DeSaix et al. 2024), although calibration

4

between stable-isotope values in the local environment and those in tissues needs to be established (Hobson et al. 2012*b*). As a trade-off, these connections are often geographically broad compared to other connectivity estimates gained from band returns, for example. As stable isotopes are an integral component of my dissertation, these methods are described in more detail later in this chapter.

1.3　Management

Long-distance movements of migratory waterfowl across national borders require collaborative strategies to ensure fair allocation of harvested birds among countries (Nichols et al. 2007) and effective conservation efforts (North American Waterfowl Management Plan 2018). To avoid overexploitation, harvest strategies must incorporate accurate information on connectivity between breeding and harvest areas, which necessitates efficient assignment of origin for harvested individuals.

Across all avian taxa, we have seen drastic population losses in the last 50 years (Rosenberg et al. 2019), but waterfowl are on average showing positive to stable population trends. Apart from geese, which are on average showing massive increases (> 1,000 %), ducks are showing generally stable populations (North American Bird Conservation Initiative 2022). Despite overall stable trends, they are still at risk due to the loss or potential loss of critical habitats across the annual cycle through climate change and other anthropogenic habitat modification (Craft et al. 2009, Sofaer et al. 2016, Thompson et al. 2017). Population size estimates for Northern Pintail *Anas acuta*, American Black Duck, and Lesser Scaup *Aythya affinis* / Greater Scaup *Aythya marila* are currently below the long-term average (U.S. Fish and Wildlife Service 2022), suggesting that these species are in overall decline. Although now stabilized at a lower population level, American Black Duck population trends show marked declines across their breeding range between 1950–80 (Conroy et al. 2002). These declines have been hypothesized to be driven by hybridization and competition with Mallard, habitat loss in their core breeding range and wintering range which reduces overall carrying capacity, and overharvest, but there is little consensus (Ankney et al. 1987, 1989, Conroy et al. 1989).

1.3.1   Adaptive harvest management

North American waterfowl are managed on the flyway scale, within which a representative flyway-specific (or management unit-specific) stock (i.e., distinct breeding population of a given species) is monitored through adaptive harvest management (AHM; U.S. Fish and Wildlife Service 2021). This stock is treated as a representative of all other species in that unit. In the Pacific and Central / Mississippi flyways, management is based on either the western or midcontinent Mallard stocks, respectively, while harvest management in the Atlantic Flyway is based on multi-stock data (American Green-winged Teal *Anas crecca carolinensis*, Wood Duck, Ring-necked Duck *Aythya collaris*, and Goldeneyes *Bucephala clangula* and *B. islandica*). With the exception of a few select examples of species-specific management, where species have been highlighted as conservation concerns (Northern Pintail, American Black Duck, Lesser Scaup / Greater Scaup), all harvest management falls under this Mallard management umbrella (U.S. Fish and Wildlife Service 2021).

These AHM models rely primarily on metrics derived from three systems: aerial surveys (e.g., Waterfowl Breeding Population Habitat Survey), harvest surveys (e.g., Species Composition and Part Collection surveys; Gendron and Smith 2019, Raftovich et al. 2023), and banding. In the eastern Mallard AHM strategy, an integrated population model is used to derive annually estimated population demographics based on metrics of breeding population abundance gained from aerial surveys, harvest rates and survival estimates derived from band returns, and age ratios from band returns and harvest surveys (Roberts et al. 2022). Using these demographics, annual harvest regulations (bag limits) are determined for the eastern Mallard.

AHM models rely on several assumptions including, (1) population metrics derived from multiple surveys represent the target population and (2) population trends and production zones for the chosen population represent all species in that flyway or management unit. A potential limitation to the first assumption is that differences in sampling extent for different surveys may introduce systematic biases. For many species, banding is limited to the southern portion of Canada and the contiguous USA due to logistical issues banding in remote northern areas, whereas harvest surveys sample harvested individuals

which could originate from northern areas not surveyed by banding. Some metrics try to account for these different sources of data, such as calculating the fall age ratio using harvest data and banding data. The harvest surveys, on the other hand, are unburdened by the spatial biases mentioned above, but the current uses are limited to age and sex ratio determination.

A potential limitation to the second assumption is that while flyways are well-established continental corridors that describe the annual cycle movements of populations (Lincoln 1935), there is significant movement between flyways (Roberts et al. 2022). Within flyways, more specific source areas for species managed under this framework may not match the same source areas as the model species (e.g., the Prairie Pothole region for the midcontinent Mallard). The degree of disconnect between source areas could violate the assumptions of the current AHM frameworks, especially when source areas do not overlap at all.

1.3.2   Banding

Marking birds with aluminum leg-bands (i.e., banding or ringing), as a continent-wide coordinated effort, was first established in North America in 1909 by the American Bird Banding Association. By 1920, the management was taken over by the U.S. government's Biological Survey of the Department of Agriculture, led by Frederick C. Lincoln (Tautin 2005). Fundamentally these leg bands were meant to track migratory movements, as marking allowed for individual encounter histories. This system was a huge breakthrough for our understanding of migratory movements and the estimation of animal numbers (i.e., the 'Lincoln-Peterson method', Petersen 1896, Lincoln 1930). One of the greatest contributions was the concept of migratory flyways (Lincoln 1935), a widely adopted system used across migratory birds and maintained within current waterfowl management frameworks (U.S. Fish and Wildlife Service 2023). Currently, waterfowl banding efforts continue with roughly 300,000 bands put out each year since 1960 onto over 50 species (Celis-Murillo et al. 2022).

1.3.3　Harvest surveys

The Species Composition Survey in Canada (Gendron and Smith 2019) and the Parts Collection Survey in the United States (Raftovich et al. 2023), survey hunters who are required to submit an entire wing from every bird harvested in a season. Hunters are systematically randomly sampled, based on hunting zones and previous hunting activity, to ensure a representative sample across the harvested range (Smith et al. 2022). These wings are then processed at the annual 'Wingbee' where trained waterfowl biologists assign all individuals a species identity, age, and sex (Carney 1992). An important metric gained from these data is the fall age ratio (i.e., the number of young produced per adult), which is an estimate of preseason productivity.

1.4　Stable isotopes

Naturally occurring stable-hydrogen isotopes (δ^2H) within animal tissues (δ^2H$_{tissue}$) were first identified as a tool to study animal origins by Cormie et al. (1994) who identified a clear relationship between the δ^2H values on deer bone collagen and those of amount-weighted mean annual local rainwater (δ^2H$_p$) and relative humidity. This led to studies by Chamberlain et al. (1997) and Hobson and Wassenaar (1997) which demonstrated this relationship, with feathers, on a continental scale, highlighting the potential to infer continent-wide origins for migratory birds (reviewed in Hobson and Wassenaar 2019). Before this breakthrough, stable isotopes had primarily been applied qualitatively to forensically determine origins based on demonstrated isotopic segregation among possible origins of a few species, such as African Elephants (*Loxodonta africana*; van der Merwe et al. 1990, Vogel et al. 1990, Koch et al. 1995).

For waterfowl, the use of stable isotopes in feathers to assign origin has mainly focused on assignment to moulting and natal/breeding areas, relying on the synchronous post-breeding moult in late summer or early autumn, where all flight feathers (primaries, secondaries, and wing coverts) are replaced simultaneously (Pyle 2005). During this period moulting individuals are flightless and generally do not move outside of a small moulting area. This is advantageous in terms of assigning animals' origins, as the feathers will be representative of a single site (e.g., moult or breeding pond).

1.4.1 Isotopic measurement

Stable isotopes are the non-radioactive forms of elements. In ecology, the most important elements are the 'light' elements which are the principal elements of hydrological and biological systems: Hydrogen (H), Carbon (C), Oxygen (O), Nitrogen (N), Sulphur (S). For each of these elements, there is an abundant light form (^{1}H, ^{12}C, ^{14}N, ^{16}O, ^{32}S) and at least one, less abundant, heavy form (^{2}H, ^{13}C, ^{15}N, ^{17}O/^{18}O, ^{33}S/^{34}S/^{36}S). Stable isotopes are expressed in delta (δ) notation as the relative difference between the ratio of heavy isotope to light isotope (Ratio = ^{H}X/^{L}X) in a sample and an international standard, expressed in parts per thousand (‰):

$$\delta_{}^{H}X = \left(\frac{Ratio_{Sample} - Ratio_{Standard}}{Ratio_{Standard}} \right) * 1,000$$

These international standards are Vienna Mean Standard Ocean Water (VSMOW) for H and O, Vienna Pee Dee Belemnite (VPDB) for C and O, atmospheric air for N, and Canon Diablo meteorite (CDT) for S.

The abundance of stable isotopes within samples is most commonly measured using a continuous-flow isotope-ratio mass spectrometer (CF-IRMS), where subsamples (~0.350–1.000 mg for δ^2H) are first combusted into gaseous forms of the elements (e.g., H$_2$, CO$_2$) using elemental analyzers, carried by a continuous flow of helium gas, separated based on mass, in a gas chromatograph column, and then fed into the CF-IRMS. Gases are then ionized and accelerated in a magnetic field, where they are separated based on their mass-to-charge ratio, and finally, abundance is measured as ions collide with Faraday-collector detectors.

For organic materials, the analysis of δ^2H is complicated by uncontrolled H exchange between exchangeable H in samples and ambient moisture in the laboratory (Wassenaar and Hobson 2003, Soto et al. 2017). If analyzed at labs in different geographic regions or at different times in the same lab, δ^2H values would differ despite following the same methods described above (Meier-Augenstein et al. 2013). To address this Wassenaar and Hobson (2003) introduced the comparative equilibration method, where samples are allowed to equilibrate in the same laboratory environment with matrix-equivalent

laboratory standards (e.g., kudu horn standard - KHS, caribou hoof standard - CBS). At room temperature, this equilibration occurs quickly (< 3 days). Then samples and standards are run in the CF-IRMS concurrently and unknown samples can be calibrated based on the expected δ^2H_{VSMOW} values of those standards. When comparing δ^2H values across studies, especially those derived with different laboratory standards or the same standards but with more recently derived calibration values (e.g., Soto et al. 2017), it is also important to convert these to the same reference scale (Magozzi et al. 2021).

1.4.2   Precipitation isoscapes

In North America, there is a strong latitudinal gradient where δ^2H_p values are generally more positive in the southeast and more negative in the northwest (Taylor 1974). This is driven in part by the gradual drying of air masses as they move across the continent (Clark and Fritz 1997). Under Rayleigh distillation, water molecules containing heavy isotopes (^2H) are preferentially condensed into water droplets (or ice crystals), fall as relatively isotopically heavy precipitation, and deplete the cloud air mass of ^2H (Clark and Fritz 1997). While the precipitate is relatively more positive in terms of δ^2H than the remaining cloud vapour, the progressive depletion of ^2H in the air mass with rainout results in precipitation becoming progressively more negative with repeated rainfall events. This fractionation is temperature dependent where at higher temperatures the fractionation is less pronounced, leading to differential effects in warmer and cooler regions (Clark and Fritz 1997). This is further complicated as regions experience different annual rainfall amounts, leading to relatively more depleted δ^2H_p values in regions with heavy rainfall, such as tropical locales (Rozanski et al. 1993). Post-precipitation processes such as mixing and evaporation of surface waters must also be accounted for, especially when hydrological sources have differing isotopic values (e.g., snowmelt) (Bowen and West 2019). In addition to the continental trends, there are also altitudinal trends driven by the same progressive drying of air masses. Here temperature dependent distillation also leads to an altitudinal gradient where more depleted δ^2H_p values are seen at higher altitudes due to orographic rainout (Siegenthaler and Oeschger 1980).

Several precipitation isoscapes (i.e., geospatial representations of isotope values; Bowen and West 2019) have been derived for use in wildlife tracking (Bowen and Revenaugh 2003, Meehan et al. 2004, Bowen et al. 2005, Terzer et al. 2013, Terzer-Wassmuth et al. 2021), all of which used long-term monthly collection of precipitation by the Global Network of Isotopes in Precipitation (GNIP) of the International Atomic Energy Association (IAEA) (International Atomic Energy Agency and World Meteorological Organization 2023). Early isoscapes relied on simple kriging methods, based on spatial distributions of δ^2H_P values alone (Hobson and Wassenaar 1997), but today interpolation methods include functions of altitude/latitude to account for temperature-driven variation in δ^2H (Bowen et al. 2005). Other more complex models have been derived (RCWIP2 model; Terzer-Wassmuth et al. 2021) but have yet to see widespread use.

Depending on the application, these amount-weighted (i.e., weighted by the monthly amount of precipitation) precipitation δ^2H_P isoscapes can be interpolated to capture values across the entire year (i.e., mean annual; Bowen and Revenaugh 2003, Bowen et al. 2005, Terzer et al. 2013, Terzer-Wassmuth et al. 2021), specific months (Bowen 2021), or values for the growing season (i.e., mean growing season; months with average temperatures > 0 °C; Meehan et al. 2004, Bowen et al. 2005). The growing season surfaces are most widely used, based on the assumption that dietary isotopes will reflect precipitation during the period of greatest vegetative growth. The appropriate calibration is less clear for aquatic and semi-aquatic species or those that eat foods that occur in aquatic emergent plant communities.

Currently, isoscapes are available as processed spatial grids, regularly updated with new annually collected data, and are paired with spatial error surfaces that provide estimates of uncertainty (Bowen 2021). More specific regional or temporally restricted isoscapes could be estimated (see Bowen 2023), but this is not recommended in most cases, as the cost of a year-specific isoscape reduced predictive accuracy due to fewer precipitation sampling points (Vander Zanden et al. 2014).

Although other isoscapes exist, such as those for $\delta^{13}C$ (Still and Powell 2010, Powell et al. 2012, Munroe et al. 2022), $\delta^{15}N$ (Craine et al. 2009), and $\delta^{87}Sr$ (Bataille et al. 2020),

they generally see less use compared to δ^2H isoscapes. Stable-carbon isoscapes, for example, are more useful in regions with broad biome-wide changes in plant groups that use different photosynthetic pathways (C3 vs C4). This is not useful for North America as the vast majority of biomes share a similar proportional composition with primarily C3 plants, except for corn monocultures which show disproportionate C4 usage. Nonetheless, δ^{13}C and δ^{15}N isoscapes have been used to create tissue-specific isoscapes in South America (García-Pérez and Hobson 2014) and Africa (Hobson et al. 2012*b*). Although these isotopes are not particularly useful for spatially explicit assignment using isoscapes in North America, they are still useful as supplementary markers to group individuals based on broad dietary niche at the time of tissue growth: δ^{13}C (e.g., marine vs. freshwater, Yerkes et al. 2008, Ashley et al. 2010), δ^{15}N (e.g., agricultural and anthropogenic inputs, Hebert and Wassenaar 2005), and δ^{34}S (e.g., marine vs. freshwater, Hebert et al. 2008, Ofukany et al. 2012). This is especially important for applications aimed at evaluating moult by birds in marine versus freshwater areas, as marine systems do not follow the same continental patterns as those driven by δ^2H$_p$. Strontium isoscapes have also been used in other migratory systems to delineate origins along an east-west gradient and isolate more regional origins (e.g., Reich et al. 2021), but have yet to be applied to waterfowl systems.

1.4.3   Calibration

Inert keratinous tissues, such as hair or feathers, experience no turnover or change in composition after growth. Therefore, their stable isotopic values do not change, with the exception of H (see H-exchange described above), and are representative of the diet during the growth period (Hobson and Clark 1992*a*), unless endogenous reserves are used during tissue formation (e.g., Fox et al. 2009).

While tissues are representative of the site of growth, incorporation of light elements into tissues involves some change in isotope ratio (i.e., isotopic discrimination) driven by the differential kinetic reaction rates between the heavy and light isotopes during various metabolic reactions (Hobson and Clark 1992*b*). Calibration equations (i.e., linear equations to relate δ^2H$_{Tissue} \sim \delta^2$H$_p$), used to convert δ^2H$_p$ values to predicted tissue δ^2H values, can be derived using tissue grown at known locations (e.g., Hobson and

Wassenaar 1997, Hobson et al. 1999, Meehan et al. 2001, Clark et al. 2006) or in lab-raised organisms (e.g., Hobson et al. 1999, 2018, Clem et al. 2023). It is also important to derive realistic estimates of error for these calibration relationships, which is often estimated as the standard deviation of the residuals (SD_{resid}).

Ideally, these equations should be species-specific (Nordell et al. 2016), with separate equations for age, when necessary (Studds et al. 2012, van Dijk et al. 2014), but the difficulty of obtaining known-origin samples has limited these precise equations to date. At the very least, calibration equations should cover as small a taxonomic group as possible, grouping based on similar diet and life history (Hobson et al. 2012*b*). See Table 1.1 for a select list of published studies containing known-origin δ^2H data for keratinous tissues (also see Hobson 2008, 2019).

1.4.4   Likelihood-based assignment

Likelihood-based assignment methods assess the support for different regions of possible origin based on similarity in δ^2H values between observed tissue δ^2H_{tissue} values and predicted δ^2H_{tissue} values in those regions, in a nominal (i.e., defined bins) or spatially explicit (i.e., continuous across a raster grid) framework (Wunder 2012). Here, each region (nominal) or cell (spatially explicit) is treated as a putative population of origin with an expected δ^2H_{tissue} value and uncertainty in this measure, derived from calibration uncertainty (i.e., SD_{resid}) and the δ^2H_p isoscape uncertainty (i.e., predictive uncertainty driven by variable in δ^2H_p values and limited geographic sample size). Incorporation of this error is important, as different individuals foraging at the same location are not expected to have the same δ^2H values, and even samples from the same individual exhibit some variation (Wassenaar and Hobson 2006). Support based on derived likelihoods is compared among different regions of possible origin and odds ratios (i.e., the probability that an outcome occurs compared to the probability that the outcome does not occur) can then be used to conservatively delineate a region of likely origin based on relative support within these likelihood surfaces. Here the most likely cells or bins are selected based on the selected odds ratio (e.g., 2/1 = upper 66.66 % of cell probabilities of origin), where any point within this region is treated as equally likely. This allows for direct comparison across many individuals while acknowledging that greater cell-specific likelihood does

13

not equate more likely origins to that specific cell. These methods, and the mathematical definitions, are described at length throughout the thesis.

Many early assignments used the nominal approach (Royle and Rubenstein 2004, Norris et al. 2006), as spatially explicit methods were not adopted until relatively later (Hobson et al. 2009*b*). While simpler, the nominal approach works well for colonial nesting species where *a priori* expectations for grouped origins are defined such as Arctic breeding birds (e.g., geese, gulls, and eiders). But, even in these cases, using multiple markers to better characterize these known groups likely allows for more precise assignment (e.g., $\delta^{13}C$ and $\delta^{15}N$, Alisauskas and Hobson 1993).

For species with no *a priori* expectations of grouped origin, the spatially explicit approach is recommended, especially with user-friendly packages that streamline this workflow for continuous surfaces (i.e., assignR, Ma et al. 2020; isocat, Campbell et al. 2020). Spatially explicit assignment has been successfully applied to determine the origins of many waterfowl species in North America (Hobson et al. 2009*b*, Ashley et al. 2010, Asante et al. 2017, Palumbo et al. 2019, 2020, Kucia et al. 2023, Schummer et al. 2023), Europe (Guillemain et al. 2014, 2019, Parejo et al. 2015, Caizergues et al. 2016), and Asia (Zhu et al. 2020). Notably, these methods have been used to delineate likely breeding areas for Mallard carriers of the influenza A virus staging in Sweden (Gunnarsson et al. 2012), estimate connectivity for the endangered Swan Goose (*Anser cygnoides*) overwintering in China (Zhu et al. 2020), and establish source areas for the harvest of various harvested species (e.g., American Black Duck, Ashley et al. 2010; Lesser Scaup, Hobson et al. 2009*b*; Mallard, Palumbo et al. 2019, Kucia et al. 2023, Schummer et al. 2023).

Table 1.1 Published known-origin δ^2H data for keratinous tissues, separated by taxonomy.

Taxa	n	Reference
Aves		
22 species[a] in Europe	128	(Hobson et al. 2004)
Columbiformes		
Common Wood Pigeon (*Columba palumbus*)	12	(Hobson et al. 2009*a*)
Anseriformes		
Swan Geese (*Anser cygnoides*)	50	(Zhu et al. 2020)
Scaly-sided Mergansers (*Mergus squamatus*)	10	(Solovyeva et al. 2016)
Mallard (*Anas platyrhynchos*)	309	(van Dijk et al. 2014)
Lesser Scaup (*Aythya affinis*)	75	(Clark et al. 2006)
Mallard Northern Pintail (*Anas acuta*)	408	(Hebert and Wassenaar 2005)
Accipitriformes, Falconiformes, Strigiformes		
Sharp-shinned Hawk (*Accipiter striatus*)	23	(Wommack et al. 2020)
Marsh Harrier (*Circus aeruginosus*)	49	(Cardador et al. 2015)
12 species[b] in North America	264	(Lott and Smith 2006)
Flammulated Owl (*Otus flammeolus*)	22	(Meehan et al. 2004)
9 species[c] in North America	112	(Lott et al. 2003)
Cooper's Hawk (*Accipiter cooperii*)	60	(Meehan et al. 2001)
Charadriiformes		
American Woodcock (*Scolopax minor*)	43	(Sullins et al. 2016)
American Woodcock	226	(Hobson et al. 2013)
Mountain Plover (*Charadrius montanus*)	465	(Wunder 2007)
Gruiformes		
14 species[d] in Asia	216	(Buchanan et al. 2018)
King Rail (*Rallus elegans*) Virginia Rail (*Rallus limicola*)	54	(Fournier et al. 2017)
Baillon's Crake (*Zapornia pusilla*) Black Crake (*Zapornia flavirostris*) Spotted Crake (*Porzana porzana*) Water Rail (*Rallus aquaticus*)	80	(Seifert et al. 2016)
Passeriformes		
Golden-winged Warbler (*Vermivora chrysoptera*)	47	(López-Calderón et al. 2019)
Prothonotary Warbler (*Protonotaria citrea*)	72	(Reese et al. 2019)
14 species[e] in North America	104	(Hobson and Koehler 2015)

Red-winged Blackbird (*Agelaius phoeniceus*)	288	(Werner et al. 2016)
Pied Flycatcher (*Ficedula hypoleuca*)	97	(Tonra et al. 2015)
Brewer's Sparrow (*Spizella breweri*) Sagebrush Sparrow (*Artemisiospiza nevadensis*)	346	(Knick et al. 2014)
Reed Warbler (*Acrocephalus scirpaceus*)	214	(Procházka et al. 2013)
Hermit Thrush (*Catharus guttatus*) Wilson's Warbler (*Wilsonia pusilla*)	186	(Rundel et al. 2013)
Loggerhead Shrike (*Lanius ludovicianus*)	546	(Chabot et al. 2012)
40 species[f] in North America	544	(Hobson et al. 2012*b*)
Wilson's Warbler	63	(Paxton et al. 2007)
Wilson's Warbler	63	(Kelly et al. 2002)
Bicknell's Thrush (*Catharus bicknelli*)	64	(Hobson et al. 2001)
Red-winged Blackbird	64	(Wassenaar and Hobson 2000)
Black-throated Blue Warbler (*Setophaga caerulescens*)	143	(Chamberlain et al. 1997)
6 species[g] in North America	175	(Hobson and Wassenaar 1997)

Insecta
Coleoptera

	34	(Miller et al. 1988)

Diptera

Eupeodes americanus Oblique Streaktail	15*	(Clem et al. 2023)
Episyrphus balteatus	62	(Raymond et al. 2014)
Episyrphus balteatus	18	(Ouin et al. 2011)

Lepidoptera

true army worm (*Mythimna unipuncta*)	200*	(Hobson et al. 2018)
peacock butterfly (*Inachis io*) southern small white butterfly (*Pieris mannii*) wall brown butterfly (*Lasiommata megera*)	175	(Brattström et al. 2008, 2010)
monarch (*Danaus plexippus*)	144	(Hobson et al. 1999)

Odonata

blue dasher (*Pachydiplax longipennis*) shadow darner (*Aeshna umbrosa*) variable darner (*Aeshna interrupta*)	186	(Hobson et al. 2012*a*)

Mammalia
Artiodactyla

mule deer (*Odocoileus hemionus*) white-tailed deer (*Odocoileus virginianus*)	38	(Cormie et al. 1994)

Chiroptera

brown long-eared bat (*Plecotus auritus*) grey long-eared bat (*Plecotus austriacus*)	178	(Popa-Lisseanu et al. 2012)

meridonal serotine (*Eptesicus isabellinus*)		
serotine bat (*Eptesicus serotinus*)		
western barbastelle (*Barbastella barbastellus*)		
eastern red bat (*Lasiurus borealis*)		
Indiana bat (*Myotis sodalis*)	215	(Britzke et al. 2009)
little brown bat (*Myotis lucifugus*)		
Myotis septentrionalis		
hoary bat (*Lasiurus cinereus*)	104	(Cryan et al. 2004)

* – indicates that tissues were obtained from animals in captivity

[a-g] – indicates studies with ≥ 5 species. Full species lists are provided here: [a] Black Grouse (*Lyrurus tetrix*), Black Woodpecker (*Dryocapus maritus*), Blue Tit (*Cyanistes caeruleus*), Chaffinch (*Fringilla coelebs*), Common Wood Pigeon, Eurasian Blackbird (*Turdus merula*), Eurasian Curlew (*Numenius arquata*), European Serin (*Serinus serinus*), Fieldfare (*Turdus pilaris*), Hazel Grouse (*Tetrastes bonasia*), House Sparrow (*Passer domesticus*), Lapwing (*Vanellus vanellus*), Partridge (*Perdix perdix*), Pheasant (*Phasianus colchicus*), Red Grouse (*Lagopus lagopus scotica*), Redwing (*Turdus iliacus*), Rock Pigeon (*Columba livia*), Song Thrush (*Turdus philomelos*), Warbler sp., Willow Grouse (*Lagopus lagopus lagopus*); [b] American Kestrel (*Falco sparverius*), Broad-winged Hawk (*Buteo platypterus*), Cooper's Hawk, Merlin (*Falco columbarius*), American Goshawk (*Accipiter atricapillus*), Northern Harrier (*Circus hudsonius*), Peregrine Falcon (*Falco peregrinus*), Prairie Falcon (*Falco mexicanus*), Rough-legged Hawk (*Buteo lagopus*), Red-tailed Hawk (*Buteo jamaicensis*), Sharp-shinned Hawk (*Accipiter striatus*), Swainson's Hawk (*Buteo swainsoni*); [c] American Kestrel, Broad-winged Hawk, Cooper's Hawk, Merlin, Northern Harrier, Peregrine Falcon, Red-shouldered Hawk, Red-tailed Hawk, Sharp-shinned Hawk; [d] Common Sandpiper (*Actitis hypoleucos*), Black-tailed Godwit (*Limosa limosa*), Black-winged Stilt (*Himantopus himantopus*), Common Lapwing, Common Redshank (*Tringa totanus*), Eurasian Curlew, Eurasian Oystercatcher (*Haematopus ostralegus*), Eurasian Whimbrel (*Numenius phaeopus*), Green Sandpiper (*Tringa ochropus*), Kentish Plover (*Anarhynchus alexandrinus*), Little Ringed Plover (*Charadrius dubius*), Marsh Sandpiper (*Tringa stagnatilis*), Pied Avocet (*Recurvirostra avosetta*), Sociable Lapwing (*Vanellus gregarius*); [e] American Redstart (*Setophaga ruticilla*), Black-and-white Warbler (*Mniotilta varia*), Carolina Chickadee (*Poecile carolinensis*), Carolina Wren (*Thryothorus ludovicianus*), Common Yellowthroat (*Geothlypis trichas*), Golden-winged Warbler, Hooded Warbler (*Setophaga citrina*), MacGillivray's Warbler (*Geothlypis tolmiei*), Song Sparrow (*Melospiza melodia*), Tufted Titmouse (*Baeolophus bicolor*), White-eyed Vireo (*Vireo griseus*), Wilson's Warbler (*Cardellina pusilla*), Yellow-breasted Chat (*Icteria virens*), Yellow Warbler (*Setophaga petechia*); [f] Abert's Towhee (*Melozone aberti*), American Redstart, American Robin (*Turdus migratorius*), Bewick's Wren (*Thryomanes bewickii*), Black-and-white Warbler, Black-capped Chickadee (*Poecile atricapillus*), Blue-winged Warbler (*Vermivora cyanoptera*), Carolina Chickadee, Carolina Wren, Chipping Sparrow (*Spizella passerina*), Common Yellowthroat, Chestnut-sided Warbler (*Setophaga pensylvanica*), Dark-eyed Junco (*Junco hyemalis oregonus*), Golden-winged Warbler, Gray Catbird (*Dumetella carolinensis*), Hermit Thrush, Hooded Warbler, House Sparrow, House Wren (*Troglodytes aedon*), Kentucky Warbler (*Geothlypis formosa*), MacGillivray's Warbler, Nashville Warbler (*Leiothlypis ruficapilla*), Northern Cardinal (*Cardinalis cardinalis*), Orange-crowned Warbler (*Leiothlypis celata*), Ovenbird (*Seiurus aurocapilla*), Red-eyed Vireo (*Vireo olivaceus*), Rufous-crowned Sparrow (*Aimophila ruficeps*), Rusty Blackbird (*Euphagus carolinus*), Song Sparrow, Sprague's Pipit (*Anthus spragueii*), Swainson's Thrush (*Catharus ustulatus*), Tree Swallow (*Tachycineta bicolor*), Tufted Titmouse, Veery (*Catharus fuscescens*), White-eyed Vireo, Wilson's Warbler, Wood Thrush (*Hylocichla mustelina*), Yellow-breasted Chat, Yellow-rumped Warbler (*Setophaga coronataa auduboni*), Yellow Warbler; [g] American Redstart, Least Flycatcher (*Empidonax minimus*), Tennessee Warbler (*Leiothlypis peregrinus*), Swainson's Thrush, Ovenbird, Wood Thrush

Within likelihood-based assignment models, prior information (i.e., prior probabilities of origin) can refine regions of likely origin based on Bayesian methods (Royle and Rubenstein 2004). Prior probabilities can be applied on an individual basis based on intrinsic traits (e.g., genetic profiles; Ruegg et al. 2017) or could apply to all individuals in a given cohort or population (e.g., relative abundance; Fournier et al. 2017). For waterfowl, banding data is the most common prior that has been applied, with priors representing flyway of origin (Asante et al. 2017, Palumbo et al. 2019), directional movement vectors (Gunnarsson et al. 2012, Guillemain et al. 2014), and movement probabilities among regions (Ashley et al. 2010).

1.5   Dissertation structure

My dissertation consists of four research chapters, examining the harvest connectivity of waterfowl in North America. The overall objective was to use stable-hydrogen isotopes to inform direct connections between harvest and source areas for harvested waterfowl in eastern North America while assessing and improving on current methods.

In Chapter 2, I used δ^{13}C and δ^2H measurements of feathers to evaluate differences in the natal and moult origin of harvested American Black Ducks across their range. For the American Black Duck, a species of conservation concern, estimates for the fall age ratio at harvest differed depending on whether harvest data was derived from Canada or the United States, suggesting regional differences. Within Canada, hunters in Atlantic Canada were more likely to harvest black ducks from nearby breeding locations compared to hunters in southern Ontario and Quebec, Canada, who were more likely to harvest individuals from the Boreal Softwood and Taiga Shield of eastern Canada. Black ducks harvested in the United States are thought to originate predominantly from northern portions of the breeding range, leading to the flyover hypothesis, which postulates that black ducks produced in the Boreal Softwood and Taiga Shield region are less susceptible to harvest by hunters in Atlantic Canada and northeastern United States. To test the flyover hypothesis, I examined regional and temporal differences in the origins of harvested black ducks using feathers from wings (n = 664) submitted by hunters to the species composition and parts collection surveys across three hunting seasons (2017–18, 2018–19, 2019–20). I used a likelihood-based assignment method that

relied on feather stable-hydrogen isotopes (δ^2H) and stable-carbon isotopes (δ^{13}C) to determine the natal or moult origin of individuals harvested within eastern Canada and the United States. I also used a spatial clustering technique to group harvested individuals by area of origin without *a priori* knowledge of such regions. Adult female black ducks originated farther south compared to males and juveniles. All sexes and ages of black ducks harvested in Atlantic Canada showed predominantly southern origins, while those harvested in the United States and other Canadian provinces primarily originated farther north within the boreal, supporting the flyover hypothesis. By contrast, I found no relationship between the timing of harvest or peaks of migration and individual origin. After combining band returns and stable isotopes, I inferred two distinct stocks: the Mississippi Flyway stock and the Atlantic Flyway stock. Based on the results of this chapter, I recommend that regional demographic parameters, particularly for Atlantic Canada, be directly measured to promote more effective conservation of black ducks and optimize harvest opportunities in the United States and Canada.

In Chapter 3, I critically evaluated the current methods used to predict stable isotopes in waterfowl feathers. Establishing links between breeding, stopover, and wintering sites for migratory species is important for their effective conservation and management. Isotopic assignment methods used to create these connections rely on the use of predictable, established relationships between the isotopic composition of environmental hydrogen and that of the non-exchangeable hydrogen in animal tissues, often in the form of a calibration equation relating feather (δ^2H$_f$) values derived from known-origin individuals and amount-weighted long-term precipitation (δ^2H$_p$) data. The efficacy of assigning waterfowl to moult origin using stable isotopes depends on the accuracy of these relationships and their statistical uncertainty. Most current calibrations for terrestrial species in North America are done using amount-weighted mean growing-season δ^2H$_p$ values, but the calibration relationship is less clear for aquatic and semi-aquatic species. My objective was to critically evaluate current methods used to calibrate δ^2H$_p$ isoscapes to predicted δ^2H$_f$ values for waterfowl. Specifically, I evaluated the strength of the relationships between δ^2H$_p$ values from three commonly used isoscapes and known-origin δ^2H$_f$ values three published datasets and one collected as part of this study, also grouping these data into foraging guilds (dabbling vs. diving ducks). I then evaluated the

performance of assignments using these calibrations by applying a cross-validation procedure. It remains unclear if any of the tested δ^2H_p isoscapes better predict surface water inputs into food webs for foraging waterfowl. I found only marginal differences in the performance of the tested known-origin datasets, where the combined foraging-guild-specific datasets showed lower assignment precision and model fit compared to data for individual species. Based on these results, I recommend the use of the more conservative combined foraging-guild-specific datasets to assign geographic origin for all dabbling duck species. Refining these relationships is important for improved waterfowl management and contributes to a better understanding of the limitations of assignment methods when using the isotope approach.

In Chapter 4, I explored spatiotemporal patterns in the natal sources of waterfowl in eastern North America using direct band returns. Under AHM in North America, most species are managed based on the status of one of three flyway-specific stocks with the assumption that the trends should represent the overall trends of species in that flyway. While flyways are well-established movement corridors, source areas for species managed under this framework may not match the same source areas as the modelled species. Many estimates of connectivity and source areas are based on preseason band-return data, but a systematic exploration of spatiotemporal trends in these source areas is lacking to date. Specifically, how variable source areas are based on timing and location of harvest and whether these changes vary systematically across species are poorly understood. Using 60 years of band-return data, I examined spatiotemporal changes in the spatial distribution of natal sources for waterfowl harvested in the Mississippi and Atlantic flyways, using kernel density estimation to delineate species-specific spatially explicit natal sources across the harvest period (September–February), at different harvest latitudes (25–30°, 30–35°, 35–40°, 40–45°, 45–50°, 50–55° N), and for the two flyways (Mississippi, Atlantic). I hypothesized that individuals harvested later in the harvest season originate from relatively farther north compared to those harvested earlier in the season, especially at northern latitudes, and that individuals harvested at lower latitudes come from broader catchments. I found evidence for northward directional expansion of natal sources over the harvest period, but rather than shifting, natal sources generally expanded northward while maintaining southern source areas. Despite temporal trends,

flyway and latitude of harvest explained variation in natal sources more than the timing of harvest. On average, I found evidence for management-unit-specific harvest, supporting AHM assumptions. The results from this chapter provide a first look into spatiotemporal dynamics of connectivity for waterfowl harvested in Eastern North America.

In Chapter 5, I critically evaluated the use of band returns as a prior probability of origin and directly compared source areas derived from band returns and feather δ^2H values. Likelihood-based assignment methods, utilizing measurements of stable isotopes in feathers can be paired with prior probabilities of origin (i.e., priors) in a Bayesian framework, to refine regions of likely natal / breeding origins. Using feathers collected from 11 species of harvested waterfowl across the Great Lakes region (n = 747; 2017–21), I estimated their likely natal origins using direct recoveries and δ^2H$_f$ measurements, directly comparing and combining two different sources of connectivity information. I explored how these two complementary data sources can be best integrated into likelihood-based assignment methods to refine origin estimates for harvested waterfowl in three frameworks: (1) by flyway, (2) by 5° longitudinal zone, and (3) by treating movement as a directional vector. I also explored the scale at which these priors are defined, where I compared the use of a prior derived for the entire Great Lakes region versus one derived at a finer spatial scale based on harvest location. Lastly, I directly compared origin based on δ^2H$_f$ and current banding effort to evaluate the overlap, determine potential gaps in the current banding program, and highlight priority areas of future banding efforts to supplement the existing banding framework. Across all species, the use of flyways and longitudinal zones as prior probabilities of origin showed more promising results compared to the directional movement vector priors. Longitudinal zones, compared to flyways, provided more fine-scale priors while allowing for the same longitudinal differentiation in likely origins. I also highlighted the importance of assessing these priors at different spatial scales, as deriving priors for the entire study region compared to a finer spatial scale significantly affected final regions of likely origins. Finally, taking advantage of δ^2H$_f$ as an intrinsic marker, I identified regions in northwestern Ontario and northern Manitoba as potential targets for future multi-species banding efforts to fill gaps in the current banding framework. The results from this

chapter reinforce the fundamentals of these methods and provide guidance to better integrate these data to establish source areas.

In the final chapter (Chapter 6), I provide a synthesis of the primary findings from my research chapters and describe the next steps for the use of stable isotopes to provide connectivity estimates for harvested waterfowl.

1.6   References

Abraham, K. F., J. O. Leafloor, and D. H. Rusch. 1999. Molt migrant Canada Geese in northern Ontario and western James Bay. The Journal of Wildlife Management 63:649–655.

Alisauskas, R. T., and K. A. Hobson. 1993. Determination of Lesser Snow Goose diets and winter distribution using stable isotope analysis. The Journal of Wildlife Management 57:49–54.

Ankney, C. D., D. G. Dennis, and R. C. Bailey. 1987. Increasing Mallards, decreasing American Black Ducks: coincidence or cause and effect? The Journal of Wildlife Management 51:523–529.

Ankney, C., D. Dennis, and R. C. Bailey. 1989. Increasing Mallards, decreasing American Black Ducks-no evidence for cause and effect: a reply. Journal of Wildlife Management 53:1072–1075.

Asante, C. K., T. D. Jardine, S. L. Van Wilgenburg, and K. A. Hobson. 2017. Tracing origins of waterfowl using the Saskatchewan River Delta: incorporating stable isotope approaches in continent-wide waterfowl management and conservation. The Condor 119:261–274.

Ashley, P., K. A. Hobson, S. L. Van Wilgenburg, N. North, and S. A. Petrie. 2010. Linking Canadian harvested juvenile American Black Ducks to their natal areas using stable isotope (δD, δ^{13}C, and δ^{15}N) methods. Avian Conservation and Ecology 5:7.

Baldassarre, G. A. 2014. Ducks, Geese, and Swans of North America. Volume 2. JHU Press, Baltimore, MD, USA.

Bataille, C. P., B. E. Crowley, M. J. Wooller, and G. J. Bowen. 2020. Advances in global bioavailable strontium isoscapes. Palaeogeography, Palaeoclimatology, Palaeoecology 555:109849.

Bellrose, F. C., and D. J. Holm. 1994. Ecology and Management of the Wood Duck. Stackpole Books, Mechanicsburg, PA, USA.

Boulet, M., and D. R. Norris. 2006. The past and present of migratory connectivity. Ornithological Monographs 61:1–13.

Bowen, G. 2023. isoWater: Discovery, Retrieval, and Analysis of Water Isotope Data. R package version 1.1.2. <https://CRAN.R-project.org/package=isoWate>.

Bowen, G. J. 2021. Gridded maps of the isotopic composition of meteoric waters. <http://www.waterisotopes.org.>. Accessed 23 Aug 2021.

Bowen, G. J., and J. Revenaugh. 2003. Interpolating the isotopic composition of modern meteoric precipitation. Water Resources Research 39:1299.

Bowen, G. J., L. I. Wassenaar, and K. A. Hobson. 2005. Global application of stable hydrogen and oxygen isotopes to wildlife forensics. Oecologia 143:337–348.

Bowen, G. J., and J. B. West. 2019. Isoscapes for terrestrial migration research. Pages 53–84 *in* K. A. Hobson and L. I. Wassenaar, editors. Tracking Animal Migration with Stable Isotopes. Second edition. Academic Press, Cambridge, MA, USA.

Bowers, E. F., and R. B. Hamilton. 1977. Derivation of northern Wood Ducks harvested in southern states of the Mississippi Flyway. Proceedings of the Annual Conference of the Southeastern Association of Fish and Wildlife Agencies 31:90–98.

Brattström, O., S. Bensch, L. I. Wassenaar, K. A. Hobson, and S. Åkesson. 2010. Understanding the migration ecology of European red admirals *Vanessa atalanta* using stable hydrogen isotopes. Ecography 33:720–729.

Brattström, O., L. I. Wassenaar, K. A. Hobson, and S. Åkesson. 2008. Placing butterflies on the map – testing regional geographical resolution of three stable isotopes in Sweden using the monophagus peacock *Inachis io*. Ecography 31:490–498.

Britzke, E. R., S. C. Loeb, K. A. Hobson, C. S. Romanek, and M. J. Vonhof. 2009. Using hydrogen isotopes to assign origins of bats in the eastern United States. Journal of Mammalogy 90:743–751.

Buchanan, G. M., A. L. Bond, N. J. Crockford, J. Kamp, J. W. Pearce-Higgins, and G. M. Hilton. 2018. The potential breeding range of Slender-billed Curlew *Numenius tenuirostris* identified from stable-isotope analysis. Bird Conservation International 28:228–237.

Caizergues, A., S. L. Van Wilgenburg, and K. A. Hobson. 2016. Unraveling migratory connectivity of two European diving ducks: a stable isotope approach. European Journal of Wildlife Research 62:701–711.

Campbell, C. J., M. C. Fitzpatrick, H. B. Vander Zanden, and D. M. Nelson. 2020. Advancing interpretation of stable isotope assignment maps: comparing and summarizing origins of known-provenance migratory bats. Animal Migration 7:27–41.

Cardador, L., J. Navarro, M. G. Forero, K. A. Hobson, and S. Mañosa. 2015. Breeding origin and spatial distribution of migrant and resident harriers in a Mediterranean wintering area: insights from isotopic analyses, ring recoveries and species distribution modelling. Journal of Ornithology 156:247–256.

Carney, S. M. 1992. Species, age and sex identification of ducks using wing plumage. U.S. Fish and Wildlife Service, Department of the Interior, Washington, DC, USA. < https://www.fws.gov/media/species-age-and-sex-identification-ducks-using-wing-plumage>

Celis-Murillo, A., M. Malorodova, and E. Nakash. 2022. North American Bird Banding Dataset 1960–2022 retrieved 2022-07-14. U.S. Geological Survey, Eastern Ecological Science Center at the Patuxent Research Refuge, Laurel, MD, USA.

Chabot, A. A., K. A. Hobson, S. L. Van Wilgenburg, G. J. McQuat, and S. C. Lougheed. 2012. Advances in linking wintering migrant birds to their breeding-ground origins using combined analyses of genetic and stable isotope markers. PLOS One 7:e43627.

Chamberlain, C. P., J. D. Blum, R. T. Holmes, X. Feng, T. W. Sherry, and G. R. Graves. 1997. The use of isotope tracers for identifying populations of migratory birds. Oecologia 109:132–141.

Clark, I., and P. Fritz. 1997. Environmental Isotopes in Hydrogeology. Lewis Publishers, Boca Raton, FL, USA.

Clark, R. G., K. A. Hobson, and L. I. Wassenaar. 2006. Geographic variation in the isotopic (δD, δ^{13}C, δ^{15}N, δ^{34}S) composition of feathers and claws from Lesser Scaup and Northern Pintail: implications for studies of migratory connectivity. Canadian Journal of Zoology 84:1395–1401.

Clem, C. S., K. A. Hobson, and A. N. Harmon-Threatt. 2023. Insights into natal origins of migratory Nearctic hover flies (Diptera: Syrphidae): new evidence from stable isotope (δ^2H) assignment analyses. Ecography 2023:e06465.

Conroy, M., G. Barnes, R. Bethke, and T. Nudds. 1989. Increasing Mallards, decreasing American Black Ducks: no evidence for cause and effect: a comment. The Journal of Wildlife Management 53:1065–1071.

Conroy, M. J., M. W. Miller, and J. E. Hines. 2002. Identification and synthetic modeling of factors affecting American Black Duck populations. Wildlife Monographs 150:1–64.

Cormie, A. B., B. Luz, and H. P. Schwarcz. 1994. Relationship between the hydrogen and oxygen isotopes of deer bone and their use in the estimation of relative humidity. Geochimica et Cosmochimica Acta 58:3439–3449.

Craft, C., J. Clough, J. Ehman, S. Joye, R. Park, S. Pennings, H. Guo, and M. Machmuller. 2009. Forecasting the effects of accelerated sea-level rise on tidal marsh ecosystem services. Frontiers in Ecology and the Environment 7:73–78.

Craine, J. M., A. J. Elmore, M. P. M. Aidar, M. Bustamante, T. E. Dawson, E. A. Hobbie, A. Kahmen, M. C. Mack, K. K. McLauchlan, A. Michelsen, G. B. Nardoto, L. H. Pardo, J. Peñuelas, P. B. Reich, E. A. G. Schuur, W. D. Stock, P. H. Templer, R. A. Virginia, J. M. Welker, and I. J. Wright. 2009. Global patterns of foliar nitrogen isotopes and their relationships with climate, mycorrhizal fungi, foliar nutrient concentrations, and nitrogen availability. New Phytologist 183:980–992.

Cryan, P. M., M. A. Bogan, R. O. Rye, G. P. Landis, and C. L. Kester. 2004. Stable hydrogen isotope analysis of bat hair as evidence for seasonal molt and long-distance migration. Journal of Mammalogy 85:995–1001.

Davis, R. A., R. N. Jones, C. D. MacInnes, and A. J. Pakulak. 1985. Molt migration of Large Canada Geese on the west coast of Hudson Bay. The Wilson Bulletin 97:296–305.

De Sobrino, C. N., C. L. Feldheim, and T. W. Arnold. 2017. Distribution and derivation of dabbling duck harvests in the Pacific Flyway. California Fish and Game 103:118–137.

DeSaix, M. G., M. D. Rodriguez, K. C. Ruegg, and E. C. Anderson. 2024. Population assignment from genotype likelihoods for low-coverage whole-genome sequencing data. Methods in Ecology and Evolution 15:493–510.

van Dijk, J. G., W. Meissner, and M. Klaassen. 2014. Improving provenance studies in migratory birds when using feather hydrogen stable isotopes. Journal of Avian Biology 45:103–108.

Egevang, C., I. J. Stenhouse, R. A. Phillips, A. Petersen, J. W. Fox, and J. R. D. Silk. 2010. Tracking of Arctic terns *Sterna paradisaea* reveals longest animal migration. Proceedings of the National Academy of Sciences 107:2078–2081.

Finch, T., S. J. Butler, A. M. A. Franco, and W. Cresswell. 2017. Low migratory connectivity is common in long-distance migrant birds. Journal of Animal Ecology 86:662–673.

Fournier, A. M. V., A. R. Sullivan, J. K. Bump, M. Perkins, M. C. Shieldcastle, and S. L. King. 2017. Combining citizen science species distribution models and stable isotopes reveals migratory connectivity in the secretive Virginia rail. Journal of Applied Ecology 54:618–627.

Fox, A. D., K. A. Hobson, and J. Kahlert. 2009. Isotopic evidence for endogenous protein contributions to greylag goose *Anser anser* flight feathers. Journal of Avian Biology 40:108–112.

García-Pérez, B., and K. A. Hobson. 2014. A multi-isotope (δ^2H, δ^{13}C, δ^{15}N) approach to establishing migratory connectivity of Barn Swallow (*Hirundo rustica*). Ecosphere 5:art21.

Geis, A. D. 1971. Breeding and wintering areas of mallards harvested in various states and provinces. U.S. Department of the Interior, Fish and Wildlife Service, Bureau of Sport Fisheries and Wildlife, Washington, DC, USA.

Geis, A. D. 1972. Use of banding data in migratory game bird research and management. U.S. Department of the Interior, Fish and Wildlife Service, Bureau of Sport Fisheries and Wildlife, Washington, DC, USA.

Geis, A. D. 1974. Breeding and wintering areas of Canvasbacks harvested in various states and provinces. U.S. Department of the Interior, Fish and Wildlife Service, Washington, DC, USA.

Geis, A. D., R. I. Smith, and J. P. Rogers. 1971. Black duck distribution, harvest characteristics, and survival. U.S. Department of the Interior, Fish and Wildlife Service, Bureau of Sport Fisheries and Wildlife, Washington, DC, USA.

Gendron, M., and A. Smith. 2019. National Harvest Survey website. Canadian Wildlife Service, Environment and Climate Change Canada, Ottawa, Ontario. <https://wildlife-species.canada.ca/harvest-survey>. Accessed 28 Jan 2020.

Greenberg, R., and P. P. Marra. 2005. Birds of two worlds: the ecology and evolution of migration. JHU Press, Baltimore, MD, USA.

Guillemain, M., L. Bacon, K. J. Kardynal, A. Olivier, M. Podhrazsky, P. Musil, and K. A. Hobson. 2019. Geographic origin of migratory birds based on stable isotope analysis: the case of the greylag goose (*Anser anser*) wintering in Camargue, southern France. European Journal of Wildlife Research 65:67.

Guillemain, M., S. L. Van Wilgenburg, P. Legagneux, and K. A. Hobson. 2014. Assessing geographic origins of Teal (*Anas crecca*) through stable-hydrogen (δ^2H) isotope analyses of feathers and ring-recoveries. Journal of Ornithology 155:165–172.

Gunnarsson, G., N. Latorre-Margalef, K. A. Hobson, S. L. Van Wilgenburg, J. Elmberg, B. Olsen, R. A. M. Fouchier, and J. Waldenström. 2012. Disease dynamics and bird migration — Linking Mallards *Anas platyrhynchos* and subtype diversity of the Influenza A virus in time and space. PLOS One 7:e35679.

Handrigan, S. A., M. L. Schummer, S. A. Petrie, and D. R. Norris. 2016. Range expansion and migration of Trumpeter Swans *Cygnus buccinator* re-introduced in southwest and central Ontario. Wildfowl 66:60–74.

Hebert, C. E., M. Bur, D. Sherman, and J. L. Shutt. 2008. Sulphur isotopes link overwinter habitat use and breeding condition in Double-crested Cormorants. Ecological Applications 18:561–567.

Hebert, C. E., and L. I. Wassenaar. 2005. Feather stable isotopes in western North American waterfowl: spatial patterns, underlying factors, and management applications. Wildlife Society Bulletin 33:92–102.

Heitmeyer, M., and L. Fredrickson. 1981. Do wetland conditions in the Mississippi Delta hardwoods influence mallard recruitment? Transactions of the North American Wildlife and Natural Resources Conferences (USA), no. 46.

Hobson, K. A. 2019. Application of isotopic methods to tracking animal movements. Pages 85–115 *in* K. A. Hobson and L. I. Wassenaar, editors. Tracking Animal Migration with Stable Isotopes. Second Edition. Academic Press, Cambridge, MA, USA.

Hobson, K. A., G. J. Bowen, L. I. Wassenaar, Y. Ferrand, and H. Lormee. 2004. Using stable hydrogen and oxygen isotope measurements of feathers to infer geographical origins of migrating European birds. Oecologia 141:477–488.

Hobson, K. A., and R. G. Clark. 1992*a*. Assessing avian diets using stable isotopes I: turnover of ^{13}C in tissues. The Condor 94:181–188.

Hobson, K. A., and R. G. Clark. 1992*b*. Assessing avian diets using stable isotopes II: factors influencing diet-tissue fractionation. The Condor 94:189–197.

Hobson, K. A., K. Doward, K. J. Kardynal, and J. N. McNeil. 2018. Inferring origins of migrating insects using isoscapes: a case study using the true armyworm, *Mythimna unipuncta*, in North America. Ecological Entomology 43:332–341.

Hobson, K. A., and G. Koehler. 2015. On the use of stable oxygen isotope (δ^{18}O) measurements for tracking avian movements in North America. Ecology and Evolution 5:799–806.

Hobson, K. A., H. Lormée, S. L. Van Wilgenburg, L. I. Wassenaar, and J. M. Boutin. 2009*a*. Stable isotopes (δD) delineate the origins and migratory connectivity of harvested animals: the case of European woodpigeons. Journal of Applied Ecology 46:572–581.

Hobson, K. A., K. P. McFarland, L. I. Wassenaar, C. C. Rimmer, and J. E. Goetz. 2001. Linking breeding and wintering grounds of Bicknell's Thrushes using stable isotope analyses of feathers. The Auk 118:16–23.

Hobson, K. A., D. X. Soto, D. R. Paulson, L. I. Wassenaar, and J. H. Matthews. 2012*a*. A dragonfly (δ^2H) isoscape for North America: a new tool for determining natal origins of migratory aquatic emergent insects. Methods in Ecology and Evolution 3:766–772.

Hobson, K. A., S. L. Van Wilgenburg, Y. Ferrand, F. Gossman, and C. Bastat. 2013. A stable isotope (δ^2H) approach to deriving origins of harvested woodcock (*Scolopax rusticola*) taken in France. European Journal of Wildlife Research 59:881–892.

Hobson, K. A., S. L. Van Wilgenburg, L. I. Wassenaar, and K. Larson. 2012*b*. Linking hydrogen (δ^2H) isotopes in feathers and precipitation: sources of variance and consequences for assignment to isoscapes. PLOS One 7:e35137.

Hobson, K. A., and L. I. Wassenaar. 1997. Linking breeding and wintering grounds of neotropical migrant songbirds using stable hydrogen isotopic analysis of feathers. Oecologia 109:142–148.

Hobson, K. A., and L. I. Wassenaar. 2018. Tracking Animal Migration with Stable Isotopes. Second Edition. Academic Press, Cambridge, MA, USA.

Hobson, K. A., L. I. Wassenaar, and O. R. Taylor. 1999. Stable isotopes (δD and δ^{13}C) are geographic indicators of natal origins of monarch butterflies in eastern North America. Oecologia 120:397–404.

Hobson, K. A., M. B. Wunder, S. L. Van Wilgenburg, R. G. Clark, and L. I. Wassenaar. 2009*b*. A method for investigating population declines of migratory birds using stable isotopes: origins of harvested Lesser Scaup in North America. PLOS One 4:e7915.

Hobson, K., S. Van Wilgenburg, L. Wassenaar, R. Powell, C. Still, and J. Craine. 2012. A multi-isotope (δ^{13}C, δ^{15}N, δ^2H) feather isoscape to assign Afrotropical migrant birds to origins. Ecosphere 3:44.

Hobson, Keith A. 2008. Applying isotopic methods to tracking animal movements. Pages 45–78 *in* K. A. Hobson and L. I. Wassenaar, editors. Tracking Animal Migration with Stable Isotopes. First Edition. Academic Press, London, UK.

International Atomic Energy Agency and World Meteorological Organization. 2023. Global Network of Isotopes in Precipitation. The GNIP database. <https://nucleus.iaea.org/wiser>.

Kaimal, B., R. Johnson, and R. Hannigan. 2009. Distinguishing breeding populations of Mallards (*Anas platyrhynchos*) using trace elements. Journal of Geochemical Exploration 102:44–48.

Kelly, J. F., V. Atudorei, Z. D. Sharp, and D. M. Finch. 2002. Insights into Wilson's Warbler migration from analyses of hydrogen stable-isotope ratios. Oecologia 130:216–221.

Klimstra, J. D., and P. I. Padding. 2012. Harvest distribution and derivation of Atlantic flyway Canada Geese. Journal of Fish and Wildlife Management 3:43–55.

Knick, S. T., M. Leu, J. T. Rotenberry, S. E. Hanser, and K. A. Fesenmyer. 2014. Diffuse migratory connectivity in two species of shrubland birds: evidence from stable isotopes. Oecologia 174:595–608.

Koch, P. L., J. Heisinger, C. Moss, R. W. Carlson, M. L. Fogel, and A. K. Behrensmeyer. 1995. Isotopic tracking of change in diet and habitat use in African Elephants. Science 267:1340–1343.

Kucia, S. R., M. L. Schummer, J. W. Kusack, K. A. Hobson, and C. A. Nicolai. 2023. Origins of Mallards harvested in the Atlantic flyway of North America: implications for conservation and management. Avian Conservation and Ecology 18:10.

Lincoln, F. C. 1930. Calculating waterfowl abundance on the basis of banding returns. U.S. Department of Agriculture, Washington, DC, USA.

Lincoln, F. C. 1935. The waterfowl flyways of North America. U.S. Department of Agriculture, Washington, DC, USA.

López-Calderón, C., S. L. Van Wilgenburg, A. M. Roth, D. J. Flaspohler, and K. A. Hobson. 2019. An evaluation of isotopic (δ^2H) methods to provide estimates of avian breeding and natal dispersal. Ecosphere 10:e02663.

Lott, C. A., T. D. Meehan, and J. A. Heath. 2003. Estimating the latitudinal origins of migratory birds using hydrogen and sulfur stable isotopes in feathers: influence of marine prey base. Oecologia 134:505–510.

Lott, C. A., and J. P. Smith. 2006. A Geographic-Information-System approach to estimating the origin of migratory raptors in North America using stable hydrogen isotope ratios in feathers. The Auk 123:822–835.

Luukkonen, D. R., H. H. Prince, and R. C. Mykut. 2008. Movements and survival of molt migrant Canada Geese from southern Michigan. The Journal of Wildlife Management 72:449–462.

Ma, C., H. B. Vander Zanden, M. B. Wunder, and G. J. Bowen. 2020. assignR: an R package for isotope-based geographic assignment. Methods in Ecology and Evolution 11:996–1001.

Magozzi, S., C. P. Bataille, K. A. Hobson, M. B. Wunder, J. D. Howa, A. Contina, H. B. Vander Zanden, and G. J. Bowen. 2021. Calibration chain transformation improves the comparability of organic hydrogen and oxygen stable isotope data. Methods in Ecology and Evolution 12:732–747.

Marra, P. P., K. A. Hobson, and R. T. Holmes. 1998. Linking winter and summer events in a migratory bird by using stable-carbon isotopes. Science 282:1884–1886.

Meehan, T. D., J. T. Giermakowski, and P. M. Cryan. 2004. GIS-based model of stable hydrogen isotope ratios in North American growing-season precipitation for use in animal movement studies. Isotopes in Environmental and Health Studies 40:291–300.

Meehan, T., C. Lott, Z. Sharp, R. Smith, R. Rosenfield, A. Stewart, and R. Murphy. 2001. Using hydrogen isotope geochemistry to estimate the natal latitudes of immature Cooper's Hawks migrating through the Florida Keys. The Condor 103:11–20.

Meier-Augenstein, W., K. A. Hobson, and L. I. Wassenaar. 2013. Critique: measuring hydrogen stable isotope abundance of proteins to infer origins of wildlife, food and people. Bioanalysis 5:751–767.

van der Merwe, N. J., J. A. Lee-Thorp, J. F. Thackeray, A. Hall-Martin, F. J. Kruger, H. Coetzee, R. H. V. Bell, and M. Lindeque. 1990. Source-area determination of elephant ivory by isotopic analysis. Nature 346:744–746.

Miller, R. F., P. Fritz, and A. V. Morgan. 1988. Climatic implications of D/H ratios in beetle chitin. Palaeogeography, Palaeoclimatology, Palaeoecology 66:277–288.

Mowbray, T. B., C. R. Ely, J. S. Sedinger, and R. E. Trost. 2020. Canada Goose (*Branta canadensis*), version 1.0. P. G. Rodewald, editor. Birds of the World. Cornell Lab of Ornithology, Ithaca, NY, USA. <https://doi.org/10.2173/bow.cangoo.01>.

Munro, R. E., and C. F. Kimball. 1982. Population ecology of the mallard: VII. Distribution and derivation of the harvest. Resource Publication, Report, Washington, DC, USA. <http://pubs.er.usgs.gov/publication/5230180>.

Munroe, S. E. M., G. R. Guerin, F. A. McInerney, I. Martín-Forés, N. Welti, M. Farrell, R. Atkins, and B. Sparrow. 2022. A vegetation carbon isoscape for Australia built by combining continental-scale field surveys with remote sensing. Landscape Ecology 37:1987–2006.

Nichols, J. D., M. C. Runge, F. A. Johnson, and B. K. Williams. 2007. Adaptive harvest management of North American waterfowl populations: a brief history and future prospects. Journal of Ornithology 148:343–349.

Nordell, C. J., S. Haché, E. M. Bayne, P. Sólymos, K. R. Foster, C. M. Godwin, R. Krikun, P. Pyle, and K. A. Hobson. 2016. Within-site variation in feather stable

hydrogen isotope (δ^2H_f) values of boreal songbirds: implications for assignment to molt origin. PLOS One 11:e0163957.

Norris, D. R., P. P. Marra, G. J. Bowen, L. M. Ratcliffe, J. A. Royle, and T. K. Kyser. 2006. Migratory connectivity of a widely distributed songbird, the American Redstart (*Setophaga ruticilla*). Ornithological Monographs 61:14–28.

North American Bird Conservation Initiative. 2022. The State of the Birds, United States of America, 2022. North American Bird Conservation Initiative. <StateoftheBirds.org>. Accessed 16 Apr 2024.

North American Waterfowl Management Plan. 2018. 2018 North American Waterfowl Management Plan (NAWMP) update: connecting people, waterfowl, and wetlands. <https://nawmp.org/timeline/2018-update >

Ofukany, A. F. A., K. A. Hobson, and L. I. Wassenaar. 2012. Connecting breeding and wintering habitats of migratory piscivorous birds: implications for tracking contaminants (Hg) using multiple stable isotopes. Environmental Science & Technology 46:3263–3272.

Ouin, A., P. Menozzi, M. Coulon, A. J. Hamilton, J. P. Sarthou, N. Tsafack, A. Vialatte, and S. Ponsard. 2011. Can deuterium stable isotope values be used to assign the geographic origin of an auxiliary hoverfly in south-western France? Rapid Communications in Mass Spectrometry 25:2793–2798.

Palumbo, M. D., J. W. Kusack, D. C. Tozer, S. W. Meyer, C. Roy, and K. A. Hobson. 2020. Source areas of Blue-winged Teal harvested in Ontario and Prairie Canada based on stable isotopes: implications for sustainable management. Journal of Field Ornithology 91:64–76.

Palumbo, M. D., D. C. Tozer, and K. A. Hobson. 2019. Origins of harvested Mallards from Lake St. Clair, Ontario: a stable isotope approach. Avian Conservation and Ecology 14:3.

Parejo, M., J. G. Navedo, J. S. Gutiérrez, J. M. Abad-Gómez, A. Villegas, C. Corbacho, J. M. Sánchez-Guzmán, and J. A. Masero. 2015. Geographical origin of dabbling ducks wintering in Iberia: sex differences and implications for pair formation. Ibis 157:536–544.

Paxton, K. L., C. Van Riper III, T. C. Theimer, and E. H. Paxton. 2007. Spatial and temporal migration patterns of Wilson's Warbler (*Wilsonia Pusilla*) in the southwest as revealed by stable isotopes. The Auk 124:162–175.

Petersen, C. G. J. 1896. The yearly immigration of young plaice in the Limfjord from the German sea. Report of the Danish Biological Station 6:1–48.

Popa-Lisseanu, A. G., K. Sörgel, A. Luckner, L. I. Wassenaar, C. Ibáñez, S. Kramer-Schadt, M. Ciechanowski, T. Görföl, I. Niermann, G. Beuneux, R. W. Mysłajek, J. Juste, J. Fonderflick, D. H. Kelm, and C. C. Voigt. 2012. A triple-isotope approach to predict the breeding origins of European bats. PLOS One 7:e30388.

Powell, L. A., and G. A. Klaasen. 1998. Distribution and derivation of Mallard band recoveries from the upper Mississippi River, 1961-1989. North American Bird Bander 23:1–12.

Powell, R. L., E.-H. Yoo, and C. J. Still. 2012. Vegetation and soil carbon-13 isoscapes for South America: integrating remote sensing and ecosystem isotope measurements. Ecosphere 3:art109.

Procházka, P., S. L. Van Wilgenburg, J. M. Neto, R. Yosef, and K. A. Hobson. 2013. Using stable hydrogen isotopes (δ^2H) and ring recoveries to trace natal origins in a Eurasian passerine with a migratory divide. Journal of Avian Biology 44:541–550.

Pyle, P. 2005. Molts and plumages of ducks (*Anatinae*). Waterbirds 28:208–219.

Raftovich, R., K. Fleming, S. Chandler, and C. Cain. 2023. Migratory bird hunting activity and harvest during the 2021-22 and 2022-23 hunting seasons. U.S. Fish and Wildlife Service, Laurel, MD, USA.

Raveling, D. G., and M. E. Heitmeyer. 1989. Relationships of population size and recruitment of pintails to habitat conditions and harvest. The Journal of Wildlife Management 1088–1103.

Raymond, L., A. Vialatte, and M. Plantegenest. 2014. Combination of morphometric and isotopic tools for studying spring migration dynamics in *Episyrphus balteatus*. Ecosphere 5:art88.

Reese, J., C. Viverette, C. M. Tonra, N. J. Bayly, T. J. Boves, E. Johnson, M. Johnson, P. Marra, E. M. Ames, A. Caguazango, M. DeSaix, A. Matthews, A. Molina, K. Percy, M. C. Slevin, and L. Bulluck. 2019. Using stable isotopes to estimate migratory connectivity for a patchily distributed, wetland-associated Neotropical migrant. The Condor 121:duz052.

Reich, M. S., D. T. T. Flockhart, D. R. Norris, L. Hu, and C. P. Bataille. 2021. Continuous-surface geographic assignment of migratory animals using strontium isotopes: a case study with monarch butterflies. Methods in Ecology and Evolution 12:2445–2457.

Roberts, A, J. Hostetler, J. Stiller, P. K. Devers, W. Link, and G. S. Boomer. 2022. Eastern Mallard Adaptive Harvest Management Strategy, 2022. U.S. Fish and Wildlife Service, Laurel, MD, USA.

Roberts, A., A. L. Scarpignato, A. Huysman, J. A. Hostetler, and E. B. Cohen. 2022. Migratory connectivity of North American waterfowl across administrative flyways. Ecological Applications 33:e2788.

Rosenberg, K. V., A. M. Dokter, P. J. Blancher, J. R. Sauer, A. C. Smith, P. A. Smith, J. C. Stanton, A. Panjabi, L. Helft, M. Parr, and P. P. Marra. 2019. Decline of the North American avifauna. Science 366:120.

Royle, J. A., and D. R. Rubenstein. 2004. The role of species abundance in determining breeding origins of migratory birds with stable isotopes. Ecological Applications 14:1780–1788.

Rozanski, K., L. Araguás-Araguás, and R. Gonfiantini. 1993. Isotopic patterns in modern global precipitation. Climate change in continental isotopic records 78:1–36.

Ruegg, K. C., E. C. Anderson, R. J. Harrigan, K. L. Paxton, J. F. Kelly, F. Moore, and T. B. Smith. 2017. Genetic assignment with isotopes and habitat suitability (gaiah), a migratory bird case study. Methods in Ecology and Evolution 8:1241–1252.

Rundel, C. W., M. B. Wunder, A. H. Alvarado, K. C. Ruegg, R. Harrigan, A. Schuh, J. F. Kelly, R. B. Siegel, D. F. DeSante, and T. B. Smith. 2013. Novel statistical methods for integrating genetic and stable isotope data to infer individual-level migratory connectivity. Molecular Ecology 22:4163–4176.

Salomonsen, F. 1968. The moult migration. Wildfowl 19:5–24.

Schummer, M. L., J. Simpson, B. Shirkey, S. R. Kucia, P. Lavretsky, and D. C. Tozer. 2023. Population genetics and geographic origins of mallards harvested in northwestern Ohio. PLOS One 18:e0282874.

Sedinger, J. S., and R. T. Alisauskas. 2014. Cross-seasonal effects and the dynamics of waterfowl populations. Wildfowl Special Issue No. 4:277–304.

Sedinger, J. S., and M. P. Herzog. 2012. Harvest and dynamics of duck populations. The Journal of Wildlife Management 76:1108–1116.

Sedinger, J. S., J. L. Schamber, D. H. Ward, C. A. Nicolai, and B. Conant. 2011. Carryover effects associated with winter location affect fitness, social status, and population dynamics in a long-distance migrant. The American Naturalist 178:E110–E123.

Seifert, N., M. Haase, S. L. Van Wilgenburg, C. C. Voigt, and A. Schmitz Ornés. 2016. Complex migration and breeding strategies in an elusive bird species illuminated by genetic and isotopic markers. Journal of Avian Biology 47:275–287.

Siegenthaler, U., and H. Oeschger. 1980. Correlation of ^{18}O in precipitation with temperature and altitude. Nature 285:314–317.

Sharp, C. M., K. F. Abraham, K. A. Hobson, and G. Burness. 2013. Allocation of nutrients to reproduction at high latitudes: Insights from two species of sympatrically nesting geese. The Auk 130:171–179.

Sheaffer, S. E., R. A. Malecki, B. L. Swift, J. Dunn, and K. Scribner. 2007. Management implications of molt migration by the Atlantic flyway resident population of Canada geese, *Branta canadensis*. The Canadian Field-Naturalist 121:313–320.

Smith, A. C., T. Villeneuve, and M. Gendron. 2022. Hierarchical Bayesian integrated model for estimating migratory bird harvest in Canada. The Journal of Wildlife Management 86:e22160.

Sofaer, H. R., S. K. Skagen, J. J. Barsugli, B. S. Rashford, G. C. Reese, J. A. Hoeting, A. W. Wood, and B. R. Noon. 2016. Projected wetland densities under climate change: habitat loss but little geographic shift in conservation strategy. Ecological Applications 26:1677–1692.

Solovyeva, D., K. A. Hobson, N. Kharitonova, J. Newton, J. W. Fox, V. Afansyev, and A. D. Fox. 2016. Combining stable hydrogen (δ^2H) isotopes and geolocation to assign Scaly-sided Mergansers to moult river catchments. Journal of Ornithology 157:663–669.

Soto, D., G. Koehler, L. Wassenaar, and K. Hobson. 2017. Determination of stable hydrogen isotopic compositions of complex organic materials: contrasting the role of exchangeable hydrogen and residual moisture. Rapid Communications in Mass Spectrometry 31:1193–1203.

Stewart, R. E., A. D. Geis, and C. D. Evans. 1958. Distribution of populations and hunting kill of the canvasback. The Journal of Wildlife Management 22:333–370.

Still, C. J., and R. L. Powell. 2010. Continental-scale distributions of vegetation stable carbon isotope ratios. Pages 179–193 *in* J. B. West, G. J. Bowen, T. E. Dawson, and K. P. Tu, editors. Isoscapes: Understanding movement, pattern, and process on Earth through isotope mapping. Springer Netherlands, Dordrecht, NL.

Studds, C. E., K. P. McFarland, Y. Aubry, C. C. Rimmer, K. A. Hobson, P. P. Marra, and L. I. Wassenaar. 2012. Stable-hydrogen isotope measures of natal dispersal reflect observed population declines in a threatened migratory songbird. Diversity and Distributions 18:919–930.

Stutchbury, B. J. M., S. A. Tarof, T. Done, E. Gow, P. M. Kramer, J. Tautin, J. W. Fox, and V. Afanasyev. 2009. Tracking long-distance songbird migration by using geolocators. Science 323:896–896.

Sullins, D. S., W. C. Conway, D. A. Haukos, K. A. Hobson, L. I. Wassenaar, C. E. Comer, and I.-K. Hung. 2016. American woodcock migratory connectivity as indicated by hydrogen isotopes. The Journal of Wildlife Management 80:510–526.

Szymanski, M. L., and J. A. Dubovsky. 2013. Distribution and derivation of the Blue-winged Teal (*Anas discors*) harvest, 1970-2003. United States Department of the Interior, Fish and Wildlife Service, Washington, DC, USA.

Tautin, J. 2005. Frederick C. Lincoln and the formation of the North American bird banding program. US Forest Service General Technical Report PSW-GTR-191. US Forest Service, Washington, DC, USA.

Taylor, H. P. 1974. The application of oxygen and hydrogen isotope studies to problems of hydrothermal alteration and ore deposition. Economic Geology 69:843–883.

Taylor, P. D., T. Crewe, S. Mackenzie, D. Lepage, Y. Aubry, Z. Crysler, G. Finney, C. Francis, C. Guglielmo, D. Hamilton, R. Holberton, P. Loring, G. Mitchell, R. Norris, J. Paquet, R. Ronconi, J. Smetzer, P. Smith, L. Welch, and B. Woodworth. 2017. The Motus Wildlife Tracking System: a collaborative research network to enhance the understanding of wildlife movement. Avian Conservation and Ecology 12:8.

Terzer, S., L. I. Wassenaar, L. J. Araguás-Araguás, and P. K. Aggarwal. 2013. Global isoscapes for δ^{18}O and δ^2H in precipitation: improved prediction using

regionalized climatic regression models. Hydrology and Earth System Sciences 17:4713–4728.

Terzer-Wassmuth, S., L. I. Wassenaar, J. M. Welker, and L. J. Araguás. 2021. Improved high-resolution global and regionalized isoscapes of δ^{18}O, δ^2H, and d-excess in precipitation. Hydrological Processes 35:e14254.

Thompson, C., C. A. Mendoza, and K. J. Devito. 2017. Potential influence of climate change on ecosystems within the Boreal Plains of Alberta. Hydrological Processes 31:2110–2124.

Tonra, C. M., C. Both, and P. P. Marra. 2015. Incorporating site and year-specific deuterium ratios (δ^2H) from precipitation into geographic assignments of a migratory bird. Journal of Avian Biology 46:266–274.

U.S. Fish and Wildlife Service. 2021. Adaptive Harvest Management: 2022 hunting season. U.S. Department of the Interior, Washington, DC, USA.

U.S. Fish and Wildlife Service. 2022. Waterfowl population status, 2022. U.S. Department of the Interior, Washington, DC, USA.

U.S. Fish and Wildlife Service. 2023. Adaptive Harvest Management: 2024 Hunting Season. U.S. Department of the Interior, Washington, DC, USA.

Vander Zanden, H. B., M. B. Wunder, K. A. Hobson, S. L. Van Wilgenburg, L. I. Wassenaar, J. M. Welker, and G. J. Bowen. 2014. Contrasting assignment of migratory organisms to geographic origins using long-term versus year-specific precipitation isotope maps. Methods in Ecology and Evolution 5:891–900.

Vogel, J. C., B. Eglington, and J. M. Auret. 1990. Isotope fingerprints in elephant bone and ivory. Nature 346:747–749.

Wassenaar, L. I., and K. A. Hobson. 2000. Stable-carbon and hydrogen isotope ratios reveal breeding origins of Red-winged Blackbirds. Ecological Applications 10:911–916.

Wassenaar, L. I., and K. A. Hobson. 2003. Comparative equilibration and online technique for determination of non-exchangeable hydrogen of keratins for use in animal migration studies. Isotopes in Environmental and Health Studies 39:211–217.

Wassenaar, L. I., and K. A. Hobson. 2006. Stable-hydrogen isotope heterogeneity in keratinous materials: mass spectrometry and migratory wildlife tissue subsampling strategies. Rapid Communications in Mass Spectrometry 20:2505–2510.

Webster, M. S., P. P. Marra, S. M. Haig, S. Bensch, and R. T. Holmes. 2002. Links between worlds: unraveling migratory connectivity. Trends in Ecology & Evolution 17:76–83.

Werner, S. J., K. A. Hobson, S. L. Van Wilgenburg, and J. W. Fischer. 2016. Multi-isotopic (δ^2H, δ^{13}C, δ^{15}N) tracing of molt origin for Red-winged Blackbirds associated with agro-ecosystems. PLOS One 11:e0165996.

Wommack, E. A., L. C. Marrack, S. Mambelli, J. M. Hull, and T. E. Dawson. 2020. Using oxygen and hydrogen stable isotopes to track the migratory movement of Sharp-shinned Hawks (*Accipiter striatus*) along Western Flyways of North America. PLOS One 15:e0226318.

Wunder, M. B. 2007. Geographic structure and dynamics in Mountain Plover. PhD Dissertation. Colorado State University, Fort Collins, CO.

Wunder, M. B. 2012. Determining geographic patterns of migration and dispersal using stable isotopes in keratins. Journal of Mammalogy 93:360–367.

Yerkes, T., K. A. Hobson, L. I. Wassenaar, R. Macleod, and J. M. Coluccy. 2008. Stable isotopes (δD, δ^{13}C, δ^{15}N) reveal associations among geographic location and condition of Alaskan Northern Pintails. The Journal of Wildlife Management 72:715–725.

Zhu, Q., K. A. Hobson, Q. Zhao, Y. Zhou, I. Damba, N. Batbayar, T. Natsagdorj, B. Davaasuren, A. Antonov, J. Guan, X. Wang, L. Fang, L. Cao, and A. David Fox. 2020. Migratory connectivity of Swan Geese based on species' distribution models, feather stable isotope assignment and satellite tracking. Diversity and Distributions 26:944–957.

Zuwerink, D. A. 2001. Changes in the derivation of mallard harvests from the northern US and Canada, 1966-1998. MSc Thesis. Ohio State University, Columbus, OH, USA.

<center>Chapter 2</center>

2 Origins of harvested American black ducks: stable isotopes support the flyover hypothesis

A version of this chapter has been published in the Journal of Wildlife Management through permissions provided in Appendix E. Citation:

Kusack, **J. W.**, D. C. Tozer, M. L. Schummer, and K. A. Hobson. 2022. Origins of harvested American black ducks: stable isotopes support the flyover hypothesis. The Journal of Wildlife Management 87:e22324.

2.1 Introduction

Conservation and management of migratory species is more effective when based on detailed knowledge of connectivity between breeding, stopover, and non-breeding areas. For game species, identifying linkages between locations where individuals are harvested and their natal origins (for juveniles) or breeding sites (for adults) is especially important when preparing adaptive harvest management strategies (Nichols et al. 2007). Current understanding of where harvested individuals originate is based primarily on mark-recapture approaches using preseason (i.e., before the fall harvest period) banding (Geis et al. 1971, Munro and Kimball 1982, Szymanski and Dubovsky 2013). This method assumes that the banded portion of a population is representative of the population of interest with respect to migration, mortality, and movement (Munro and Kimball 1982). Key demographic data are often missing if a significant proportion of hunted individuals nest or are produced in remote areas where banding effort is minimal because of logistical and financial difficulties in reaching these areas. Naturally occurring stable isotopes within tissues of harvested individuals can augment traditional banding efforts, as they are a reliable marker of geographic origin for migratory individuals (Hobson et al. 2009, Ashley et al. 2010, Asante et al. 2017). Stable-isotope methods avoid banding-effort biases associated with tagging because these intrinsic markers require no initial capture, especially in logistically difficult areas (Hobson and Wassenaar 2018).

In North America, predictable patterns of stable-hydrogen isotopes within annual or growing-season precipitation (δ^2H_p) occur because of heavy-isotope depletion from the

<center>36</center>

southeast to the northwest (Bowen et al. 2005). Waterfowl exhibit a synchronous moult where all flight feathers are replaced simultaneously at a single location. Thus, the stable-isotopic value of flight feathers is directly related to the weighted-average stable-isotopic value of environmental waters at the moulting site for adults or the natal site for juveniles (Clark et al. 2006, 2009; van Dijk et al. 2014). These stable-isotopic values can then be integrated with a prior probability of origin based on banding data in Bayesian-based models to further refine estimates of likely origins (Wunder 2012, Van Wilgenburg and Hobson 2011, Asante et al. 2017, Palumbo et al. 2019).

The American Black Duck (*Anas rubripes*; black duck) is a species of conservation and management concern that breeds across eastern Canada and the northeastern United States and overwinters along the Atlantic coast of North America (Longcore et al. 2020). According to the Midwinter Waterfowl Inventory, black duck populations declined by approximately 50 % between 1955 and the mid-1980s (Rusch et al. 1989) but have since stabilized at a lower population level (Ringelman and Williams 2018). Circumstantial evidence suggests that several varied and likely multi-faceted factors have contributed to the population decline (Conroy et al. 2002, Ringelman and Williams 2018), including overharvest (Francis et al. 1998, Longcore et al. 2000), competition and hybridization with Mallard (*Anas platyrhynchos*; Ankney et al. 1987, 1989), and loss or degradation of breeding and wintering habitat. Current adaptive harvest management of black ducks assumes a single population (U.S. Fish and Wildlife Service [USFWS] 2021), despite evidence of different stocks within the breeding population (Geis et al. 1971, Pendleton and Sauer 1992). These stocks may relate to differing autumn movement patterns of birds between the Mississippi and Atlantic flyways and between Canada and the United States (Lavretsky et al. 2014). Further, data from the North American breeding bird survey (BBS) have shown differential population trends across the black duck breeding range, especially in the Atlantic provinces of Canada (New Brunswick, Newfoundland and Labrador, Nova Scotia, and Prince Edward Island) where populations were stable while Ontario and Quebec showed pronounced declines (Conroy et al. 2002). Demographic information for specific population stocks would enhance the management of this species, as hunting effort and bag limits could be directed more effectively toward specific production areas or management interests (Black Duck Joint Venture 2018).

The adaptive harvest management model for black ducks relies on metrics of breeding-ground abundance, age-specific and sex-specific harvest rates and survival rates, and the fall (autumn) age ratio (number of young produced per adult). This age ratio is an estimate of preseason productivity, which uses information from leg-band returns from the previous fall hunt and wings collected during harvest. Estimates for the fall age ratio differ depending on whether they are derived from harvest data from Canada or the United States, suggesting that black ducks harvested within those countries, or in different regions within them, may represent different stocks (Black Duck Joint Venture 2018). What is not clear is which regions are driving this difference. Black ducks currently breed in Atlantic Canada, northeastern United States, northern Ontario, and northern Quebec. Atlantic Canada and the northeastern United States are the only breeding regions that overlap with high-density human populations and may be more heavily harvested near breeding locations. This led to the adoption of the flyover hypothesis, which postulates that black ducks produced in the Boreal Softwood and Taiga Shield region of northeastern Canada are less susceptible to harvest by hunters in Atlantic Canada and the northeastern United States, areas that primarily harvest birds produced relatively close to harvest sites (Black Duck Joint Venture 2018). For hunters in other regions of the United States and Canada, I hypothesize that they mainly harvest birds from the Boreal Softwood and Taiga Shield, where the highest density of black ducks breed (Baldassarre 2014).
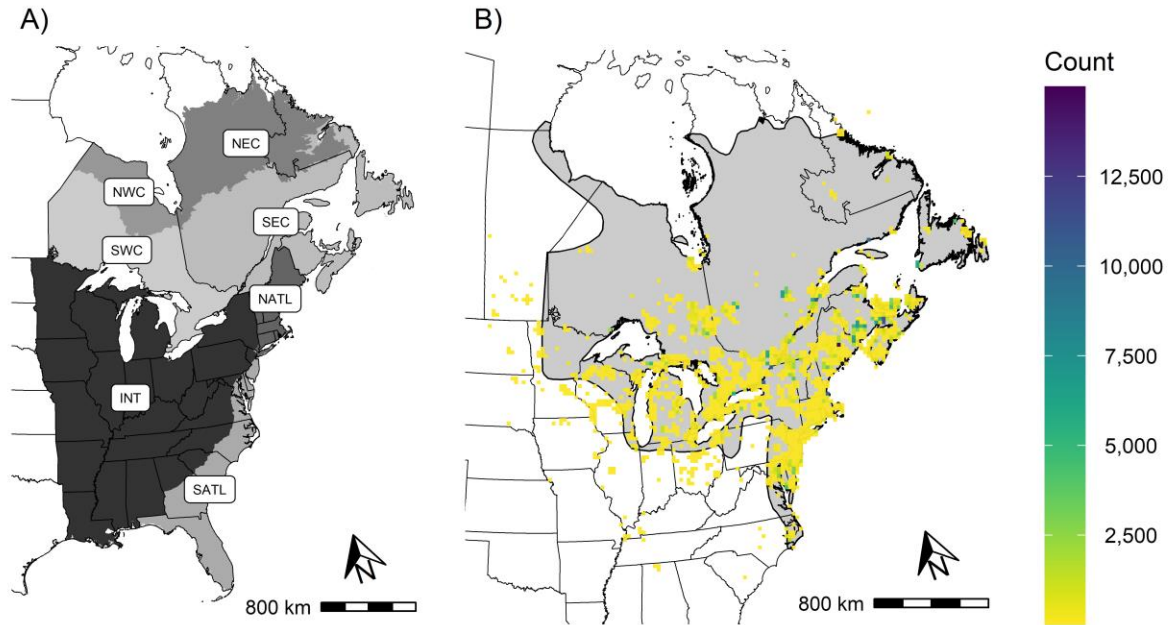
Figure 2.1 A) Black duck conservation regions and B) count of juvenile (i.e., local, juvenile, hatch-year) black ducks banded between July and September. A) The black duck conservation regions (northwestern Canada [NWC], northeastern Canada [NEC], southwestern Canada [SWC], southeastern Canada [SEC], interior United States [INT], north Atlantic United States [NATL], south Atlantic United States [SATL]), as defined by the Black Duck Joint Venture (Robinson et al. 2016) and B) count of juvenile (i.e., local, juvenile, hatch year) black ducks banded between July and September (1913–2020), summarized by 1° blocks and overlaid on the black duck breeding range (light grey; Baldassarre 2014). I obtained summary banding data from the United States Geological Survey's Bird Banding Laboratory (U.S. Geological Survey 2021).

Current banding effort is focused largely on the southern, road-accessible portion of the breeding range (Figure 2.1B); therefore, northern-bred ducks are likely underrepresented in the preseason banding data and may experience differential but undocumented harvest vulnerability and productivity. Previous evidence for the flyover hypothesis was provided by the isotopic study of Ashley et al. (2010). They showed that juvenile black ducks harvested in Atlantic Canada exhibited a more southern origin compared to those harvested in Ontario and Quebec (west of 70° W), which were likely from areas far to the north, in the Boreal Softwood Shield, Hudson Plains, and Taiga Shield, relatively more distant from where they were harvested (Ashley et al. 2010). Roy et al. (2015) also showed that birds banded in the Canadian Maritime provinces, including along the Saint Lawrence River, were more likely to be harvested within Canada. To date, no studies have isotopically examined black ducks harvested within the United States, nor have they included adults.

My objective was to test the flyover hypothesis by determining regional and temporal differences in the natal and moult origins of black ducks harvested across their range in eastern Canada and the United States. First, to better understand contemporary population trends within the updated black duck conservation regions, I repeated the analysis of Conroy et al. (2002) using the North American BBS data. Next, I investigated which harvest regions were driving differences in the fall age ratios between Canada and the United States. We expected Atlantic Canada to be the major contributor to the differences in age ratio seen between the United States and Canada. I then used a likelihood-based assignment method relying on feather stable-hydrogen isotopes (δ^2H) to determine the natal or feather moult origin of individuals harvested across their breeding range in eastern Canada and the United States. I examined three non-mutually exclusive predictions that natal and feather moult origin differs for Atlantic Canada and the northeastern United States black duck conservation region, compared to the other harvest regions, because of 1) timing, where I expected black ducks harvested earlier in the season to show more southern origin compared to those harvested later; 2) local peaks in abundance of migrants, where I expected black ducks to show more southern origin if harvested before the peak in southbound migrants and more northerly origin if harvested after the peak in migrants; and 3) regional differences, where I expected black ducks

harvested in Atlantic Canada and the north Atlantic United States black duck conservation region to show more southern origin regardless of timing and those harvested elsewhere to show more northerly origin. I examined regional differences between the Black Duck Joint Venture conservation regions (Figure 2.1A) and investigated age and sex effects on natal and moult origin, to account for behavioural differences between juvenile and adult black ducks. In particular, I wanted to control for differences in origin driven by moult migration, often exhibited by adult males (Longcore et al. 2020). Lastly, I used stable-carbon isotope values (δ^{13}C) within feathers to isolate individuals that moulted in marine or brackish environments (Hobson and Sealy 1991), as the δ^2H values of feathers grown in marine systems cannot be associated with terrestrial geographical regions based on the modeled terrestrial precipitation gradient (Ashley et al. 2010, Reed et al. 2018).

2.2 Study area

I conducted the study across eastern Canada and the United States, during the fall harvest period (Sep–Feb; post-breeding, fall migratory, and overwintering periods), wherever black ducks are harvested, which covers much of the Atlantic and Mississippi flyways for the United States and Canada (all states east of ~95° W; area = 5,970,000 km^2). The overwintering range for black ducks spans from the southern portion of their breeding range (i.e., Great Lakes, St. Lawrence, and Atlantic Canada) down to the Gulf of Mexico (i.e., Mississippi, Alabama, and northern Florida). Each year, > 5 million individuals from over 20 species of waterfowl are harvested in the Atlantic (μ ± 95 % CI = 1,361,600 ± 7 % in 2020; Raftovich et al. 2021) and Mississippi flyways (4,408,800 ± 5 % in 2020; Raftovich et al. 2021), including Wood Duck (*Aix sponsa*), Mallard, Green-winged Teal (*Anas crecca*), Ring-necked Duck (*Aythya collaris*), and Bufflehead (*Bucephala albeola*). Within this area, I delineated harvest regions by the Black Duck Joint Venture conservation regions (Figure 2.1A): southwestern Canada (SWC), southeastern Canada (SEC), interior United States (INT), north Atlantic United States (NATL), south Atlantic United States (SATL), and separating southeastern Canada (Quebec [QC], Atlantic Canada [ATL]), based on differences highlighted by Ashley et al. (2010) and Roy et al. (2015). Canadian regions were named relative to the known range of black ducks, not the

true portion of Canada (e.g., southwestern Canada is the part of Canada that is in the southwestern part of the black duck range; Robinson et al. 2016).

My study area covers the majority of the eastern United States and Canada; therefore, I summarized the habitat composition of the black duck conservation areas using Bird Conservation Regions (BCRs; https://nabci-us.org/resources/bird-conservation-regions/, accessed 8 Aug 2022). For each black duck conservation region, I reported all overlapping BCRs and the percent area covered by that BCR within the conservation area: SWC = Boreal Hardwood Transition (BCR 12; 27.3 %), Boreal Softwood Shield (BCR 8; 62.1 %), and Lower Great Lakes–St. Lawrence Plain (BCR 13; 10.6 %); SEC = Atlantic Northern Forests (BCR 14; 18.6 %), Boreal Hardwood Transition (BCR 12; 16.2 %), Boreal Softwood Shield (BCR 8; 62.6 %), and Lower Great Lakes–St. Lawrence Plain (BCR 13; 2.6 %), INT = Appalachian Mountains (BCR 28; 16.7 %), Atlantic Northern Forests (BCR 14; 1.2 %), Boreal Hardwood Transition (BCR 12; 9.6 %), Central Hardwoods (BCR 24; 11.5 %), Eastern Tallgrass Prairie (BCR 22; 16.9 %), Gulf Coastal Prairie (BCR 37; 1 %), Lower Great Lakes–St. Lawrence Plain (BCR 13; 3.7 %), Mississippi Alluvial Valley (BCR 27; 4.1 %), Piedmont (BCR 29; 7.4 %), Prairie Hardwood Transition (BCR 23; 10.9 %), Prairie Potholes (BCR 11; 4.4 %), Southeastern Coastal Plain (BCR 27; 8.2 %), and West Gulf Coastal Plain–Ouachitas (BCR 25; 4.2 %); NATL = Atlantic Northern Forests (BCR 14; 76.5 %) and New England–MidAtlantic Coast (BCR 30; 23.5 %); SATL = New England–MidAtlantic Coast (BCR 30; 12.3 %), Peninsular Florida (BCR 31; 22.4 %), and Southeastern Coastal Plain (BCR 27; 65.3 %).

The black duck breeding range (area = 3,600,000 km^2) covers seven BCRs within Canada and the United States: Taiga Shield and Hudson Plain (BCR 7), Boreal Softwood Shield (BCR 8), Boreal Hardwood Transition (BCR 12), Lower Great Lakes–St. Lawrence Plain (BCR 13), Atlantic Northern Forests (BCR 14), Prairie Hardwood Transition (BCR 23), and New England–MidAtlantic Coasts (BCR 30). Much of the core black duck breeding area occurs within the Canadian Shield and boreal forest in the northern Quebec and Atlantic Canada (BCRs 7, 8, 12, 14; Baldassarre 2014). In the Taiga Shield and Hudson Plain, coastal marshes and tidal flats line the coast and the northern forests are dominated by black spruce (*Picea mariana*) and jack pine (*Pinus banksiana*) with alder (*Alnus* spp.),

tamarack (*Larix laricina*), and willow (*Salix* spp.) fens and bogs (Ecological Stratification Working Group 1995). In the Boreal Softwood Shield and Boreal Hardwood Transition, which together makeup the Boreal Shield Ecozone, northern forests are mainly coniferous, dominated by balsam fir (*Abies balsamea*), tamarack, white spruce (*Picea glauca*), and black spruce (Ecological Stratification Working Group 1995). In the hardwood transition zone to the south, broadleaf trees are more common, including white birch (*Betula papyrifera*), trembling aspen (*Populus tremuloides*), and balsam poplar (*P. balsamifera*), with red pine (*Pinus resinosa*) and white pine (*P. strobus*; Ecological Stratification Working Group 1995). South of the Canadian shield, the Atlantic Northern Forests are a mixed conifer-deciduous forest dominated by balsam fir, sugar maple (*Acer saccharum*), yellow birch (*Betula alleghaniensis*), and red spruce (*Picea rubens*), although many boreal species are still present (Ecological Stratification Working Group 1995). In general, the Canadian Shield is characterized by vast forest and peat-covered lowlands dotted with an abundance of freshwater bodies (i.e., lakes, rivers, wetlands). Nesting habitats for black ducks are diverse, with the majority of pairs nesting in freshwater systems (e.g., beaver ponds, wooded wetlands, bogs, shallow lakes), although some coastal pairs nest in brackish or salt marshes (Longcore et al. 2020). Other waterfowl species reported to breed in this area and occupy the same waterbodies include Bufflehead, Common Goldeneye (*Bucephala clangula*), Green-winged Teal, Greater Scaup (*Aythya marila*), Lesser Scaup (*A. affinis*), Mallard, and Ring-necked Duck (Baldassarre 2014, Schummer et al. 2018, Roberts et al. 2020).

2.3   Methods

I performed all statistics, geospatial data manipulation, and visualizations in the R statistical environment (version 4.1.1, R Core Team 2021) within RStudio (version 1.4.1717, RStudio Team 2021) using the raster (version 3.4-13, Hijmans 2020), sf (version 1.0-3, Pebesma 2018), and sp (version 1.4-5, Pebesma and Bivand 2005) packages.

2.3.1   Breeding bird survey trends

I determined regional indices of black duck abundance using the North American BBS data (1966–2019; Pardieck et al. 2020) analyzed using hierarchical Bayesian analysis within the bbsBayes package (version 2.3.8.2020, Edwards and Smith 2021). I used a general additive model with a random year effect, the current model used by the Canadian Wildlife Service (Edwards and Smith 2021). Otherwise, I used the default model parameters (e.g., burn-in = 10,000, chains = 3, iterations = 20,000, thinning = 10) with a heavy-tailed t-distribution for the extra-Poisson error distribution, as suggested by Edwards and Smith (2021). Only black duck conservation regions where enough survey routes were available could be modeled (i.e., ≥ 3 routes with black duck observations; ≥ 3 years with non-zero observations on ≥ 1 route). From these indices, I calculated region-specific population trends for southwestern Canada, Quebec, Atlantic Canada, interior United States, north Atlantic United States, and south Atlantic United States.

2.3.2   Fall age ratio

I analyzed differences in region-specific age ratios for harvested black ducks using banding data and harvest data. For age ratios based on band returns (B_j/B_a), I determined the number of preseason (Jul–Sep) banded adults (i.e., after hatch-year or older) and juveniles (i.e., local, juvenile, hatch-year) that were harvested in a specified region within a given year during the harvest season (Sep–Feb), then divided the number of banded juveniles that were harvested (B_j) by the number of banded adults that were harvested (B_a). I obtained banding data from the United States Geological Survey's Bird Banding Laboratory (U.S. Geological Survey 2021). For Canadian age ratios based on harvest data (W_j/W_a), I compiled data available online from the National Harvest Survey website (Gendron and Smith 2019), again dividing the number of juveniles that were harvested (W_j) by the number of adults that were harvested (W_a). For the United States harvest data, I extracted harvest age ratios directly from the yearly USFWS Migratory Bird Hunting Activity and Harvest reports (Raftovich et al. 2021). These country-wide harvest age ratios for the United States have been calculated by weighting the ratio from each state in proportion to the estimated harvest within that state compared to the overall harvest (Raftovich et al. 2021). I examined annual data between 2000–18, as more recent data

were not publicly available from the Canadian Harvest Survey (Gendron and Smith 2019). Lastly, fall age ratios were then derived as the ratio of these two ratios:

$$R = \frac{\dfrac{W_j}{W_a}}{\dfrac{B_j}{B_a}}$$

I first calculated age ratios by province or state of harvest (except for U.S. harvest ratios) using simple arithmetic counts. Following the Migratory Bird Hunting Activity and Harvest reports, I calculated age ratios for each country and region (i.e., Atlantic Canada) by weighting the age ratio of each province or state by the proportion of the estimated harvest for that province or state compared to the region or country of interest, using harvest estimates from the National Harvest Survey (Gendron and Smith 2019) and Waterfowl Harvest Survey (Raftovich et al. 2021). I applied this weighting to both banding and harvest age ratios. For regional comparisons, I stratified by province and state rather than black duck conservation regions because harvest survey results are not summarized by the same geographic boundaries. I used simple arithmetic counts to determine age ratios rather than hierarchical Bayesian models, which the National Harvest Survey will use for future estimates (Smith et al. 2022). When Smith et al. (2022) compared these Bayesian estimates to previous estimates, results were consistent with data-rich species, such as black duck, at least for Canadian metrics. I used a paired 2-tailed t-test to compare average values in age ratios between regions. I tested for differences between Canada and the United States and between Atlantic Canada, Ontario, and Quebec for fall age ratios, banding age ratios, and harvest age ratios.

2.3.3 Sample collection

I obtained the first primary feather (P1) from wings submitted to the Species Composition Survey in Canada (Gendron and Smith 2019) and Parts Collection Survey in the United States (USFWS 2019). Trained waterfowl biologists assigned all individuals a species identity, age, and sex, if possible (Carney 1992). The hunter reported the date and location of harvest. These surveys sample hunters randomly, based on hunting zones and previous hunting activity, ensuring a representative sample across the harvested range

(Smith et al. 2022). From available feathers, I selected individuals for stable-isotope analysis stratified by black duck conservation region, sex, age, and date of harvest, where possible (Table 2.1).

I assigned individuals to a region of harvest based on the provided latitude and longitude of harvest (or the listed province when missing latitude and longitude) for feathers obtained from the Species Composition Survey, and county of harvest, for feathers obtained from the Parts Collection Survey. In the few cases (n = 43) where the county spanned 2 conservation regions, I assigned the individual to the conservation region within which the county centroid fell. For all black ducks harvested in the United States, I used the county centroid in visual depictions of harvest location.

2.3.4 Stable isotopes

Feathers were processed for δ^2H and δ^{13}C at the Laboratory for Stable Isotope Science Advanced Facility for Avian Research lab (LSIS-AFAR; Western University, London, ON, Canada) and the Cornell Lab of Ornithology Isotope Lab (COIL; Cornell University, Ithaca, NY, USA). All feathers were processed for δ^2H. All feathers from adult males were processed for δ^{13}C, but only a subset of samples from adult females (n = 42) and juveniles (n = 90) was processed for δ^{13}C. Feathers were cleaned of surface oils and contaminants using a 2:1 chloroform:methanol solution, where feathers were soaked for a minimum of 12 hours, and then rinsed and dried for 24 hours in a fume hood.

Table 2.1 Sample sizes used for analyses (n), sample sizes for individuals that were excluded from analyses because of marine δ^{13}C signatures (Marine), and mean (μ) feather δ^2H values for harvested black ducks (n = 664, 2017–20) summarized by country, black duck conservation region, age (juvenile, adult), and sex.

Country	Region[1]	Unknown n	Female n	Female Marine	Female δ^2H (‰) μ (SD)	Male n	Male Marine	Male δ^2H (‰) μ (SD)
Juvenile								
CA	SWC	1	21	0	-117.86 (13.88)	19	0	-124.98 (14.04)
	SEC$_{QC}$	0	37	0	-125.13 (16.67)	37	0	-123.79 (16.26)
	SEC$_{ATL}$	0	44	0	-97.91 (15.76)	51	0	-97.53 (18.68)
USA	INT	0	46	0	-118.05 (17.18)	44	0	-122.40 (11.67)
	NATL	0	40	0	-121.22 (23.70)	40	0	-120.77 (19.59)
	SATL	0	40	1	-121.46 (23.45)	44	0	-119.84 (20.33)
Adult								
CA	SWC		11	0	-107.31 (18.74)	16	0	-121.96 (21.17)
	SEC$_{QC}$		14	0	-112.72 (19.63)	19	1	-115.33 (15.33)
	SEC$_{ATL}$		6	1	-90.87 (8.72)	6	5	-98.87 (26.01)
USA	INT		31	0	-118.05 (15.41)	40	3	-117.94 (21.04)
	NATL		14	0	-100.27 (22.84)	8	3	-128.92 (12.46)
	SATL		12	2	-118.74 (24.39)	5	2	-128.26 (16.72)

[a] Black Duck Management Regions: northwestern Canada (NWC), northeastern Canada (NEC), southwestern Canada (SWC), southeastern Canada-Quebec (SEC$_{QC}$), southeastern Canada-Atlantic (SEC$_{ATL}$), interior United States (INT), north Atlantic United States (NATL), south Atlantic United States (SATL)

For δ^2H analyses, I clipped and weighed 0.35 ± 0.02 mg of feather vane from the distal end of the feather into silver cups. At the LSIS-AFAR lab, prepared samples were loaded, simultaneously with laboratory standards, in a Uni-Prep autosampler (Eurovector, Milan, Italy), heated to 60 °C, flushed with dry helium and maintained under helium pressure (Wassenaar et al. 2015). Samples were combusted using flash pyrolysis (~1,350 °C) on glassy carbon, separated via a Eurovector 3000 elemental analyzer interfaced with a Thermo Delta V Plus continuous-flow isotope-ratio mass spectrometer (CF-IRMS; Thermo Instruments, Bremen, Germany). At COIL, gases were separated following combustion using a Temperature Conversion Elemental Analyzer (Thermo Instruments) interfaced with a Thermo Delta V Plus mass spectrometer. In both laboratories, values of δ^2H were derived using the comparative equilibration method of Wassenaar and Hobson (2003) using 2 keratin standards (caribou hoof standard [CBS], δ^2H = -197 ‰; kudu horn standard [KHS], δ^2H = −54.1 ‰) corrected for linear instrumental drift. At LSIS-AFAR, based on within-run analyses (n = 16 trays, each containing 10 standards for every 38 unknowns) of these keratin standards, the measurement standard deviation was 2.2 ‰ (CBS) and 2.7 ‰ (KHS). At COIL, an internal laboratory standard (keratin) included every 10 samples resulted in a standard deviation of 2.8 ‰ per run. All values are reported relative to the Vienna Standard Mean Ocean Water Precipitation (VSMOW) scale in delta (δ) notation in units of per mil (‰).

For δ^{13}C analysis, I clipped and weighed 0.5 ± 0.02 mg of feather vane from the distal end of the feather into tin cups. At LSIS-AFAR, samples were combusted and separated using a Costech Elemental Analyzer (Costech Analytical Technologies; Valencia, CA, USA) interfaced with a Thermo Delta V Plus CF-IRMS. Standards (USGS-40, δ^{13}C = -26.4 ‰; USGS-41, δ^{13}C = +37.6 ‰) were included every 10 samples along with an internal laboratory standard (keratin spectrum 1) to control for drift, resulting in an overall standard deviation of 0.16 ‰. At COIL, samples were analyzed using an NC2500 elemental analyzer interfaced with a Thermo Delta V IRMS (ThermoFisher Scientific; Waltham, MA, USA). Internal laboratory standards with known δ^{13}C values (Cayuga brown trout [CBT], δ^{13}C = -25.58 ‰; ground corn [KCRN], δ^{13}C = -13.01 ‰) along with an in-house standard (deer) were included every 10 samples, resulting in run-specific

standard deviations of 0.08 ‰ and 0.14 ‰. Values of $\delta^{13}C$ were calibrated to Vienna Pee Dee Belemnite (VPDB).

2.3.5   Assignment to origin

I determined moult or natal origin using spatially explicit likelihood-based assignment methods (Royle and Rubenstein 2004, Hobson et al. 2009, Wunder 2012, Campbell et al. 2020). I used a calibration equation derived for Mallard ($\delta^2H_f = \delta^2H_p \times 1.36 - 21.9$; van Dijk et al. 2014) to convert an amount-weighted growing-season precipitation isoscape (δ^2H_p; Bowen et al. 2005, International Atomic Energy Agency and World Meteorological Organization 2015, Bowen 2021) into a predicted feather isoscape (δ^2H_f; Figure 2.2) for North America. I excluded all individuals with $\delta^{13}C$ values > -20 ‰ (Ashley et al. 2010) from assignments to remove individuals with potential marine inputs to diets. Using functions within the isocat R package (version 0.2.6, Campbell et al. 2020), I first created individual-specific probability surfaces using a normal probability density function:

$$f(y_*|\mu_c, \sigma_c) = \left(\frac{1}{\sigma_c\sqrt{2\pi}}\right)\exp\left[-\frac{(y_* - \mu_c)^2}{2\sigma_c^2}\right]$$

where $f(y_*|\mu_c, \sigma_c)$ represents the probability that a given cell (c) within the δ^2H_f isoscape represents the origin of an individual (y_*), given the expected mean (μ_c; Figure 2.3A) and error (σ_c). Error incorporated both isoscape model error (Figure 2.3B; Bowen et al. 2005, International Atomic Energy Agency and World Meteorological Organization 2015, Bowen 2021) and residual error from the calibration relationship (12.8 ‰; Clark et al. 2006, 2009):

$$\sigma_c = \sqrt{\sigma_{iso}^2 + \sigma_{cal}^2}.$$

I normalized probabilities to sum to 1, estimating a probability of origin surface for each individual. I selected the upper 66 % of probabilities of origin (2:1 odds ratio), creating a binary surface. To depict likely origins across all individuals, I subsequently summed surfaces across individuals.

To further refine these estimates, I explored the use of movement probabilities (Robinson et al. 2016) as prior probabilities of origin (Royle and Rubenstein 2004, Wunder 2012). Specifically, I created separate probability surfaces for each black duck conservation region where the probability of originating at a given cell was the movement probability between the black duck conservation region where the theoretical origin cell (i.e., banding region) and harvest location (i.e., encounter region; Robinson et al. 2016) occurred. Because these probabilities were based entirely on banding information, and may strongly bias the results, I presented my final assignments with and without the prior included. I conducted all visualizations of raster data using the R package rasterVis (version 0.50.3, Lamigueiro and Hijmans 2020).

I also used clustering methods from Campbell et al. (2020) within isocat to identify similarities between continuous probability surfaces. In short, I calculated a similarity matrix using pairwise Schoener's *D*-metric among all individuals within the given assignment grouping and applied hierarchical clustering (package pvclust version 2.2-0; Suzuki and Shimodaira 2013) by correlation distance (Campbell et al. 2020). I cut each dendrogram tree at a height of 0.5, which I arbitrarily chose from initial investigations, as this value consistently produced 2–4 clusters for any given cohort per harvest region. As with the previous assignments, I applied a 2:1 odds ratio and summed across individuals. This clustering procedure ultimately grouped individuals by areas of origin without *a priori* knowledge of such regions to help further visualize and quantify where harvested individuals originated from. This method is particularly useful when examining the origins of many individuals with diverse origins. I applied clustering to all assignment cohorts and on all samples simultaneously, to represent groupings within the overall population.
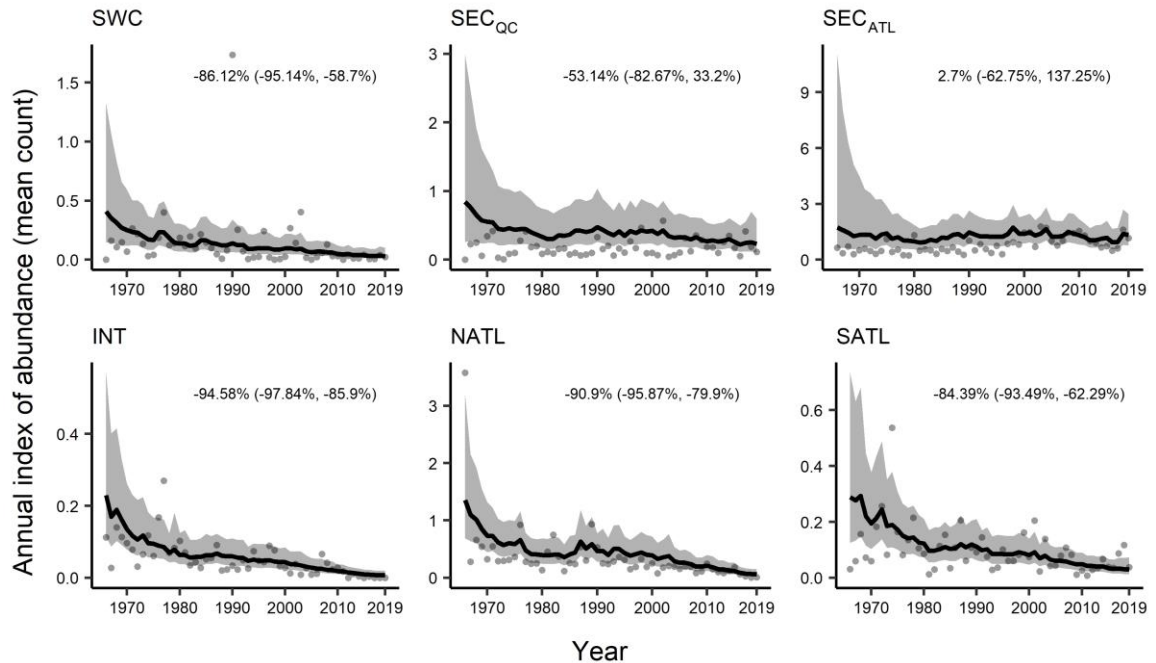
Figure 2.2 Regional annual indices of black duck abundance based on breeding bird survey data. Regional annual indices of black duck abundance based on breeding bird survey data (1966–2019; Pardieck et al. 2020). Lines are smoothed annual index with 95 % credible intervals (grey) and points are observed as annual means. Values are regional percent change (1970–2018, with 95 % credible interval). I modeled only black duck conservation regions where enough survey routes were available: southwestern Canada (SWC), southeastern Canada-Quebec (SEC$_{QC}$), southeastern Canada-Atlantic (SEC$_{ATL}$), interior United States (INT), north Atlantic United States (NATL), south Atlantic United States (SATL).
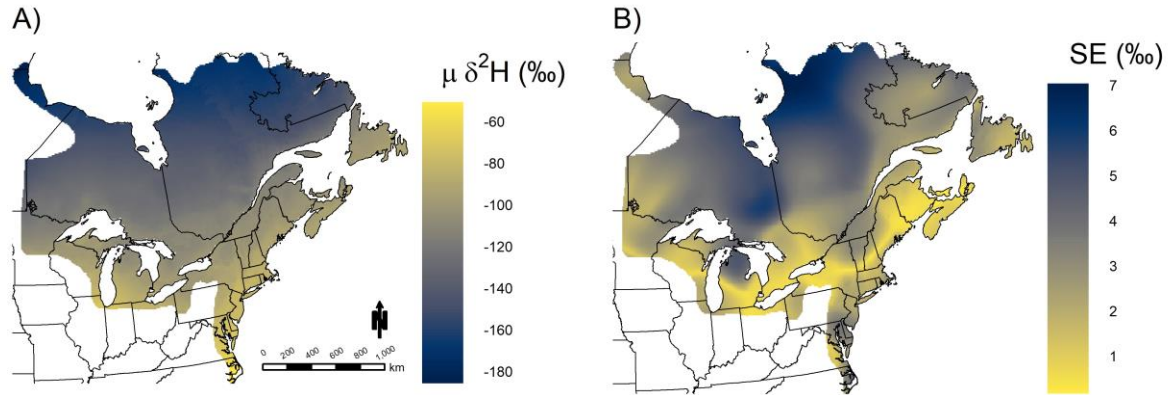
Figure 2.3 Isoscape showing A) mean (µ) predicted feather δ^2H values and B) predicted standard error (SE) of mean amount-weighted growing-season δ^2H values. I produced the mean predicted feather δ^2H isoscape through calibration of a mean predicted amount-weighted growing- δ^2H surface season (Bowen et al. 2005, International Atomic Energy Agency and World Meteorological Organization 2015, Bowen 2021) using a calibration equation for Mallard (van Dijk et al. 2014). Both surfaces were restricted to the black duck breeding range across eastern Canada and the northeastern United States (Baldassarre 2014) and used for likelihood-based assignment of harvest black ducks, 2017–19.

2.3.6　Statistical analyses

To test for differences between $\delta^2 H_f$ values between groups, I used linear models with $\delta^2 H_f$ as the response and the following predictors: age (factor: adult, juvenile), sex (factor: female, male), harvest season (factor: 2017–18, 2018–19, 2019–20), date of harvest (integer), region of harvest (factor), and harvest relative to the peak of migrants (factor). I assessed parameter significance using p-values, using < 0.05 as an indicator of significance. Global models included all predictors and I performed backwards stepwise model selection using Akaike's Information Criterion to determine the most parsimonious model. Global models also included an interaction term between age and sex to account for age- and sex-specific differences, such as moult migration. To assess collinearity between predictors, I assessed variance inflation factors for the global and best models (package DAAG version 1.24, Maindonald and Braun 2021), and none exceeded 3 in the final model. I assessed model fit by investigating normality and homoscedasticity of model residuals.

I used eBird Status and Trends data to estimate the timing of peak migration based on changes in weekly relative abundance (Auer et al. 2020; package ebirdst version 0.30, Fink et al. 2020*b*). These annually updated data products use statistical and machine learning models that use observer effort, and temporal and environmental covariates to estimate occurrence and abundance while accounting for variability associated with citizen science data (Fink et al. 2020*a*). Because of the imprecision of the harvest location (i.e., at the level of county in some cases), I used a low-resolution (27-km grid) map for relative abundance and extracted values using bilinear interpolation (i.e., nearest 4 raster cells) at the point of harvest. I extracted weekly relative abundance from the beginning of the harvest season (1 Sep, week 35) to the last day that 1 of these birds were harvested (26 Jan, week 4) and determined the week of highest relative abundance during this period. I then determined whether each individual was harvested before the week of highest relative abundance (coding these as 0) or during / after the week of highest relative abundance (coding these as 1).

I determined differences between multi-level factors using a Tukey *post hoc* test. I calculated the date of harvest as the number of days since 1 September, which I then

standardized (i.e., centered to a mean of 0 and scaled to an SD of 1). I removed individuals with missing dates (n = 1), unknown sex (n = 1), and missing coordinates (n = 11), and those harvested in areas without relative abundance data (n = 11) from all linear models.

2.4   Results

2.4.1   Population metrics

There were differential declines across the black duck breeding range (Figure 2.2) similar to those from Conroy et al. (2002). Specifically, Atlantic Canada was the only region showing little support for a decline (regional % change = 2.7 %) over the sampling period (1970–2018). Relative abundance was also highest in Atlantic Canada.

Fall age ratios (Appendix A) tended to be greater (i.e., more juveniles in the harvest data compared to the band-return data) when calculated using harvest data for Canada compared to the United States (mean difference = 0.22, t_{18} = 3.41, p < 0.01). Harvest age ratios (mean difference = 2.28, t_{18} = 11.90, p < 0.001) and band-return age ratios (mean difference = 3.10, t_{18} = 6.23, p < 0.001) were also on average greater when calculated for Canada. Within Canada, the fall age ratio for Atlantic Canada was on average less than the fall age ratio from Quebec (mean difference = -0.26, t_{18} = -2.16, p = 0.045), but otherwise there were no differences between age ratios for Atlantic Canada and either Quebec or Ontario.

2.4.2   Stable-isotope assignment

I collected feathers from 1,424 black ducks from three harvest seasons (2017–18, 2018–19, 2019–20) from across eastern Canada and the United States. After sub-sampling by region, age, and sex (Table 2.1), I processed 664 feathers for stable-isotope analysis (LSIS-AFAR, δ^2H, n = 615 and δ^{13}C, n = 63; COIL, δ^2H, n = 49 and δ^{13}C, n = 177). Only 14 of 108 (13 %) adult males were identified as moulting feathers in marine environments, all of which were removed from further analyses. The prevalence of marine moulting within the selected sample of adult females and juveniles was low (3 of 42 and 1 of 90 respectively); therefore, I did no further δ^{13}C sampling for juveniles.

Feather δ^2H values were best predicted by a model containing region (separating SEC into SEC_{ATL} and SEC_{QC}) and an interaction between age and sex (n = 622, $F_{8, 613} = 14.05$, p < 0.001), which supported my prediction of regional differences. By contrast, harvest date, season, and harvest timing relative to migration peak did not explain δ^2H values. Juvenile birds showed more negative δ^2H values compared to adults, indicating more northern origin (β [SE] = −8.30 [2.39], t = −3.48, p < 0.001). The same effect was seen for males, where adult males showed more northern origin (β [SE] = −6.60 [2.80], t = −2.36, p = 0.019), although for juvenile males there was a weaker effect due to a positive interaction between age and sex (β [SE] = 5.92 [3.32], t = 1.78, p = 0.075). Despite an effect of region, the only differences in feather δ^2H were between Atlantic Canada and all other regions, where individuals harvested in Atlantic Canada showed, on average, 20 ‰ more positive δ^2H values (Tukey *post-hoc* test, all p < 0.001; region-specific mean δ^2H [SD], SWC = -119.12 ‰ [17.40], SEC_{QC} = -121.24 ‰ [17.24], SEC_{ATL} = -98.43 ‰ [17.98], INT = -119.21 ‰ [16.61], NATL = -118.77 ‰ [22.42], SATL = -120.77 ‰ [21.74]).

Probabilistic assignments incorporating movement probabilities showed varied origins across the black duck breeding range, although the assignments generally corroborate the patterns based on the analysis of feather δ^2H values above. Black ducks harvested in Atlantic Canada showed more southern origins along with adult females in Quebec, the north Atlantic United States, and the south Atlantic United States black duck conservation regions, which supported my prediction of regional differences (Figure 2.4 and Figure 2.5; for assignments without the priors see Figure A1 and Figure A2). Overall, I assigned northern origins for juveniles and adult males across all harvest regions but to a lesser extent in Atlantic Canada (Figure 2.4 and Figure 2.5), again providing support for my prediction of regional differences. For adult females, likely regions of origin were generally farther south compared to juveniles and adult males within each black duck conservation region (Figure 2.4 and Figure 2.5). When movement probabilities were incorporated as a prior probability of origin, likely origins for harvested individuals showed strong flyway fidelity in all harvest regions except the south Atlantic United States black duck conservation region (Figure 2.4 and Figure 2.5). Further, in the southwestern black duck conservation region of Canada, which consists of southern and

central Ontario, there was a low probability of staying within the region after banding, based on movement probabilities. This created a dead-zone where black ducks were likely originating from all surrounding regions but not within that zone (Figure 2.4). In the southeastern Canada black duck conservation region, a similar pattern was seen where the probability of originating from northeastern Canada was greater than the probability of staying within southeastern Canada, but the effect was much less pronounced (Figure 2.4).

Using the clustering methods, I identified four latitudinal bands or clusters (Table 2.2; Figure 2.6). The two northernmost clusters, representing the Boreal Softwood Shield and Taiga Shield and Hudson Plains, were the predominant origins for juveniles (excluding Atlantic Canada) and adult males (excluding the interior United States black duck conservation region; Table 2.2; Figure 2.6). The next most southern cluster, representing the mixed forests south of the boreal, was the predominant region of origin for harvested juveniles in Atlantic Canada and adult female black ducks across all regions but the interior United States black duck conservation region (Table 2.2; Figure 2.6). Lastly, while identified as a cluster, there were only 12 individuals assigned to the southernmost cluster, representing the Atlantic coast (Table 2.2; Figure 2.6).
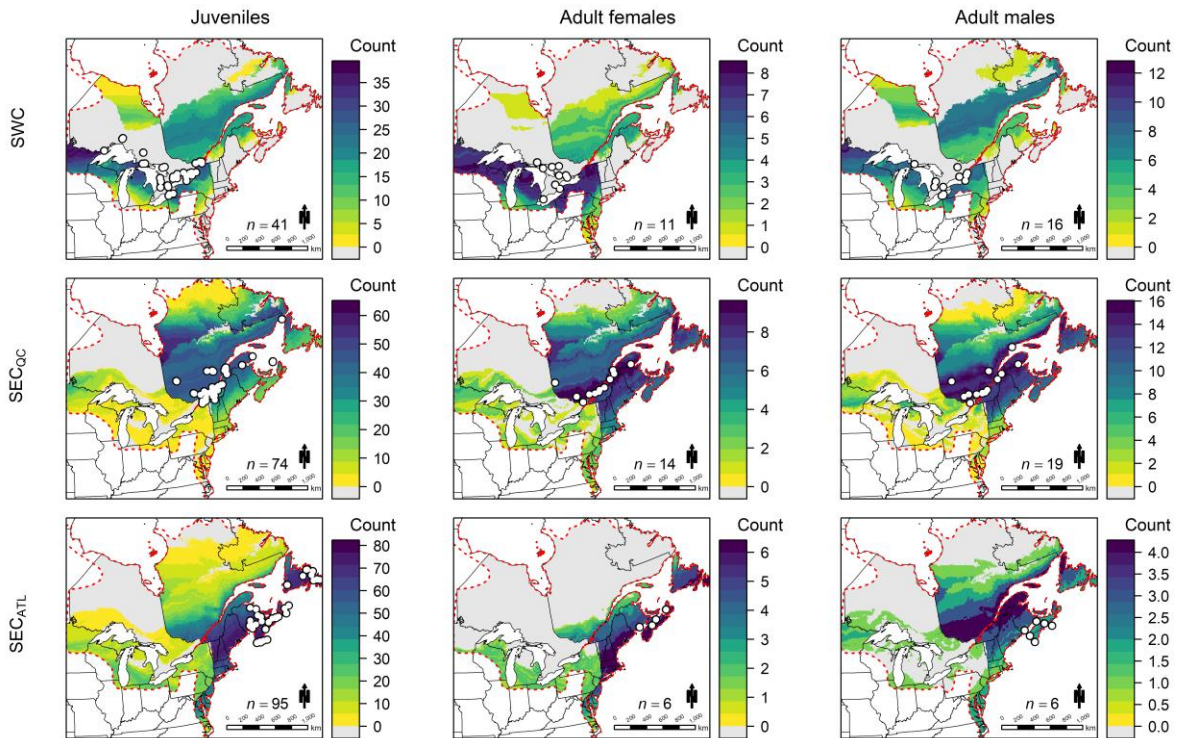
Figure 2.4 Likely origins of black ducks harvested within Canada from 2017–19.

Likely origins of black ducks harvested within Canada from 2017–19, incorporating movement probabilities between regions as a prior probability of origin (Robinson et al. 2016). I grouped individuals by age and sex cohort (columns; juvenile, adult female, adult male) and black duck conservation region of harvest (rows; southwestern Canada [SWC], southeastern Canada-Quebec [SEC$_{QC}$], southeastern Canada-Atlantic [SEC$_{ATL}$]). Sample sizes show the number of individuals harvested and circles are harvest locations. The scale represents the number of individuals assigned to a given pixel, under a 2:1 odds ratio.
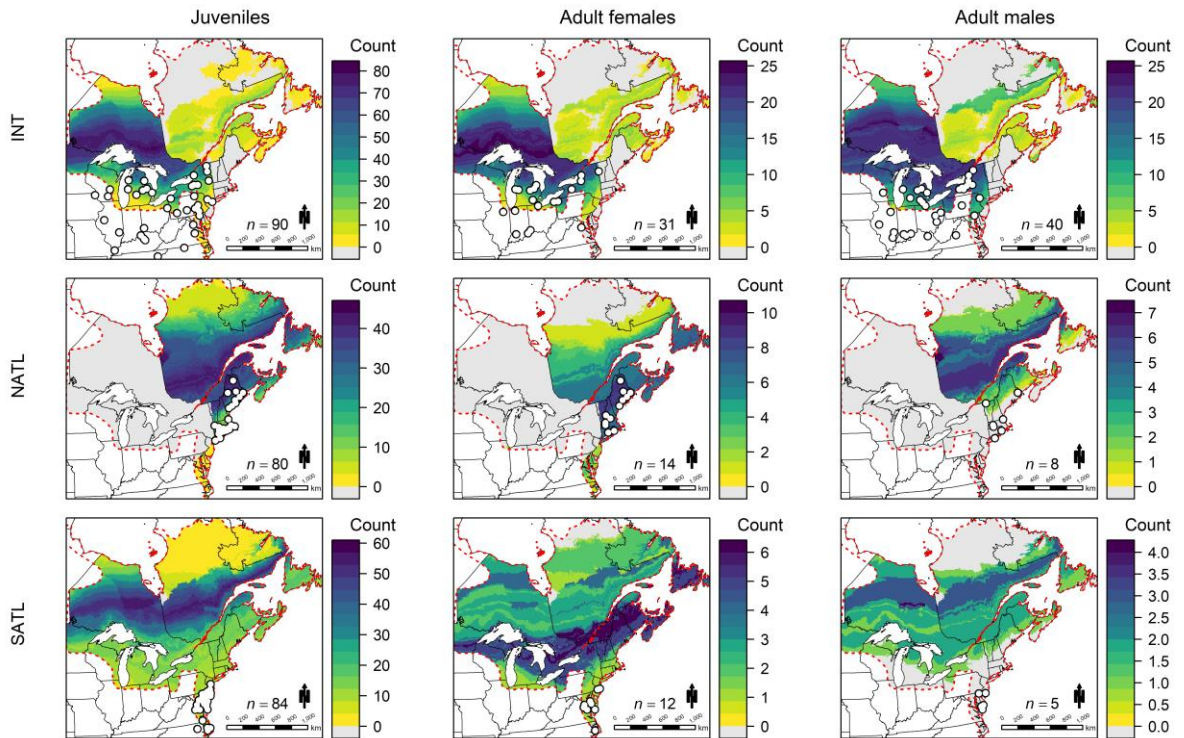
Figure 2.5 Likely origins of black ducks harvested within the United States from 2017–20. Likely origins of black ducks harvested within the United States from 2017–20, incorporating movement probabilities between regions as a prior probability of origin (Robinson et al. 2016). I grouped individuals by age and sex cohort (columns; juvenile, adult female, adult male) and black duck conservation region of harvest (rows; interior United States [INT], north Atlantic United States [NATL], south Atlantic United States [SATL]). Sample sizes show the number of individuals harvested and circles are harvest locations. The scale represents the number of individuals assigned to a given pixel, under a 2:1 odds ratio.

Table 2.2 The proportion of black ducks that were probabilistically assigned to each cluster (1 = Taiga Shield and Hudson Plain, 2 = Boreal Softwood Shield and Boreal Hardwood Transition, 3 = Lower Great Lakes–St. Lawrence Plain and Atlantic Northern Forests, 4 = New England–MidAtlantic Coast), summarized by age, sex, and black duck conservation region of harvest, 2017–20.

For each group, the cluster with the greatest proportion, indicated with an asterisk, indicates the predominant region of origin (moult location [adults] or natal area [juveniles]). Harvest regions include southwestern Canada (SWC), southeastern Canada-Quebec (SEC_{QC}), southeastern Canada-Atlantic (SEC_{ATL}), interior United States (INT), north Atlantic United States (NATL), and south Atlantic United States (SATL).

	Juvenile				Adult female				Adult male			
Region	1	2	3	4	1	2	3	4	1	2	3	4
SWC	0.37	0.44*	0.20	0	0.09	0.36	0.55*	0	0.44*	0.25	0.31	0
SEC_{QC}	0.41*	0.41*	0.19	0	0.21	0.36	0.43*	0	0.21	0.47*	0.32	0
SEC_{ATL}	0.05	0.17	0.74*	0.04	0	0	1*	0	0	0.50*	0.33	0.17
INT	0.28	0.52*	0.19	0.01	0.29	0.42*	0.29	0	0.32	0.28	0.40*	0
NATL	0.40	0.35*	0.24	0.01	0.07	0.36	0.50*	0.07	0.50*	0.50*	0	0
SATL	0.43*	0.35	0.19	0.04	0.33	0.17	0.50*	0	0.60*	0.20	0.20	0
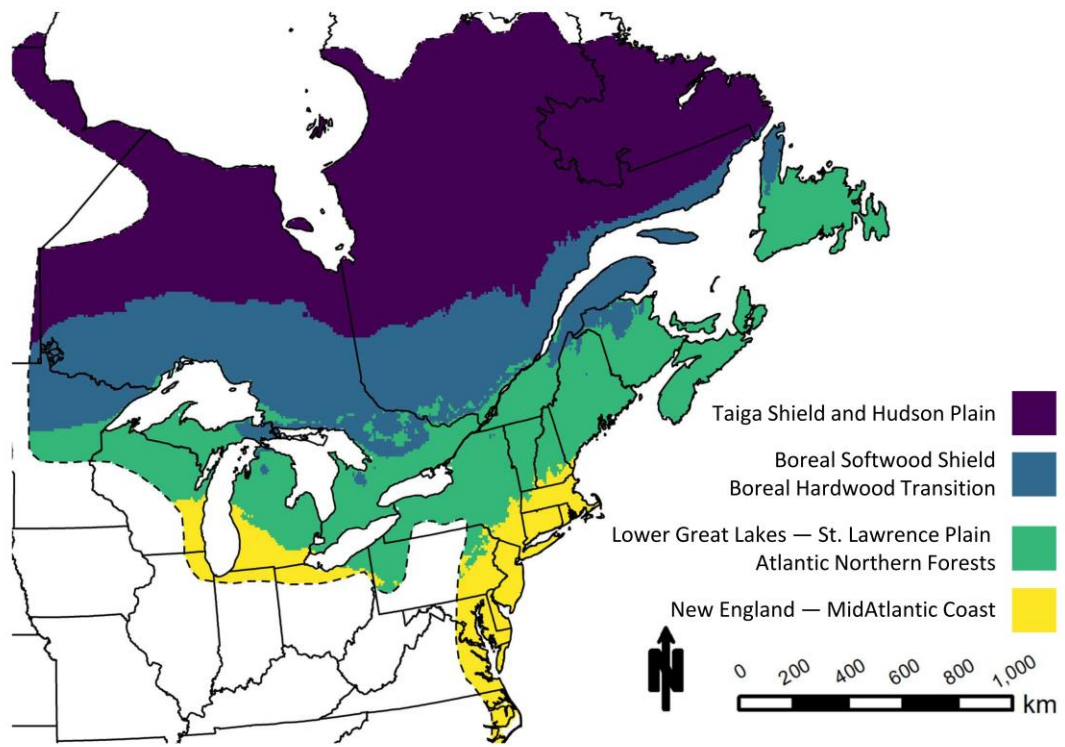
Figure 2.6 Clustered areas of origin for black ducks harvested in the United States and Canada. Clustered areas of origin for black ducks harvested in the United States and Canada, 2017–19. This procedure grouped individuals by areas of origin without *a priori* knowledge of such regions. I named each origin location based on the dominant Bird Conservation Regions.

2.5   Discussion

I tested the flyover hypothesis for black ducks using multiple intrinsic markers (feather δ^2H, δ^{13}C) and prior knowledge of movement patterns derived from banding to identify region-specific, age-specific, and sex-specific origins of harvested individuals throughout the United States and Canada. I more completely tested the flyover hypothesis by incorporating adult black ducks and those harvested within the United States. Black ducks harvested in Atlantic Canada had more southern origins, indicative of nearby breeding locations with relatively few individuals assigned to breeding regions farther north. In general, the opposite pattern in all other black duck conservation regions was evident, where δ^2H$_f$ values were mostly assigned to northern boreal areas, well north of harvest areas, which provided strong support for regional differences predicted under the flyover hypothesis. The δ^2H$_f$ values in the Quebec and the north Atlantic United States black duck conservation regions showed some, but much weaker, support for the flyover hypothesis (i.e., a portion of the harvest showed some sign of local origins) compared to Atlantic Canada.

My results combined with the findings of Ashley et al. (2010) and Roy et al. (2015) suggest that regional black duck harvest regulations may improve harvest management. Previous studies have shown support for independent stocks for black ducks (Geis et al. 1971, Pendleton and Sauer 1992), but my results further highlight regional connectivity between breeding and harvest areas. Current adaptive harvest management treats the black duck population as a continuous entity with population-wide demographic parameters (e.g., harvest rates, survival rates) and no regional metrics (USFWS 2021). At least for Atlantic Canada, these population-wide parameters may not represent localized stock-specific parameters, although collection and interpretation of this regional information is difficult. As previously identified, the fall age ratio, and both age-ratio components, are greater for black ducks harvested in Canada compared to the United States. Despite this difference, Atlantic Canada, which I expected to drive these differences between the 2 countries, did not show different age ratios to the other Canadian provinces (apart from differences in fall age ratio between Atlantic Canada and Quebec).

My data showed no difference in origin based on the timing of harvest, indicative of migration strategies where a mix of local breeders and northern migrants were harvested independently of harvest date. This result has also been seen in Mallard, where even at northern harvest locations early in the season, some northern-produced individuals and some nearby breeders are harvested (Kucia 2021). Black ducks have been expanding their winter range farther north and east (Brook et al. 2009) and some individuals breeding in Atlantic Canada, specifically in Nova Scotia, remain in Canada over winter (Peck et al. 2022). If some individuals are permanent residents in this area, they should be available for harvest early in the hunting season with a larger proportion of the harvest representing boreal origins later in the season, especially because the harvest season for Canada generally begins as early as 1 September (range of start dates 2021–22: 1–25 Sep in ON; 1–25 Sep in QC, 1–15 Oct in NB, 1–8 Oct in NS) compared to the United States (e.g., 25 Sep to 9 Oct in MI, 2 Oct to 20 Nov in NY, 27 Sep to 6 Nov in ME). Early boreal migrants arriving at the beginning of the harvest season in these northern areas likely obscure this temporal effect in natal and moult origin. In the southwestern Canada conservation region, the extremely low breeding densities of black ducks likely further prevent any temporal effects in origin because so few local black ducks are available to hunters early in the hunting season (compare abundance indices in Figure 2.2).

Adult males showed more northern origins compared to adult females, but not juveniles, suggesting similar moulting latitude of adult males and juvenile hatch locations. Across waterfowl, the direction of moult migration movements is variable depending on the life-history of the species but often involves the aggregation of many individuals and movement to separate (from the breeding area) communal moulting sites (Salomonsen 1968). Moult migratory movements are not well documented for black ducks (Baldassarre 2014), but studies report moulting birds on the northern coast of Labrador (Bowman and Brown 1992) and the Hudson Bay and James Bay lowlands (Bellrose and Kortright 1976, Ross 1984, Reed et al. 1996), many of which are generally at the north edge of their breeding range or beyond. Two studies have tracked annual cycle movements of black ducks, but neither conclusively showed northward moult migratory movements (Coluccy et al. 2020, Peck et al. 2022). Coluccy et al. (2020) investigated only adult females and treated the breeding and moult location as the same. Although

Peck et al. (2022) did acknowledge that two of their five male black ducks may have exhibited moult migration to the north, they were not confident in classifying moult migration in these cases. Other tracking studies determining moult migratory movements have focused more on geese and diving ducks, where northward movements to moulting sites such as the Hudson and James Bay lowlands and Ungava Peninsula are documented for eastern populations of these groups (Robert et al. 2002, Sheaffer et al. 2007, Luukkonen et al. 2008). For black ducks, these coastal moulting habitats are often in tidal flats and saltwater or brackish ponds (Ross 1984), suggesting marine inputs for such moulting birds. Therefore, I would expect my sample of males, 14 of which were excluded because of marine inputs, to show more northern moult origins indicative of moult migratory movements if these individuals could be reliably assigned to origin. In the interior United States black duck conservation region, adult males originated farther south than juveniles and adult females, potentially indicating a southward moult migration for these adult males, although this phenomenon was not seen in southwestern Canada.

Harvested adult females showed more southern origin relative to juveniles within any given region. Successful adult females and juveniles grow their feathers at the breeding site; therefore, the difference in origin indicates natal areas for juveniles are on average more northerly compared to the average breeding areas for all adult females for a given harvest area. This could indicate increasing productivity of females with increasing latitude, where more northern breeding females are more productive. Comparisons between agricultural breeding black ducks and those breeding in peatland and forested landscapes show that agricultural-origin birds are generally less productive (Maisonneuve et al. 2000). Alternatively, the pattern I saw in harvest by latitude could also indicate differential harvest vulnerability for juveniles and adult females where southern breeding adults are more likely to be harvested compared to juveniles at the same sites. Additionally, this effect could be driven by adult females with failed clutches, as they abandon the breeding grounds to moult at communal moulting grounds (Salomonsen 1968) and would show different $\delta^2 H_f$ values. Lastly, although I identified sex-specific and age-specific origins, sample sizes for adults were lower than those of juveniles. This limitation was due to the reduced representation of adults within the parts collection and

63

harvest surveys compared to juveniles and due to the greater proportion of adult birds that were excluded because they moulted in marine systems.

Despite the relative lack of banding in the northern boreal, band returns as a source of connectivity information can be useful for refining origin, but the results should be carefully interpreted. Movement between breeding and harvest regions (Robinson et al. 2016), incorporated as a Bayesian prior for isotopic assignment, provided reliable longitudinal refinement, where individuals harvested in the Mississippi flyway (INT) and Atlantic flyway (SEC and NATL) generally showed natal or moult origins within the same flyway. This flyway fidelity is supported for black ducks, although individuals banded in southern Ontario show a higher probability of migrating to the Atlantic coast to overwinter (Lavretsky et al. 2014), as my data support for black ducks harvested in the south Atlantic United States black duck conservation region. In this case, incorporating movement estimates generally mirrored previous methods to restrict waterfowl by flyway of origin within probabilistic assignments (Asante et al. 2017, Palumbo et al. 2019), whereas movement probabilities provided little useful latitudinal refinement (e.g., SEC, NEC). By incorporating these movement estimates, I inferred a Mississippi Flyway stock produced in the Boreal Shield and Hudson Plains of Ontario that is harvested in the Great Lakes and interior of Canada and the United States and an Atlantic Flyway stock harvested both as local breeders and with some migrants from northern Quebec and Newfoundland and Labrador in the Boreal Softwood and Taiga Shield. This supports the findings of Peck et al. (2022), where some individuals spent the entire annual cycle in Nova Scotia, while others migrated north to breed. This is especially important because these interior regions showed more negative population trends compared to Atlantic Canada, although I did not model the northern breeding individuals because of inadequate BBS coverage in the northeastern and northwestern Canada black duck conservation regions. Farther down the Atlantic coast, individuals originate from broad northern origins across both the Mississippi and Atlantic flyways.

Despite the usefulness for most harvest regions, for black ducks harvested in the southwestern Canada black duck conservation region, movement priors disproportionately restricted likely origins away from local breeding regions. Stable-

isotope values for harvested black ducks in southwestern Canada indicated likely origins across much of the Great Lakes and northern Atlantic forests, but movement probabilities indicated a low likelihood of origins in these regions compared to the interior United States black duck conservation region. This disconnect between the band-return and stable-isotope data could indicate a bias for banding data in the southwestern Canada black duck conservation region, where northern Ontario breeding black ducks are not adequately sampled during banding compared to the less harvested but more heavily banded southern breeders. Alternatively, this could represent a true effect where hunters in this region are more likely to harvest birds from the United States. I incorporated the most contemporary estimates for movement probabilities, estimated using hierarchical Bayesian models (Robinson et al. 2016), which indicate a low probability of banding and subsequently encountering a black duck within the southwestern Canada black duck conservation region ($\Psi = 0.002$) compared to all other regions such as the interior United States black duck conservation region ($\Psi = 0.1$; Robinson et al. 2016). Looking at previous movement estimates for black ducks, likelihood of banding and encounter within this area was much higher ($\Psi = 0.975$ and 0.979, sex-specific estimates; Zimpfer and Conroy 2006), although these estimates were calculated using different regions where Canada was separated into western, central, and eastern breeding strata with no north–south separation. The southwestern Canada black duck conservation region is a prime example of where prior information, in this case banding data, needs to be critically evaluated before incorporating with probabilistic assignments, which also must be interpreted with and without prior information, as I have done here.

2.5.1   Management implications

The adaptive harvest management model for black ducks relies on metrics of breeding-ground abundance, age-specific and sex-specific harvest rates and survival rates, and the fall age ratio, and in doing so, assumes that these processes operate across a single, range-wide population. Although I did not measure population metrics, apart from the fall age ratios, my results suggest the possibility of regional difference in these metrics with additional evidence of 2 distinct stocks (Mississippi and Atlantic flyway). Based on my results, I recommend that regional demographic parameters, particularly for Atlantic

Canada, be directly measured. Incorporating demographic information from regional stocks will likely be challenging because of a suite of analytical and operational issues, but it could help optimize harvest opportunities in the United States and Canada and promote more effective conservation of black ducks.

2.6   References

Ankney, C. D., D. G. Dennis, and R. C. Bailey. 1987. Increasing mallards, decreasing American black ducks: coincidence or cause and effect? Journal of Wildlife Management 51:523–529.

Ankney, C., D. G. Dennis, and R. C. Bailey. 1989. Increasing mallards, decreasing American black ducks–no evidence for cause and effect: a reply. Journal of Wildlife Management 53:1072–1075.

Asante, C. K., T. D. Jardine, S. L. Van Wilgenburg, and K. A. Hobson. 2017. Tracing origins of waterfowl using the Saskatchewan River Delta: incorporating stable isotope approaches in continent-wide waterfowl management and conservation. The Condor 119:261–274.

Ashley, P., K. A. Hobson, S. L. Van Wilgenburg, N. North, and S. A. Petrie. 2010. Linking Canadian harvested juvenile American black ducks to their natal areas using stable isotope (δD, δ^{13}C, and δ^{15}N) methods. Avian Conservation and Ecology 5:7.

Auer, T., D. Fink, and M. Strimas-Mackey. 2020. ebirdst: tools for loading, plotting, mapping and analysis of eBird Status and Trends data products. R Package version 1.0.0. <https://cornelllaboforniothology.github.io/ebirdst/>.

Baldassarre, G. A. 2014. Ducks, Geese, and Swans of North America. Volume 2. JHU Press, Baltimore, MD, USA.

Bellrose, F. C., and F. H. Kortright. 1976. Ducks, Geese & Swans of North America. Stackpole Books, Mechanicsburg, PA, USA.

Black Duck Joint Venture. 2018. Notice of funding opportunity, Migratory Bird Joint Ventures (Black Duck Joint Venture) Catalog of Federal Domestic Assistance (CFDA) Number 15.637. U.S. Fish and Wildlife Service, Division of Migratory Bird Management, Washington, DC, USA.

Bowen, G. J. 2021. Gridded maps of the isotopic composition of meteoric waters. <http://www.waterisotopes.org.>. Accessed 19 Sep 2019.

Bowen, G. J., L. I. Wassenaar, and K. A. Hobson. 2005. Global application of stable hydrogen and oxygen isotopes to wildlife forensics. Oecologia 143:337–348.

Bowman, T. D., and P. W. Brown. 1992. Site fidelity of male black ducks to a molting area in Labrador. Journal of Field Ornithology 63:32–34.

Brook, R. W., R. K. Ross, K. F. Abraham, D. L. Fronczak, and J. C. Davies. 2009. Evidence for black duck winter distribution change. Journal of Wildlife Management 73:98–103.

Campbell, C. J., M. C. Fitzpatrick, H. B. Vander Zanden, and D. M. Nelson. 2020. Advancing interpretation of stable isotope assignment maps: comparing and summarizing origins of known-provenance migratory bats. Animal Migration 7:27–41.

Carney, S. M. 1992. Species, age and sex identification of ducks using wing plumage. U.S. Department of the Interior, U.S. Fish and Wildlife Service, Washington, DC, USA.

Clark, R. G., K. A. Hobson, and L. I. Wassenaar. 2006. Geographic variation in the isotopic (δD, δ^{13}C, δ^{15}N, δ^{34}S) composition of feathers and claws from lesser scaup and northern pintail: implications for studies of migratory connectivity. Canadian Journal of Zoology 84:1395–1401.

Clark, R. G., K. A. Hobson, and L. I. Wassenaar. 2009. Corrigendum—Geographic variation in the isotopic (δD, δ^{13}C, δ^{15}N, δ^{34}S) composition of feathers and claws from lesser scaup and northern pintail: implications for studies of migratory connectivity. Canadian Journal of Zoology 87:553–554.

Coluccy, J. M., K. A. Anderson, T. Yerkes, and J. L. Bowman. 2020. Migration routes and chronology of American Black Duck *Anas rubripes*. Wildfowl 70:148–166.

Conroy, M. J., M. W. Miller, and J. E. Hines. 2002. Identification and synthetic modeling of factors affecting American Black Duck populations. Wildlife Monographs 150:1–64.

van Dijk, J. G. B., W. Meissner, and M. Klaassen. 2014. Improving provenance studies in migratory birds when using feather hydrogen stable isotopes. Journal of Avian Biology 45:103–108.

Ecological Stratification Working Group. 1995. A national ecological framework for Canada. Agriculture and Agri-Food Canada, Research Branch, Centre for Land and Biological Resources Research and Environment Canada, State of the Environment Directorate, Ecozone Analysis Branch, Ottawa, ON, Canada.

Edwards, B. P. M., and A. C. Smith. 2021. bbsBayes: an R package for hierarchical Bayesian analysis of North American Breeding Bird Survey data. Journal of Open Research Software 9:19.

Fink, D., T. Auer, A. Johnston, V. Ruiz-Gutierrez, W. M. Hochachka, and S. Kelling. 2020*a*. Modeling avian full annual cycle distribution and population trends with citizen science data. Ecological Applications 30:e02056.

Fink, D., T. Auer, A. Johnston, M. Strimas-Mackey, O. Robinson, S. Ligocki, B. Petersen, C. Wood, I. Davies, and B. Sullivan. 2020*b*. eBird status and trends, data version: 2018; released: 2020. Cornell Lab of Ornithology, Ithaca, NY, USA.

Francis, C. M., J. R. Sauer, and J. R. Serie. 1998. Effect of restrictive harvest regulations on survival and recovery rates of American black ducks. Journal of Wildlife Management 62:1544–1557.

Geis, A. D., R. I. Smith, and J. P. Rogers. 1971. Black duck distribution, harvest characteristics, and survival. U.S. Department of the Interior, Fish and Wildlife Service, Bureau of Sport Fisheries and Wildlife, Washington, DC, USA.

Gendron, M., and A. Smith. 2019. National Harvest Survey website. Canadian Wildlife Service, Environment and Climate Change Canada, Ottawa, Ontario. <https://wildlife-species.canada.ca/harvest-survey>. Accessed 13 May 2022.

Hijmans, R. J. 2020. raster: geographic data analysis and modeling. R package version 3.3-13. <https://CRAN.R-project.org/package=raster>.

Hobson, K. A., and S. G. Sealy. 1991. Marine protein contributions to the diet of northern saw-whet owls on the Queen Charlotte Islands: a stable-isotope approach. The Auk 108:437–440.

Hobson, K. A., and L. I. Wassenaar. 2018. Tracking Animal Migration with Stable Isotopes. Second Edition. Academic Press, Cambridge, MA, USA.

Hobson, K. A., M. B. Wunder, S. L. Van Wilgenburg, R. G. Clark, and L. I. Wassenaar. 2009. A method for investigating population declines of migratory birds using stable isotopes: origins of harvested lesser scaup in North America. PLOS One 4:e7915.

International Atomic Energy Agency and World Meteorological Organization. 2015. Global Network of Isotopes in Precipitation. The GNIP database. <https://nucleus.iaea.org/wiser>. Accessed 10 Oct 2022.

Kucia, S. R. 2021. Natal origins and breeding habitat associations of the eastern mallard population. MSc Thesis. State University of New York College of Environmental Science and Forestry, Syracuse, USA.

Kusack, J. W., D. C. Tozer, M. L. Schummer, and K. A. Hobson. 2022. Stable-isotopes (δ^2H, δ^{13}C) within feathers from harvested American black ducks (2017-2020). Dryad <doi:10.5061/dryad.95x69p8nm>

Lamigueiro, O. P., and R. Hijmans. 2020. rasterVis. R Package version 0.48. https://CRAN.R-project.org/package=rasterVis

Lavretsky, P., J. H. Miller, V. Bahn, and J. L. Peters. 2014. Exploring fall migratory patterns of American black ducks using eight decades of band-recovery data. Journal of Wildlife Management 78:997–1004.

Longcore, J. R., D. G. McAuley, D. A. Clugston, C. M. Bunck, J.-F. Giroux, C. Ouellet, G. R. Parker, P. Dupuis, D. B. Stotts, and J. R. Goldsberry. 2000. Survival of American black ducks radiomarked in Quebec, Nova Scotia, and Vermont. Journal of Wildlife Management 64:238–252.

Longcore, J. R., D. G. McAuley, G. R. Hepp, and J. M. Rhymer. 2020. American black duck (*Anas rubripes*), version 1.0. Account *in* A.F. Poole and F.B. Gill, editors. Birds of the World. Cornell Lab of Ornithology, Ithaca, New York, USA.

<https://doi-org.proxy1.lib.uwo.ca/10.2173/bow.ambduc.01>. Accessed 14 Apr 2020.

Luukkonen, D. R., H. H. Prince, and R. C. Mykut. 2008. Movements and survival of molt migrant Canada geese from southern Michigan. Journal of Wildlife Management 72:449–462.

Maindonald, J. H., and J. W. Braun. 2021. DAAG: data analysis and graphics data and functions. R package version 1.24. <https://CRAN.R-project.org/package=DAAG>.

Maisonneuve, C., R. McNicoll, and A. Desrosiers. 2000. Comparative productivity of American black ducks and mallards nesting in agricultural landscapes of southern Québec. Waterbirds 23:378–387.

Munro, R. E., and C. F. Kimball. 1982. Population ecology of the mallard: VII. Distribution and derivation of the harvest. U.S. Fish and Wildlife Service, Washington, DC, USA. <http://pubs.er.usgs.gov/publication/5230180>.

Nichols, J. D., M. C. Runge, F. A. Johnson, and B. K. Williams. 2007. Adaptive harvest management of North American waterfowl populations: a brief history and future prospects. Journal of Ornithology 148:343–349.

Palumbo, M. D., D. C. Tozer, and K. A. Hobson. 2019. Origins of harvested mallards from Lake St. Clair, Ontario: a stable isotope approach. Avian Conservation and Ecology 14:3.

Pardieck, K., D. Ziolkowski, Jr, M. Lutmerding, V. Aponte, and M.-A. Hudson. 2020. North American Breeding Bird Survey Dataset 1966-2019: U.S. Geological Survey data release. Eastern Ecological Science Center, Kearneysville, West Virginia, USA.

Pebesma, E. 2018. Simple features for R: standardized support for spatial vector data. R Journal 10:439–446.

Pebesma, E., and R. Bivand. 2005. Classes and methods for spatial data in R. R News 5:9–13.

Peck, L. E., M. D. English, G. J. Robertson, S. R. Craik, and M. L. Mallory. 2022. Migration chronology and movements of adult American black ducks *Anas rubripes* wintering in Nova Scotia, Canada. Wildlife Biology 2022:e01000.

Pendleton, G. W., and J. R. Sauer. 1992. Black duck population units as determined by patterns of band recovery. Pages 687–695 *in* D. R. McCullough and R. H. Barrett, editors. Wildlife 2001: populations. Springer, Dordrecht, NL.

R Core Team. 2021. R: a language and environment for statistical computing. R Foundation for Statistical Computing, Vienna, AT.

Raftovich, R., K. Fleming, S. Chandler, and C. Cain. 2021. Migratory bird hunting activity and harvest during the 2019-20 and 2020-21 hunting seasons. U.S. Fish and Wildlife Service, Laurel, MD, USA.

Reed, A., R. Benoit, R. Lalumière, and M. Julien. 1996. Duck use of the coastal habitats of northeastern James Bay. Canadian Wildlife Service Occasional Paper Number 90:1–47.

Reed, E. T., K. J. Kardynal, J. A. Horrocks, and K. A. Hobson. 2018. Shorebird hunting in Barbados: using stable isotopes to link the harvest at a migratory stopover site with sources of production. The Condor 120:357–370.

Ringelman, K. M., and C. K. Williams. 2018. The American black duck: three decades of science-based adaptive management. Case Studies in the Environment 2:1–8.

Robert, M., R. Benoit, and J.-P. L. Savard. 2002. Relationship among breeding, molting, and wintering areas of male Barrow's goldeneyes (*Bucephala islandica*) in eastern North America. The Auk 119:676–684.

Roberts, A. J., J. A. Royle, P. I. Padding, P. K. Devers, C. Lepage, and D. Bordage. 2020. Occupancy patterns of breeding American black ducks. Journal of Wildlife Management 84:150–160.

Robinson, O. J., C. P. McGowan, and P. K. Devers. 2016. Updating movement estimates for American black ducks (*Anas rubripes*). PeerJ 4:e1787.

Ross, R. 1984. Use of James Bay and Hudson Bay coasts of Ontario by dabbling ducks. Pages 69–76 *in* S. Curtis, D. G. Dennis, and H. Boyd, editors. Waterfowl studies in Ontario, 1973 to 1981. Canadian Wildlife Service Occasional Paper Number 54, Ottawa, ON, CA.

Roy, C., S. G. Cumming, and E. J. B. McIntire. 2015. Spatial and temporal variation in harvest probabilities for American black duck. Ecology and Evolution 5:1992–2004.

Royle, J. A., and D. R. Rubenstein. 2004. The role of species abundance in determining breeding origins of migratory birds with stable isotopes. Ecological Applications 14:1780–1788.

RStudio Team. 2021. RStudio: integrated development for R. RStudio, Inc., Boston, MA, USA.

Rusch, D. H., C. D. Ankney, H. Boyd, J. R. Longcore, F. Montalbano III, J. K. Ringelman, and V. D. Stotts. 1989. Population ecology and harvest of the American black duck: a review. Wildlife Society Bulletin 17:379–406.

Salomonsen, F. 1968. The moult migration. Wildfowl 19:5–24.

Schummer, M. L., A. D. Afton, S. S. Badzinski, S. A. Petrie, G. H. Olsen, and M. A. Mitchell. 2018. Evaluating the waterfowl breeding population and habitat survey for scaup. Journal of Wildlife Management 82:1252–1262.

Sheaffer, S. E., R. A. Malecki, B. L. Swift, J. Dunn, and K. Scribner. 2007. Management implications of molt migration by the Atlantic flyway resident population of Canada geese, *Branta canadensis*. Canadian Field-Naturalist 121:313–320.

Smith, A. C., T. Villeneuve, and M. Gendron. 2022. Hierarchical Bayesian integrated model for estimating migratory bird harvest in Canada. Journal of Wildlife Management 86:e22160.

Suzuki, R., and H. Shimodaira. 2013. pvclust: hierarchical clustering with P-values via multiscale bootstrap resampling. R package version 2.2-0. <https://rdrr.io/cran/pvclust/>

Szymanski, M. L., and J. A. Dubovsky. 2013. Distribution and derivation of the Blue-winged Teal (*Anas discors*) harvest, 1970-2003. United States Department of the Interior, Fish and Wildlife Service, Washington, DC, USA.

U.S. Fish and Wildlife Service [USFWS]. 2019. Waterfowl population status, 2019. U.S. Department of the Interior, Washington, DC, USA.

U.S. Fish and Wildlife Service [USFWS]. 2021. Adaptive harvest management: 2022 hunting season. U.S. Department of the Interior, Washington, DC, USA.

U.S. Geological Survey. 2021. GameBirds. U.S. Geological Survey, Laurel, Maryland, USA.

Wassenaar, L. I., and K. A. Hobson. 2003. Comparative equilibration and online technique for determination of non-exchangeable hydrogen of keratins for use in animal migration studies. Isotopes in Environmental and Health Studies 39:211–217.

Wassenaar, L. I., K. A. Hobson, and L. Sisti. 2015. An online temperature-controlled vacuum-equilibration preparation system for the measurement of δ^2H values of non-exchangeable-H and of δ^{18}O values in organic materials by isotope-ratio mass spectrometry. Rapid Communications in Mass Spectrometry 29:397–407.

Van Wilgenburg, S. L., and K. A. Hobson. 2011. Combining stable-isotope (δD) and band recovery data to improve probabilistic assignment of migratory birds to origin. Ecological Applications 21:1340–1351.

Wunder, M. B. 2012. Determining geographic patterns of migration and dispersal using stable isotopes in keratins. Journal of Mammalogy 93:360–367.

Zimpfer, N. L., and M. J. Conroy. 2006. Modeling movement and fidelity of American black ducks. Journal of Wildlife Management 70:1770–1777.

Chapter 3

3 Assigning harvested waterfowl to geographic origin using feather δ^2H isoscapes: What is the best analytical approach?

A version of this chapter has been published in PLOS One and is reproduced under the Creative Commons Attribution 4.0 International (CC BY) license. Citation:

Kusack, **J. W.**, D. C. Tozer, K. M. Harvey, M. L. Schummer, and K. A. Hobson. 2023. Assigning harvested waterfowl to geographic origin using feather δ^2H isoscapes: What is the best analytical approach? PLOS One 18:e0288262.

3.1   Introduction

Establishing links between breeding, stopover, and wintering sites for migratory species is important for the effective conservation and management of those species and their habitats (Webster et al. 2002, Boulet and Norris 2006). The development of extrinsic tracking tools has greatly increased our ability to establish patterns of migratory connectivity (Flack et al. 2022), but there are numerous situations involving unmarked individuals where only intrinsic markers are possible for inferring these connections. Such intrinsic markers typically involve the use of genetic or chemical molecular markers. This use of spatially explicit assignments to determine the origin of unmarked, migrant individuals using measurements of tissue stable-hydrogen isotopes (δ^2H) has grown considerably over the past two decades (reviewed in Hobson 2019). In addition to numerous non-game animals, this isotopic approach has been applied to determine the geographic origins of several hunted waterfowl species across North America (Hobson et al. 2009*b*, Ashley et al. 2010, Asante et al. 2017, Palumbo et al. 2019, 2020, Kusack et al. 2022) and Eurasia (Guillemain et al. 2014, 2019, Parejo et al. 2015, Caizergues et al. 2016). In this context using the stable-isotope approach, origin is generally not a specific location, but instead describes a probabilistically defined region that likely contains the location where an individual previously grew the sampled tissue(s) such as a natal, breeding, or non-breeding site. This assignment method has been important in improving our understanding of migratory connectivity, especially between breeding and harvest

areas (Palumbo et al. 2019, 2020, Kusack et al. 2022, Kucia et al. 2023, Schummer et al. 2023), and has the potential to contribute considerably to waterfowl management.

Isotopic assignment methods depend on the use of predictable relationships between the isotopic composition of environmental hydrogen (H) (e.g., precipitation, standing surface water) and non-exchangeable H in animal tissues. This approach relies on the fact that all H in animal tissues is derived ultimately from environmental H, either through diet or drinking water. Relationships between environmental H and non-metabolically active animal tissues formed locally, such as in feathers, allow inference of origins of individuals that are otherwise unmarked or tracked remotely, and so are not biased to focal (marked) populations within a species' range. Feather hydrogen-isotope values (δ^2H_f) reflect the source of H in local food webs following isotopic discrimination (i.e., the preferential assimilation of the heavy, ^2H, or light, ^1H, form), which occurs during incorporation through food webs and ultimately into consumer tissues. Feathers are inert following formation, so the non-exchangeable δ^2H values of feathers are representative of the environmental conditions present during feather growth (Hobson and Wassenaar 1997), assuming no endogenous reserves are used during feather formation (Fox et al. 2009). As waterfowl exhibit synchronous flight-feather moult after breeding (Pyle 2005), stable isotopes within these newly-formed feathers should reflect stable-isotope abundance present within the environment at the moulting site for adults. Similarly, stable isotopes present in feathers from juvenile waterfowl should reflect stable isotopes present within the environment at the natal site of those individuals.

Relating these baseline environmental H isotope values, driven primarily by precipitation (δ^2H_p), to δ^2H_f values requires a calibration or transfer function (Wunder 2010), often in the form of a linear equation (hereafter calibration equation). To derive these relationships, researchers primarily target known-origin, wild individuals whose tissues can confidently be related to a given location and relate their δ^2H values to an averaged δ^2H_p at that location. For some animals, such as insects, calibrations can be derived in the laboratory using isotopically-known, dietary substrates (Hobson et al. 1999, 2018). Sample sizes and geographic coverage needed to adequately capture these broad-scale relationships often necessitates lumping of taxa with similar life history (Hobson and

Wassenaar 1997, Hobson et al. 2004, 2012*b*, *a*, Hebert and Wassenaar 2005, Lott and Smith 2006, Popa-Lisseanu et al. 2012, Buchanan et al. 2018). Over the past 30 years, these relationships have been derived for many taxa (see Table B1), including bats (Cryan et al. 2004, 2014, Britzke et al. 2009, Popa-Lisseanu et al. 2012), butterflies and moths (Hobson et al. 1999, 2018, 2019), dragonflies (Hobson et al. 2012*a*), hoverflies (Ouin et al. 2011), raptors (Lott et al. 2003, Lott and Smith 2006, Wommack et al. 2020, Crowley et al. 2021), songbirds (Bowen et al. 2005, Hobson et al. 2009*a*, 2012*b*, Procházka et al. 2013, Tonra et al. 2015), and waterfowl (Table 3.1).

Calibration equations estimating the transfer of H from precipitation to tissue can vary among taxa and age classes within taxa (Studds et al. 2012, van Dijk et al. 2014), as life history and foraging strategies influence isotopic source and routing (Hobson et al. 2012*b*). For example, for individual songbirds captured at the same moulting location, species is an important predictor of δ^2H_f values (Nordell et al. 2016). Waterfowl species can be broadly grouped into two guilds with differing foraging strategies: dabblers (i.e., feed on aquatic vegetation and invertebrates beneath the surface of the water) and divers (i.e., dive to feed upon fish, invertebrates, and vegetation). Although the diets and behaviour of dabbling and diving ducks are varied and can overlap, these broad foraging strategies partition the dietary niche of these ducks to different microhabitats (dabblers – surface; divers – benthos or water column), which could theoretically influence these calibration relationships, although this is largely unknown for waterfowl.

Table 3.1 Summary of published calibration equations and associated statistics relating δ2Hp to δ^2H_f for waterfowl, waterbirds, and shorebirds

Common name	Scientific name	Calibration equation	δ^2H_p[a]	R^2	SD_{resid}	Source
Anseriformes						
Lesser Scaup	*Aythya affinis*	$\delta^2H_f = -31.6 + 0.93 * \delta^2H_p$	MGS_{B-2005}	0.78	12.8 ‰	(Clark et al. 2006, 2009)
Mallard Northern Pintail	*Anas platyrhynchos, Anas acuta*	$\delta^2H_f = -57 + 0.83 * \delta^2H_p$	MGS_M	-	-	(Hebert and Wassenaar 2005)
-	-	$\delta^2H_f = -61 + 0.67 * \delta^2H_p$	MA_{B-2005}	-	-	(Hebert and Wassenaar 2005)
Mallard	*Anas platyrhynchos*	$\delta^2H_f = -21.9 + 1.36 * \delta^2H_p$	MGS_{B-2005}	0.61	-	(van Dijk et al. 2014)
Swan Goose	*Anser cygnoides*	$\delta^2H_f = 9.03 + 1.71 * \delta^2H_p$	MGS_{B-2005}	0.43	8.89 ‰	(Zhu et al. 2020)
Waterbirds and Shorebirds						
Virginia Rail, King Rail	*Rallus limicola, R. elegans*	$\delta^2H_f = -43.82 + 1.16 * \delta^2H_p$	MGS_{B-2005}	0.76	8.6 ‰	(Fournier et al. 2017)
4 rail species		$\delta^2H_f = -74 + 1.16 * \delta^2H_p$	MM_B[b]	-	-	(Seifert et al. 2016)
14 wader species		$\delta^2H_f = -37.56 + 0.34 * \delta^2H_p$	MGS_B[b]	-	-	(Buchanan et al. 2018)

SD_{resid}, Standard deviation of residuals.

[a] MGS_{B-2005}, *Amount-weighted mean growing-season precipitation δ^2H* (Bowen et al. 2005); MGS_M, (Meehan et al. 2004); MA_{B-2005}, *Amount-weighted mean annual precipitation δ^2H* (Bowen and Revenaugh 2003, Bowen et al. 2005); MM_B, *Amount-weighted mean monthly precipitation (Nov-Feb; Apr-Aug) δ^2H* (Bowen 2021:202); MGS_B, (Bowen 2021:202).

[b] Isoscape was downloaded at the time of publication and may not represent the current form available in the reference.

'-' indicates information repeated from the line above; blanks indicate unreported information.

When using precipitation isoscapes to assign individuals to origin, it is important to understand how H in precipitation contributes to H in a consumer's tissues. For terrestrial-foraging species, most current calibrations in North America are done using amount-weighted mean growing-season (hereafter MGS) $\delta^2 H_p$ isoscapes, which incorporate isotope data for months with average temperatures > 0ºC (Meehan et al. 2004, Bowen et al. 2005) (Table B1). These calibrations work on the assumption that consumer $\delta^2 H_f$ will relate to the $\delta^2 H_p$ during the period of greatest vegetative growth, as these precipitation signals are translated into plant biomass and to consumers. The appropriate calibration is less clear for aquatic and semi-aquatic species or those that eat foods that occur in aquatic emergent plant communities. Despite this, the focus for waterfowl calibration studies has been on the relationship between consumer tissues and MGS $\delta^2 H_p$ values, as all but one waterfowl calibration relationship has utilized MGS $\delta^2 H_p$ values (Table 3.1), although few studies have directly measured surface water $\delta^2 H$ to compare with consumer tissues (Coulton et al. 2009, Solovyeva et al. 2016). The other isoscape used is the amount-weighted mean annual (hereafter MA) $\delta^2 H_p$ grid, which incorporates precipitation isotope data across all months (Bowen et al. 2005, Terzer et al. 2013, Terzer-Wassmuth et al. 2021). The main difference for the MA grid is the potential contribution of snowmelt to the surface water. Although no studies have directly measured this relationship, snowmelt entering waterbodies likely influences dietary $\delta^2 H$ especially for northern moulting waterfowl. Therefore, it is not clear which isoscape captures this relationship more accurately.

The efficacy of assigning waterfowl to a geographic origin using the stable-isotope approach also depends upon the accuracy of the calibration relationship between $\delta^2 H_f$ and $\delta^2 H_p$, as well as the variance one might expect for such a calibration. This involves isotopic measurement error (Wunder and Norris 2008) and intrinsic differences between individuals (e.g., behaviour, metabolism), in addition to error associated with the derivation of $\delta^2 H_p$ isoscapes (i.e., $\delta^2 H_p$ measurement error, interpolation uncertainty, annual environmental effects). As such, modern $\delta^2 H_p$ isoscape grids are generally accompanied by a spatially explicit estimate of $\delta^2 H_p$ variability (Bowen 2021), where error is generally greater in regions with fewer sampling points (Bowen and Revenaugh

2003). To capture the remaining calibration error, variability is often approximated using the standard deviation of calibration model residuals (hereafter SD_{resid}), which includes uncertainty in δ^2H_f values (e.g., measurement error, inter- and intraspecific intrinsic variability) and site-specific δ^2H_p values (e.g., interpolation error, climatic variability). For waterfowl, annual climatic variation such as dry summers leading to increased evaporation in shallow ponds and more positive surface water δ^2H values (Coulton et al. 2009) likely contributes to increased variability. Propagating as much of the known error as possible into assignments is the objective of most practitioners and with the adoption of newer assignment algorithms (Campbell et al. 2020, Ma et al. 2020) these sources of error can be incorporated into likelihood-based assignment algorithms, to provide the most complete estimates of assignment error.

The primary goal of my research was to critically evaluate current methods used to calibrate precipitation-hydrogen isoscapes to predicted δ^2H_f values and, by extension, evaluate likelihood-based assignment methods for waterfowl. Specifically, I aimed to test whether known-origin waterfowl δ^2H_f values correlated better with MA δ^2H_p or with MGS δ^2H_p, and which calibration relationship is best for different foraging guilds of ducks (dabbling vs. diving). To test these correlations, I used published δ^2H_f data for known-origin waterfowl and collected additional data from across northeastern North America, a region that has been unrepresented to date. Using these data and published isoscapes, I derived calibrations between measured and predicted δ^2H_f values and then evaluated the accuracy and precision of assignments by applying a cross-validation procedure. Lastly, as a proof-of-concept, I reanalyzed a published dataset (Palumbo et al. 2020), applied my derived calibration methods, and compared the results to the previous utilized method.

3.2   Materials and methods

3.2.1   Isoscapes

I compiled three δ^2H_p isoscapes from two sources that represent the most complete precipitation isoscapes available at the time of publication. Both sources utilized the long-term datasets compiled by the Global Network of Isotopes in Precipitation (GNIP)

of the International Atomic Energy Association (IAEA) (International Atomic Energy Agency and World Meteorological Organization 2023). From the WaterIsotopes website (Bowen 2021), I obtained a predicted amount-weighted (i.e., weighted by the monthly amount of precipitation) mean annual $\delta^2 H_p$ grid (5 arc-minute resolution, hereafter MA_B), amount-weighted mean growing-season $\delta^2 H_p$ grid (5 arc-minute resolution, hereafter MGS_B), and associated uncertainty (1 standard deviation) grids for MGS_B and MA_B predictions. Using monthly station-specific $\delta^2 H_p$ values (largely from GNIP), these isoscapes are typically interpolated using algorithms that rely on spatial (e.g., latitude, elevation) correlates to account for variation in $\delta^2 H_p$ (Bowen and Revenaugh 2003, Bowen et al. 2005), although the versions I used include more recent precipitation $\delta^2 H_p$ data (International Atomic Energy Agency and World Meteorological Organization 2015). From the IAEA (International Atomic Energy Agency and World Meteorological Organization 2023), I obtained an amount-weighted mean annual $\delta^2 H_p$ grid (30 arc-second resolution, hereafter MA_T; accessed August 23, 2021), modelled using the updated Regionalized Cluster-Based Water Isotope Prediction Version 2 model (RCWIP2) (Terzer-Wassmuth et al. 2021). This model updated the previous RCWIP model (Terzer et al. 2013) and included an additional seven years of $\delta^2 H_p$ data (1960–2006). In addition to the spatial correlates included in the (Bowen and Revenaugh 2003, Bowen et al. 2005) model (i.e., latitude and altitude), the RCWIP2 model included additional climatic (e.g., air temperature, vapour pressure) and geographical predictors (e.g., land mass fraction; for a complete list see Terzer-Wassmuth et al. 2021). The RCWIP2 isoscape grids are available as 1800 x 1800 arcminute GeoTIFF files (accessed May 27, 2022), which I downloaded separately and combined into a global grid (Terzer-Wassmuth et al. 2021). These RCWIP2 isoscapes provide $\delta^2 H_p$ values at the highest resolution available, but this resolution was not logistically feasible because of computer processing time. Therefore, I reduced the resolution to match the 5 arc-minute resolution of the MGS_B and MA_B isoscapes (method: bilinear resampling).

3.2.2   Samples

I collected feathers from known-origin waterfowl across eastern Canada and the United States (n = 273, 2017–21, hereafter the 'Kusack' dataset; see Table 3.2 for sample sizes

by province and state and Figure 3.1 for geographic distribution). Most feather samples were collected from flightless hatch-year (HY) birds (i.e., 'locals') during regular banding operations, where feathers were collected opportunistically or during targeted sampling. I focused collection on primary (P1; clip ¼ inch of the distal end of the feather) and covert (secondary covert; pluck entire feather) feathers, but due to the opportunistic nature of sampling and the different ages at which banding occurred for HY birds, multiple different feather groups, including breast feathers (n = 17) were included in analyses. Samples were collected from HY American Black Duck (*Anas rubripes*), Mallard (*Anas platyrhynchos*), Ring-necked Duck (*Aythya collaris*), and Wood Duck (*Aix sponsa*). I also obtained Blue-winged Teal (*Spatula discors* n = 2) samples that were collected by Palumbo et al. (2020). Moulting adults (n = 9) were included if they were not flight-capable yet, but only newly moulted primary feathers were sampled from these birds to be sure of the local signal. Outside of banding stations, I also obtained primary feather tissue (P1) from HY Wood Duck (n = 22) banded during a Maryland breeding study, which were sampled within 5 km of their original banding site as flightless young. I obtained flight feathers (primary [P1] and primary coverts) from the Species Composition Survey (Gendron and Smith 2019) when wings from HY or adults in incomplete moult were submitted from known origins (Green-winged Teal *Anas crecca* n = 5, American Black Duck n = 1, Ring-necked Duck = 3, Common Merganser *Mergus merganser* n = 1, Wood Duck n = 2).

I obtained published known-origin δ^2H_f data from the assignR known-origin dataset repository (Ma et al. 2020) and authors directly. For dabbling ducks, I obtained δ^2H_f data on known-origin Mallard and Northern Pintail pre-fledged HY birds captured in western North America (Hebert and Wassenaar 2005) (n = 324, hereafter the 'Hebert' dataset) and known-origin juvenile and moulting adult Mallard across Europe (van Dijk et al. 2014) (n = 215, hereafter the 'van Dijk' dataset). Three samples from the van Dijk dataset were excluded from analyses as they did not overlap with the MA_T isoscape (IDs 2755, 2932, and 2933). For diving ducks, I obtained data on known-origin HY Lesser Scaup (*Aythya affinis*) in western North America (Clark et al. 2006, 2009) (n = 75, hereafter the 'Clark' dataset).

Table 3.2 Summary statistics for feather stable-hydrogen isotope (δ^2H_f) values.

Country	Province	Species	n	Foraging Guild	Mean ± SD δ^2H_f (‰)[a]
Canada	NB	American Black Duck	3	Dabbling	-100.3 ± 1.3
	NS	American Black Duck	1	Dabbling	-107.5
	ON	American Black Duck	3	Dabbling	-97.3 ± 5.7
		Green-winged Teal	5	Dabbling	-105.5 ± 16.0
		Blue-winged Teal	2	Dabbling	-110.4 ± 1.8
		Common merganser	1	Diving	-112.3
		Mallard	7	Dabbling	-118.4 ± 12.8
		Ring-necked Duck	9	Diving	-132.6 ± 16.7
		Wood Duck	12	Dabbling	-115.6 ± 21.0
	QC	American Black Duck	20	Dabbling	-120.0 ± 8.0
		Mallard	8	Dabbling	-130.2 ± 7.3
USA	CT	Mallard	1	Dabbling	-111.9
	IN	Mallard	1	Dabbling	-76.3
	MA	Mallard	10	Dabbling	-100.2 ± 4.3
		Wood Duck	6	Dabbling	-97.9 ± 13.2
	MD	Wood Duck	22	Dabbling	-94.6 ± 14.8
	MI	Mallard	2	Dabbling	-90.03 ± 20.3
	NJ	Mallard	1	Dabbling	-82.5
	NY	Mallard	4	Dabbling	-123.6 ± 5.8
		Wood Duck	5	Dabbling	-104.1 ± 15.1
	OH	Wood Duck	3	Dabbling	-108.2 ± 8.7
	PA	Mallard	2	Dabbling	-111.0 ± 9.4
		Wood Duck	3	Dabbling	-108.4 ± 14.6
	VA	Wood Duck	9	Dabbling	-88.5 ± 9.8
	WI	Mallard	88	Dabbling	-119.8 ± 16.4
		Ring-necked Duck	23	Diving	-119.9 ± 14.1
		Wood Duck	24	Dabbling	-105.3 ± 7.6
Total			275		

[a] Mean δ^2H_f values were calculated without the outlier samples and sites (see Results)
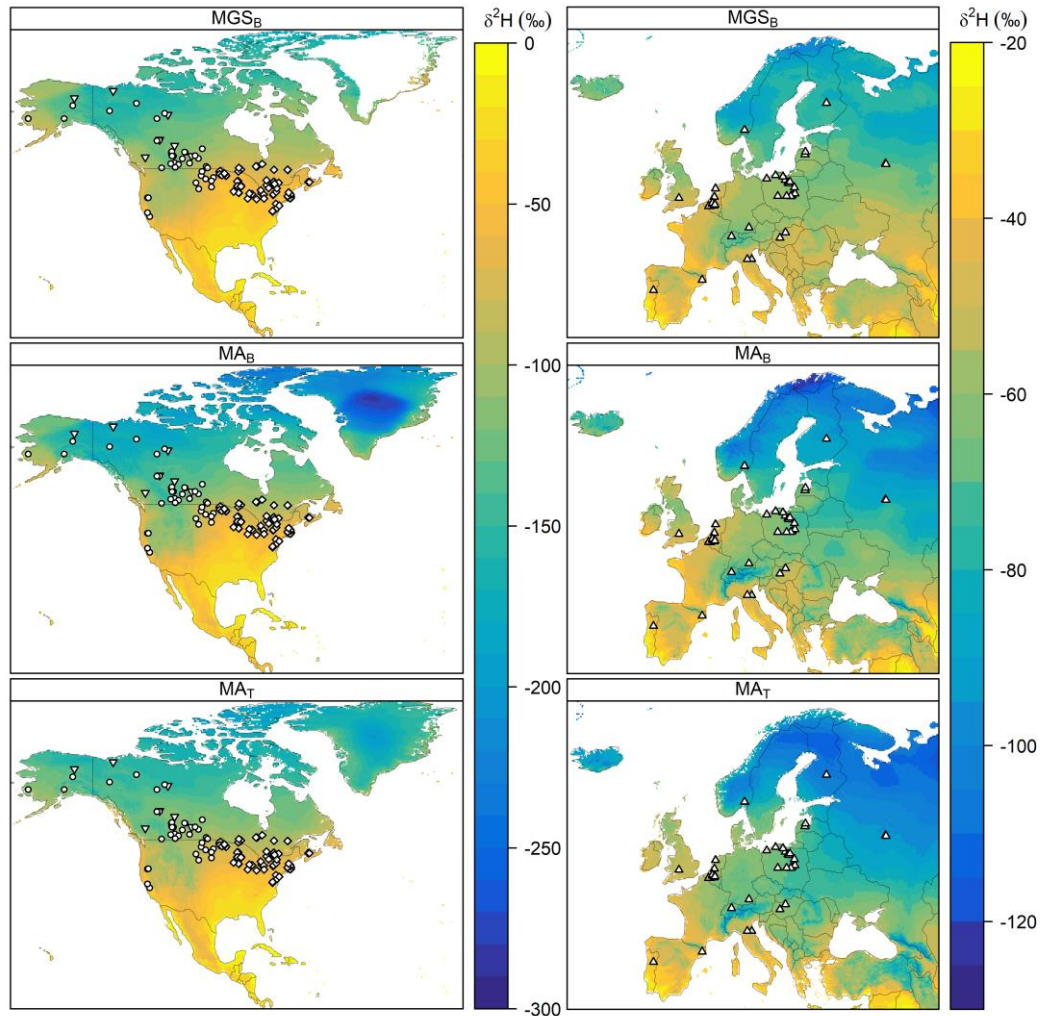
Figure 3.1 Map of sampling sites. Collection locations for North American and European known-origin ducks, overlaid on amount-weighted mean growing-season precipitation (MGS$_B$) (Bowen 2021) and amount-weighted mean annual precipitation (MA$_B$, Bowen 2021; MA$_T$, Terzer-Wassmuth et al. 2021) isoscape grids. Points show sampling location for individual samples and symbology shows the source publication (*triangle*, n = 212, 'van Dijk', van Dijk et al. 2014; *circle*, n = 324, 'Hebert', Hebert and Wassenaar 2005; *diamond*, n = 275, Kusack; *inverted triangle*, n = 75, Clark, Clark et al. 2006, 2009). Stable-hydrogen isotope values within each column are represented by the colour (scale is consistent among isoscape sources within the same continent). For more specific sampling locations for a given dataset, see the original publications.

3.2.3 Stable-isotope measurements

Feather samples were processed for $\delta^2 H_f$ measurement at the Laboratory for Stable-isotope Science - Advanced Facility for Avian Research (n = 71; LSIS-AFAR; Western University, London, ON, CA) and the Cornell Isotope Laboratory (n = 204; COIL; Cornel, Ithaca, NY, USA). Feathers were first cleaned of surface oils by soaking and rinsing in a 2:1 chloroform:methanol mixture and allowed to dry under a fume hood. I sampled the distal end of the feather vane and weighed 0.350 ± 0.03 mg of feather material into silver capsules. At LSIS-AFAR crushed capsules were then placed in a Uni-Prep carousel (Eurovector, Milan, Italy) heated to 60 °C, evacuated and then held under positive helium pressure. Feather samples were combusted using flash pyrolysis (~1350 °C) on glassy carbon in a Eurovector elemental analyzer (Eurovector, Milan, Italy) coupled with a Thermo Delta V Plus continuous-flow isotope-ratio mass spectrometer (CF-IRMS; Thermo Instruments, Bremen, Germany). At COIL, the same procedures were followed, except feather samples were combusted (> 1400 °C) using a Thermo Scientific Temperature Conversion Elemental Analyzer coupled via a Conflo IV (Thermo Scientific) to a Thermo Scientific Delta V CF-IRMS. Both labs used the comparative equilibration method of Wassenaar and Hobson (2003) using the same two keratin standards (CBS, $\delta^2 H$ = -197 ‰; KHS, $\delta^2 H$ = -54.1 ‰) corrected for linear instrumental drift. All results are reported for non-exchangeable H expressed in the typical delta notation, in units of per mil (‰), and normalized on the Vienna Standard Mean Ocean Water (VSMOW) scale. Based on within-run (n = 5 CBS at LSIS-AFAR; n = 7–9 Keratin at COIL) and across-run (n = 10 at LSIS-AFAR; n = 13 at COIL) analyses of standards, measurement error was approximately $\pm$ 2.5 ‰ (LSIS-AFAR) and $\pm$ 2.2 ‰ (COIL). All $\delta^2 H_f$ values are reported relative to the Vienna Standard Mean Ocean Water–Standard Light Antarctic Precipitation scale. All published data used in this study were processed using the same comparative equilibration methods (Wassenaar and Hobson 2003), using the same standards as Wassenaar and Hobson (2003) (i.e., CFS, CHS, BWB) or used standards that have been calibrated relative to the standards in Wassenaar and Hobson (2003) (i.e., KHS, CBS), and therefore should be comparable without any additional transformations (Magozzi et al. 2021).

3.2.4   Statistics

All statistics were performed within the R statistical environment (version 4.2.2, R Core Team 2021) using RStudio (version 2022.12.0, RStudio Team 2021). Spatial data manipulations were performed using the packages sf (version 1.0-9, Pebesma 2018) and terra (version 1.6-47, Hijmans 2021). All isoscape depictions and assignment procedures were done using the original coordinate system of the isoscapes (WGS84; EPSG:4326), but final depictions of assignment maps were converted to an Albers equal-area projection for North America (NAD83; EPSG:42303).

I used general linear models to derive calibration equations based on the relationship between known-origin δ^2H_f values and δ^2H_p values at the location of sampling. I removed outliers on a site-specific basis, where individuals with δ^2H_f values more positive than the third quartile + 1.5 x the interquartile range, for that site, were removed from the calibration, as were those with δ^2H_f values more negative than the first quartile – 1.5 x the interquartile range. Separate calibration equations were derived for each published known-origin data source (Hebert and Wassenaar 2005, Clark et al. 2006, 2009, van Dijk et al. 2014), as well as my data, paired with each precipitation isoscape (Bowen 2021, Terzer-Wassmuth et al. 2021). I also grouped all dabbling ducks (American Black Duck, Blue-winged Teal, Green-winged Teal, Mallard, Wood Duck; hereafter the 'Dabblers' dataset) and diving ducks (Common Merganser, Lesser Scaup, Ring-necked Duck; hereafter the 'Divers' dataset). From each calibration equation, I reported the SD_{resid} and adjusted R^2 to approximate model fit.

3.2.5   Model validation

To validate the performance of known-origin δ^2H_f datasets, isoscapes, and any resulting calibration (δ^2H_f vs δ^2H_p) equations, I performed a cross-validation procedure, similar to those used by Ma et al. (Ma et al. 2020). Half of the given dataset, chosen at random, was used to produce a calibration equation, while the other half was used to validate the derived equation. These isoscapes were then converted to predicted δ^2H_f isoscapes using the calibration equation derived from the calibration subset. As the known-origin data were collected within North America and Europe, isoscapes were limited to these

83

continents. Specifically, North America (extent: longitude -170 to -10º, latitude 7 to 84º) was masked to exclude South America while Europe (extent: longitude -25 to 50º, latitude 35 to 72º) was masked to exclude Africa. Geopolitical shapefiles were obtained from the R package rnaturalearth (version 0.1.0, South 2017). Isoscapes were not masked to any breeding range since I was assessing multispecies data, and waterfowl can migrate to moult outside of the breeding range (Salomonsen 1968).

I then assessed the likelihood that any given cell within the $\delta^2 H_f$ isoscape was the origin of an individual duck using the procedures and functions from the isocat package (version 0.2.6, Campbell et al. 2020), which uses normal probability density function (Royle and Rubenstein 2004, Wunder 2010) incorporating both calibration error (σ_{cal}) and isoscape error (σ_{iso}) into the expected standard deviation of a given isoscape cell (σ_c). Calibration error was derived directly from the residuals of the calibration relationship (SD_{resid}) between the isoscape and calibration data. Isoscape error was extracted directly from the isoscape uncertainty raster. For the MA_T isoscape, which did not have an error grid, I used a placeholder grid with no uncertainty (i.e., $\sigma_{isoscape} = 0$), which simplified the error calculation to just the calibration error, while still using the isocat functions. Probabilities were normalized to sum to 1, estimating a probability of origin, and the upper 66.6 % of probabilities of origin (i.e., a 2:1 odds ratio) were selected, creating a uniform region of likely origins (i.e., all cells are equally likely). As some of the grouped datasets contained samples from both North America and Europe, I limited the likely origins for a given individual to the continent (see above) where sampled. I evaluated the performance of each known-origin dataset and isoscape using estimates of accuracy, precision, and minimum distance. I measured accuracy by determining the proportion of individuals that were correctly assigned under the applied odds ratio (i.e., the binary grid contains the sampling point for known-origin feathers, Reese et al. 2019). Other validation methods examined the performance of these thresholds on a spectrum (0–1) (Campbell et al. 2020, Ma et al. 2020), rather than a single odds ratio, but as I was focussing on the calibration data and isoscapes rather than the assignment methods, I chose to examine the performance of these methods using a single, conservative, odds ratio instead (2:1). I measured precision as the proportion of cells in the raster which were

likely assigned compared to the total number of cells (Reese et al. 2019). This procedure was repeated 25 times for each dataset and isoscape pairing, with precision and minimum distance being summarized as the mean value across individuals within a given iteration. For inaccurately assigned individuals, I also measured the minimum distance (km) between the location of sampling for the known-origin individual and the closest cell of the region of likely origin (hereafter 'minimum distance'). I followed methods from Campbell et al. (2020) but used the function 'distance' within the package terra.

3.2.6   Test dataset

As a proof-of-concept, I reanalyzed data from Palumbo et al. (2020) on Blue-winged Teal harvested across Canada (2014–18; n = 144). This study represents a case where a diving duck (Lesser Scaup) calibration (Clark et al. 2006, 2009) was used to assign the geographic origins of a dabbling duck. This has been common in waterfowl studies to date, as six of eight published assignments for unknown-origin dabbling ducks or geese have used this equation (Ashley et al. 2010, Gunnarsson et al. 2012, Parejo et al. 2015, Roberts and Conover 2015, Asante et al. 2017, Guillemain et al. 2019, Palumbo et al. 2019, 2020). I chose to reanalyze Palumbo et al. (2020), as this study has direct management implications for the connectivity of harvested Blue-winged Teal. To facilitate direct comparison to the original publication, as these data were assigned separately for each harvest region, I subsetted these data and only analyzed birds harvested in the southern Saskatchewan harvest region because of its larger sample size (n = 47).

To assess the consequences of using different calibration equations to assign waterfowl origins, I repeated the assignment procedures above, but with the updated δ^2H_P grids (Bowen et al. 2005, Bowen 2021, Terzer-Wassmuth et al. 2021) and the calibration equations derived from the Dabblers and Divers datasets. Therefore, I applied six assignments: MGS_B + Dabblers, MA_B + Dabblers, MA_T + Dabblers, MGS_B + Divers, MA_B + Divers, and MA_T + Divers. I masked this isoscape to the Blue-winged Teal breeding range (BirdLife International and Handbook of the Birds of the World 2021). As these are unknown origin samples, there is no way to truly validate the accuracy of any

method, but my intention was simply to demonstrate the scale of differences relative to each other.

3.3   Results

I collected and processed $\delta^2 H_f$ values of 273 known-origin ducks (American Black Duck [n = 27], Green-winged Teal [n = 5], Blue-winged Teal [n = 2], Common Merganser [n = 1], Mallard [n = 124], Ring-necked Duck [n = 32], Wood Duck [n = 82]) across eastern North America (2017–21; Table 3.2). One site in Wisconsin showed more positive $\delta^2 H_f$ values than expected (mean [SD] = -85.8 ‰ [10.3 ‰]; Mallard [n = 7] and Wood Duck [n = 4]) likely due to irrigation and increased effect of evapotranspiration in shallow water due to the site's location on a cranberry farm. I removed 35 outliers whose $\delta^2 H_f$ values deviated from the site-specific mean $\delta^2 H_f$ (Clark [n = 2], van Dijk [n= 10], Hebert [n = 19], Kusack [n = 4]). These samples were excluded from all further analyses.

3.3.1   Calibration equations

Calibration relationships were generally consistent, with a positive linear relationship between $\delta^2 H_f$ and $\delta^2 H_p$ values within each dataset (Figure 3.2 and Figure 3.3). All calibration equations had a negative intercept term (range: -82.6 to -9.9 ‰) and a positive slope term (range: 0.5 to 1.2), but the magnitude of these terms varied (Table 3.3). Within each respective known-origin dataset, calibration equation model fit was only marginally different when derived using $\delta^2 H_p$ values that were extracted from the three different isoscapes (Table 3.3). Comparing different known-origin datasets there was a greater difference in model fit. For dabbling ducks (Figure 3.2), the calibration equation derived using the Hebert dataset showed almost double the amount of residual variation (~21 ‰) compared to van Dijk (~10 ‰) and Kusack (~14 ‰). For the calibration derived from the Dabblers dataset, model fit improved marginally (~17 ‰) compared to Hebert but was still greater than the other individual datasets. For diving ducks (Figure 3.3), where only a few additional samples (n = 33) were added to the Clark dataset, model fit was reduced slightly (Table 3.3).

Table 3.3 Summary of derived calibration equations.

Dataset	Isoscape[a]	Calibration	n	SD_{resid}	R^2
Dabblers	MGS_B	$\delta^2H_f = -69.9 + 0.7 * \delta^2H_p$	734	17.7	0.56
	MA_B	$\delta^2H_f = -71.7 + 0.6 * \delta^2H_p$	734	17.2	0.58
	MA_T	$\delta^2H_f = -62.0 + 0.7 * \delta^2H_p$	734	17.3	0.58
van Dijk (van Dijk et al. 2014)	MGS_B	$\delta^2H_f = -38.5 + 1.2 * \delta^2H_p$	202	10.0	0.65
	MA_B	$\delta^2H_f = -52.9 + 0.9 * \delta^2H_p$	202	9.6	0.68
	MA_T	$\delta^2H_f = -54.2 + 0.8 * \delta^2H_p$	202	9.9	0.65
Hebert (Hebert and Wassenaar 2005)	MGS_B	$\delta^2H_f = -59.1 + 0.7 * \delta^2H_p$	305	21.7	0.44
	MA_B	$\delta^2H_f = -62.7 + 0.6 * \delta^2H_p$	305	21.6	0.45
	MA_T	$\delta^2H_f = -62.9 + 0.7 * \delta^2H_p$	305	22.0	0.43
Kusack (Dabblers)	MGS_B	$\delta^2H_f = -66.9 + 0.8 * \delta^2H_p$	227	14.8	0.28
	MA_B	$\delta^2H_f = -76.7 + 0.5 * \delta^2H_p$	227	14.9	0.27
	MA_T	$\delta^2H_f = -75.1 + 0.5 * \delta^2H_p$	227	14.4	0.32
Divers	MGS_B	$\delta^2H_f = -82.6 + 0.5 * \delta^2H_p$	106	14.7	0.54
	MA_B	$\delta^2H_f = -78.4 + 0.5 * \delta^2H_p$	106	14.1	0.58
	MA_T	$\delta^2H_f = -63.1 + 0.6 * \delta^2H_p$	106	14.8	0.54
Clark (Clark et al. 2006, 2009)	MGS_B	$\delta^2H_f = -37.5 + 0.9 * \delta^2H_p$	73	12.6	0.63
	MA_B	$\delta^2H_f = -41.7 + 0.7 * \delta^2H_p$	73	12.4	0.64
	MA_T	$\delta^2H_f = -9.9 + 1.0 * \delta^2H_p$	73	13.1	0.60

SD_{resid}, standard deviation of residuals.

[a] MGS_B, Amount-weighted mean growing-season precipitation (Bowen 2021); MA_B, Amount-weighted mean annual precipitation (Bowen 2021); MA_T, Amount-weighted mean annual precipitation (Terzer-Wassmuth et al. 2021).
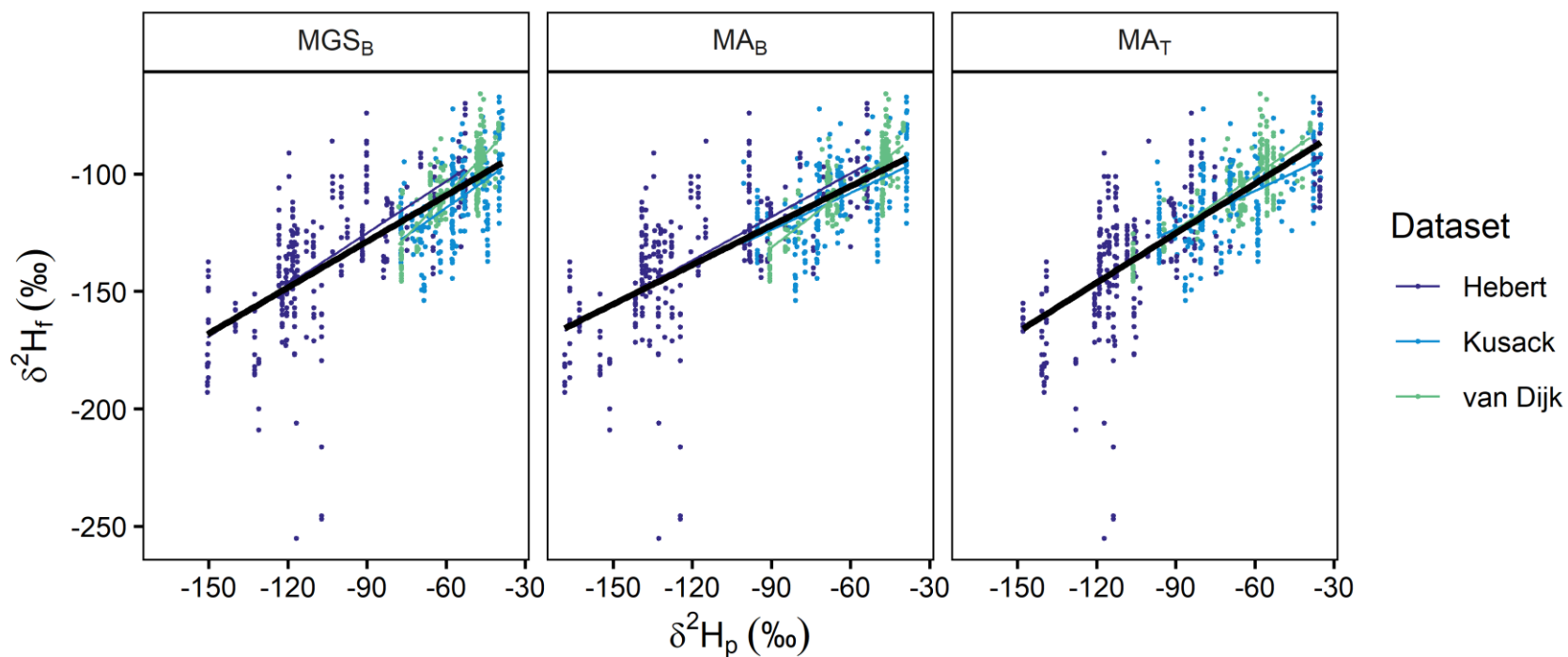
Figure 3.2 Dabbling duck calibration relationships. Linear relationships between δ^2H_p (amount-weighted mean growing-season precipitation, MGS$_B$, Bowen 2021; amount-weighted mean annual precipitation, MA$_B$, Bowen 2021; MA$_T$, Terzer-Wassmuth et al. 2021) and δ^2H_f from known-origin dabbling ducks. The solid black line shows an overall linear relationship and smaller lines show dataset-specific calibration relationships. Points show individual known-origin ducks, separated by dataset (shown in different colours).
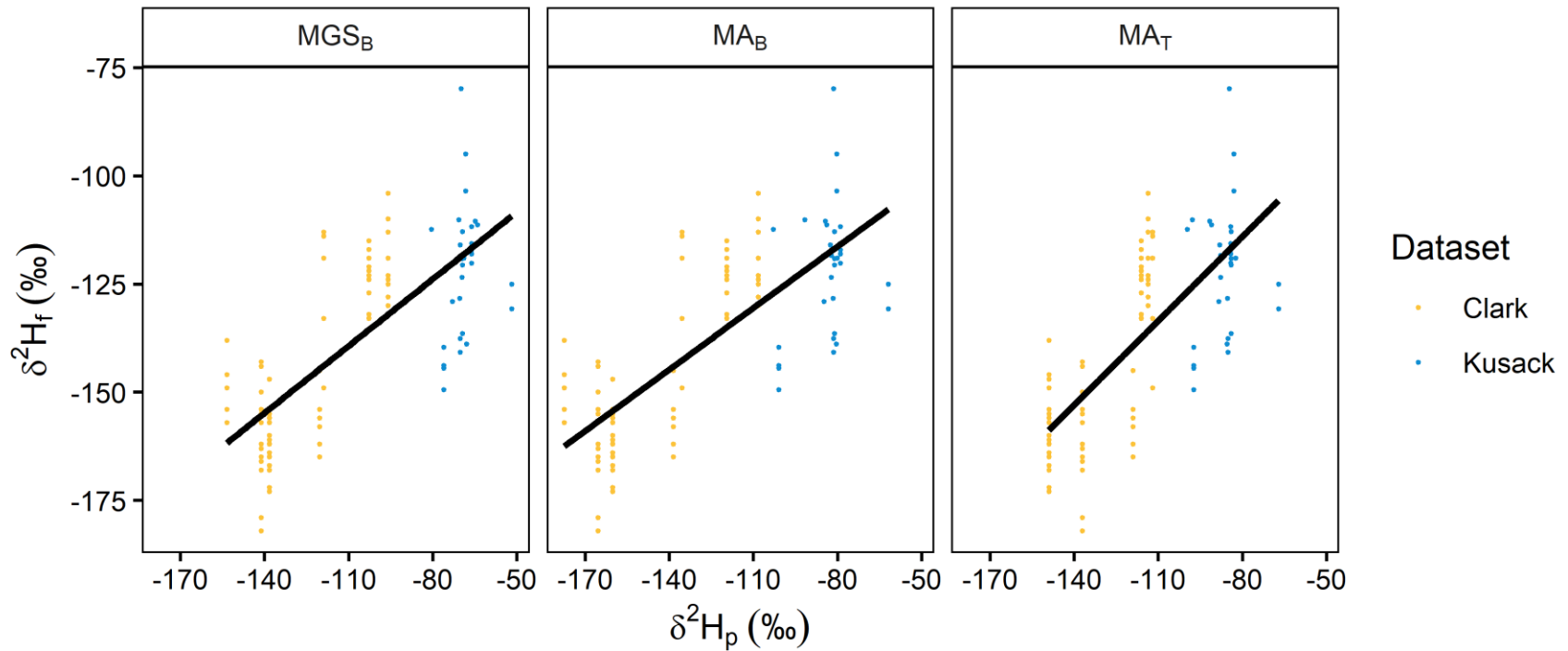
Figure 3.3 Diving duck calibration relationships. Linear relationships between δ^2H_p (amount-weighted mean growing-season precipitation, MGS$_B$, Bowen 2021; amount-weighted mean annual precipitation, MA$_B$, Bowen 2021; MA$_T$, Terzer-Wassmuth et al. 2021) and δ^2H_f from known-origin diving ducks. The solid black line shows an overall linear relationship. Points show individual known-origin ducks, separated by dataset (shown in different colours).

3.3.2   Model validation

Accuracy in assignment did not differ consistently among isoscapes when considering the same known-origin dataset but differed marginally among known-origin datasets (Figure 3.4). Estimates of mean accuracy from cross-validation procedures applied to dabbling duck datasets (van Dijk, Hebert, Kusack, Dabblers) all fell within a proportion of 0.66 ± 0.07 accurately assigned individuals (range = 0.63 to 0.73) while estimates for diving duck datasets (Clark, Divers) all fell within 0.66 ± 0.05 (range = 0.61 to 0.71), both consistent with the accuracy that I expected for the applied odds ratio (i.e., 0.66 for 2:1). The Dabblers dataset showed the highest accuracy, which was greater than expected (> 0.66), in all but four iterations across all three isoscapes. For the diving duck datasets, accuracy was more variable, and consistently lower than expected, on average, for the Divers dataset (accuracy < 0.66 for 61 of 75 iterations). Minimum distance showed some variability between datasets, but no strong differences were identified between the three isoscapes (Figure 3.4). Specifically, the van Dijk and Clark datasets showed the lowest values for minimum distance, but otherwise, the datasets showed similar minimum distances (mean [SD]; 290 km [52] Dabblers; 298 km [63] Hebert; 246 km [45] Kusack).

Mean precision was more variable between datasets compared to accuracy (Figure 3.4). For the van Dijk, Hebert, Clark, and Divers datasets, the MA_B calibrations showed the best precision follow by the MA_T and MGS_B grids respectfully, but again showed no consistent differences among the isoscapes for the Kusack and Dabblers datasets (Figure 3.4). The Kusack and Clark datasets showed the best precision (Figure 3.4), despite the Kusack dataset having the lowest R^2 (Table 3.3). For the Dabblers and Hebert datasets, precision was low and did not exceed 0.4 (Figure 3.4). For the Divers dataset, precision and accuracy were lower with the inclusion of the diving ducks from the Kusack dataset (Figure 3.4), despite a slight increase in sample size.
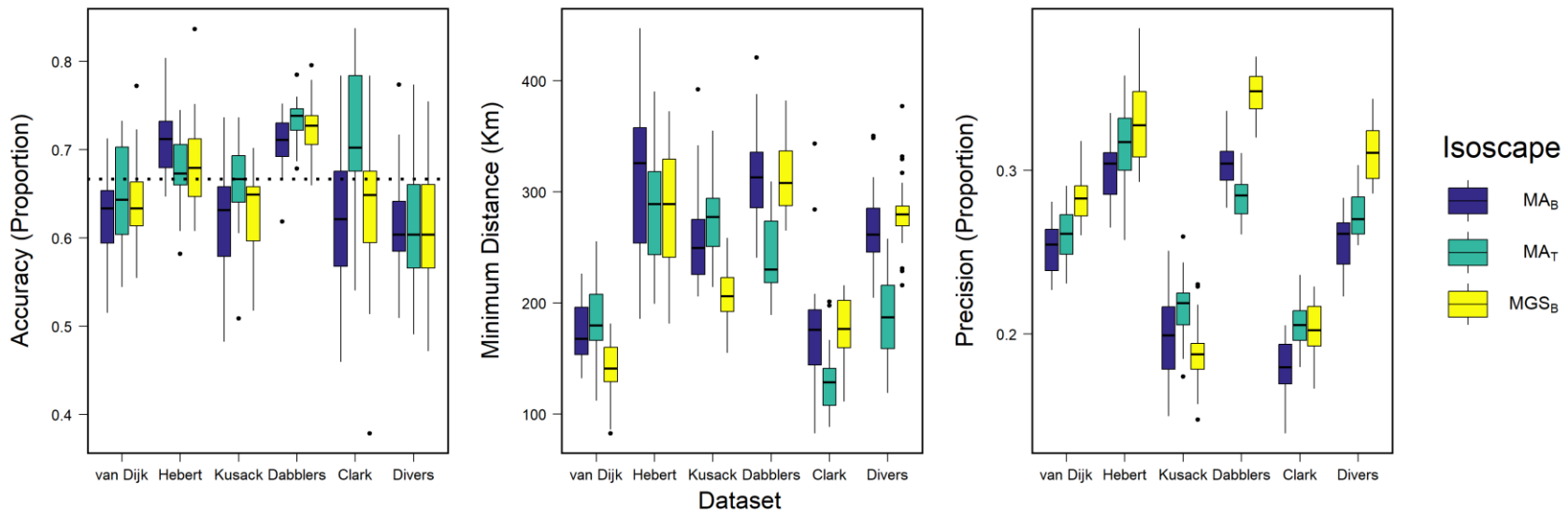
Figure 3.4 Accuracy, precision, and minimum distance distributions. Box and whisker plots showing distributions of accuracy, minimum distance, and precision from cross-validation procedures applied to the listed datasets. Validation results for different isoscapes (amount-weighted mean growing-season precipitation, MGS_B, Bowen 2021; amount-weighted mean annual precipitation, MA_B, Bowen 2021; MA_T, Terzer-Wassmuth et al. 2021) are shown in different colours. Boxplots show medians (horizontal lines within boxes), 25th and 75th quantiles (upper and lower limits of the boxes), upper and lower extreme values (whiskers), and outliers as values outside of 1.5 x the interquartile range (points). Dotted line (left) shows the expected accuracy for the applied odds ratio (2:1 or 0.66).

3.3.3   Test dataset

Likely origins were not noticeably altered by using the updated calibration equations for Dabblers or Divers (Figure 3.5), which showed likely origins of Blue-winged Teal in the northwestern Boreal Forest of northern British Columbia and Alberta (see Figure B1 for a recreation of the figure from Palumbo et al. 2020). This general result matches the results in the original publication, although at a higher resolution. Using the calibration equation derived from the Divers dataset tended to bias likely origins towards the northwest compared to using the Dabblers calibration, which showed similar origins to the original publication apart from greater likelihood to the south (Figure 3.5). As the residual standard deviation was greater (range = 14.1–17.7 ‰) than what was used in the original publication (12.8 ‰), the larger area of potential origin is not unexpected. The original publication also did not include isoscape uncertainty, as I have included in the MGS_B and MA_B assignments, which likely contributes to the broader areas. Aside from minor fluctuations in the upper and lower range and the maximum number of individuals assigned, the use of any specific isoscape did not significantly alter the final depiction, within each foraging guild.
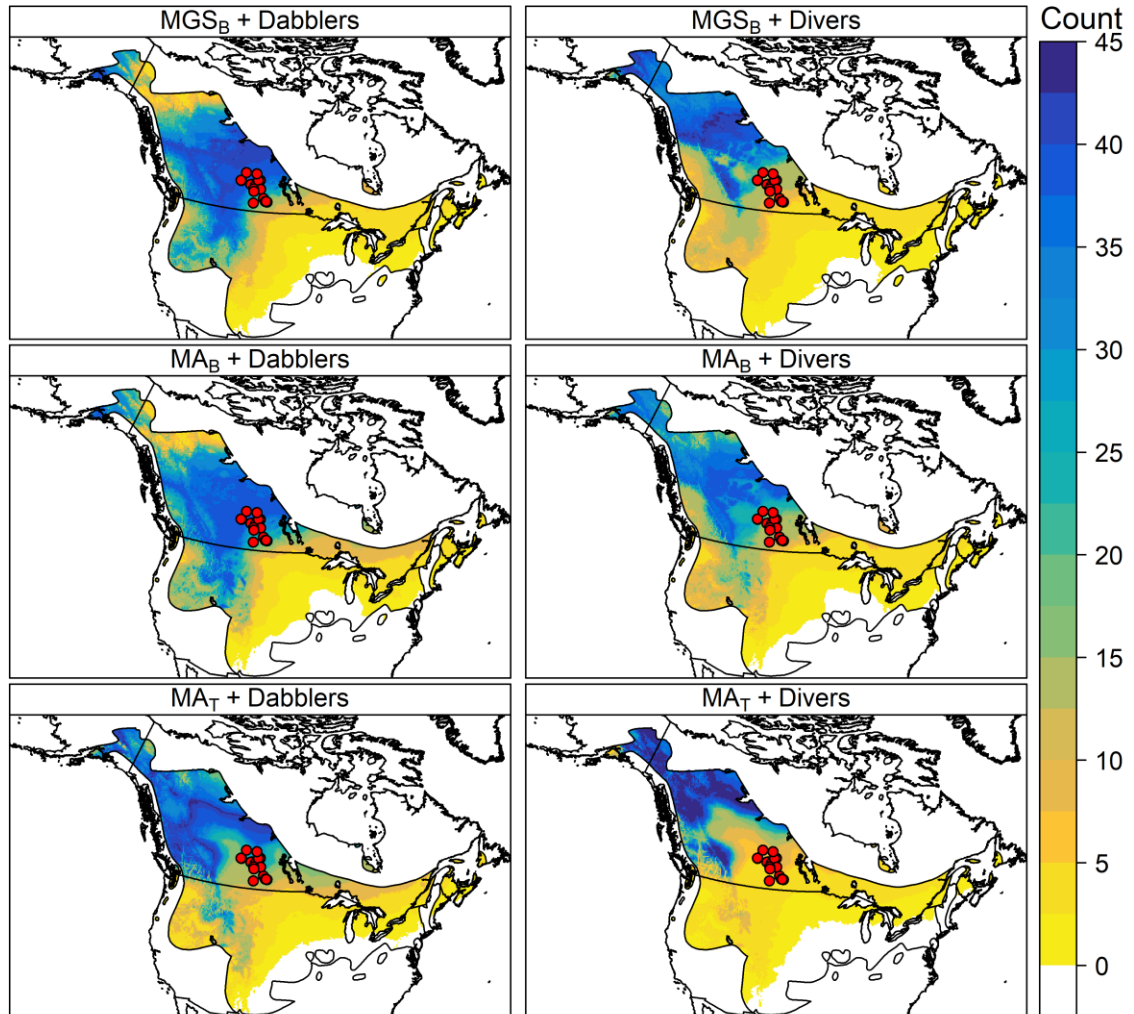
Figure 3.5 Test dataset results. Likely origins of Blue-winged Teal (*Spatula discors*) harvested in southern Saskatchewan (n = 47, 2014–18, Palumbo et al. 2020) using different assignment methods. Panels show likely origins determined using different precipitation isoscapes (amount-weighted mean growing-season precipitation, MGS$_B$ Bowen 2021; amount-weighted mean annual precipitation, MA$_B$ Bowen 2021; MA$_T$ Terzer-Wassmuth et al. 2021) and calibration equations (listed in the panel strip text: isoscape + calibration equation). The colour indicates the number of individuals that were assigned to a given pixel under a 2:1 odds ratio. Harvest locations for samples are shown as red points.

3.4   Discussion

Combining published and newly collected data, I (1) critically evaluated the relationship between δ^2H values of waterfowl feathers and precipitation at known sites of feather growth;(2) empirically tested the performance of three publicly-available isoscapes and four calibration datasets, including newly collected samples; and (3) derived updated calibration equations for diving and dabbling ducks that can be applied to future waterfowl studies in North America and Europe. As with numerous other studies, I found a strong positive relationship between δ^2H_f and δ^2H_p values, reinforcing the usefulness of using stable isotopes to determine likely origin for unknown-origin individuals. The MA and MGS isoscapes showed similar relationships with known-origin δ^2H_f values, suggesting that either MA or MGS is suitable for predicting δ^2H_f values. Finally, when I applied these different assignment methods to a test dataset, the region of most likely origin remained consistent overall, with some minor discrepancies.

Few studies have directly compared the suitability of MA and MGS methods for deriving isoscapes and relating them to consumer tissues. Bowen et al. (2005) compared the relationship between δ^2H_p and δ^2H_f for known-origin North American and European birds (based entirely on Hobson and Wassenaar 1997 for North America and Hobson et al. 2004 for Europe), using their derived MA and MGS grids, and found that neither isoscape fit significantly better (North America: MA $R^2 = 0.67$ and MGS $R^2 = 0.65$; Europe: MA $R^2 = 0.85$ and MGS $R^2 = 0.86$). In this study and ours, European birds showed a slightly better fit compared to North American birds, as demonstrated by the van Dijk dataset which had the highest coefficient of determination ($R^2 = 0.65–0.67$) compared to the North American datasets ($R^2 = 0.27–0.45$). I found that the van Dijk dataset showed the lowest minimum distance measures, which could be driven by the relatively smaller area in Europe compared to North America.

My results suggest that MA or MGS perform equally well for predicting surface water inputs into food webs for foraging waterfowl, regardless of foraging strategy, as both δ^2H_p values correlated comparably with known-origin δ^2H_f values. It is worth noting that calibration relationships using MA or MGS δ^2H_p never explained more than ~ 50–60 % of the variance. These values are consistent with what has been seen in other single-

species or multi-taxa studies (e.g., Accipitriformes and Falconiformes $R^2 = 0.64$, Crowley et al. 2021; Charadriiformes, Columbiformes, Galliformes, Passeriformes, and Piciformes $R^2 = 0.54$–0.66, Hobson et al. 2004; Northern long-eared bat *Myotis septentrionalis* $R^2 = 0.47$–0.53, Britzke et al. 2009), although other, better fitting, examples exist (e.g., Chiroptera $R^2 = 0.72$, Popa-Lisseanu et al. 2012; Coleoptera $R^2 = 0.74$–0.78, Gröcke et al. 2006; Odonata $R^2 = 0.75$, Hobson et al. 2012*a*; Passeriformes $R^2 = 0.83$, Hobson and Wassenaar 1997; see Table B1 for further examples). The single most likely contributor to this variation for waterfowl is the mismatch between predicted food web water δ^2H based on precipitation and that manifested on the ground. Other authors have pointed to the effects of evapotranspiration in small wetlands (Coulton et al. 2009) as well as differential inputs from snowmelt and complex hydrology (Cavallaro et al. 2022), but other sources of inter- and intraspecific variation, such as diet, timing of moult, and metabolic routing (Wunder et al. 2012, Nordell et al. 2016), also undoubtedly contribute. This unexplained variability within these calibration models may be enough to mask these differences in fit between the MA or MGS methods, nullifying the usefulness of more specific or more general δ^2H_p measurements.

I initially expected that MA δ^2H_p would provide better integration of water isotope data compared to MGS δ^2H_p values for northern-origin individuals. The contribution of snowmelt to waterfowl feathers would be more pronounced for individuals breeding in the far north, where prolonged colder temperatures lead to more snowfall and a greater contribution of snowmelt to waterbodies. Here it would be expected to see relatively more negative δ^2H_f values due to the greater contribution of snowmelt, which for a given location should have relatively more negative δ^2H_p values compared to rain (Clark and Fritz 1997). For my sampling in eastern Canada and the USA, these far northern individuals were mostly unavailable as I relied entirely on pre-existing banding operations to collect feathers, none of which were farther north than ~50 °N. For southern-origin waterfowl, fewer months below freezing means the MGS grid approximates the MA grid (Figure B2), so these differences are mostly negligible. At more northern latitudes, with colder climates, it would be expected to have a greater contribution of snowmelt (Coulton et al. 2009). What I found instead was greater variability in δ^2H_f for known-origin ducks in regions with more negative δ^2H_p values,

which generally are found in the far north. In the Hebert dataset, individuals sampled at locations with lower δ^2H_p values (< -100 ‰), variability in δ^2H_f was greater, with more δ^2H_f values being lower than the predicted δ^2H_f values. Many individuals in this range were also removed as outliers before analysis (n = 18). From these outliers, the majority were found in the prairies (n = 15; 14 Mallard and 1 Northern Pintail) although they were not restricted to a specific species/region and did not represent the entirety of samples at any given site. This is surprising as I would expect relatively higher δ^2H_f values due to surface water becoming progressively more enriched in deuterium during evaporative processes (Clark and Fritz 1997, Coulton et al. 2009), but this was not the case. For these outliers, especially for those in the far north (n = 1 Alaska, n = 2 Northwest Territories), this may indicate that snowmelt was disproportionately important, but without further investigation, it is difficult to be sure. That said, I still saw many individuals clustered around the predicted δ^2H_f values.

Comparing calibration equations derived from dabblers and divers, there were clear differences, but the sample size disparity between the two was significant (n = 734 and 106, respectively). As such, it is difficult to validate the performance of the diving duck data. When additional diving duck samples were added from my samples to the Clark dataset, performance decreased across all measures, including accuracy. This slight decrease in accuracy is not unexpected as this equation included multiple diving duck species compared to the Clark dataset which was only Lesser Scaup. It is clear from these results that additional samples for known-origin diving ducks should be collected to build a more robust diving duck calibration dataset.

3.4.1 Limitations

Propagating realistic estimates of error into isotopic assignments using isoscapes is integral to achieving realistic results useful for conservation and management (Wunder and Norris 2008). Although I incorporated calibration error in these likelihood-based assignments, I did not explicitly account for isoscape interpolation error when validating the MA_T grid, as this measure was unavailable. If these error estimates are available in the future, these methods can properly incorporate isoscape error into these assessments. Regardless, my current focus on choosing the best calibration algorithm remains

unaffected as even without this error measurement, the assignments for the test dataset showed overall the same regions of likely origin.

I did not account for age effects in my models, despite including adults in the samples collected here and those from the van Dijk dataset (van Dijk et al. 2014). In van Dijk et al. (2014), accounting for age effects, while simultaneously controlling for year effects, resulted in a marginally better calibration model fit (0.71 compared to 0.61). Here, juvenile feathers showed lower δ^2H_f values compared to adults (difference = -6.8 ‰), which is consistent across other avian taxa, such as American Redstart *Setophaga ruticilla* (Langin et al. 2007), Bicknell's Thrush *Catharus bicknelli* (Studds et al. 2012), Cooper's Hawk *Accipiter cooperii* (Meehan et al. 2003), and Ovenbird *Seiurus aurocapilla* (Haché et al. 2012). This effect is likely to be driven by adult birds experiencing higher body water loss due to increased provisioning effort before moult leading to enriched δ^2H_f values (Studds et al. 2012), different feather growth rates, or dietary routing or microclimate differences between nestlings and adults (Langin et al. 2007). In practice, this difference in δ^2H_f of adults and juveniles may not lead to a noticeable difference in the assignment. For example, using the Blue-winged Teal test dataset, randomly selecting an individual (ID = 2014_SK-01, δ^2H_f = -159.3 ‰), increase and decrease the δ^2H_f value by 6.8 ‰, and repeat the assignment procedures, I get a distance of 192 and 383 km between the centroids of the resulting binary regions and the centroid of the binary region from the original value. With the geographic scales that I am working with in most of these assignments (usually the breeding range of a species), these distances would be negligible. Regardless, for my analyses, this information was not available in the assignR database, but access to this information would improve the usefulness of these and future known-origin data.

I relied on published isoscape grids rather than year-specific, month-specific, or other custom isoscapes produced using platforms such as isoMAP (Bowen et al. 2014). This choice served two main purposes: 1) these freely-available grids are the main isoscapes already used in waterfowl calibration studies (only three publications used custom surfaces (Tonra et al. 2015, Reese et al. 2019, Wommack et al. 2020), other than the kriged surfaces used before 2005) and 2) these grids represent the most user-friendly

source of isotope data. Further, while short-term δ^2H_p measures may be more specific, they often result in increased uncertainty due to reduced spatial coverage from sampling points (Vander Zanden et al. 2014). At the time of this publication, the isoMAP server was unsupported and may not be available for future studies. Overall, my intention here was to provide actionable and easily accessible recommendations that can be used by waterfowl managers and researchers.

I assembled as large a sample of known-origin waterfowl feathers as possible to maximize power for describing calibration relationships although this work could be further improved with larger sample sizes. For example, banding operations, especially those occurring in remote areas, should consider collecting feathers from local HY birds during regular banding operations. Several other studies contain known-origin duck tissues (Szymanski et al. 2007, Coulton et al. 2009), which could be integrated with the growing database to define these relationships. Another valuable, but uncommon, source is banded known-origin HY birds submitted to the North American Waterfowl Parts Collection (Raftovich et al. 2022) and Species Composition Surveys (Gendron and Smith 2019), although using these incidental sources of feather collection comes with some necessary assumptions (e.g., harvested individuals have not opportunistically regrown feathers since banding). These surveys are excellent sources of feathers from harvested birds (Palumbo et al. 2020, Kusack et al. 2022, Kucia et al. 2023) but have been underutilized to date. All δ^2H_f data used here are available (Kusack et al. 2023) for future calibration studies and help build upon the literature describing these relationships (see Table B1). As this isotopic database grows, researchers will be able to combine and compartmentalize the data to directly derive the necessary calibration equations from their own environmental water measurements or other custom isoscape. This workflow is recommended in packages like assignR (Ma et al. 2020). Adding to these databases allows us to not only better describe these $\delta^2H_f \sim \delta^2H_p$ relationships, in a changing world, but also to refine these into more specific (e.g., by taxa, age, diet) calibration relationships, as necessary.

3.4.2   Recommendations

Waterfowl conservation and management can benefit greatly from the adoption of stable-isotope methods. These assignment techniques are not new to waterfowl applications (Hobson et al. 2009*b*, Ashley et al. 2010, Gunnarsson et al. 2012, Guillemain et al. 2014, 2019, Parejo et al. 2015, Roberts and Conover 2015, Caizergues et al. 2016, Asante et al. 2017, Palumbo et al. 2019, 2020) but have yet to be used routinely or other than for a few specific species. In the early days of isotopic assignment, use of published calibration equations was often necessary, but we are now at the stage where users can use publicly available known-origin data to derive or supplement calibrations as needed. Whether deriving the calibration using such data or using the equations presented here (see Table 3.3), I recommend the use of the combined foraging-guild-specific calibration datasets (Dabblers, MGS_B: $\delta^2H_f = -69.9 + 0.7 * \delta^2H_p$; MA_B: $\delta^2H_f = -71.7 + 0.6 * \delta^2H_p$ and Divers, MGS_B: $\delta^2H_f = -82.6 + 0.5 * \delta^2H_p$; MA_B: $\delta^2H_f = -78.4 + 0.5 * \delta^2H_p$) for general applications to assign unknown-origin waterfowl in North America and Europe. For regional and species-specific studies, such as the assignment of unknown origin Mallard in Europe, the use of the more specific dataset for that species and/or region (van Dijk ~ MGS_B in this case) is warranted. Although the Dabblers dataset showed lower precision and model fit compared to the individual dabbling duck datasets, I consider the Dabblers dataset to be the most conservative and realistic relationship. Similarly, for diving ducks my derived calibration equation for the combined Divers dataset offers little improvement over the Clark dataset, but I still recommend using the more general dataset including multiple diving duck species, unless the application is for Lesser Scaup specifically. While the RCWIP2 isoscape has advantages based on more advanced algorithms (Terzer-Wassmuth et al. 2021), it is computationally challenging due to computer memory requirements and currently has no associated error estimates. Although (Terzer-Wassmuth et al. 2021) lists the "40-fold" increase in resolution as an overall improvement, use of the RCWIP2 isoscape is currently limited. Ultimately, for waterfowl, neither MGS_B nor MA_B measurements presented a markedly better relationship and the use of either grid could is justified, although precision was marginally better for MA_B. Refining these relationships is important, but understanding

the limitations of the approach is absolutely necessary to interpret results from isotopic assignment methods.

3.5   References

Asante, C. K., T. D. Jardine, S. L. Van Wilgenburg, and K. A. Hobson. 2017. Tracing origins of waterfowl using the Saskatchewan River Delta: incorporating stable isotope approaches in continent-wide waterfowl management and conservation. The Condor 119:261–274.

Ashley, P., K. A. Hobson, S. L. Van Wilgenburg, N. North, and S. A. Petrie. 2010. Linking Canadian harvested juvenile American Black Ducks to their natal areas using stable isotope (δD, δ^{13}C, and δ^{15}N) methods. Avian Conservation and Ecology 5:7.

BirdLife International and Handbook of the Birds of the World. 2021. Bird species distribution maps of the world. Version 2020.1. <http://datazone.birdlife.org/species/requestdis.>. Accessed 16 May 2021.

Boulet, M., and D. R. Norris. 2006. The past and present of migratory connectivity. Ornithological Monographs 61:1–13.

Bowen, G. J. 2021. Gridded maps of the isotopic composition of meteoric waters. <http://www.waterisotopes.org.>. Accessed 23 Aug 2021.

Bowen, G. J., Z. Liu, H. B. Vander Zanden, L. Zhao, and G. Takahashi. 2014. Geographic assignment with stable isotopes in IsoMAP. Methods in Ecology and Evolution 5:201–206.

Bowen, G. J., and J. Revenaugh. 2003. Interpolating the isotopic composition of modern meteoric precipitation. Water Resources Research 39:1299.

Bowen, G. J., L. I. Wassenaar, and K. A. Hobson. 2005. Global application of stable hydrogen and oxygen isotopes to wildlife forensics. Oecologia 143:337–348.

Britzke, E. R., S. C. Loeb, K. A. Hobson, C. S. Romanek, and M. J. Vonhof. 2009. Using hydrogen isotopes to assign origins of bats in the eastern United States. Journal of Mammalogy 90:743–751.

Buchanan, G. M., A. L. Bond, N. J. Crockford, J. Kamp, J. W. Pearce-Higgins, and G. M. Hilton. 2018. The potential breeding range of Slender-billed Curlew *Numenius tenuirostris* identified from stable-isotope analysis. Bird Conservation International 28:228–237.

Caizergues, A., S. L. Van Wilgenburg, and K. A. Hobson. 2016. Unraveling migratory connectivity of two European diving ducks: a stable isotope approach. European Journal of Wildlife Research 62:701–711.

Campbell, C. J., M. C. Fitzpatrick, H. B. Vander Zanden, and D. M. Nelson. 2020. Advancing interpretation of stable isotope assignment maps: comparing and summarizing origins of known-provenance migratory bats. Animal Migration 7:27–41.

Cavallaro, M. C., C. I. Michelson, T. L. Lewis, A. DuBour, M. Lindberg, K. A. Hobson, and R. G. Clark. 2022. Characterizing spatial and temporal variation in stable hydrogen isotopes (δ^2H) between two distinct lentic freshwater food webs. Aquatic Sciences 84:51.

Clark, I., and P. Fritz. 1997. Environmental Isotopes in Hydrogeology. Lewis Publishers, Boca Raton, FL, USA.

Clark, R. G., K. A. Hobson, and L. I. Wassenaar. 2006. Geographic variation in the isotopic (δD, δ^{13}C, δ^{15}N, δ^{34}S) composition of feathers and claws from Lesser Scaup and Northern Pintail: implications for studies of migratory connectivity. Canadian Journal of Zoology 84:1395–1401.

Clark, R. G., K. A. Hobson, and L. I. Wassenaar. 2009. Corrigendum—Geographic variation in the isotopic (δD, δ^{13}C, δ^{15}N, δ^{34}S) composition of feathers and claws from Lesser Scaup and Northern Pintail: implications for studies of migratory connectivity. Canadian Journal of Zoology 87:553–554.

Coulton, D. W., R. G. Clark, K. A. Hobson, L. I. Wassenaar, and C. E. Hebert. 2009. Temporal sources of deuterium (δD) variability in waterfowl feathers across a prairie-to-boreal gradient. The Condor 111:255–265.

Crowley, B. E., C. P. Bataille, B. A. Haak, and K. M. Sommer. 2021. Identifying nesting grounds for juvenile migratory birds with dual isotope: an initial test using North American raptors. Ecosphere 12:e03765.

Cryan, P. M., M. A. Bogan, R. O. Rye, G. P. Landis, and C. L. Kester. 2004. Stable hydrogen isotope analysis of bat hair as evidence for seasonal molt and long-distance migration. Journal of Mammalogy 85:995–1001.

Cryan, P. M., C. A. Stricker, and M. B. Wunder. 2014. Continental-scale, seasonal movements of a heterothermic migratory tree bat. Ecological Applications 24:602–616.

van Dijk, J. G., W. Meissner, and M. Klaassen. 2014. Improving provenance studies in migratory birds when using feather hydrogen stable isotopes. Journal of Avian Biology 45:103–108.

Flack, A., E. O. Aikens, A. Kölzsch, E. Nourani, K. R. S. Snell, W. Fiedler, N. Linek, H.-G. Bauer, K. Thorup, J. Partecke, M. Wikelski, and H. J. Williams. 2022. New frontiers in bird migration research. Current Biology 32:R1187–R1199.

Fournier, A. M. V., A. R. Sullivan, J. K. Bump, M. Perkins, M. C. Shieldcastle, and S. L. King. 2017. Combining citizen science species distribution models and stable isotopes reveals migratory connectivity in the secretive Virginia rail. Journal of Applied Ecology 54:618–627.

Fox, A. D., K. A. Hobson, and J. Kahlert. 2009. Isotopic evidence for endogenous protein contributions to greylag goose *Anser anser* flight feathers. Journal of Avian Biology 40:108–112.

Gendron, M., and A. Smith. 2019. National Harvest Survey website. Canadian Wildlife Service, Environment and Climate Change Canada, Ottawa, Ontario. <https://wildlife-species.canada.ca/harvest-survey>. Accessed 28 Jan 2020.

Gröcke, D. R., A. Schimmelmann, S. Elias, and R. F. Miller. 2006. Stable hydrogen-isotope ratios in beetle chitin: preliminary European data and re-interpretation of North American data. Quaternary Science Reviews 25:1850–1864.

Guillemain, M., L. Bacon, K. J. Kardynal, A. Olivier, M. Podhrazsky, P. Musil, and K. A. Hobson. 2019. Geographic origin of migratory birds based on stable isotope analysis: the case of the greylag goose (*Anser anser*) wintering in Camargue, southern France. European Journal of Wildlife Research 65:67.

Guillemain, M., S. L. Van Wilgenburg, P. Legagneux, and K. A. Hobson. 2014. Assessing geographic origins of Teal (*Anas crecca*) through stable-hydrogen (δ^2H) isotope analyses of feathers and ring-recoveries. Journal of Ornithology 155:165–172.

Gunnarsson, G., N. Latorre-Margalef, K. A. Hobson, S. L. Van Wilgenburg, J. Elmberg, B. Olsen, R. A. M. Fouchier, and J. Waldenström. 2012. Disease dynamics and bird migration — Linking Mallards *Anas platyrhynchos* and subtype diversity of the Influenza A virus in time and space. PLOS One 7:e35679.

Haché, S., K. A. Hobson, M.-A. Villard, and E. M. Bayne. 2012. Assigning birds to geographic origin using feather hydrogen isotope ratios (δ^2H): importance of year, age, and habitat. Canadian Journal of Zoology 90:722–728.

Hebert, C. E., and L. I. Wassenaar. 2005. Feather stable isotopes in western North American waterfowl: spatial patterns, underlying factors, and management applications. Wildlife Society Bulletin 33:92–102.

Hijmans, R. J. 2021. terra: spatial data analysis. R package version 1.1-4. <https://CRAN.R-project.org/package=terra>.

Hobson, K. A. 2019. Application of isotopic methods to tracking animal movements. Pages 85–115 *in* K. A. Hobson and L. I. Wassenaar, editors. Tracking Animal Migration with Stable Isotopes. Second Edition. Academic Press, Cambridge, MA, USA.

Hobson, K. A., G. J. Bowen, L. I. Wassenaar, Y. Ferrand, and H. Lormee. 2004. Using stable hydrogen and oxygen isotope measurements of feathers to infer geographical origins of migrating European birds. Oecologia 141:477–488.

Hobson, K. A., K. Doward, K. J. Kardynal, and J. N. McNeil. 2018. Inferring origins of migrating insects using isoscapes: a case study using the true armyworm, *Mythimna unipuncta*, in North America. Ecological Entomology 43:332–341.

Hobson, K. A., K. J. Kardynal, and G. Koehler. 2019. Expanding the isotopic toolbox to track Monarch butterfly (*Danaus plexippus*) origins and migration: on the utility of stable oxygen isotope (δ^{18}O) measurements. Frontiers in Ecology and Evolution 7:224.

Hobson, K. A., H. Lormée, S. L. Van Wilgenburg, L. I. Wassenaar, and J. M. Boutin. 2009*a*. Stable isotopes (δD) delineate the origins and migratory connectivity of harvested animals: the case of European woodpigeons. Journal of Applied Ecology 46:572–581.

Hobson, K. A., D. X. Soto, D. R. Paulson, L. I. Wassenaar, and J. H. Matthews. 2012*a*. A dragonfly (δ^2H) isoscape for North America: a new tool for determining natal origins of migratory aquatic emergent insects. Methods in Ecology and Evolution 3:766–772.

Hobson, K. A., S. L. Van Wilgenburg, L. I. Wassenaar, and K. Larson. 2012*b*. Linking hydrogen (δ^2H) isotopes in feathers and precipitation: sources of variance and consequences for assignment to isoscapes. PLOS One 7:e35137.

Hobson, K. A., and L. I. Wassenaar. 1997. Linking breeding and wintering grounds of neotropical migrant songbirds using stable hydrogen isotopic analysis of feathers. Oecologia 109:142–148.

Hobson, K. A., L. I. Wassenaar, and O. R. Taylor. 1999. Stable isotopes (δD and δ^{13}C) are geographic indicators of natal origins of monarch butterflies in eastern North America. Oecologia 120:397–404.

Hobson, K. A., M. B. Wunder, S. L. Van Wilgenburg, R. G. Clark, and L. I. Wassenaar. 2009*b*. A method for investigating population declines of migratory birds using stable isotopes: origins of harvested Lesser Scaup in North America. PLOS One 4:e7915.

International Atomic Energy Agency and World Meteorological Organization. 2015. Global Network of Isotopes in Precipitation. The GNIP database. <https://nucleus.iaea.org/wiser>.

International Atomic Energy Agency and World Meteorological Organization. 2023. Global Network of Isotopes in Precipitation. The GNIP database. <https://nucleus.iaea.org/wiser>.

Kucia, S. R., M. L. Schummer, J. W. Kusack, K. A. Hobson, and C. A. Nicolai. 2023. Origins of Mallards harvested in the Atlantic flyway of North America: implications for conservation and management. Avian Conservation and Ecology 18:10.

Kusack, J. W., D. C. Tozer, K. M. Harvey, M. L. Schummer, and K. A. Hobson. 2023. Data from: Assigning harvested waterfowl to geographic origin using feather δ2H isoscapes: What is the best analytical approach? Dryad, Dataset. <https://doi.org/10.5061/dryad.9w0vt4bmd>.

Kusack, J. W., D. C. Tozer, M. L. Schummer, and K. A. Hobson. 2022. Origins of harvested American black ducks: stable isotopes support the flyover hypothesis. The Journal of Wildlife Management 87:e22324.

Langin, K. M., M. W. Reudink, P. P. Marra, D. R. Norris, T. K. Kyser, and L. M. Ratcliffe. 2007. Hydrogen isotopic variation in migratory bird tissues of known origin: implications for geographic assignment. Oecologia 152:449–457.

Lott, C. A., T. D. Meehan, and J. A. Heath. 2003. Estimating the latitudinal origins of migratory birds using hydrogen and sulfur stable isotopes in feathers: influence of marine prey base. Oecologia 134:505–510.

Lott, C. A., and J. P. Smith. 2006. A Geographic-Information-System approach to estimating the origin of migratory raptors in North America using stable hydrogen isotope ratios in feathers. The Auk 123:822–835.

Ma, C., H. B. Vander Zanden, M. B. Wunder, and G. J. Bowen. 2020. assignR: an R package for isotope-based geographic assignment. Methods in Ecology and Evolution 11:996–1001.

Magozzi, S., C. P. Bataille, K. A. Hobson, M. B. Wunder, J. D. Howa, A. Contina, H. B. Vander Zanden, and G. J. Bowen. 2021. Calibration chain transformation improves the comparability of organic hydrogen and oxygen stable isotope data. Methods in Ecology and Evolution 12:732–747.

Meehan, T. D., J. T. Giermakowski, and P. M. Cryan. 2004. GIS-based model of stable hydrogen isotope ratios in North American growing-season precipitation for use in animal movement studies. Isotopes in Environmental and Health Studies 40:291–300.

Meehan, T. D., R. N. Rosenfield, V. N. Atudore, J. Bielefeldt, L. J. Rosenfield, A. C. Stewart, W. E. Stout, and M. A. Bozek. 2003. Variation in hydrogen stable-isotope ratios between adult and nestling Cooper's Hawks. The Condor 105:567–572.

Nordell, C. J., S. Haché, E. M. Bayne, P. Sólymos, K. R. Foster, C. M. Godwin, R. Krikun, P. Pyle, and K. A. Hobson. 2016. Within-site variation in feather stable hydrogen isotope (δ^2H$_f$) values of boreal songbirds: implications for assignment to molt origin. PLOS One 11:e0163957.

Ouin, A., P. Menozzi, M. Coulon, A. J. Hamilton, J. P. Sarthou, N. Tsafack, A. Vialatte, and S. Ponsard. 2011. Can deuterium stable isotope values be used to assign the geographic origin of an auxiliary hoverfly in south-western France? Rapid Communications in Mass Spectrometry 25:2793–2798.

Palumbo, M. D., J. W. Kusack, D. C. Tozer, S. W. Meyer, C. Roy, and K. A. Hobson. 2020. Source areas of Blue-winged Teal harvested in Ontario and Prairie Canada based on stable isotopes: implications for sustainable management. Journal of Field Ornithology 91:64–76.

Palumbo, M. D., D. C. Tozer, and K. A. Hobson. 2019. Origins of harvested Mallards from Lake St. Clair, Ontario: a stable isotope approach. Avian Conservation and Ecology 14:3.

Parejo, M., J. G. Navedo, J. S. Gutiérrez, J. M. Abad-Gómez, A. Villegas, C. Corbacho, J. M. Sánchez-Guzmán, and J. A. Masero. 2015. Geographical origin of dabbling ducks wintering in Iberia: sex differences and implications for pair formation. Ibis 157:536–544.

Pebesma, E. 2018. Simple features for R: standardized support for spatial vector data. The R Journal 10:439–446.

Popa-Lisseanu, A. G., K. Sörgel, A. Luckner, L. I. Wassenaar, C. Ibáñez, S. Kramer-Schadt, M. Ciechanowski, T. Görföl, I. Niermann, G. Beuneux, R. W. Mysłajek, J. Juste, J. Fonderflick, D. H. Kelm, and C. C. Voigt. 2012. A triple-isotope approach to predict the breeding origins of European bats. PLOS One 7:e30388.

Procházka, P., S. L. Van Wilgenburg, J. M. Neto, R. Yosef, and K. A. Hobson. 2013. Using stable hydrogen isotopes (δ^2H) and ring recoveries to trace natal origins in a Eurasian passerine with a migratory divide. Journal of Avian Biology 44:541–550.

Pyle, P. 2005. Molts and plumages of ducks (*Anatinae*). Waterbirds 28:208–219.

R Core Team. 2021. R: a language and environment for statistical computing. R Foundation for Statistical Computing, Vienna, AT.

Raftovich, R., K. Fleming, S. Chandler, and C. Cain. 2022. Migratory bird hunting activity and harvest during the 2020-21 and 2021-22 hunting seasons. U.S. Fish and Wildlife Service, Laurel, MD, USA.

Reese, J., C. Viverette, C. M. Tonra, N. J. Bayly, T. J. Boves, E. Johnson, M. Johnson, P. Marra, E. M. Ames, A. Caguazango, M. DeSaix, A. Matthews, A. Molina, K. Percy, M. C. Slevin, and L. Bulluck. 2019. Using stable isotopes to estimate migratory connectivity for a patchily distributed, wetland-associated Neotropical migrant. The Condor 121:duz052.

Roberts, A. J., and M. R. Conover. 2015. Breeding origins of Northern Shovelers (*Anas clypeata*) wintering on the Great Salt Lake, Utah. The Wilson Journal of Ornithology 127:233–238.

Royle, J. A., and D. R. Rubenstein. 2004. The role of species abundance in determining breeding origins of migratory birds with stable isotopes. Ecological Applications 14:1780–1788.

RStudio Team. 2021. RStudio: integrated development for R. RStudio, Inc., Boston, MA, USA.

Salomonsen, F. 1968. The moult migration. Wildfowl 19:5–24.

Schummer, M. L., J. Simpson, B. Shirkey, S. R. Kucia, P. Lavretsky, and D. C. Tozer. 2023. Population genetics and geographic origins of mallards harvested in northwestern Ohio. PLOS One 18:e0282874.

Seifert, N., M. Haase, S. L. Van Wilgenburg, C. C. Voigt, and A. Schmitz Ornés. 2016. Complex migration and breeding strategies in an elusive bird species illuminated by genetic and isotopic markers. Journal of Avian Biology 47:275–287.

Solovyeva, D., K. A. Hobson, N. Kharitonova, J. Newton, J. W. Fox, V. Afansyev, and A. D. Fox. 2016. Combining stable hydrogen (δ^2H) isotopes and geolocation to assign Scaly-sided Mergansers to moult river catchments. Journal of Ornithology 157:663–669.

South, A. 2017. rnaturalearth: world map data from natural earth. R package version 0.1.0. <https://CRAN.R-project.org/package=rnaturalearth>.

Studds, C. E., K. P. McFarland, Y. Aubry, C. C. Rimmer, K. A. Hobson, P. P. Marra, and L. I. Wassenaar. 2012. Stable-hydrogen isotope measures of natal dispersal reflect observed population declines in a threatened migratory songbird. Diversity and Distributions 18:919–930.

Szymanski, M. L., A. D. Afton, and K. A. Hobson. 2007. Use of stable isotope methodology to determine natal origins of Mallards at a fine scale within the Upper Midwest. The Journal of Wildlife Management 71:1317–1324.

Terzer, S., L. I. Wassenaar, L. J. Araguás-Araguás, and P. K. Aggarwal. 2013. Global isoscapes for δ^{18}O and δ^2H in precipitation: improved prediction using regionalized climatic regression models. Hydrology and Earth System Sciences 17:4713–4728.

Terzer-Wassmuth, S., L. I. Wassenaar, J. M. Welker, and L. J. Araguás. 2021. Improved high-resolution global and regionalized isoscapes of δ^{18}O, δ^2H, and d-excess in precipitation. Hydrological Processes 35:e14254.

Tonra, C. M., C. Both, and P. P. Marra. 2015. Incorporating site and year-specific deuterium ratios (δ^2H) from precipitation into geographic assignments of a migratory bird. Journal of Avian Biology 46:266–274.

Vander Zanden, H. B., M. B. Wunder, K. A. Hobson, S. L. Van Wilgenburg, L. I. Wassenaar, J. M. Welker, and G. J. Bowen. 2014. Contrasting assignment of migratory organisms to geographic origins using long-term versus year-specific precipitation isotope maps. Methods in Ecology and Evolution 5:891–900.

Wassenaar, L. I., and K. A. Hobson. 2003. Comparative equilibration and online technique for determination of non-exchangeable hydrogen of keratins for use in animal migration studies. Isotopes in Environmental and Health Studies 39:211–217.

Webster, M. S., P. P. Marra, S. M. Haig, S. Bensch, and R. T. Holmes. 2002. Links between worlds: unraveling migratory connectivity. Trends in Ecology & Evolution 17:76–83.

Wommack, E. A., L. C. Marrack, S. Mambelli, J. M. Hull, and T. E. Dawson. 2020. Using oxygen and hydrogen stable isotopes to track the migratory movement of Sharp-shinned Hawks (*Accipiter striatus*) along Western Flyways of North America. PLOS One 15:e0226318.

Wunder, M. B. 2010. Using isoscapes to model probability surfaces for determining geographic origins. Pages 251–270 *in* J. B. West, G. J. Bowen, T. E. Dawson, and K. P. Tu, editors. Isoscapes: Understanding movement, pattern, and process on Earth through isotope mapping. Springer Netherlands, Dordrecht. <https://doi.org/10.1007/978-90-481-3354-3_12>.

Wunder, M. B., J. R. Jehl Jr, and C. A. Stricker. 2012. The early bird gets the shrimp: confronting assumptions of isotopic equilibrium and homogeneity in a wild bird population. Journal of Animal Ecology 81:1223–1232.

Wunder, M. B., and D. R. Norris. 2008. Improved estimates of certainty in stable-isotope-based methods for tracking migratory animals. Ecological Applications 18:549–559.

Zhu, Q., K. A. Hobson, Q. Zhao, Y. Zhou, I. Damba, N. Batbayar, T. Natsagdorj, B. Davaasuren, A. Antonov, J. Guan, X. Wang, L. Fang, L. Cao, and A. David Fox. 2020. Migratory connectivity of Swan Geese based on species' distribution models, feather stable isotope assignment and satellite tracking. Diversity and Distributions 26:944–957.

Chapter 4

4 Spatiotemporal changes in natal sources of waterfowl harvested in the Mississippi and Atlantic Flyways

4.1 Introduction

To prepare effective harvest management strategies, connectivity between breeding and harvest locations must be estimated (Nichols et al. 2007). Much of our understanding of connectivity for harvested species is based on leg-band returns (Geis 1971, Munro and Kimball 1982, Klimstra and Padding 2012, Szymanski and Dubovsky 2013, De Sobrino et al. 2017) through coordinated annual preseason leg-banding programs that target post-breeding waterfowl near or on the breeding grounds. Bands are recovered and reported by hunters through a massive-scale citizen science effort. For management purposes, connectivity is described using harvest derivations, which describe the proportion of individuals originating from different source (breeding) areas after correcting for regional harvest rates and population size (Munro and Kimball 1982). To date, these derivations have been performed by stratifying harvest areas into geopolitical boundaries (Szymanski and Dubovsky 2013, De Sobrino et al. 2017) or management units (Munro and Kimball 1982, Powell and Klaasen 1998). Most frequently, derivations have been done on species-specific basis (e.g., American Black Duck *Anas rubripes*, Geis et al. 1971; Canada Goose *Branta canadensis*, Klimstra and Padding 2012; Canvasback *Aythya valisineria*, Stewart et al. 1958, Geis 1974; Mallard *Anas platyrhynchos*, Geis 1971, 1972, Munro and Kimball 1982, Powell and Klaasen 1998, Zuwerink 2001; Wood Duck *Aix sponsa*, Bowers and Hamilton 1977; Blue-winged Teal *Spatula discors*, Szymanski and Dubovsky 2013), but range-wide connectivity measures are lacking for many species. More recently, multi-species regional derivations such as those defined for the entire Pacific Flyway have been performed (De Sobrino et al. 2017).

Under adaptive harvest management (AHM) in North America, most species are managed based on the status of one of three flyway-specific stocks (U.S. Fish and Wildlife Service 2023). The assumption with flyway-level management is that the population trends for the chosen stock should represent the overall trends of any species

in that flyway and management decisions can be made based on a single species. Management in the Central and Mississippi flyways (i.e., the midcontinent) is based on the status of Mallard breeding primarily in the Prairie Pothole region while management in the Atlantic Flyway is based on 'multi-stock' trends incorporating data from four populations (American Green-winged Teal *Anas crecca carolinensis*, Wood Duck, Ring-necked Duck *Aythya collaris*, and Common / Barrow's Goldeneye *Bucephala clangula* and *B. islandica* combined; U.S. Fish and Wildlife Service 2023). While flyways are well-established continental corridors that describe the annual cycle movements of populations (Lincoln 1935), it is known that there is significant movement between flyways (Roberts et al. 2022). Source areas for species managed under this framework likely do not match the same precise source areas as the model species (e.g., the Prairie Pothole region for the midcontinent Mallard), but the degree of disconnect between source areas could violate the assumptions of the current AHM frameworks, especially source areas do not overlap at all.

Although a single continuous population with negligible variation in demographics is assumed within these regions, there may also be heterogeneity in connectivity or demographics, at smaller scales than flyways, that is not captured by current AHM frameworks. For example, harvest connectivity varies across the American Black Duck range where individuals from Atlantic Canada are disproportionately harvested as locals compared to other harvest regions (Ashley et al. 2010, Roy et al. 2015, Kusack et al. 2022). This difference in connectivity led to differences in fall age ratios, an important metric of productivity used in AHM (Black Duck Joint Venture 2018). Although American Black Duck are managed under a separate, species-specific AHM model, this model also assumes a single range-wide population (U.S. Fish and Wildlife Service 2023). This variation in the connectivity between breeding and harvest locations must be estimated regularly to validate the underlying assumptions of AHM and ensure overexploitation does not occur.

Whether source areas vary based on the timing and location of harvest and whether these changes differ systematically across species are poorly understood. Recent studies have explored spatiotemporal trends in band-return data in a spatially explicit way, but much

of the focus has been on examining recovery locations (Lavretsky et al. 2014, Cox et al. 2023, Verheijen et al. 2023) compared to the banding locations (but see Roy et al. 2015). Evidence for spatial changes in source areas from other markers is mixed. Studies using stable isotopes to determine breeding / natal origins suggest more northerly origins later in the harvest period (Palumbo et al. 2019) but other studies suggest that the harvest date is not related to the latitude of origin (Palumbo et al. 2020, Kusack et al. 2022). Examining these banding locations can provide spatially explicit estimates of source areas, allowing for more fine-scale estimation of sources.

Using 60 years of band-return data, I examined spatiotemporal changes in the spatial distribution of natal sources for waterfowl harvested in the Mississippi and Atlantic flyways. My objective was to use kernel density estimation to delineate species-specific spatially explicit natal sources across the harvest period (September–February), at different harvest latitudes (25–30°, 30–35°, 35–40°, 40–45°, 45–50°, 50–55° N), and for two flyways (Mississippi, Atlantic). I then examined spatiotemporal changes in natal sources across the harvest period, while controlling harvest location (latitude and flyway). This kernel density estimation approach is similar to those of Lavretsky et al. (2014) and Cox et al. (2023) but uses banding locations in place of harvest locations. As I was interested in broad patterns across species, I considered all diving or dabbling duck species harvested in the Mississippi and Atlantic flyways as candidates for this modelling, contingent on available band return data.

I tested three main hypotheses. First, I hypothesized that individuals harvested later in the harvest season originate from relatively farther north compared to those harvested earlier in the season, especially at northern latitudes where harvest of locals is possible (Munro and Kimball 1982). I predicted that natal sources would shift and expand to the north later in the harvest period. Second, I hypothesized that individuals harvested at lower latitudes come from broader catchments, indicative of weaker connectivity at lower latitudes. Here, I predicted that natal sources would increase in area for individuals harvested at lower latitudes. Third, I hypothesized that the Mississippi and Atlantic flyways are the primary sources for their respective harvests, at least for the species with possible natal sources in those flyways. I predicted that the harvest in the Mississippi and

Atlantic flyways would show natal sources consistent with the management unit (midcontinent or Atlantic Flyway) of harvest and match those of the representative species for that unit (e.g., Mallard in the Mississippi Flyway), supporting AHM assumptions.

4.2   Methods

4.2.1   Banding data

I obtained banding and encounter data for harvested waterfowl in North America (n = 15,994,986, 1960–2022, Figure 4.1) from the Patuxent Wildlife Research Center (Laurel, MD, USA). I considered all diving and dabbling duck species that are harvested in North America, excluding geese and any hybrids. I stratified the banding records based on the flyway and latitudinal strata of harvest. For the flyways, I used the administrative boundary shapefiles from the U.S. Fish and Wildlife Service (U.S. Fish and Wildlife Service 2017).

I restricted these data to birds that met all of the following criteria: (i) were normal wild birds banded and released in the same location, (ii) hatch-years, juveniles, or locals, (iii) direct recovery (i.e., banded during the preseason (July–September) and recovered during the hunting season (September–February) directly following their preseason banding), (iv) harvested in the Mississippi or Atlantic Flyway, (v) no external trackers (e.g., Passive integrated transponder, GPS, or radio tags), and (vi) locational uncertainty for both banding and encounter was ≤ 1°. I focused on hatch-year birds because I was primarily interested in the spatial distribution of sources of production for the fall harvest.
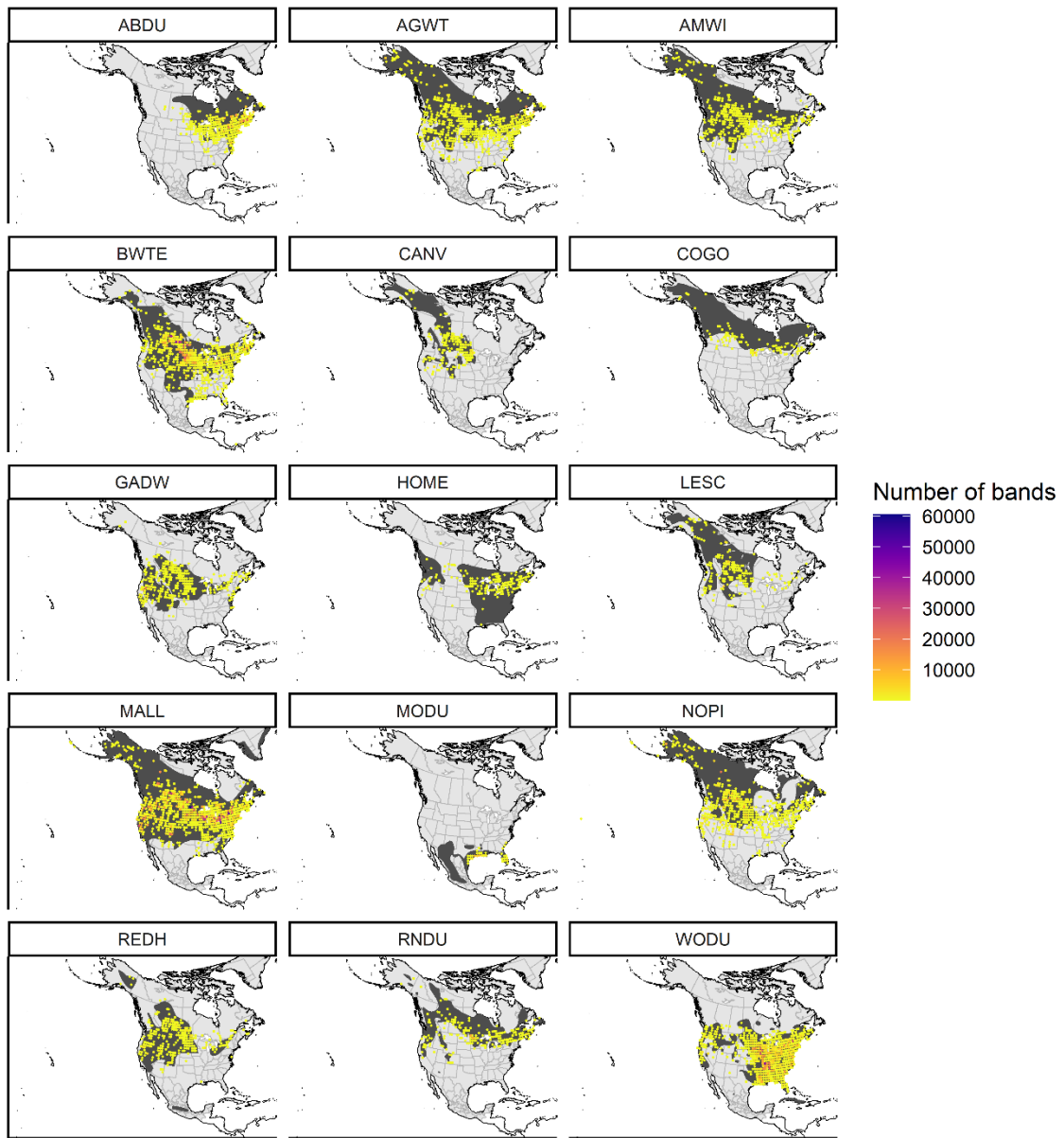
Figure 4.1 Distribution of historic preseason banding records. Distribution of all banding records (n = 5,131,946) relative to the breeding distribution (dark grey; BirdLife International and Handbook of the Birds of the World 2021) of that species. Banding locations are shown as points and the colour of those points represents the number of individuals banded. See Table 4.1 for species alpha-code definitions.

The final dataset contained 5,206,634 banding records and 213,107 direct recoveries from 24 species (Table 4.1): American Black Duck, American Green-winged Teal (*Anas crecca carolinensis*), American Wigeon (*Mareca americana*), Bufflehead (*Bucephala albeola*), Blue-winged Teal, Canvasback, Cinnamon Teal (*Spatula cyanoptera*), Common Eider (*Somateria mollissima*), Common Goldeneye, Common Merganser (*Mergus merganser*), Gadwall (*Mareca strepera*), Greater Scaup (*Aythya marila*), Hooded Merganser (*Lophodytes cucullatus*), Lesser Scaup (*Aythya affinis*), Long-tailed Duck (*Clangula hyemalis*), Mallard, Mottled Duck (*Anas fulvigula*), Northern Pintail (*Anas acuta*), Northern Shoveler (*Spatula clypeata*), Redhead (*Aythya americana*), Ring-necked Duck, Ruddy Duck (*Oxyura jamaicensis*), Wood Duck, and White-winged Scoter (*Melanitta deglandi*).

From these species, in the Mississippi and Atlantic flyways, the most heavily harvested (> 100,000 estimated individuals harvested in 2022–23 in at least one flyway; Raftovich et al. 2023) are Mallard (981,547 and 169,537 respectively) American Green-winged Teal (555,419 and 123,658), Blue-winged Teal / Cinnamon Teal (419,913 and 53,492), Gadwall (371,974 and 43,354), Northern Shoveler (110,989 and 16,895), Ring-necked Duck (160,342 and 94,165), and Wood Duck (384,182 and 311,549). Among species with direct recoveries (see below), Canvasback (27,344 and 3,599), Common Goldeneye (20,549 and 3,024, also includes Barrow's Goldeneye), Common Merganser (3,331 and 13,465, also includes Red-breasted Merganser *Mergus serrator*), Common Eider (0 and 1,516, also includes other eiders), and Ruddy Duck (4,001 and 7,316) exhibited the lowest (< 5,000 individuals) number of harvested individuals (Raftovich et al. 2023).

Table 4.1 Monthly and total flyway-specific sample sizes for direct recoveries (i.e., banded during the preseason and recovered during the hunting season directly following their preseason banding) summarized by species.

Alpha-code	Common name (*Scientific name*)	Flyway	n						
			Total	Sep	Oct	Nov	Dec	Jan	Feb
ABDU	American Black Duck (*Anas rubripes*)	Atlantic	9,526	46	3,503	2,376	3,601	1,690	9
		Mississippi	1,685	17	718	478	472	254	4
AGWT	American Green-winged Teal (*Anas crecca carolinensis*)	Atlantic	2,424	61	860	892	611	569	17
		Mississippi	1,918	126	564	699	529	341	7
AMWI	American Wigeon (*Mareca americana*)	Atlantic	428	3	140	114	171	111	2
		Mississippi	620	21	325	164	110	70	1
BUFF	Bufflehead (*Bucephala albeola*)	Atlantic	9	-	-	3	6	1	-
		Mississippi	22	-	12	10	-	-	-
BWTE	Blue-winged Teal (*Spatula discors*)	Atlantic	1,734	221	931	292	290	197	4
		Mississippi	10,923	5,344	3,675	1,242	662	361	1
CANV	Canvasback (*Aythya valisineria*)	Atlantic	91	-	4	30	57	34	1
		Mississippi	812	56	467	201	88	61	-
CITE	Cinnamon Teal (*Spatula cyanoptera*)	Mississippi	3	1	-	-	2	-	-
COEI	Common Eider (*Somateria mollissima*)	Atlantic	13	1	4	3	5	1	-
COGO	Common Goldeneye (*Bucephala clangula*)	Atlantic	46	-	15	13	18	6	-
		Mississippi	734	43	480	155	56	18	1
COME	Common Merganser (*Mergus merganser*)	Atlantic	5	-	2	1	2	1	-
		Mississippi	62	2	34	22	4	-	-
GADW	Gadwall (*Mareca strepera*)	Atlantic	197	1	51	59	86	57	2
		Mississippi	832	6	113	340	373	191	2
GRSC	Greater Scaup (*Aythya marila*)	Atlantic	2	-	-	1	1	-	-
		Mississippi	7	1	-	6	-	-	-
HOME	Hooded Merganser (*Lophodytes cucullatus*)	Atlantic	78	-	8	27	43	55	1
		Mississippi	181	18	87	47	29	21	-

Code	Common Name	Flyway							
LESC	Lesser Scaup (*Aythya affinis*)	Atlantic	39	-	2	8	29	10	-
		Mississippi	469	-	129	252	88	24	-
LTDU	Long-tailed Duck (*Clangula hyemalis*)	Atlantic	1	-	-	1	-	-	-
		Mississippi	1	-	-	1	-	-	-
MALL	Mallard (*Anas platyrhynchos*)	Atlantic	22,427	285	10,446	5,724	5,972	3,855	49
		Mississippi	63,026	2,863	27,274	17,621	15,268	10,051	121
MODU	Mottled Duck (*Anas fulvigula*)	Atlantic	458	14	1	197	246	182	9
		Mississippi	1,408	2	5	959	442	259	1
NOPI	Northern Pintail (*Anas acuta*)	Atlantic	354	5	124	97	128	64	-
		Mississippi	1,892	29	419	751	693	463	5
NSHO	Northern Shoveler (*Spatula clypeata*)	Atlantic	59	-	17	15	27	26	1
		Mississippi	186	2	65	64	55	19	-
REDH	Redhead (*Aythya americana*)	Atlantic	167	-	17	50	100	72	-
		Mississippi	1,676	55	1,110	376	135	53	1
RNDU	Ring-necked Duck (*Aythya collaris*)	Atlantic	578	-	62	210	306	267	8
		Mississippi	3,174	242	2,177	488	267	172	1
RUDU	Ruddy Duck (*Oxyura jamaicensis*)	Atlantic	8	-	3	2	3	2	-
		Mississippi	35	1	21	10	3	1	-
WODU	Wood Duck (*Aix sponsa*)	Atlantic	14,385	301	6,373	3,578	4,133	3,966	69
		Mississippi	40,559	9,577	12,733	9,262	8,987	5,908	97
WWSC	White-winged Scoter (*Melanitta deglandi*)	Atlantic	2	-	1	1	-	1	-
		Mississippi	3	-	-	3	-	-	-

4.2.2   Distributions of natal source

All statistics and spatial data manipulation were performed in the R statistical computing environment (version 4.3.1, R Core Team 2023) within RStudio (version 2023.09.1, RStudio Team 2023). Spatial data manipulations were performed using the package sf (version 1.0-3, Pebesma 2018) using an Albers equal-area conic projection for North America.

Derivations were done for each monthly period, stratifying samples by flyway and latitude of harvest. As determination of natal sources necessitates grouping, I used 5° latitudinal zones between 25° and 55° (25–30°, 30–35°, 35–40°, 40–45°, 45–50°, 50–55° N) in place of the exact harvest latitude. To convert banding locations (points) into a continuous surface representing the banding densities for harvested individuals, I used spatial kernel density estimation (KDE) in the package SpatialKDE (version 0.8.2, Caha 2023). Kernel density estimates were estimated to a raster grid (cell size 1°) using a quartic kernel. I performed KDE using a 1° grid to reflect the upper threshold of uncertainty with the banding data. As a conservative estimate of the natal sources, I then extracted cells representing 90 % of the kernel density estimate and converted this to a polygon. This 90 % density polygon was defined as the 'natal source'. To avoid complications with KDE with few banding points, only periods with ≥ 50 encounter records were modelled.

To determine the optimal bandwidth (scaling parameter for the width of the kernel) for KDE, I used Scott's rule-of-thumb for multivariate kernel estimators (Scott 2015) using species- (i), month- (j), latitudinal zone- (k), and flyway-specific (m) banding points:

$$h_{ijkm} = \left(\frac{4}{d+2}\right)^{\frac{1}{d+4}} \times \sqrt{\sigma^2_{x,ijkm} + \sigma^2_{y,ijkm}} \times n_{ijkm}^{\frac{-1}{(d+4)}}$$

Where h_{ijkm} represents the bandwidth, d represents the number of dimensions, $\sigma^2_{x,ijkm}$ and $\sigma^2_{y,ijkm}$ represents the variance in x and y coordinates (in °) of banding points, and n_{ijkm} represents the sample size. As these coordinates are bivariate (i.e., $d = 2$), the coefficient simplifies to 1.

I used spatial-temporal analysis of moving polygons (STAMP; package stampr version 0.3, Long et al. 2018) to analyze changes in natal sources between months of harvest, within a flyway-specific latitudinal block. STAMP allows for hierarchical classification of spatial changes between polygons at two discrete time points, within which overlapping and nearby polygons are grouped for direction- and distance-based metrics (Long et al. 2018). I analyzed STAMP events at the first hierarchical level and calculated directional movements (cone method, n = 8) for generation (i.e., polygonal areas present in the first period but not in the second) and disappearance (i.e., polygonal areas present in the second period but not in the first) events relative to polygons in the first period. More specifically, I calculated areas of generation and disappearance event polygons within cones radiating from the centroid of the polygons in the first period. I defined groups using a 100 km distance threshold. Across all groups identified for a given period, directionality was summarized by adding the areas captured by each respective directional cone together. Lastly, I calculated a circular mean (package circular version 0.5-0, Angostinelli and Lund 2023) weighted by the area captured by each directional cone, for each period and used these as an average directional measure of polygonal expansion.

4.2.3   Statistical modelling

To examine latitudinal shifts in natal sources, utilizing individual band-returns directly, I attempted two approaches: (1) linear mixed-effect model (LMM; package lme4 version 1.1-34, Bates et al. 2015) including all species that met the sample size threshold (see above) and a nested random-effect structure (intercept), where flyway was nested within species, to account for the potentially different natal sources for the two flyways and (2) separate species-specific LMMs. In both models, I included fixed effects for the harvest day (number of days since September 1st; continuous) and harvest latitude (continuous), and second-order polynomial terms for both day and latitude of harvest. I included polynomial terms here as I expected the relationship between the predictors and banding latitude/area to level off, as the upper/limit for the response is theoretically bounded by geographic restraints. In the first model, I also included random slope terms which allowed the effect of day of harvest and day of harvest^2 to vary by species. Day of harvest

was defined as the number of days since September 1st. Records with missing information on day of harvest were removed from this analysis (n = 8,810) reducing the total sample size.

To examine the trends in the area of the natal sources over time, I used a LMM with polygon area (log-transformed) as the response, harvest month (continuous) and harvest latitudinal zone(continuous) as fixed effects. Again, I included second-order polynomial terms for harvest month and latitudinal zone to account for curvilinear relationships. I included the same nested random effect structure as the latitude model above but without the random slope due to the low sample size. To account for the increased harvest derivation area due to the increased number of band-returns alone, I also included the number of monthly band-returns (continuous) as a fixed effect. I considered the removal of outliers (i.e., very small banding areas in northern harvest areas), but parameter significance was not affected, so they were retained.

Parameter significance was determined by calculating confidence intervals and determining whether they overlapped with zero. Model fit was assessed using the Nakagawa et al. (2017) method to determine conditional (considering both random and fixed effects) and marginal (considering only fixed effects) R^2 values for mixed-effect models (package performance version 0.10.8, Lüdecke et al. 2021). Model selection was not formally performed, as the random effect structure was necessary to control for the hierarchical structure of the data, I only considered < 5 fixed effects in the global models (considering polynomial terms as two terms), and polynomial terms in the global model were almost always retained in preliminary investigations. Models were fit with restricted maximum likelihood to ensure unbiased parameter estimates (Pinhero and Bates 2000). All continuous predictors were standardized. Model assumptions (normality and homogeneity of variance) were assessed using diagnostic plots and multicollinearity was tested using variance inflation factors (cutoff = 2; Zuur et al. 2009), using orthogonal polynomial terms when assessing higher-order terms.

4.3   Results

Fifteen of 24 species met the sample-size threshold (≥ 50) to construct at least one monthly flyway- and latitudinal-specific natal sources. Of these, two species (Common Goldeneye, Hooded Merganser; Figure C4 and Figure C6) had sufficient samples in only one period and were omitted from STAMP and modelling. American Black Duck (Figure 4.2), American Green-winged Teal (Figure 4.3), American Wigeon (Figure C2), Blue-winged Teal (Figure 4.4), Canvasback (Figure C3), Gadwall (Figure C5), Lesser Scaup (Figure C7), Mallard (Figure 4.5), Mottled Duck (Figure C8), Northern Pintail (Figure C9), Redhead (Figure C10), Ring-necked Duck (Figure C11), and Wood Duck (Figure 4.6) all allowed for sequential temporal comparisons, within a specific flyway and latitudinal band, of at least two time periods. Canvasback, Gadwall, Lesser Scaup, and Redhead, only allowed for temporal comparisons within the Mississippi Flyway, although Gadwall had one month with enough returns to estimate a natal source in the Atlantic Flyway (December, 35–40° N). Mottled Duck had banding areas restricted to the south, as expected, but met the sample size and temporal criteria to be included and was retained in the analyses below. For subsequent models, I refer to these 13 species as the 'focal' species. See supplementary materials (Figure C2–Figure C11) for derivation plots for all species with at least one monthly natal source.
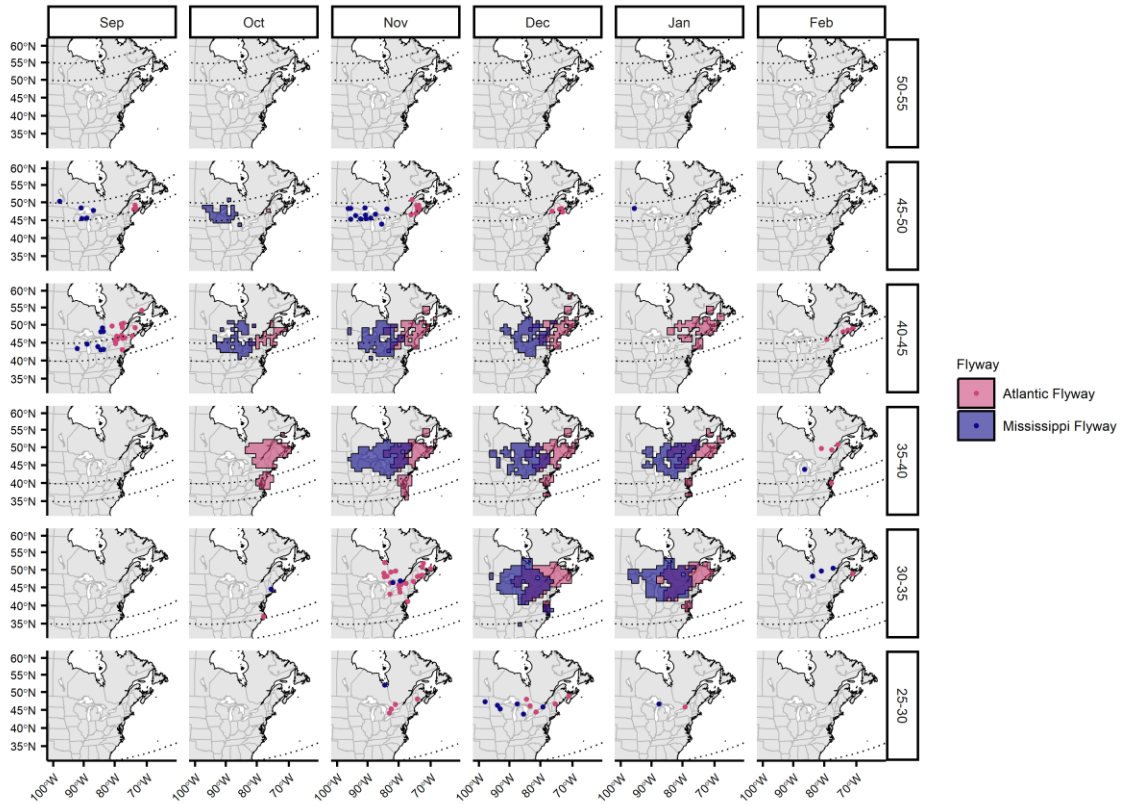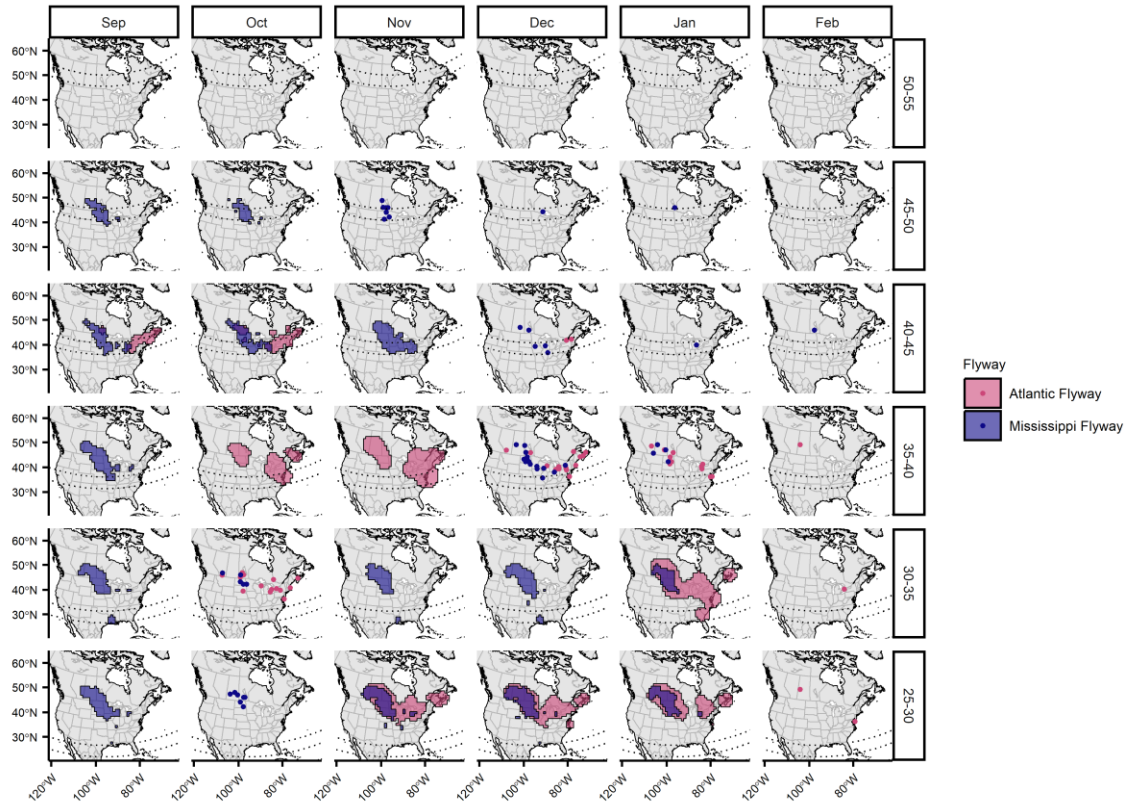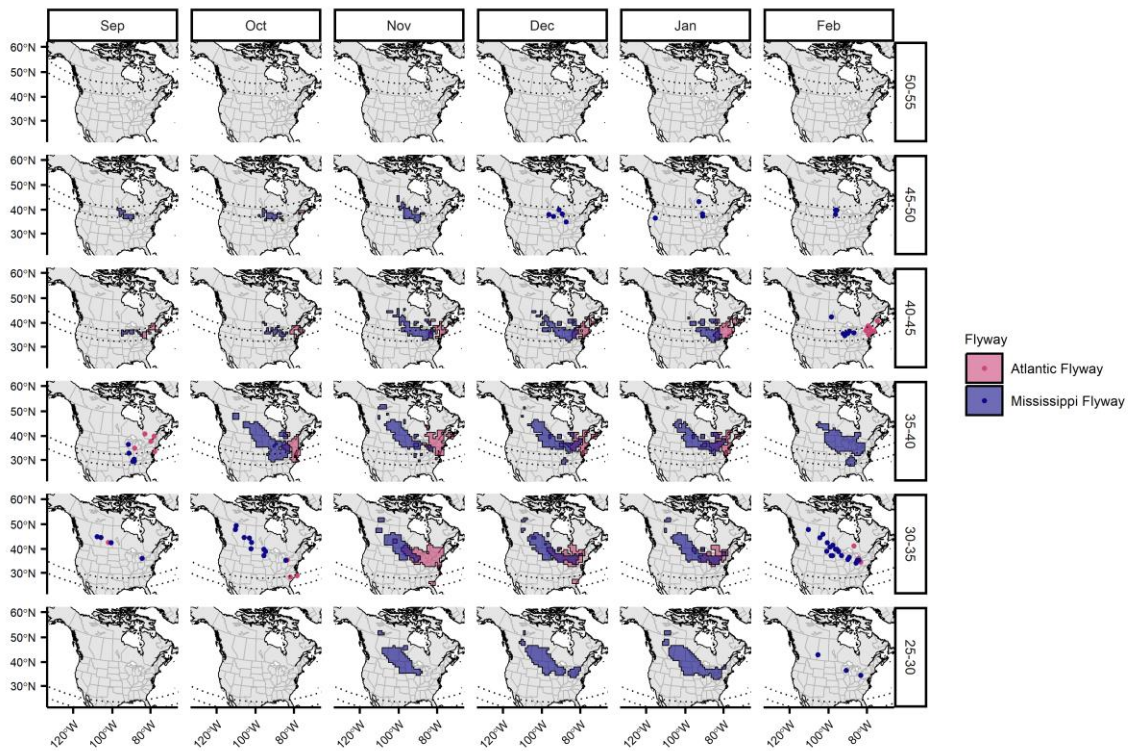
Figure 4.2 Natal sources for American Black Duck. Kernel density estimated natal source areas (90 % density area) for American Black Duck (*Anas rubripes*) harvested in the Mississippi (blue; n = 1,685, 1960–2022) and Atlantic (pink; n = 9,526, 1960–2022) flyways, separated by month of harvest (September–February) and latitude of harvest (25–55, by 5° bands). The upper and lower limits of the harvest area (latitudinal band) are shown with dotted curved lines. Points show banding locations when sample sizes were < 50.
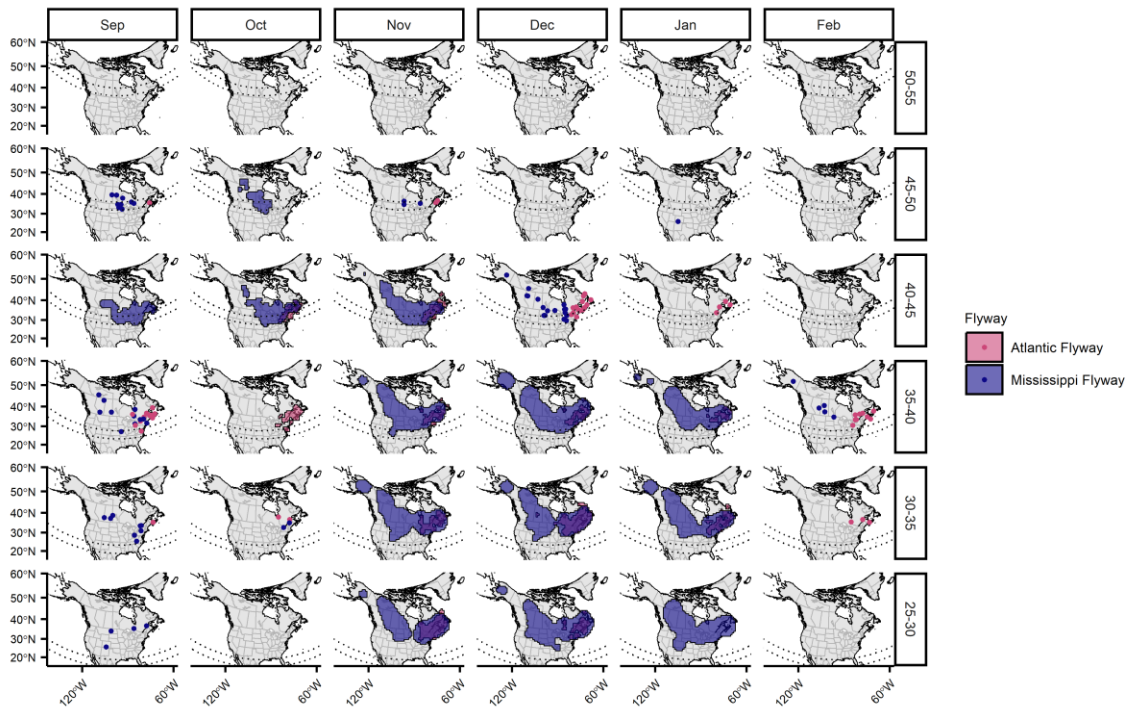
Figure 4.3 Natal sources for American Green-winged Teal. Kernel density estimated natal source areas (90 % density area) for American Green-winged Teal (*Anas crecca carolinensis*) harvested in the Mississippi (blue; n = 1,918, 1960–2022) and Atlantic (pink; n = 2,424, 1960–2022) flyways, separated by month of harvest (September–February) and latitude of harvest (25–55, by 5° bands). The upper and lower limits of the harvest area (latitudinal band) are shown with dotted curved lines. Points show banding locations when sample sizes were < 50.
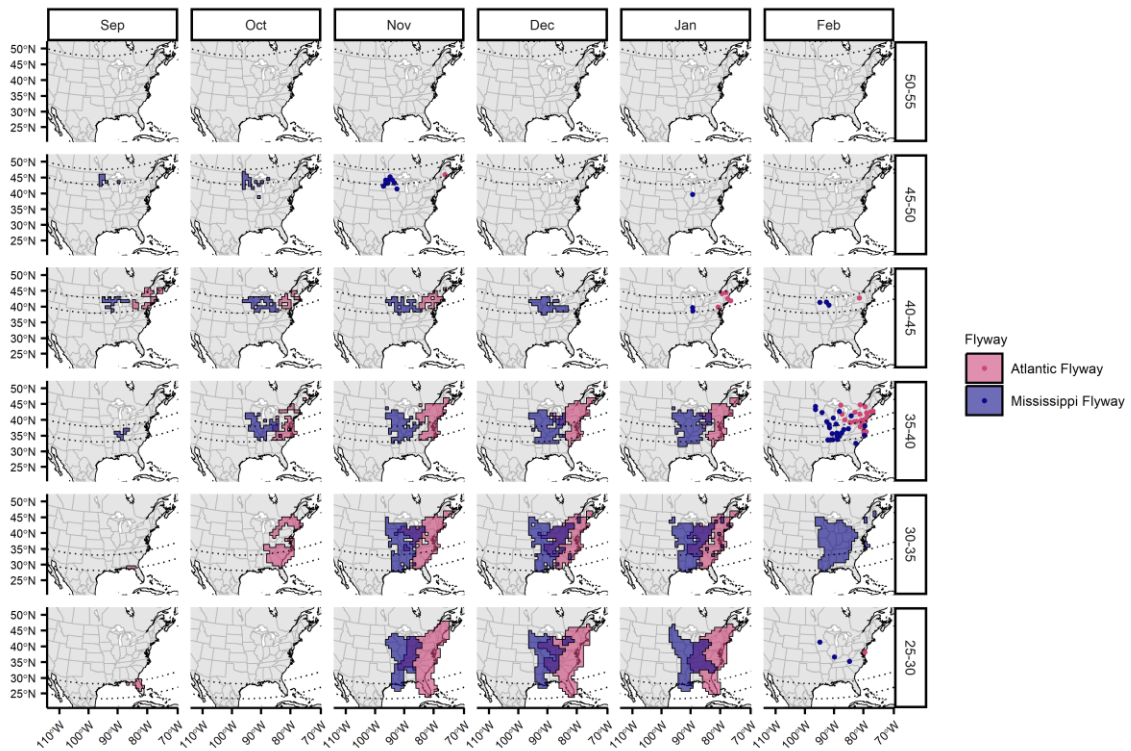
Figure 4.4 Natal sources for Blue-winged Teal. Kernel density estimated natal source areas (90 % density area) for Blue-winged Teal (*Spatula discors*) harvested in the Mississippi (blue; n = 10,923, 1960–2022) and Atlantic (pink; n = 1,734, 1960–2022) flyways, separated by month of harvest (September–February) and latitude of harvest (25–55, by 5° bands). The upper and lower limits of the harvest area (latitudinal band) are shown with dotted curved lines. Points show banding locations when sample sizes were < 50.

Figure 4.5 Natal sources for Mallard. Kernel density estimated natal source areas (90 % density area) for Mallard (*Anas platyrhynchos*) harvested in the Mississippi (blue; n = 63,026, 1960–2022) and Atlantic (pink; n = 22,427, 1960–2022) flyways, separated by month of harvest (September–February) and latitude of harvest (25–55, by 5° bands). The upper and lower limits of the harvest area (latitudinal band) are shown with dotted curved lines. Points show banding locations when sample sizes were < 50.

Figure 4.6 Natal sources for Wood Duck. Kernel density estimated natal source areas (90 % density area) for Wood Duck (*Aix sponsa*) harvested in the Mississippi (blue; n = 40,559, 1960–2022) and Atlantic (yellow; n = 14,385, 1960–2022) flyways, separated by month of harvest (September–February) and latitude of harvest (25–55, by 5° bands). The upper and lower limits of the harvest area (latitudinal band) are shown with dotted curved lines. Points show banding locations when sample sizes were < 50.

4.3.1 Temporal trends

Looking at temporal trends in the geographic extent of natal sources, within a flyway and latitudinal band, most species showed no strong spatial shifts over time. The direction of generation events (from STAMP) between time periods also showed no clear patterns (Figure 4.7), although a few species (American Green-winged Teal, Mallard, Northern Pintail, Redhead) showed directional expansion at northern harvest areas early in the season. This was mainly limited to the Mississippi Flyway where natal sources shifted to the northwest, particularly between September and November at harvest areas between 40–50° latitude (Figure 4.7). The only other clear directionality in the expansion of natal sources was seen in Wood Duck, which showed strong directional expansion to the west for the Atlantic Flyway harvest (Figure 4.7).

4.3.2 Latitudinal trends

Changes in natal sources with harvest latitude followed two general patterns or showed no obvious directionality, depending on the species and flyway of harvest. First, in more southern harvest regions there was a general expansion in natal sources to the northwest in the Mississippi Flyway. This occurred most notably in Mallard (Figure 4.5) and American Green-winged Teal (Figure 4.3). Second, natal sources expanded to include the south while still maintaining the regions in the north, which occurred most prominently in Blue-winged Teal (Figure 4.4) and Wood Duck (Figure 4.6) but also in American Black Duck in the Atlantic Flyway (Figure 4.2). In these cases, the highest density regions shifted to include the harvest latitude (e.g., Wood Duck in Mississippi Flyway; Figure C12), suggesting that a significant portion of the harvest was represented by local individuals. In all other species, natal sources showed omnidirectional expansion/fluctuation or no change with harvest latitude.
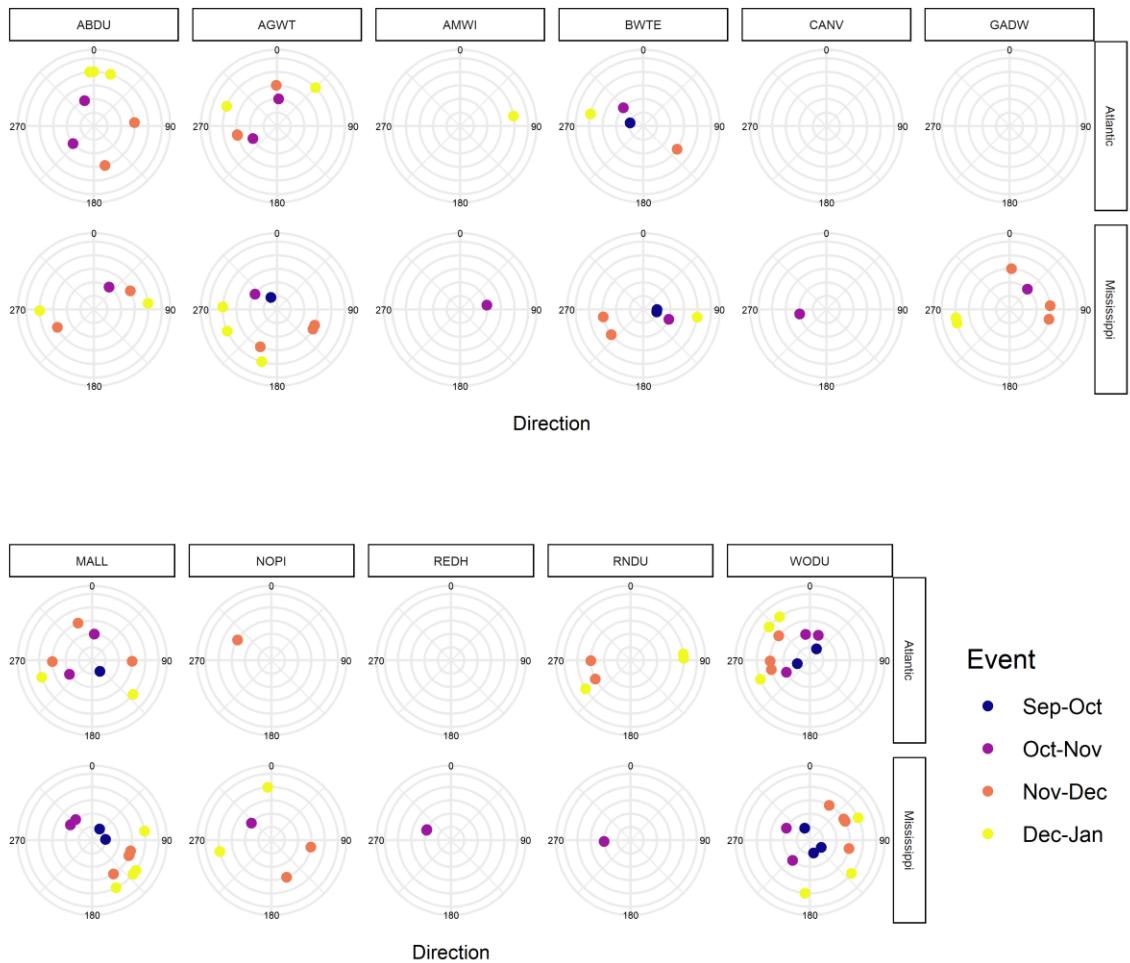
Figure 4.7 Directionality of STAMP generation events. Direction of generation events from Spatial Temporal Analysis of Moving Polygons (STAMP). Points show the weighted circular mean direction of generation events, relative to the first time period, for each latitudinal band and flyway. Within a flyway, generation events for all latitudinal bands (separate points) are shown on the same panel. Colour and distance from center signifies the comparison period (e.g., Sep–Oct). See Table 4.1 for species alpha-code definitions.

4.3.3   Individual banding data

In the multi-species model, I found evidence for a positive decelerating curvilinear relationship between banding latitude and harvest day (LMM; n = 202,762, species:flyway = 26, species = 13; β_{day} = 1.39 ± 0.26, 95 % CI [0.85, 1.92], t = 5.24; β_{day^2} = -0.59 ± 0.16, 95 % CI [-0.93, -0.26], t = -3.64) where banding latitude was on average lower in the beginning of the season and peaked toward the end of the season (Figure 4.8). Although this pattern occurred overall, the model fit Mottled Duck data poorly (Figure 4.8). Banding latitude was also strongly related to harvest latitude ($\beta_{harvest\ latitude}$ = 1.06 ± 0.01, 95 % CI [1.04, 1.09], t = 83.77; $\beta_{harvest\ latitude^2}$ = 0.71 ± 0.01, 95 % CI [0.70, 0.73], t = 75.54; Figure S13). The random intercept (variance components: species:flyway = 35.52, species = 2.58, residual = 11.32) and slope terms (β_{day} = 0.89, β_{day^2} = 0.33) accounted for a significant amount of variability ($R^2_{conditional}$ = 0.76, $R^2_{marginal}$ = 0.03).

The relationship between banding latitude and timing of harvest was supported by the species-specific models (Figure C14), where all species except American Wigeon, Mottled Duck, and Northern Pintail showed positive relationships between banding latitude and harvest day. American Black Duck and Gadwall showed evidence of a positive linear relationship rather than a curvilinear one (Figure C14). Many of these species had overall low sample sizes, leading to model singularity being an issue in species-specific models.
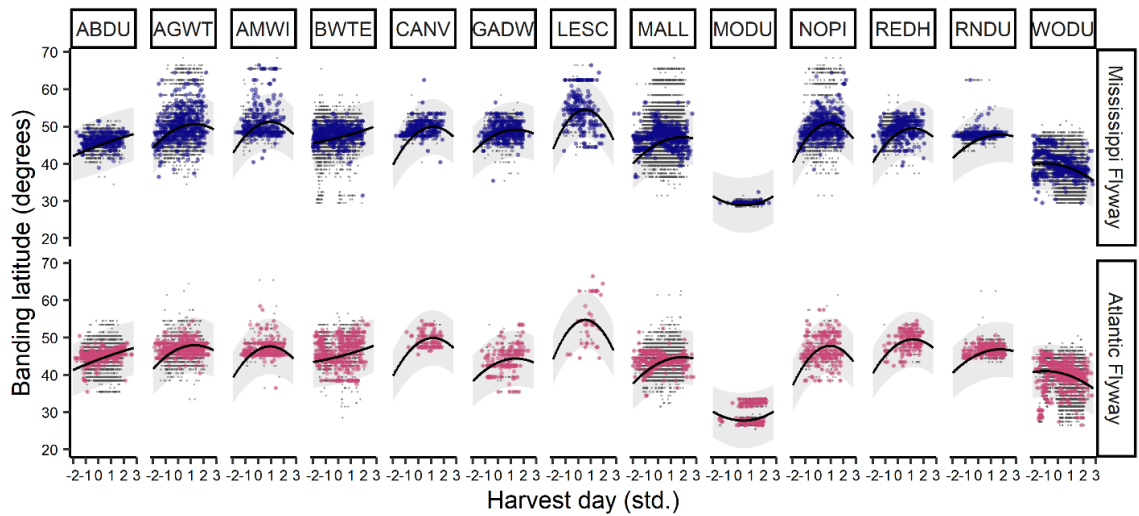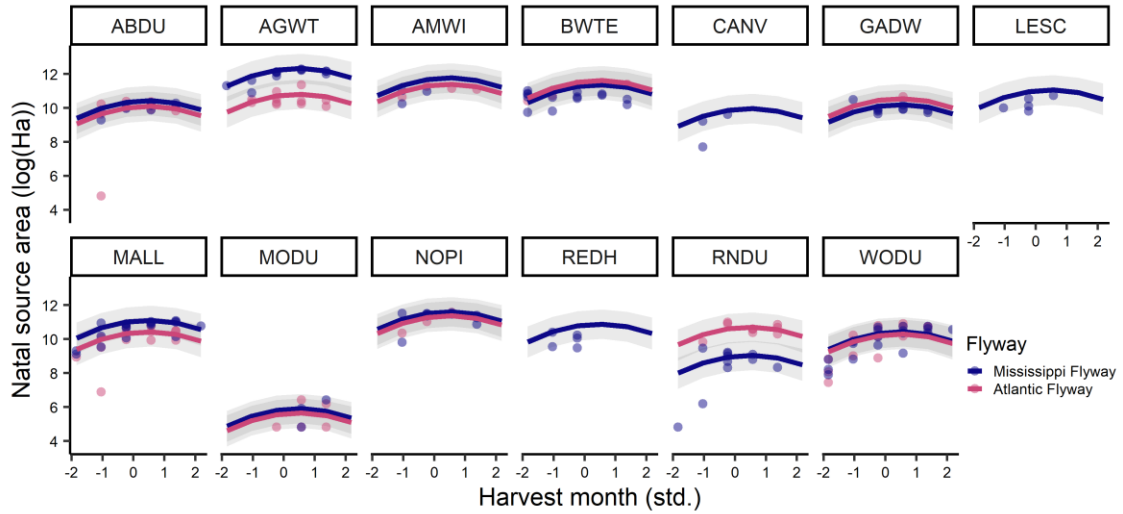
Figure 4.8 Change in banding latitude over the hunting season. Relationship between banding latitude (°) and harvest day (standardized) for 13 species of waterfowl harvested in the Great Lakes region (n = 202762, 1920–2020). The line colour represents the flyway of harvest. Lines are the estimated marginal means from the multi-species linear mixed-effect model (fitted with 'ggpredict' from ggeffects package version 1.3.2, Lüdecke 2018), holding the effect of sample size and date constant. The grey region represents the prediction intervals. Raw data are shown as grey points. Mean banding latitude for each unique harvest day in a given latitudinal band are shown in colour to give a visual representation of centrality. See Table 4.1 for species alpha-code definitions.

4.3.4   Natal source area

I detected a positive decelerating curvilinear relationship between area and harvest month (LMM, n = 206, species:flyway = 23, species = 13; β_{month} = 0.19 ± 0.05, 95 % CI [0.09, 0.28], t = 3.83; β_{month^2} = -0.19 ± 0.04, 95 % CI [-0.27, -0.11], t = -4.81), where natal source area was smallest at the beginning of the season, peaked mid-to-late season, and decreased toward the end of the season (Figure 4.9). Natal source area also showed a negative curvilinear relationship with harvest latitude ($\beta_{harvest\ latitude}$ = -0.30 ± 0.05, 95 % CI [-0.40, -0.20], t = -5.82; $\beta_{harvest\ latitude^2}$ = -0.27 ± 0.05, 95 % CI [-0.36, -0.18], t = -5.98), where area was greatest at lower latitudes and decreased at higher latitudes (Figure S12). The number of band-returns was not significantly related to natal source area (β_n = 0.0024 ± 0.04, 95 % CI [-0.08, 0.08], t = -0.06). The random effects (variance components: species:flyway = 0.35, species = 2.21, residual = 0.32) accounted for a significant amount of variability ($R^2_{conditional}$ = 0.90, $R^2_{marginal}$ = 0.11). For random intercept terms, natal source area was generally consistent between the two flyways, but it was noticeably greater in the Mississippi Flyway for American Green-winged Teal and in the Atlantic Flyway for Ring-necked Duck (Figure 4.9).

Figure 4.9 Change in harvest derivation area over the hunting season. Relationship between natal source area (log(Ha)) and harvest month (standardized) for 13 species of waterfowl harvested in the Great Lakes region (n = 206, 1920–2020). The line colour represents the flyway of harvest. Lines are the estimated marginal means from a linear mixed-effect model (fitted with 'ggpredict' from ggeffects package version 1.3.2, Lüdecke 2018), holding the effect of sample size and date constant. The grey region represents the prediction intervals. For species with derivations in only one flyway, marginal means were only shown for that flyway. See Table 4.1 for species alpha-code definitions.

4.3.5   Flyway-specific natal sources

Comparing natal sources between the flyways, the Mississippi Flyway showed natal sources in the Central and Mississippi flyways in all species but the American Green-winged Teal which showed natal sources in all four flyways (Figure 4.3). Northern Pintail harvested in the Mississippi Flyway also showed natal sources in the Pacific Flyway, but not the Atlantic Flyway (Figure C9). Although constrained to the Mississippi Flyway, Wood Duck natal sources were considerably more south than other species (Figure 4.6). Overall, natal sources for all other species harvested in the Mississippi Flyway matched those of Mallard, showing origins in the Prairie Pothole and Boreal Taiga Plains (Figure 4.5).

For the Atlantic Flyway, natal sources were shown to be consistent with within-flyway origins for American Black Duck (Figure 4.2), American Green-winged Teal (Figure 4.3), Gadwall (Figure C5), Mallard (Figure 4.5), Mottled Duck (Figure C8), Northern Pintail (Figure C9), and Wood Duck (Figure 4.6). American Wigeon (Figure C2), Blue-winged Teal (Figure 4.4), and Ring-necked Duck (Figure C11) showed natal sources within the Atlantic Flyway but also in the Central and Mississippi flyways. Lastly, Canvasback, Redhead, and Lesser Scaup showed natal sources in the Central and Mississippi flyways regardless of the flyway of harvest. As in the Mississippi Flyway, natal sources for Wood Duck were considerably more south compared to other species (Figure 4.6).

Despite the longitudinal separation in natal sources between the Mississippi and Atlantic flyways in some species, natal sources regularly showed areas of overlap. For American Black Duck (Figure 4.2), Blue-winged Teal (Figure 4.4), Mallard (Figure 4.5), and Wood Duck (Figure 4.6), overlap in flyway-specific natal sources was more pronounced at lower harvest latitudes.

4.4   Discussion

Across the 13 focal species, I found some evidence for northward directional expansion of natal sources over the harvest period. Species-specific natal sources and their spatiotemporal relationships with harvest timing and location differed. Still, I detected a

general trend of increased catchment area and more northern sources later in the harvest period. Rather than a complete shift, natal sources generally expanded, as regions included in the sources early in the season were still sources later in the season despite increasing overall catchment area. On average, flyway and latitude of harvest explained more variation in natal sources than the timing of harvest. I found evidence for flyway-specific natal sources for seven of 13 species harvested in the Atlantic Flyway and natal sources in the midcontinent (i.e., Central and Mississippi flyways) for all species harvested in the Mississippi Flyway except American Green-winged Teal.

4.4.1   Spatiotemporal trends

Consistent with my original hypothesis, I found some evidence of northern expansion for natal sources over the harvest period, at least for the Mississippi Flyway. Examining the geographic extent of natal sources showed more ambiguous temporal differences, as all species other than American Green-winged Teal and Northern Pintail did not show visually obvious shifts in natal sources over the harvest period at a given latitude. Instead, temporal shifts in banding latitude were detected when examining the individual band returns. This suggests a northward shift in the density of natal sources but less drastic changes in these source areas' absolute upper and lower margins. Further, these differences could be driven by the different treatment of harvest timing as natal source polygons were analyzed month-by-month, while the individual banding data was analyzed treating harvest timing as a continuous predictor. Overall, this effect suggests a chain migration strategy where individuals later in the harvest period originate from natal sources farther north (Palumbo et al. 2019). Alternatively, sampled individuals were unlikely to be at their wintering locations, especially earlier in the season, and this chain migration pattern could just indicate a delayed migration timing towards the same wintering location.

Temporal shifts in natal sources were less clear for the Atlantic Flyway. Evidence from stable isotopes from American Black Duck supports that harvest date is not related to breeding latitude (Kusack et al. 2022), at least for this species in the Mississippi and Atlantic flyways. The lack of a shift in natal sources may be due to reduced banding effort in the far north of Quebec and Labrador (Figure 4.1). It is unclear whether temporal

shifts would be seen with greater banding effort in the northeast. Alternatively, as the harvest in the Atlantic Flyway was mainly derived from within that flyway, which is supported by AHM frameworks (U.S. Fish and Wildlife Service 2023), the smaller geographic area of available breeding habitats in the northeast may limit my ability to detect these spatial trends. In the Mississippi Flyway, natal sources were spread across the boreal forest, and into Alaska in some cases, allowing for larger potential source areas.

The interpretation of chain migration is complicated as some species showed natal sources that suggest differential migration patterns. Even late in the harvest period (December–January) Mallard and Wood Duck harvested at northern latitudes showed local natal sources. Previous derivations have shown early-season northern harvested birds showed some local origins (Munro and Kimball 1982), but these local natal sources in the north appear more prevalent in my derivations. This is not unexpected, as both species exhibit strategies to remain on the breeding grounds as north as possible despite harsh winter temperatures (Bellrose and Holm 1994, Baldassarre 2014) and wintering locations have been shifting north in recent decades (Cox et al. 2023, Verheijen et al. 2023).

4.4.2   Future directions

Future analyses should continue to explore these spatiotemporal changes between historic and more recent banding data. I used direct recoveries of hatch-year birds, which necessitated lumping all available data across many years of collection, but the yearly distribution of band returns differed between species (Figure C1). American Black Duck, Blue-winged Teal, and Redhead had more direct recoveries in the 1950s compared to the 2000s, whereas Mallard, Green-winged Teal, and Wood Duck showed the opposite distribution (Figure C1). For the species where banding records mainly reflect historic banding, it is not clear whether the trends I found reflect contemporary harvest derivations. Recent studies have shown that harvest locations, and by extension wintering locations, have been shifting to the north (Cox et al. 2023, Verheijen et al. 2023) and autumn migration has been more delayed in recent years (Thurber et al. 2020, Frei et al.

2024). Despite this, other studies have shown that transition probabilities between the flyways have remained relatively constant among species (Roberts et al. 2022).

Harvest pressures, banding effort, and reporting rates differ spatially and temporally, limiting the interpretation of my results. Rather than summarize the harvest derivation by geopolitical boundaries, which would have allowed me to incorporate many of these metrics, I chose to analyze these data in a spatially explicit framework. Although this approach has the advantage of ignoring biologically arbitrary geopolitical boundaries, it also comes with some drawbacks. First, I was unable to account for spatially explicit estimates of population size and banding effort which would have provided a direct recovery rate (De Sobrino et al. 2017). As such, the density of these estimates should not be overinterpreted. To avoid this, I used polygonal boundaries for these distributions rather than explicit density surfaces. Second, I only included hatch-year birds and lumped locals with juveniles/hatch-year birds. Many traditional derivations include adult males and females, estimating cohort-specific direct recovery rates (Munro and Kimball 1982, De Sobrino et al. 2017). Munro and Kimball (1982) showed that the differences in harvest derivations between age classes, including locals and immature birds, were significant. Here I was primarily interested in outlining natal sources and general spatiotemporal patterns seen across species, which necessitated spatially and temporally stratified data.

Intrinsic markers can also be used to derive regions of past occupancy (e.g., genetics, Inman et al. 2003; stable isotopes, Palumbo et al. 2019, 2020), but have yet to receive full support in AHM. I encourage comparing multiple harvest derivation estimates between those derived from different data sources (e.g., banding, genetics, stable isotopes, radio tagging). For example, our recent publication on harvested Blue-winged Teal (Palumbo et al. 2020) provided evidence that breeding origin based on stable-isotope assignment contrasted with previous banding derivations (Szymanski and Dubovsky 2013). These derivations should be carefully interpreted, as banding information is limited to areas where banding occurs. Many waterfowl species or populations are banded unequally throughout their range (see Figure 4.1), especially if a portion of their breeding range reaches remote northern regions where banding is logistically and financially prohibitive.

Using banding data alone to derive connectivity estimates has the potential to introduce bias, especially for some far northern breeding species like the Greater Scaup where banding on the breeding grounds is rare. There is concern that parameters derived from banding may be biased to southern portions of the population (Roy et al. 2015), as population models assume that the banded cohort is representative of the population of interest (Munro and Kimball 1982). To circumvent these biases, band-return data should be analyzed in tandem with intrinsic markers to estimate these harvest derivations.

4.4.3   Conclusions

Understanding the connections between breeding and harvest areas is integral for the maintenance and health of waterfowl populations. Here I have shown evidence for latitudinal shifts and general expansion of natal source areas over the harvest period for harvested waterfowl in the Mississippi and Atlantic flyways. These expansions generally maintained management unit-specific (i.e., midcontinent or Atlantic Flyway) harvest, supporting the assumptions of AHM. Notably, American Green-winged Teal harvested in the Mississippi Flyway did not strictly follow the assumptions of AHM and instead showed natal sources from Alaska to the Atlantic Coast. These broad natal sources may not pose a significant mismatch between teal population trends and midcontinent Mallard trends, especially for a species of minimal conservation concern, but at the very least these connectivity metrics should be further explored. Here I provide an initial look into spatiotemporal dynamics of source areas and connectivity for waterfowl harvested in eastern North America, but these metrics can be explored in more detail on a species-by-species basis. This research provides a framework to spatiotemporally visualize flyway- and species-specific source areas and derive subsequent connectivity estimates (e.g., Cohen et al. 2018, Roberts et al. 2022) that can directly inform AHM decisions and maintain effective conservation efforts for these species.

4.5   References

Angostinelli, C., and U. Lund. 2023. circular: Circular Statistic. R Package version 0.5-0. <https://CRAN.R-project.org/package=circular>.

Ashley, P., K. A. Hobson, S. L. Van Wilgenburg, N. North, and S. A. Petrie. 2010. Linking Canadian harvested juvenile American Black Ducks to their natal areas

using stable isotope (δD, δ^{13}C, and δ^{15}N) methods. Avian Conservation and Ecology 5:7.

Baldassarre, G. A. 2014. Ducks, Geese, and Swans of North America. Volume 2. JHU Press, Baltimore, MD, USA.

Bates, D., M. Maechler, B. Bolker, and S. Walker. 2015. Fitting linear mixed-effects models using lme4. Journal of Statistical Software 67:1–48.

Bellrose, F. C., and D. J. Holm. 1994. Ecology and Management of the Wood Duck. Stackpole Books, Mechanicsburg, PA, USA.

BirdLife International and Handbook of the Birds of the World. 2021. Bird species distribution maps of the world. Version 2020.1. <http://datazone.birdlife.org/species/requestdis.>. Accessed 16 May 2021.

Black Duck Joint Venture. 2018. Notice of funding opportunity, Migratory Bird Joint Ventures (Black Duck Joint Venture) Catalog of Federal Domestic Assistance (CFDA) Number 15.637. U.S. Fish and Wildlife Service, Division of Migratory Bird Management. Washington, DC, USA.

Bowers, E. F., and R. B. Hamilton. 1977. Derivation of northern Wood Ducks harvested in southern states of the Mississippi Flyway. Proceedings of the Annual Conference of the Southeastern Association of Fish and Wildlife Agencies 31:90–98.

Caha, J. 2023. SpatialKDE: Kernel Density Estimation for Spatial Data. R package version 0.8.2. <https://CRAN.R-project.org/package=SpatialKDE>.

Cohen, E. B., J. A. Hostetler, M. T. Hallworth, C. S. Rushing, T. S. Sillett, and P. P. Marra. 2018. Quantifying the strength of migratory connectivity. Methods in Ecology and Evolution 9:513–524.

Cox, A. R., B. Frei, S. E. Gutowsky, F. B. Baldwin, K. Bianchini, and C. Roy. 2023. Sixty-years of community-science data suggest earlier fall migration and short-stopping of waterfowl in North America. Ornithological Applications 125:duad041.

De Sobrino, C. N., C. L. Feldheim, and T. W. Arnold. 2017. Distribution and derivation of dabbling duck harvests in the Pacific Flyway. California Fish and Game 103:118–137.

Frei, B., A. R. Cox, A. C. Morales, and C. Roy. 2024. Community-science reveals delayed fall migration of waterfowl and spatiotemporal effects of a changing climate. Journal of Animal Ecology 93:377–392.

Geis, A. D. 1971. Breeding and wintering areas of mallards harvested in various states and provinces. U.S. Department of the Interior, Fish and Wildlife Service, Bureau of Sport Fisheries and Wildlife, Washington, DC, USA.

Geis, A. D. 1972. Use of banding data in migratory game bird research and management. U.S. Department of the Interior, Fish and Wildlife Service, Bureau of Sport Fisheries and Wildlife, Washington, DC, USA.

Geis, A. D. 1974. Breeding and wintering areas of Canvasbacks harvested in various states and provinces. U.S. Department of the Interior, Fish and Wildlife Service, Washington, DC, USA.

Geis, A. D., R. I. Smith, and J. P. Rogers. 1971. Black duck distribution, harvest characteristics, and survival. U.S. Department of the Interior, Fish and Wildlife Service, Bureau of Sport Fisheries and Wildlife, Washington, DC, USA.

Inman, R. L., K. T. Scribner, H. H. Prince, J. A. Warrillow, D. R. Luukkonen, and P. I. Padding. 2003. A novel method for Canada goose harvest derivation using genetic analysis of tail feathers. Wildlife Society Bulletin 1126–1131.

Klimstra, J. D., and P. I. Padding. 2012. Harvest distribution and derivation of Atlantic flyway Canada Geese. Journal of Fish and Wildlife Management 3:43–55.

Kusack, J. W., D. C. Tozer, M. L. Schummer, and K. A. Hobson. 2022. Origins of harvested American black ducks: stable isotopes support the flyover hypothesis. The Journal of Wildlife Management 87:e22324.

Lavretsky, P., J. H. Miller, V. Bahn, and J. L. Peters. 2014. Exploring fall migratory patterns of American black ducks using eight decades of band-recovery data. The Journal of Wildlife Management 78:997–1004.

Lincoln, F. C. 1935. The waterfowl flyways of North America. U.S. Department of Agriculture, Washington, DC, USA.

Long, J., C. Robertson, and T. Nelson. 2018. stampr: Spatial-Temporal Analysis of Moving Polygons in R. Journal of Statistical Software, Code Snippets 84:1–19.

Lüdecke, D. 2018. ggeffects: Tidy data frames of marginal effects from regression models. Journal of Open Source Software 3:772.

Lüdecke, D., M. S. Ben-Shachar, I. Patil, P. Waggoner, and D. Makowski. 2021. performance: An R package for assessment, comparison and testing of statistical models. Journal of Open Source Software 6:3139.

Munro, R. E., and C. F. Kimball. 1982. Population ecology of the mallard: VII. Distribution and derivation of the harvest. Resource Publication, Report, Washington, D.C. <http://pubs.er.usgs.gov/publication/5230180>.

Nakagawa, S., P. C. Johnson, and H. Schielzeth. 2017. The coefficient of determination R^2 and intra-class correlation coefficient from generalized linear mixed-effects models revisited and expanded. Journal of the Royal Society Interface 14:20170213.

Nichols, J. D., M. C. Runge, F. A. Johnson, and B. K. Williams. 2007. Adaptive harvest management of North American waterfowl populations: a brief history and future prospects. Journal of Ornithology 148:343–349.

Palumbo, M. D., J. W. Kusack, D. C. Tozer, S. W. Meyer, C. Roy, and K. A. Hobson. 2020. Source areas of Blue-winged Teal harvested in Ontario and Prairie Canada based on stable isotopes: implications for sustainable management. Journal of Field Ornithology 91:64–76.

Palumbo, M. D., D. C. Tozer, and K. A. Hobson. 2019. Origins of harvested Mallards from Lake St. Clair, Ontario: a stable isotope approach. Avian Conservation and Ecology 14:3.

Pebesma, E. 2018. Simple features for R: standardized support for spatial vector data. The R Journal 10:439–446.

Pinhero, J., and D. Bates. 2000. Mixed-effects models in S and S-PLUS. Springer-Verlag, New York, NY, USA.

Powell, L. A., and G. A. Klaasen. 1998. Distribution and derivation of Mallard band recoveries from the upper Mississippi River, 1961-1989. North American Bird Bander 23:1–12.

R Core Team. 2023. R: a language and environment for statistical computing. R Foundation for Statistical Computing, Vienna, AT.

Raftovich, R., K. Fleming, S. Chandler, and C. Cain. 2023. Migratory bird hunting activity and harvest during the 2021-22 and 2022-23 hunting seasons. U.S. Fish and Wildlife Service, Laurel, MD, USA.

Roberts, A., A. L. Scarpignato, A. Huysman, J. A. Hostetler, and E. B. Cohen. 2022. Migratory connectivity of North American waterfowl across administrative flyways. Ecological Applications 33:e2788.

Roy, C., S. G. Cumming, and E. J. B. McIntire. 2015. Spatial and temporal variation in harvest probabilities for American black duck. Ecology and Evolution 5:1992–2004.

RStudio Team. 2023. RStudio: integrated development for R. RStudio, Inc., Boston, MA, USA.

Scott, D. 2015. Multivariate Density Estimation: Theory, Practice, and Visualization. 2nd edition. John Wiley & Sons, Inc., New York, NY, USA.

Stewart, R. E., A. D. Geis, and C. D. Evans. 1958. Distribution of populations and hunting kill of the canvasback. The Journal of Wildlife Management 22:333–370.

Szymanski, M. L., and J. A. Dubovsky. 2013. Distribution and derivation of the Blue-winged Teal (*Anas discors*) harvest, 1970-2003. United States Department of the Interior, Fish and Wildlife Service, Washington, DC, USA.

Thurber, B. G., C. Roy, and J. R. Zimmerling. 2020. Long-term changes in the autumn migration phenology of dabbling ducks in southern Ontario and implications for waterfowl management. Wildlife Biology 2020:wlb.00668.

U.S. Fish and Wildlife Service. 2017. USFWS Administrative Waterfowl Flyway Boundaries. U.S. Fish and Wildlife Service, Natural Resource Program Center. <https://ecos.fws.gov/ServCat/Reference/Profile/42276>. Accessed 20 Sep 2019.

U.S. Fish and Wildlife Service. 2023. Adaptive Harvest Management: 2024 Hunting Season. U.S. Department of the Interior, Washington, DC, USA.

Verheijen, B. H. F., E. B. Webb, M. G. Brasher, and H. M. Hagy. 2023. Spatiotemporal dynamics of duck harvest distributions in the Central and Mississippi flyways, 1960–2019. The Journal of Wildlife Management 88:e22521.

Zuur, A., E. N. Ieno, N. Walker, A. A. Saveliev, and G. M. Smith. 2009. Mixed effects models and extensions in ecology with R. Springer, Berlin, DE.

Zuwerink, D. A. 2001. Changes in the derivation of mallard harvests from the northern US and Canada, 1966-1998. PhD Dissertation. Ohio State University, Columbus, OH, USA.

Chapter 5

5   Combining stable-hydrogen isotopes with band-returns to determine the natal origins of Great Lakes harvested waterfowl

5.1   Introduction

Although waterfowl are one of the most heavily managed (North American Waterfowl Management Plan 2018) and tracked group of birds in North America (Scarpignato et al. 2023), much of our understanding of where harvested individuals originate is based on leg-band returns (Munro and Kimball 1982, Klimstra and Padding 2012, Szymanski and Dubovsky 2013, De Sobrino et al. 2017). Waterfowl banding programs in North America are unrivalled worldwide, with a staggering $303,000 \pm 61,000$ bands put out each year since 1960 onto over 50 species (Celis-Murillo et al. 2022). Banding data support diverse uses including estimating population size (Alisauskas et al. 2014), fine-scale regional demographics (e.g., Ellis et al. 2022), annual survival (e.g., Devers et al. 2021), migration phenology (e.g., Cox et al. 2023), and movement probabilities (e.g., Robinson et al. 2016). Mark-recapture data produced by banding and subsequent recoveries also provide important connections between breeding and harvest areas (Munro and Kimball 1982, Klimstra and Padding 2012, Szymanski and Dubovsky 2013, De Sobrino et al. 2017). To establish many of these connections, coordinated annual preseason leg-banding programs, which target post-breeding waterfowl near or on the breeding grounds, are used. However, one of the assumptions of this method is that banded samples are representative of population mortality, movement, and migration (Munro and Kimball 1982). However, this assumption is often violated when at least a portion of the population breeds in remote areas and is not marked. Logistic and financial difficulties often preclude banding of remote waterfowl populations.

Intrinsic markers, such as naturally occurring stable isotopes of various elements (Ashley et al. 2010, Fowler et al. 2018, Palumbo et al. 2019, 2020, Kusack et al. 2022, Kucia et al. 2023) and genetics (Inman et al. 2003), can be used to estimate these breeding / natal source areas. Stable isotopes stored in animal tissues are particularly useful in the context

of harvest as they are naturally occurring and provide a snapshot of the recent life history of the individual. Stable-hydrogen isotopes (δ^2H) have been used to assign regions of likely origin to harvested migratory species including Sandhill Crane (*Grus canadensis*, Hobson et al. 2006), European Woodpigeon (*Columba palumbus*, Hobson et al. 2009), American Woodcock (*Scolopax minor*, Sullins et al. 2016), several shorebird species harvested in the Caribbean (Reed et al. 2018), the illegal harvest of Ortolan Bunting (*Emberiza hortulana*, Jiguet et al. 2019), and many waterfowl species. This technique relies on the predictable patterns of δ^2H values in amount-weighted precipitation (δ^2H$_p$), which vary on a continental scale and are incorporated into local food webs. After accounting for expected isotopic discrimination (i.e., change in isotopic ratio) that occurs between precipitation δ^2H values and that of consumer tissues (see Clark et al. 2006, van Dijk et al. 2014, Kusack et al. 2023), we can assign individuals to regions of origin using spatially explicit likelihood-based assignment methods (Royle and Rubenstein 2004). Feathers, and other inert keratinous tissue, are useful, as they 'lock-in' the dietary isotopes at the time of tissue growth (Hobson and Clark 1992). For example, feathers from adult waterfowl provide information about the previous moulting site as adults exhibit a post-breeding synchronous moult, while feathers from juveniles provide information about the natal site, both of which can be used to establishing patterns of connectivity across the annual cycle.

A major advantage of using intrinsic markers is that every capture is essentially a recapture as the stable-isotope approach only requires a single capture compared to at least two captures for traditional extrinsic markers (Hobson 2019). However, stable isotopic assignment methods are not without their drawbacks. If two regions are isotopically identical, we cannot differentiate between them using isotopes alone. In North America, precipitation δ^2H isoclines allow for latitudinal differentiation but longitudinally are less useful to inform origins. As well, spatial δ^2H patterns are broadly consistent across North America showing a strong latitudinal gradient, but this pattern reverses in Alaska, where δ^2H$_p$ values become more positive westward and resemble more southern values (Bowen et al. 2005, Terzer-Wassmuth et al. 2021). These issues can complicate the application of stable isotopes to determine the origin of waterfowl because many species breed across large areas, often including Alaska, unless other prior

information can refine isotopic assignment based on Bayesian methods (Royle and Rubenstein 2004). Prior probabilities of origin can involve multiple sources of information that can be integrated to inform the posterior probability of origin. These can be applied on an individual-by-individual basis based on intrinsic traits, such as genetic profiles (Ruegg et al. 2017), or could apply to all individuals in a given cohort or population, such as using predicted relative abundance (Fournier et al. 2017).

Banding data has been used as a prior for assignment to origin for waterfowl research primarily as a way to longitudinally restrict regions of likely origins to a given flyway (Asante et al. 2017, Palumbo et al. 2019, Kucia et al. 2023, Schummer et al. 2023). Some studies have instead used these data to establish directional movement vectors (Gunnarsson et al. 2012, Guillemain et al. 2014) and movement probabilities among regions (Ashley et al. 2010, Kusack et al. 2022). The latter approach can be useful in species-specific applications, where movement between established management regions can be estimated (Robinson et al. 2016), while the flyway approach can be more broadly applied as it relies on well-established continental movement patterns based on political boundaries (Roberts et al. 2022). The directional movement vector approach relies on estimating of movement direction (for a given season) through individual encounter histories, assuming that movement direction between banding and encounter locations represents population-wide migratory behaviour. In situations with few band returns, such as those for songbirds in North America, these individual movements can be summarized across the entire range to estimate population-wide seasonal movement directions (e.g., van Wilgenburg and Hobson 2011). In cases with ample band returns, as is the case with many waterfowl species, these movement directions can be summarized based on encounters in management regions and geopolitical boundaries, or specific harvest sites (e.g., Gunnarsson et al. 2012). With the robust banding datasets available for many waterfowl species, priors can, in theory, be established with band returns from portions of a study area, to allow for multiple priors within a given study area.

Under adaptive harvest management (AHM), outside of a few select examples of species-specific management (e.g., Northern Pintail *Anas acuta*, American Black Duck *Anas rubripes*, Greater Scaup *Aythya marila* and Lesser Scaup *Aythya affinis*), North American

waterfowl are managed at the flyway scale (U.S. Fish and Wildlife Service 2021). Within these flyways, a single population is assumed, but a species may exhibit moderate to high harvest connectivity (e.g., American Black Duck; Ashley et al. 2010, Roy et al. 2015, Kusack et al. 2022) or significant movement between regions (Roberts et al. 2022). As such, it is important to estimate the degree of harvest connectivity to ensure current management matches the underlying population.

Using feathers collected from 11 species of harvested waterfowl across the Great Lakes region, I determined their likely natal origins using direct band returns and stable-hydrogen isotope measurements of feathers (δ^2H_f), directly combining and comparing two different sources of connectivity information. I focused on the Great Lakes as my harvest area, as this provided an opportunity to compare origins among a wide suite of species breeding across Canada including some species breeding locally. I first explored how these two complementary data sources can realistically be integrated into likelihood-based assignment methods to refine origin estimates for harvested waterfowl. Specifically, I compared the use of band returns as prior probabilities of origin (hereafter 'priors') in three frameworks: (1) by flyway, (2) by 5° longitudinal zone, and (3) by treating movement as a directional vector. I also explored the scale at which these priors are defined, where I compared the use of a prior derived for the entire Great Lakes region versus one derived at a finer spatial scale based on harvest location within the Great Lakes region. Lastly, I directly compared origin based on δ^2H_f, origin based on direct band returns, and banding effort to evaluate the overlap, determine potential gaps in the current banding program, and highlight priority areas of future banding efforts to supplement the existing framework.

5.2   Methods

5.2.1   Study area

The Great Lakes region is a prime breeding, stopover, and overwintering location for many waterfowl, with more than 30 species occupying the area at some point during the year (Prince et al. 1992). The Great Lakes region includes waterfowl harvest from the Mississippi and Atlantic flyways of North America. This region is a mix of abundant

open waterbodies, diverse wetland types, and extensive river systems that flow into the Great Lakes. Terrestrially, the southern portions of the Great Lakes are heavily modified environments with several large urban centers (e.g., Chicago, Cleveland, Detroit, Toronto) and regions of intensive row crop agriculture. Moving south to north, the basin covers four ecoregions (Level II, U.S. Environmental Protection Agency 2010), representing a gradient from mixed forest and grasslands to the Boreal Forest: Mixed Woods Plain, Central USA Plains, Mixed Wood Shield, and Softwood Shield.

5.2.2   Study species

I examined the natal origins of 11 species of harvested ducks: American Black Duck, American Green-winged Teal, Bufflehead (*Bucephala albeola*), Canvasback (*Aythya valisineria*), Greater Scaup, Lesser Scaup, Mallard, Northern Pintail, Redhead (*Aythya americana*), Ring-necked Duck (*Aythya collaris*), and Wood Duck (*Aix sponsa*). Species were chosen as a broad representation of the Great Lakes harvest, with variable harvest rates, band returns, and banding effort. I also specifically wanted to compare species with southern (e.g., Wood Duck) versus far northern breeding areas (e.g., Greater Scaup), as I expect southern breeding species to have greater banding effort, in terms of spatial coverage, as their range overlaps more with human-occupied areas. Within Ontario and Michigan, which represent the most significant provinces/states of the Great Lakes region in terms of area, number of harvested individuals (for 2020) were greatest in Mallard (72,743 and 74,043, respectively) and Wood Duck (44,657 and 39,001) with Bufflehead (3,753 and 13,209), Canvasback (1,952 and 1,584), and Greater Scaup (4,004 and 5,543) exhibiting some of the fewest harvested individuals for my study species (Raftovich et al. 2022).

5.2.3   Feather samples

Feathers (first primary, P1; n = 1,073) were collected from wings submitted to the Species Composition (Canada) and Parts Collection (USA) surveys in the 2017–18 (n = 241), 2018–19 (n = 417), 2019–20 (n = 39), and 2020–21 (n = 50) harvest seasons (Table 5.1 and Figure 5.1). Most of the sampling was done in the first two seasons, with some target species (Canvasback and Redhead) sampled specifically in later years. Through

these annual surveys, hunters are systematically randomly selected and must send in an entire wing from each individual they harvest in a season, providing information on the location and date of harvest for each individual. Wings were identified, aged, and sexed by trained biologists (Carney 1992). I limited the collection to feathers from juvenile birds, which are grown at the natal site for that individual.

For wings submitted to the Species Composition Survey, I had specific harvest locations (latitude and longitude), but for the Parts Collection Survey, I used the centroid of the county of harvest in place of the specific harvest location. Using these harvest locations, I then filtered the data to only include feathers that were collected within the Great Lakes watershed (Grannemann 2010), which reduced the number of feathers to 747. Some Northern Pintail feathers came directly from another concurrent project (n = 238; Wojtaszek 2022) but were included in this study because they were harvested in the Great Lakes.

Due to sampling based on hunter-killed birds and the inclusion of data collected for other projects, the spatial coverage of certain species was not homogenous throughout the Great Lakes watershed. As expected, fewer samples were collected in the northern areas compared to more populated areas in the south (Figure 5.1). Mallard collection, in particular, was biased toward the eastern edge of the watershed, as 62 % of the samples included there were harvested in New York state. I included these samples to increase the sample size of Great Lakes harvested Mallard, but this introduced some spatial heterogeneity in the Mallard dataset.

Table 5.1 Sample sizes and summary statistics (sample size [n], mean [μ], standard deviation [SD]), by species and country of harvest, for feather stable-hydrogen isotope values (δ^2H_f).

Species	Scientific name	Country	n	μ	SD
				δ^2H_f	
American Black Duck	*Anas rubripes*	CA	31	-118.75	14.18
		USA	39	-120.86	11.26
American Green-winged Teal	*Anas crecca carolinensis*	CA	41	-123.35	15.16
		USA	19	-127.43	18.99
Bufflehead	*Bucephala albeola*	CA	59	-144.14	18.92
		USA	19	-147.97	21.02
Canvasback	*Aythya valisineria*	CA	21	-159.87	25.45
		USA	1	-166.4	
Greater Scaup	*Aythya marila*	CA	13	-150.17	22.99
		USA	18	-163.46	22.4
Lesser Scaup	*Aythya affinis*	CA	17	-137.68	15.88
		USA	25	-152.66	20.57
Mallard	*Anas platyrhynchos*	CA	55	-120.8	16.5
		USA	114	-119.46	17.38
Northern Pintail	*Anas acuta*	CA	64	-144.77	19.89
		USA	42	-142.51	22.94
Redhead	*Aythya americana*	CA	50	-146.97	18.26
		USA	37	-140.44	21.14
Ring-necked Duck	*Aythya collaris*	CA	37	-126.54	22.75
		USA	14	-134.51	27.66
Wood Duck	*Aix sponsa*	CA	31	-108.52	11.05
Total		CA	419		
		USA	328		
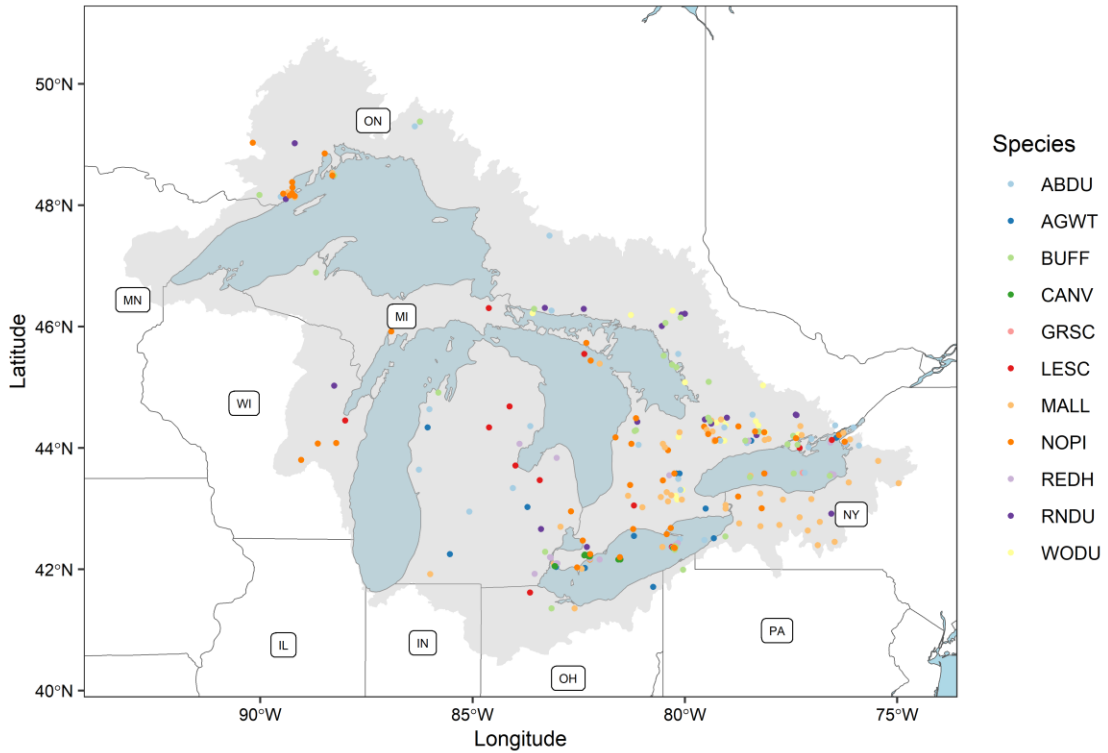
Figure 5.1 Harvest locations for juvenile ducks in the Great Lakes region. Harvest locations, or approximations (see Methods), for individual ducks are shown as points, with species represented by the points colour. The Great Lakes watershed is shown in light grey (Grannemann 2010) and the Great Lakes waterbodies are shown in light blue. Labels show state and province abbreviations for those overlapping the Great Lakes region.

5.2.4　Stable-isotope analysis

Feather samples collected for this project were processed for stable-hydrogen isotopes (δ^2H_f) at Western University's Advanced Facility for Avian Research Laboratory for Stable-Isotope Science (n = 612; LSIS-AFAR, London, ON, Canada). Feathers were first cleaned of surface oils by soaking and rinsing in a 2:1 chloroform:methanol mixture and allowed to dry under a fume hood. I sampled the distal end of the feather vane and weighed 0.350 ± 0.03 mg of feather material into silver capsules. Crushed capsules were then placed in a Uni-Prep carousel (Eurovector, Milan, Italy) heated to 60 °C, evacuated and then held under positive helium pressure. Feather samples were combusted using flash pyrolysis (~1350 °C) on glassy carbon in a Eurovector elemental analyser (Eurovector, Milan, Italy) coupled with a Thermo Delta V Plus continuous-flow isotope-ratio mass spectrometer (CF-IRMS; Thermo Instruments, Bremen, Germany), using the comparative equilibration method of Wassenaar and Hobson (2003) using the same two keratin standards (CBS, δ^2H = -197 ‰; KHS, δ^2H = -54.1 ‰) corrected for linear instrumental drift. All results are reported for non-exchangeable H expressed in the typical delta (δ) notation, in units of per mil (‰), and normalized on the Vienna Standard Mean Ocean Water (VSMOW) scale. Based on within-run and across-run analyses of standards, measurement error has been previously shown to be approximately $\pm$ 2.5 ‰ (Kusack et al. 2023).

A smaller proportion of Mallard and Northern Pintail samples, incorporated from other projects, were processed at the Cornell University Stable Isotope Laboratory (n = 136; COIL, Ithica, NY, USA). For detailed lab methods see Chapter 3. Measurements from both labs are comparable as both labs use the same comparative equilibration method, standards, and values for those standards (i.e., old ECCC scale) (Magozzi et al. 2021).

5.2.5　Direct band recoveries

I obtained band encounter data from the USGS, representing all banding and encounter records from 1960–2022 (Celis-Murillo et al. 2022). I first filtered this dataset to only include my species of interest which fit all of the following criteria: (i) normal wild birds, (ii) banded preseason (July–September), (iii) banded as a hatch-year bird (including

locals and juveniles), and (iv) not tagged with any extrinsic trackers (e.g., PIT, GPS, VHF tags). I removed any encounter or banding records where the spatial uncertainty exceeded 1°. This dataset represented the preseason banding effort, for hatch-year birds of my species (n = 4,027,431; Table 5.2).

To obtain direct recoveries, I filtered the preseason records to only include records where birds were shot in the harvest season (Sep–Mar) directly following banding and harvested in the Great Lakes watershed (Grannemann 2010). After filtering I identified 47,102 direct recoveries across the 11 species (Table 5.2).

Lastly, for the directional movement vector analysis, I also restricted this dataset to only direct recoveries originating (banded) from outside the Great Lakes watershed as a more focused sample of migrating birds. I also removed any samples encountered within 100 km of the original banding location, regardless of whether the banding location was within or outside of the Great Lakes. After filtering I identified 8,593 direct recoveries of migrants across the 11 species (Table 5.2). Throughout the manuscript, these three datasets will be referred to as the preseason banding effort, direct recoveries, and migratory direct recoveries datasets. These datasets are not independent as they are fully nested (i.e., preseason banding effort > direct recoveries > migratory direct recoveries).

5.2.6   Statistics

All statistics and geospatial exploration were done in the R Statistical Framework version 4.3.1 (R Core Team 2023) in RStudio version 2023.09.1 (RStudio Team 2023). Wherever possible I used the spatial packages terra (version 1.7-46, Hijmans 2023) and sf (version 1.0-14, Pebesma 2018) to work with spatial data and reverted to raster (version 3.6-23, Hijmans 2020) when necessary.

Table 5.2 Sample sizes for band-return data (n = 4,027,431, 1960–2022), separated by total banding effort (*b*), direct recoveries (*r*) for the Great Lakes, and direct recoveries for migrants in the Great Lakes (see methods).

Species	Scientific name	n		
		b	*r*	*r* (migrants)
American Black Duck	*Anas rubripes*	301,816	3,780	1,122
American Green-winged Teal	*Anas crecca carolinensis*	188,943	671	358
Bufflehead	*Bucephala albeola*	1,984	7	7
Canvasback	*Aythya valisineria*	25,461	229	229
Greater Scaup	*Aythya marila*	561	1	1
Lesser Scaup	*Aythya affinis*	36,724	44	43
Mallard	*Anas platyrhynchos*	1,965,401	36,240	5,678
Northern Pintail	*Anas acuta*	330,241	235	133
Redhead	*Aythya americana*	82,548	787	662
Ring-necked Duck	*Aythya collaris*	48,093	251	177
Wood Duck	*Aix sponsa*	1,045,659	4,857	183

To define the spatial extent of the flyways, I used the shapefile from the USFWS (U.S. Fish and Wildlife Service 2017). For Canada, I followed the changes from Roberts et al. (2022). British Columbia and the Yukon Territories were assigned to the Pacific Flyway. Alberta, Saskatchewan, and the Northwest Territories were assigned to the Central Flyway. Manitoba and Ontario / Nunavut west of -80° latitude were included in the Mississippi Flyway. The Maritimes provinces (NB, NS, PEI), Quebec, Newfoundland and Labrador, and Ontario / Nunavut east of -80° latitude were included in the Atlantic Flyway.

Before assignment to origin, I explored the raw δ^2H_f data in a linear modelling framework, to test for relationships between δ^2H_f values and harvest season and country of harvest across species. To test for systematic differences across species, I also included species as a predictor, but only included data from species that were sampled in the same season within a given model to avoid collinearity between season and species. Normality and heterogeneity of variance in the residuals were assessed visually. Collinearity was assessed via variance inflation factors (Zuur et al. 2009), using 2 as a cutoff.

5.2.7 Regional priors

For the entire Great Lakes region, I defined three priors per species (see "Subregional priors" section below for details on fine-scale within region priors for Mallard): (1) flyway of origin, (2) 5° longitudinal zone of origin, (3) movement direction. All priors were defined relative to being encountered (harvested) in the Great Lakes. For the likely flyway and longitudinal zone of origin, methods were similar. I determined relative harvest rates (*f*) for each flyway or longitudinal zone as:

$$f_{i,j} = \frac{r_{i,j}}{b_{i,j}}$$

where *b* is the total number of hatch-year birds banded (i.e., preseason banding effort) and *r* is the number of direct recoveries originating from a given flyway or longitudinal zone (*i*) in a given year (*j*). These harvest rates were normalized to sum to 1 within each year. In cases where no direct recoveries occurred, but banding effort existed, I treated those as 0 while cases where no banding effort existed were treated as null values. To

determine the overall prior probability of origin, for a species, I calculated the mean value across all years (ignoring null values) and normalized the resulting values to sum to 1.

To determine likely movement direction, I used the migratory direct recoveries dataset. For each individual, I determined the azimuth between the encounter (harvest) and banding location using the 'bearing' function from the geosphere package (version 1.5-18, Hijmans 2022). Previous applications of this method have applied a von Mises circular distribution to these angular trajectories to estimate the population distribution for movement direction (van Wilgenburg and Hobson 2011, Gunnarsson et al. 2012, Guillemain et al. 2014), but I wanted to allow for multimodal distributions. Therefore, I used the package BAMBI (version 2.3.5, Chakraborty and Wong 2021) to fit a Bayesian univariate angular mixing model for each species. I used the function *fit_incremental_angmix* to determine the optimal number of components (i.e., clustered groups with different parameters; max = 5) via stepwise model selection (MCMC parameters: iterations = 10,000, thin = 1, chains = 3, burn-in = 5,000). To favour parsimony in the final model, I used a Bonferroni adjustment with decreasing adjusted alphas within an increasing number of components. From the final model, I estimated the mean (μ), concentration parameter (κ), and mixing proportion (pmix) for each component.

To create the surface for movement direction priors, I used a circular buffer, split into 5° wedges created using a modified version of the function 'buffer_wedge' from the buffeRs package (version 0.31, https://github.com/cran/buffeRs). I estimated probability densities for each wedge, based on the midpoint, using the model components derived above and normalized the probabilities to sum to 1. Although previous applications of this method have used a singular capture point, I had unique harvest locations for each individual. Therefore, this circular prior probability surface was centered on the harvest location for each individual assignment (see "Assignment to origin" section below). Although each individual had a unique prior probability surface, as the center points were spatially shifted, the circular probability distribution remained the same.

5.2.8   Subregional priors

For Mallard, which had the largest sample sizes for all datasets, I also evaluated the use of a more fine-scale prior estimation that varied by harvest location within the Great Lakes region (i.e., subregional priors). Specifically, I subset the Great Lakes region into 5° cells (4 x 2 grid) and summarized direct recoveries to each of the cells based on the location of harvest. Following the same prior estimation as above, I determined eight priors (one for each cell) for each method (flyway, longitudinal zone, direction). The movement direction prior surface was still centered on the harvest location for each individual but used the cell-specific circular distribution. I used 5° cells to reflect the uncertainty at which these banding data are provided (< 1°). Although these grid cells also included areas outside of the Great Lakes watershed, only data from the Great Lakes were included in the prior estimation.

5.2.9   Assignment to origin

I created foraging guild-specific (dabblers and divers) isoscapes for the expected feather stable-hydrogen isotope (δ^2H_f) values, across North America. I used the calibration equations derived for these guilds in Kusack et al. (2023) (Dabblers: $\delta^2H_f = \delta^2H_p$ x 0.6 – 71.7 ‰, σ_{cal} = 17.2 ‰; Divers: $\delta^2H_f = \delta^2H_p$ x 0.5 – 78.4 ‰, σ_{cal} = 14.1 ‰) and used a mean-annual precipitation surface (δ^2H_p) (Bowen et al. 2005, Bowen 2021). While I previously found that amount-weighted mean growing-season δ^2H_p compared to mean annual δ^2H_p isoscapes did not show markedly better predictive accuracy or precision (Kusack et al. 2023), I chose the mean annual isoscape as it is the most parsimonious interpretation of environmental δ^2H_p values, including amount-weighted δ^2H_p measurements from all months regardless of season. Predicted δ^2H_f isoscapes were then clipped and masked to the species' breeding range (including permanent resident areas). All breeding range shapefiles were sourced from Birdlife international (BirdLife International and Handbook of the Birds of the World 2022) except for American Black Duck, which I used the range depiction from Baldassarre (2014).

I determined the likely natal regions following likelihood-based assignment methods within the isocat package (version 0.2.6, Campbell et al. 2020). For each individual of

unknown origin, spatially explicit likelihood of origin was estimated on a cell-by-cell basis, applying a normal probability density function:

$$f(y_*|\mu_c, \sigma_c) = \left(\frac{1}{\sigma_c\sqrt{2\pi}}\right) \exp\left[-\frac{(y_* - \mu_c)^2}{2\sigma_c^2}\right]$$

where, y is the δ^2H_f of the individual, μ_c is the predicted mean δ^2H_f at that cell (c), and σ_c is the predicted error at that cell. This error incorporates both isoscape error (σ_{iso}) and calibration error (i.e., standard deviation of calibration residuals; σ_{cal}):

$$\sigma_c = \sqrt{\sigma_{iso}^2 + \sigma_{cal}^2}$$

Priors were rasterized to match the resolution and extent of the isoscape and were incorporated into likelihood-based assignment using Bayes' Rule:

$$f_x = \frac{f(y|\mu_c, \sigma_c) f_b}{\Sigma f(y|\mu_c, \sigma_c) f_b}$$

Where f_x is the posterior probability of origin, f_b is the prior probability of origin, and $f(y|\mu_x, \sigma_x)$ is the likelihood. Posterior probability of origin surfaces were normalized to sum to 1 and converted into binary regions of origin using a 2:1 odds ratio (i.e., upper 66 % of probability density), to estimate regions of likely origins and compare origins across individuals. Finally, all surfaces for given species were summed to produce a final map showing the number of individuals assigned to each cell.

For the assignments using directional movement vectors as the prior probability of origin, I restricted the assignment to only include individuals that showed a δ^2H_f value consistent with migratory (non-local) origins, to match the band-return data. If the difference between observed δ^2H_f and the predicted δ^2H_f (μ_c) exceeded the predicted error (σ_c) at the harvest site, the bird was considered a migrant. Isoscape error (σ_{iso}) in the Great Lakes is low (0.1–2.5 ‰), so the predicted area at the harvest sites was equivalent to the σ_{cal} (17.2 ‰ for dabblers, and 14.1 ‰ for divers).

All assignment procedures and prior probability estimation procedures were done in the WGS 84 coordinate system (EPSG:4326) and reprojected to an Albers equal-area conic projection (EPSG:42303) for final visualization.

5.2.10   Overlap

Finally, I compared the regions of likely origins derived above to the spatial extent of (1) direct recoveries (*r*) and (2) preseason banding (*b*). I first created raster grids (1° resolution) that summarized the number of birds that were banded in each cell (preseason banding) and the number of those birds that were recovered as direct recoveries, for each species. I simplified these surfaces into binary values and compared these surfaces to the individual binary regions of likely origin from $\delta^2 H_f$ assignment procedures. Specifically, I compared the proportional area of the binary regions of likely origin that overlapped with the source areas for direct recoveries and the preseason banding. This procedure was done for each assignment framework, including each prior and no priors. Regions of likely origin were resampled to match the coarser preseason banding rasters.

As a final visualization, I highlighted regions indicated by the likely origins where no banding effort has been undertaken in the last 60 years. To be conservative, I used the likely origins based on the flyway of origin prior and subset the regions of likely origin to only include cells where at least 50 % of individuals, from a given species, were assigned.

5.3   Results

5.3.1   Priors

Across species, the number of direct recoveries and the banding effort varied greatly (Table 5.2). Mallard had the most band returns and effort (n = 36,240 and 1,965,401) and Greater Scaup had the fewest recoveries and least effort (n = 1 and 561). Using these recoveries, I derived priors for all species (Figure D2–Figure D5, Figure D7–Figure D12) except for Greater Scaup because of the lack of direct recoveries to estimate meaningful probabilities (Figure D6).

Flyway of origin priors showed the Mississippi Flyway as the most likely origins for all species except Northern Pintail and Wood Duck, which were most likely to originate in the Atlantic Flyway, although Wood Duck had more equal probability of origin across both flyways. Longitudinal zone of origin priors followed a descending pattern where zones adjacent to high probability longitudinal zones gradually decreased with distance. Redhead, for example, showed high probabilities near the eastern edge of the prairie breeding range and the western edge of Great Lakes breeding range with gradually decreasing probabilities further west and east, respectively (Figure D10). Comparing the flyway and longitudinal zone of origin, both generally supported the same regions of origin, unless the longitudinal prior indicated the highest probabilities of origin along a flyway border, as was the case most notably with American Green-winged Teal (Figure 5.2 and Figure D3) and Northern Pintail (Figure D9). In most cases, the longitudinal zone provided more fine-scale resolution within the flyway(s) of origin where certain areas were given lower probabilities and excluded from the final likely region (e.g., American Black Duck, Figure 5.2 and Figure D2).

Movement direction priors showed focused directional probabilities to the northwest for most species but showed northward origins for American Black Duck (Figure D2), northeastern origins for American Green-winged Teal (Figure D3), and southeastern origins for Wood Duck (Figure D12). Almost all species, other than those with low sample size (Bufflehead, Canvasback, Lesser Scaup), showed multiple components to the circular mixing model, but in most cases the circular means were in similar directions (e.g., American Black Duck $\mu_1 = 28.31$, pmix$_1 = 0.41$, $\mu_2 = 8.37$, pmix$_2 = 0.58$) or the mixing proportions favoured a single direction (e.g., Northern Pintail, $\mu_1 = 22.86$, proportion $= 0.71$, $\mu_2 = 305.96$, proportion $= 0.29$). Mallard was the only species to exhibit markedly bimodal directional probabilities of origin ($\mu_1 = 117.43$, pmix$_1 = 0.41$, $\mu_2 = 298.63$, pmix$_2 = 0.22$, $\mu_3 = 68.97$, pmix$_3 = 0.37$). The variance of these distributions varied among species, with some showing high variance (Wood Duck $\kappa = 2.34$ and 3.86) and others, especially those with low sample sizes, showing low variance (Bufflehead $\kappa = 56.41$). There was also low variance when the most frequent direct recoveries were from the upper edge of the banding effort (Canvasback $\kappa = 76.41$ and Redhead $\kappa = 144.44$), leading to a highly focused directional distribution.

In general, movement direction priors contrasted with the flyway and longitudinal zone priors. Northern Pintail in particular, which showed strong Atlantic Flyway origins using the previous two priors, showed likely movement probabilities to the northwest (Figure D9 and Figure D11).

5.3.2   Stable-hydrogen isotopes

For the two seasons with the most harvest data (2017–18 and 2018–19), there were only marginal differences in δ^2H_f values between harvest seasons (t = -1.70, p = 0.09) after controlling for differences in the among species ($F_{8,615}$ = 31.32, p < 0.0001). I found no differences in the δ^2H_f values between the countries of harvest (t = -0.29, p = 0.77). Only Canvasback, Northern Pintail, and Redhead were sampled across ≥ 3 years (see Table D1). For these species, I still saw no effect of the season ($F_{2,170}$ = 1.07, p = 0.34) or country of harvest (t = 1.05, p = 0.30).

5.3.3   Likelihood-based assignment

Regions of likely origin determined using δ^2H_f values alone were, as expected, broad (Figure 2 and Figure D2–Figure D12). Latitudinally, American Green-winged Teal (Figure 5.2) and Lesser Scaup (Figure D7) showed origins in the southern portions of their ranges, while Canvasback (Figure D5), Redhead (Figure D10), and Wood Duck (Figure 5.2) had more northern origins within their ranges. Northern Pintail showed origins in the latitudinal center of their range. Bufflehead, Greater Scaup, and Ring-necked duck showed variable origins with individuals showing origins across the entire breeding range (but see discussion on Greater Scaup).

After the integration of priors, there was marked restriction in the region of likely origin in almost all cases (Figure 5.2), but again, regions of likely origins did not agree in all cases, especially when considering the movement direction method. Using American Green-winged Teal as an example, all three priors concentrated likely origins to the eastern portion of the range (east of Manitoba), but within that area regions showing the most support differed (Figure 5.2). Specifically, applying the flyway prior showed probable origins in Ontario and Manitoba, to the northwest of harvest areas, while the movement direction prior showed origins in northern Quebec, to the northeast. In the

middle of these, the longitudinal zone prior showed likely origins in northern Ontario and Quebec along the flyway margin.

For Canvasback, applying the priors led to a bimodal distribution of likely origins, where likely origins based on δ^2H_f favoured origins in the northwest, but banding data were concentrated in the southeast (Figure D5). Therefore, likely origins were concentrated around gaps in the banding data. Here the longitudinal band of origin prior suggests origins in Prairie Pothole region with some minor probabilities in Alaska and the flyway of origin prior suggested some origins in northwestern boreal. Similarly, for Bufflehead, longitudinal zone of origin priors strongly restricted origin to areas where banding occurs compared to the flyway of origin prior, which included broader areas across the boreal portion of the Mississippi Flyway, where almost no banding occurs (Figure D4). Compared to a species like American Green-winged Teal, where banding effort is more consistent (longitudinally) across the range, these focused regions of origin may be more suspect.
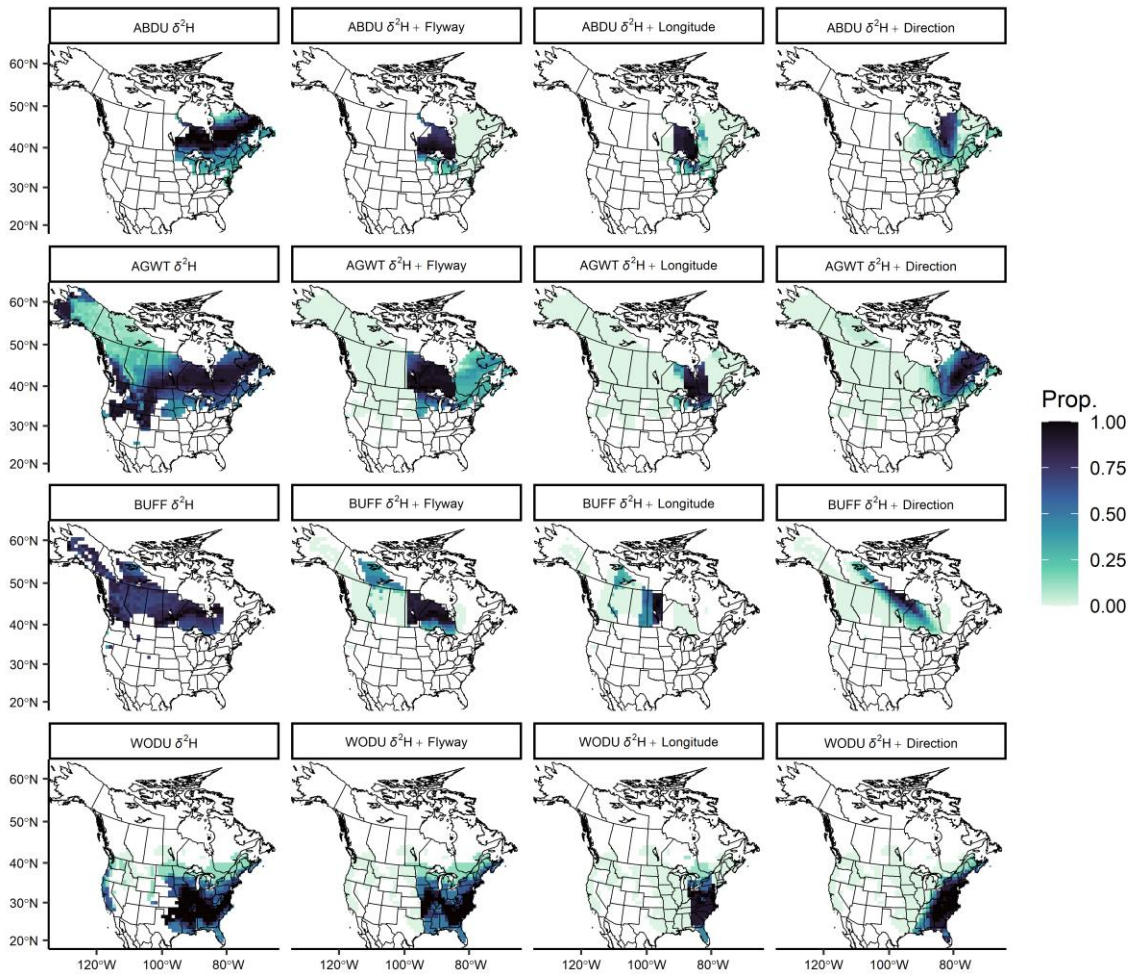
Figure 5.2 Likely origins of American Black Duck (ABDU), American Green-winged Teal (AGWT), Bufflehead (BUFF), Wood Duck (WODU) based on likelihood-based assignment using δ^2H_f and different priors: flyway (Flyway), 5° longitudinal zone (Longitude), and movement direction (Direction). Values were rescaled to be a proportion of the maximal value, to better visualize relative differences.

5.3.4　Regional vs. subregional priors

Mallard origins, without any priors applied, showed likely origins in the southern portion of their breeding range (Figure D8). Using the regional priors, estimated for the entire Great Lakes region, the most likely origins were consistent with the Mississippi and Atlantic flyways (Figure 5.3). As with many of the other species, when the longitudinal prior was applied, it allowed for more precise estimation of origins along the border of the two flyways. This suggested more local origins around the Great Lakes. Interestingly, when the subregional explicit priors were used, the flyway of origin was most focused on the Atlantic Flyway both in the flyway prior and the longitudinal zone prior (Figure 5.3). This was likely driven by the spatial bias in the Mallard δ^2H$_f$ data where most samples came from New York state.
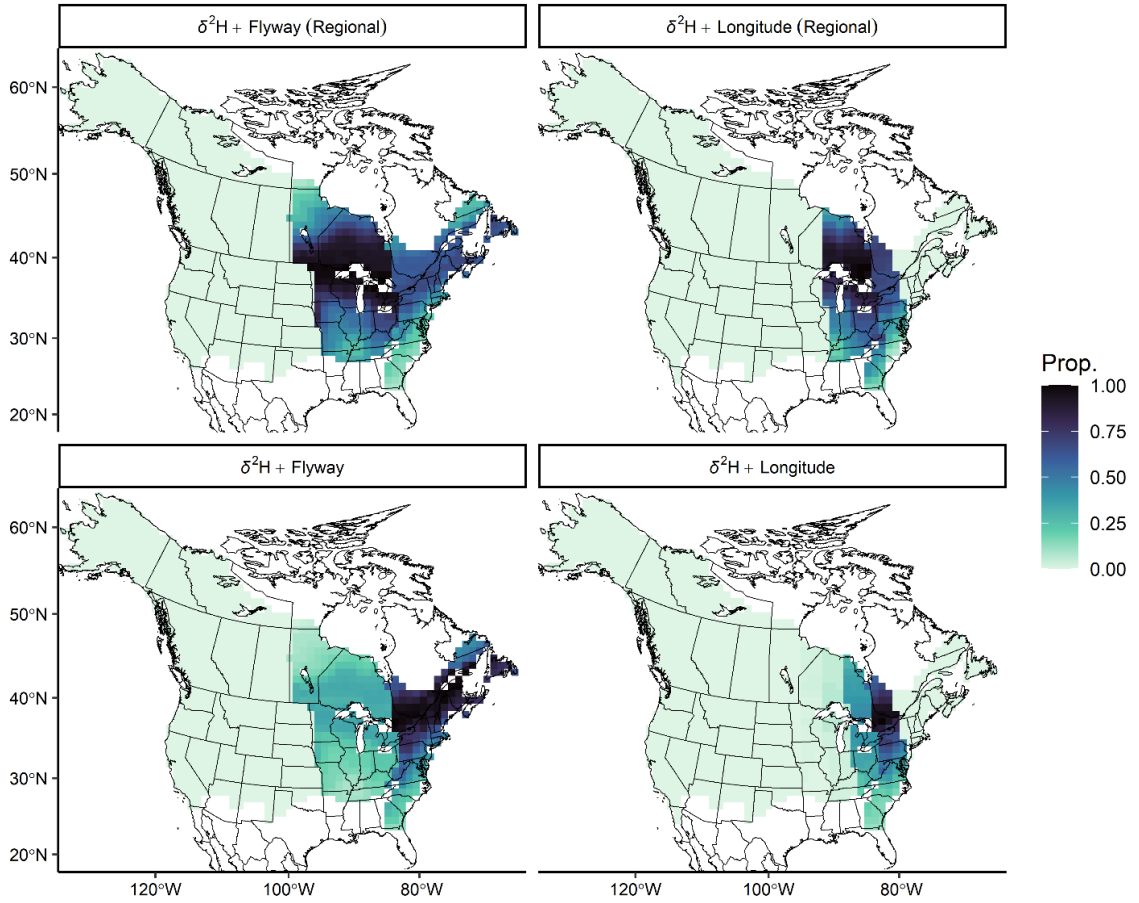
Figure 5.3 Comparison of regional priors (top row) and spatially explicit priors (bottom row) to establish the likely origins of harvested juvenile Mallard. Values were rescaled to be a proportion of the maximal value, to better visualize relative differences.

5.3.5   Overlap

Overlap between likely regions of origin and banding locations varied among species, with Wood Duck showing the greatest overlap (0.81 ± 0.07) and most other species showing moderate overlap (range in means = 0.11–0.60, Figure 5.4). Similarly, overlap between likely regions of origin and direct recoveries was highest for Wood Duck, but the overlap was on average lower (e.g., 0.27 ± 0.07 for Wood Duck). When the flyway of origin prior was incorporated, there were no major changes in either overlap measure. On average, the overlap with direct recoveries increased slightly, which makes sense as this region was informed by these data. Overlap with the banding locations fluctuated slightly with some species showing greater overlap (e.g., 0.47 ± 0.15 for Redhead) and others showing less overlap (e.g., 0.27 ± 0.17 for Northern Pintail).

For the Great Lakes harvest, priority banding regions were concentrated in northwestern Ontario and northern Manitoba (Figure D1). American Black Duck, American Green-winged Teal, Bufflehead, Lesser Scaup, Mallard, Northern Pintail, and Ring-necked Duck all showed priority banding regions in this area (Figure 5.5). Wood Duck and Redhead both showed patchy scattered regions where banding effort could be increased, indicating decent coverage already. Northern Pintail also showed priority areas in northern Quebec (Ungava Peninsula) and the north coast along the Gulf of St. Lawrence and Labrador (Figure 5.5).
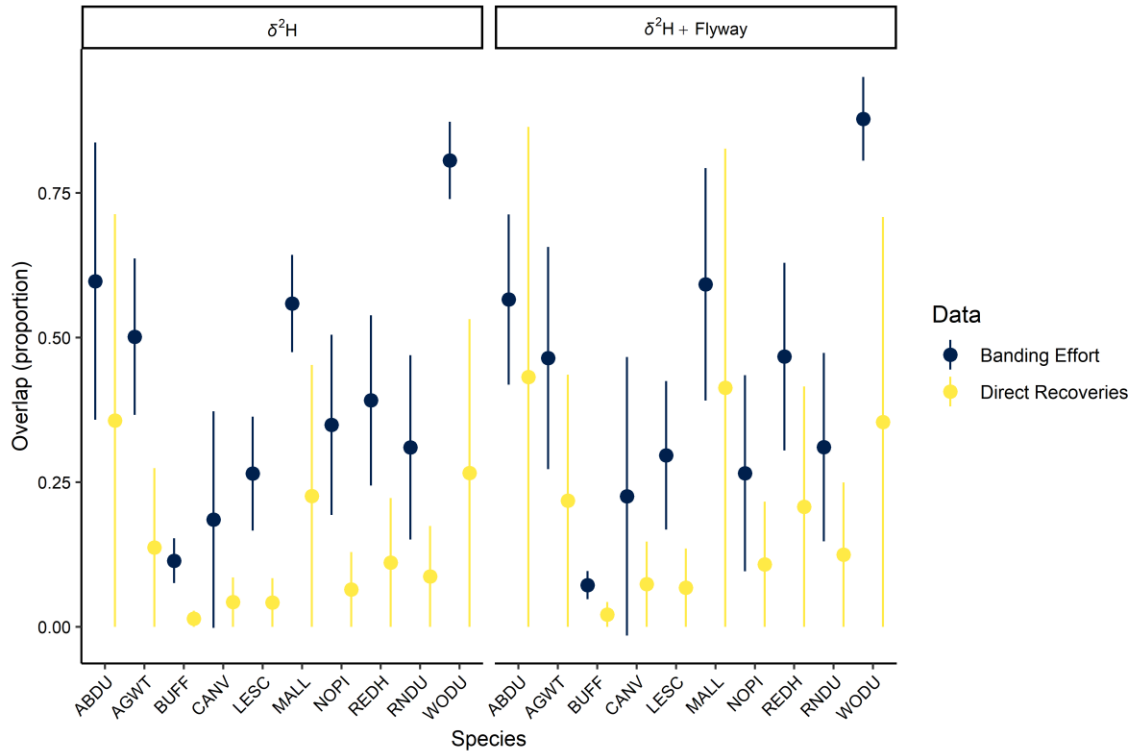
Figure 5.4 Overlap estimates (mean and SD) between regions of likely origin based on stable isotopes ($\delta^2 H_f$ – left, $\delta^2 H_f$ + flyway prior – right) and band returns, by species. Proportional overlap shows an estimate of (a) agreement between the regions of likely origin based on the two data sources (direct recoveries; yellow) and (b) the current coverage of all likely origins by banding effort (blue).
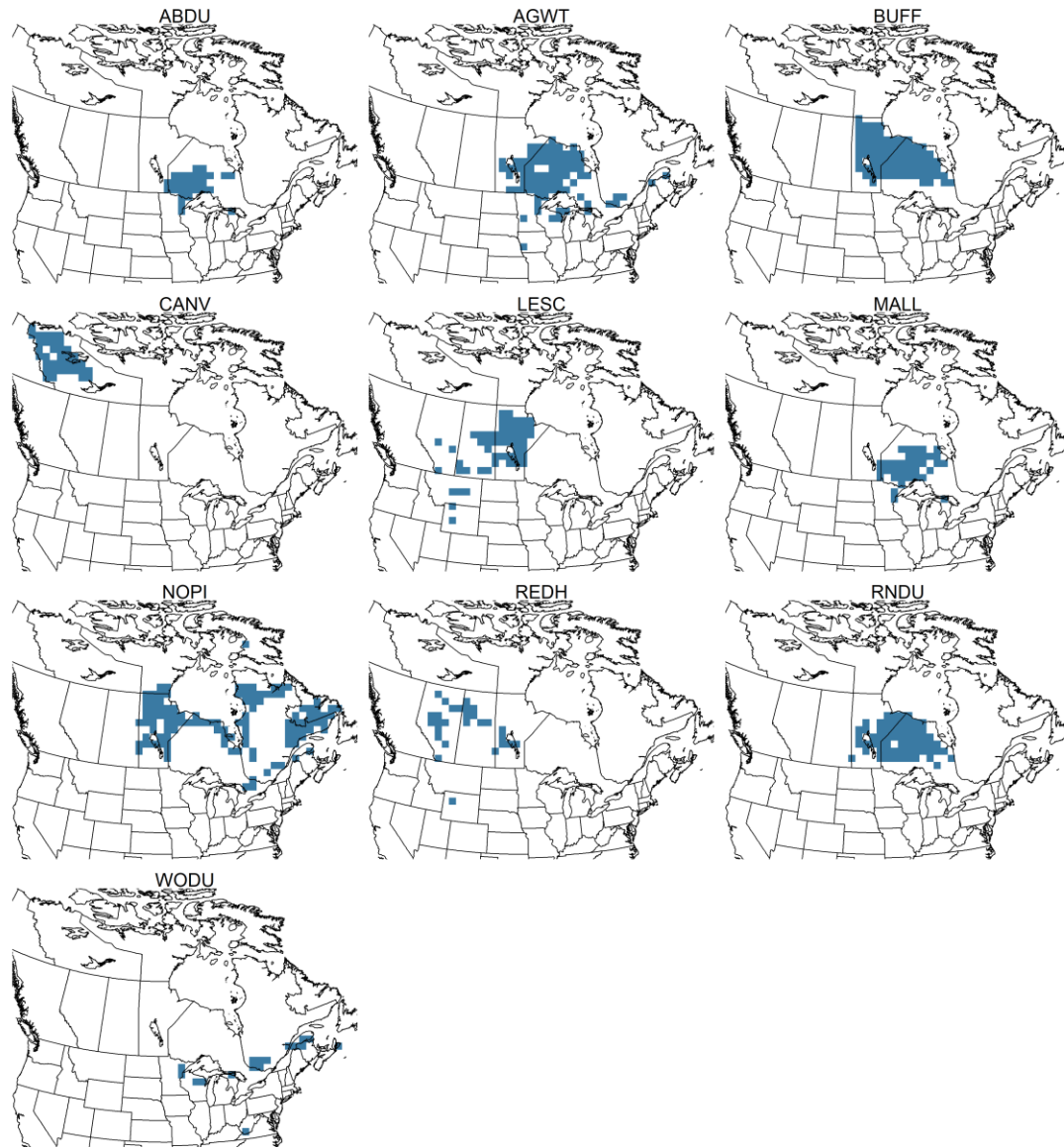
Figure 5.5 Species-specific target regions for future banding effort. Polygons shown in blue depict regions of disagreement between likely origin (δ^2H_f + flyway prior) and banding effort.

5.4   Discussion

Use of mark-recapture data from waterfowl banding has always been plagued with spatial and temporal bias that inevitably occurs during banding. Here I have demonstrated the usefulness of combining stable isotopes and 60+ years of band returns to probabilistically derive the origins of waterfowl harvested in the Great Lakes. Across all species, the use of flyways and longitudinal zones as a prior probability of origin showed the most promising results, where longitudinal zones provided more fine-scale estimation of origins while providing the same longitudinal differentiation as the flyway priors. To my knowledge, this is the first application of fine-scale longitudinal zones as a prior probability of origin. Conversely, I did not find the directional movement vector to be a useful prior when applied to the Great Lakes, but I discuss why in more detail below. Notably I also highlight the importance of assessing these priors at different spatial scales, as deriving priors at the regional level vs. sub regionally significantly affected final regions of likely origins. Finally, taking advantage of δ^2H_f as an intrinsic marker, I identified regions in northwestern Ontario and northern Manitoba as potential targets for future multi-species banding efforts to fill gaps in the current banding framework. This study joins an ever-growing body of work using stable isotopes to establish harvest connectivity (Ashley et al. 2010, Guillemain et al. 2014, 2019, Asante et al. 2017, Palumbo et al. 2019, 2020, Kucia et al. 2023, Schummer et al. 2023), and my study reinforces the fundamentals of these methods in an effort to better integrate stable-isotope data with current waterfowl management frameworks.

This discussion was intended not as a critique of banding frameworks but, rather, as a demonstration of how intrinsic markers can supplement harvest derivations. Banding data are publicly accessible, annually updated datasets (https://www.usgs.gov/labs/bird-banding-laboratory/data) that are often underused considering the massive amount of effort done annually to mark these birds. Interpretation of the banding data can be complicated, especially with an ever-growing number of banded birds (> 19 million between 1960–2022; Celis-Murillo et al. 2022), but these data provide a rich source of mark-recapture data to answer myriad questions about waterfowl migration.

5.4.1   Effect of scale

Flyway priors were less specific than longitudinal zones, as longitudinal priors highlighted likely origins in narrower regions for many species. However, careful interpretation is needed, as narrower or more fine-scale prior probabilities of origin can also be derived by fewer band returns, in cases like Bufflehead. Priors cannot provide information on regions where no effort has been applied. The other benefit of longitudinal priors was the ability to show likely origins along the borders of established flyways, as seen in American Green-winged Teal, Mallard, Northern Pintail, and Wood Duck. This is likely a result, again, of a relatively northern harvest area, where shorter-distance movement and local origins are supported over flyway-level migration patterns. This highlights the need to establish regional priors rather than relying on those derived at a scale much larger than the given harvest area. For example, transition probabilities between breeding and wintering areas for American Green-winged Teal derived continentally show some movement from the Pacific and Central flyways to the Mississippi and Atlantic flyways (Roberts et al. 2022), but band recoveries derived here, for the Great Lakes, showed greatest probabilities of breeding origin along the border of the Mississippi and Atlantic flyways. Nonetheless, for species with fewer band returns, the use of flyway transition probabilities derived at the continental scale may be necessary.

The only species I was unable to establish any priors for was Greater Scaup. This was unfortunate, as Greater Scaup is an ideal example of how intrinsic markers alone cannot adequately determine regions of likely origin. Their breeding range in North America spans a latitudinally narrow region across northern Canada and Alaska (Figure S6), which shows overlap in expected δ^2H_f values between areas in Alaska, northern Quebec and Labrador, and the Canadian territories (the Yukon, the Northwest Territories, Nunavut) as isoclines run parallel to the breeding range (Bowen 2021). At this time, even with band returns, it is difficult to differentiate between these areas using δ^2H_f alone, as banding data only exists for Alaska. Alternative markers (e.g., genetics, strontium isotopes) or additional preseason banding effort in other areas, or with the inclusion of banding data from outside of the preseason (Fleming 2022), this may be possible in

future derivations. Highlighting the importance of these banding data, there is some discussion on band-return data for scaup as an additional breeding population estimator to compliment those produced by the Waterfowl Breeding Population and Habitat Survey (Schummer et al. 2018).

Here I also provided evidence of how sub regional compartmentalization of band recoveries can allow for more appropriate estimation of priors for isotope-based assignments, especially when sampling is unbalanced, as is usually the case. Subregional priors showed that sources for Mallard were more likely from the Atlantic Flyway, which is more consistent with derivations for the New York state harvest, where the bulk of Mallard samples were collected. This exercise worked for Mallard, as it is the most widespread and the most banded duck in North America (Celis-Murillo et al. 2022), and worldwide. Unfortunately, not all species will have adequate band returns to allow for this fine-scale prior derivation. Regardless, this exercise demonstrates the nuance required when estimating prior probabilities of origin.

5.4.2   Locality

One of the primary benefits of flyway and longitudinal zone priors over movement direction priors was their ability to detect the probability of 'local' (i.e., within region) origins. This was especially important as the Great Lakes is home to 21 species of breeding waterfowl (Cadman et al. 2007), although from my study species only Mallard, Ring-necked Duck, and Wood Duck breed regularly across much of the Great Lakes basin. It is inappropriate to apply movement direction priors to birds that could show local origins because the wedge shape of the prior distorts probability densities away from the capture site. For example, in Gunnarsson et al. (2012) the final assignments after incorporation of the prior probability showed no likelihood of local origins despite a clear overlap between the origins based on isotopes and the study site where these birds were captured. In this case, if local origins are not biologically possible, then the prior can be useful to eliminate local origins, but careful consideration must be taken if the sampling location overlaps with the breeding range.

Movement direction priors may be applicable in some cases, especially when harvest areas are relatively more distant from potential breeding areas, but the power of band-return data in these applications comes from the ability to longitudinally restrict the region of likely origin. These directional vectors influence the probabilities latitudinally and longitudinally, an effect more pronounced in northern harvest areas. This method also does not account explicitly for banding effort, as circular priors were calculated from individual movement vectors. That said, some species showed partial agreement across all three priors, such as Wood Duck. Still, even in these cases the movement direction prior was not able to accurately assess local origins.

An alternative framework may be to establish movement probabilities in a state-space mark-recapture model where the probability of being a local can be explicitly accounted for (Patterson et al. 2008). Mark-recapture models assessing movement under scenarios with local breeders and migrants exist (Gourlay-Larour et al. 2014), but incorporating directional movement probabilities, similar to the way presented here, has not been explored to date. Ideally, this could be in a fully spatial framework where recovery probabilities are estimated across the breeding range for a given harvest location. However, this introduces the same concerns about spatial biases and gaps in banding in the north.

5.4.3   Gaps and biases

The agreement between derived regions of likely origins and origins based on the band returns for waterfowl harvested in the Great Lakes was low, as expected. It is worth noting that even if the direct recoveries perfectly outlined the source origins, I did not expect complete overlap for direct recoveries and regions of likely origin. Within the isotopic assignment methodology, any area within the binary region of likely origin is just as likely as the other. Therefore, the region of likely origin for an individual could encompass its true origins but also include other areas with no direct recoveries, or banding effort. This overlap metric was meant to be a relative comparison between species and between assignment methods, not an absolute measure of accuracy. For the overlap between likely origins and banding effort, these measures can approach complete overlap, if banding is constant across the entire range, as was the case with Wood Duck.

But even for Wood Duck, however, breeding densities are not constant within this range. Therefore, lower proportions of overlap in some species could be driven by gaps in banding effort within the inner portions of the range, rather than in cases of species breeding in northern areas, which likely is not contributing to systematic gaps in the banding framework.

My spatial assignment suggested that most of the sampled individuals came from the Mississippi Flyway. This was not surprising as the Great Lakes are mostly covered by that flyway. Across species, northwestern Ontario and northern Manitoba were identified as regions to target banding efforts for American Black Duck, American Green-winged Teal, Bufflehead, Lesser Scaup, Mallard, Northern Pintail, and Ring-necked Duck, to better understand connectivity for the Great Lakes. Northern areas in these regions are mostly inaccessible by road, as is the case with much of the Boreal and Hudson Bay Lowlands. Looking at recent waterfowl banding data (post-2000) from this target banding region (focusing on Ontario and Manitoba only), some ducks and geese are being banded here (total bands = 151,592, American Black Duck n = 528, American Green-winged Teal n = 346, American Wigeon *Mareca americana* n = 110, Blue-winged Teal *Spatula discors* n = 1,846, Canada Goose *Branta canadensis* n = 116,452, Hooded Merganser *Lophodytes cucullatus* n = 223, Mallard n = 12,166, and Ring-necked Duck n = 205,, Snow Goose *Anser caerulescens* n = 18,675). All other species (e.g., Common Goldeneye *Bucephala clangula*, Lesser Scaup, Northern Pintail) have fewer than 100 banded birds in the past 22 years. Increasing regular banding efforts across these regions may not be practical, for the same reasons it has not been done to date, but targeted banding of locals (flightless young) can help to establish better estimates for these natal source areas. Further, my results only highlight these regions as target banding areas for the Great Lakes harvest, but the importance of these areas to the overall harvest in the Mississippi and Atlantic flyways is not clear and should be explored by applying these methods on a larger scale and at more southern harvest areas.

5.4.4   Recommendations

My recommendation when performing likelihood-based assignment that pairs stable-isotope and band-return data, is to use flyways and longitudinal zones as a prior

probability of origin, depending on the number of band-returns available. As an initial exploration, I recommend exploring the use of both priors, for a given species and study area. For example, Bufflehead and Lesser Scaup showed narrow and patchy longitudinal zone priors due to low band returns ($<$ 100). These gaps likely do not represent zero probability of origin. In these cases, I recommend the use of a flyway-level prior over the longitudinal zone prior. Further, in cases with abundant band-returns and a large study area, consider spatially segmenting band encounters when deriving priors to better represent variations in connectivity across the study area. As an alternative to band-returns, for species with very few band returns, there are also alternative intrinsic markers such as Strontium ($\delta^{86}Sr$) stable isotopes that can provide some longitudinal differentiation to perform multi-isotope assignments based on a single encounter (Bataille et al. 2020, Reich et al. 2021). Finally, when depicting origins, I encourage others to show estimates of likely origin estimated using all sources of data (i.e., δ^2H + prior) and each source of data separately, to allow for evaluation of all data sources independently.

5.4.5 Future directions

A major assumption of the priors we developed is that all hatch-year birds are banded at or near their natal sites. For birds banded as locals (i.e., flightless young) this assumption is valid, but there is some evidence from δ^2H_f that suggests some hatch-year birds are likely immigrants from other, possibly northern, areas (Harvey 2022). If these differences are short-distance movements, this assumption may be valid at the scale I have derived these priors ($>$ 5° longitude). One option would be to explore the use of more conservative criteria, limiting these banding records to only local birds, to see how prior probabilities change. This was beyond the scope of this multispecies project but could be explored in the case of a data-rich species like Mallard. As a proof-of-concept, when I applied this filter to the Great Lakes direct recoveries, sample sizes dropped significantly (-95 % overall, -98 % for Mallard), potentially limiting the estimation of more spatially explicit priors. Overall, this further justifies the use of intrinsic markers to elucidate the origins of these birds.

The temporal mismatch between the isotope data and the band returns data may also lead to spurious relationships, especially when the historic banding effort (prior to 1990)

outnumbers contemporary effort (post 1990), as is the case with species like American Black Duck (n = 2,842 for 1960–90, n = 938 for 1991–2022). Here year-specific priors were calculated and probabilities were averaged across all years, which assumes that movement patterns or population densities are not changing over time. For a species like American Black Duck, which experienced drastic population declines (50 % between 1950–80) that differed in intensity across the breeding range (Conroy et al. 2002), this effect may be more pronounced. Across waterfowl species in North America, evidence suggests that under climate change, autumn migration behaviour is changing as migration timing has become more delayed in recent years (Thurber et al. 2020, Frei et al. 2024) and northern shifts in wintering grounds (Cox et al. 2023, Verheijen et al. 2023). Whether these patterns would lead to longitudinal shifts that could affect these priors remains to be seen but should be considered moving forward.

I also acknowledge that my interpretation of the band-return data does not account for band reporting probabilities and harvest probabilities (Arnold et al. 2020). Further, I only incorporated the direct preseason band returns for juveniles here, but other mark-recapture models include more broad classifications of band returns, including multi-year recoveries and adults. These methods involve estimating survival and recovery rates across the years (Brownie 1978), which was beyond the scope of this project. To improve these models, these considerations should be incorporated into these priors to more formally derive these probabilities of origin, especially if adults are included in the likelihood-based assignment.

5.4.6   Conclusions

Connectivity studies, like this, which examine more fine-scale harvest connectivity are important as they can identify regions or species within a region that do not follow the assumptions of AHM models. While the Great Lakes may not be a significant region in terms of harvest pressures, it is an ecologically important region for many breeding and non-breeding waterfowl. For species with population-wide management (e.g., American Black Duck, Northern Pintail), I found restricted natal origins that never spanned the entire breeding range, suggesting moderate connectivity for the harvest in this region. I also showed that harvest connectivity, for the Great Lakes in general, seems to match the

assumptions of AHM for species in this region where most species showed likely origins consistent with the Mississippi and Atlantic flyways (U.S. Fish and Wildlife Service 2023), but I was not able to segment this region into specific management regions to explicitly evaluate this. Considering Mallard, which has the most straightforward expectations based on the delineation of the three stocks, I found that Mallard showed origins consistent with origins in the eastern stock. This is just one piece of the puzzle for each of these species, but I hope that more of these studies are undertaken to further establish the harvest connectivity at continental scale.

5.5   References

Alisauskas, R. T., T. W. Arnold, J. O. Leafloor, D. L. Otis, and J. S. Sedinger. 2014. Lincoln estimates of mallard (*Anas platyrhynchos*) abundance in North America. Ecology and Evolution 4:132–143.

Arnold, T. W., R. T. Alisauskas, and J. S. Sedinger. 2020. A meta-analysis of band reporting probabilities for North American waterfowl. The Journal of Wildlife Management 84:534–541.

Asante, C. K., T. D. Jardine, S. L. Van Wilgenburg, and K. A. Hobson. 2017. Tracing origins of waterfowl using the Saskatchewan River Delta: incorporating stable isotope approaches in continent-wide waterfowl management and conservation. The Condor 119:261–274.

Ashley, P., K. A. Hobson, S. L. Van Wilgenburg, N. North, and S. A. Petrie. 2010. Linking Canadian harvested juvenile American Black Ducks to their natal areas using stable isotope (δD, δ^{13}C, and δ^{15}N) methods. Avian Conservation and Ecology 5:7.

Baldassarre, G. A. 2014. Ducks, Geese, and Swans of North America. Volume 2. JHU Press, Baltimore, MD, USA.

Bataille, C. P., B. E. Crowley, M. J. Wooller, and G. J. Bowen. 2020. Advances in global bioavailable strontium isoscapes. Palaeogeography, Palaeoclimatology, Palaeoecology 555:109849.

BirdLife International and Handbook of the Birds of the World. 2022. Bird species distribution maps of the world. Version 2022.2. <http://datazone.birdlife.org/species/requestdis.>. Accessed 16 Feb 2024.

Bowen, G. J. 2021. Gridded maps of the isotopic composition of meteoric waters. <http://www.waterisotopes.org.>. Accessed 23 Aug 2021.

Bowen, G. J., L. I. Wassenaar, and K. A. Hobson. 2005. Global application of stable hydrogen and oxygen isotopes to wildlife forensics. Oecologia 143:337–348.

Brownie, C. 1978. Statistical inference from band recovery data: a handbook. Volume 131. US Department of the Interior, Fish and Wildlife Service.

Cadman, M., D. Sutherland, G. Beck, D. Lepage, and A. Couturier, editors. 2007. Atlas of Breeding Birds of Ontario 2001–2005. Bird Studies Canada, Environment Canada, Ontario Field Ornithologists, Ontario Ministry of Natural Resources, and Ontario Nature, Toronto.

Campbell, C. J., M. C. Fitzpatrick, H. B. Vander Zanden, and D. M. Nelson. 2020. Advancing interpretation of stable isotope assignment maps: comparing and summarizing origins of known-provenance migratory bats. Animal Migration 7:27–41.

Carney, S. M. 1992. Species, age and sex identification of ducks using wing plumage. U.S. Department of the Interior, Fish and Wildlife Service, Washington, DC, USA.

Celis-Murillo, A., M. Malorodova, and E. Nakash. 2022. North American Bird Banding Dataset 1960–2022 retrieved 2022-07-14. U.S. Geological Survey, Eastern Ecological Science Center at the Patuxent Research Refuge, Laurel, MD, USA.

Chakraborty, S., and S. W. K. Wong. 2021. BAMBI: An R Package for Fitting Bivariate Angular Mixture Models. Journal of Statistical Software 99:1–69.

Clark, R. G., K. A. Hobson, and L. I. Wassenaar. 2006. Geographic variation in the isotopic (δD, δ^{13}C, δ^{15}N, δ^{34}S) composition of feathers and claws from Lesser Scaup and Northern Pintail: implications for studies of migratory connectivity. Canadian Journal of Zoology 84:1395–1401.

Conroy, M. J., M. W. Miller, and J. E. Hines. 2002. Identification and synthetic modeling of factors affecting American Black Duck populations. Wildlife Monographs 150: 1–64.

Cox, A. R., B. Frei, S. E. Gutowsky, F. B. Baldwin, K. Bianchini, and C. Roy. 2023. Sixty-years of community-science data suggest earlier fall migration and short-stopping of waterfowl in North America. Ornithological Applications 125:duad041.

De Sobrino, C. N., C. L. Feldheim, and T. W. Arnold. 2017. Distribution and derivation of dabbling duck harvests in the Pacific Flyway. California Fish and Game 103:118–137.

Devers, P. K., R. L. Emmet, G. S. Boomer, G. S. Zimmerman, and J. A. Royle. 2021. Evaluation of a two-season banding program to estimate and model migratory bird survival. Ecological Applications 31:e02425.

van Dijk, J. G., W. Meissner, and M. Klaassen. 2014. Improving provenance studies in migratory birds when using feather hydrogen stable isotopes. Journal of Avian Biology 45:103–108.

Ellis, S. L., M. G. Lohman, J. S. Sedinger, P. J. Williams, and T. V. Riecke. 2022. Long-term trends and drought: Spatiotemporal variation in juvenile sex ratios of North American ducks. Ecology and Evolution 12:e9099.

Fleming, B. 2022. Estimating origins of Greater (*Aythya marila*) and Lesser (*A. affinis*) scaup wintering along the Atlantic coast using stable isotopes and band-

recoveries. MSc Thesis. State University of New York College of Environmental Science and Forestry, Syracuse, NY, USA.

Fournier, A. M. V., A. R. Sullivan, J. K. Bump, M. Perkins, M. C. Shieldcastle, and S. L. King. 2017. Combining citizen science species distribution models and stable isotopes reveals migratory connectivity in the secretive Virginia rail. Journal of Applied Ecology 54:618–627.

Fowler, D. N., E. B. Webb, F. B. Baldwin, M. P. Vrtiska, and K. A. Hobson. 2018. A multi-isotope (δ^{13}C, δ^{15}N, δ^{34}S, δ^{2}H) approach to establishing migratory connectivity in lesser snow geese: tracking an overabundant species. PLOS One 13:e0203077.

Frei, B., A. R. Cox, A. C. Morales, and C. Roy. 2024. Community-science reveals delayed fall migration of waterfowl and spatiotemporal effects of a changing climate. Journal of Animal Ecology 93:377–392.

Gourlay-Larour, M.-L., R. Pradel, M. Guillemain, J.-S. Guitton, M. L'Hostis, H. Santin-Janin, and A. Caizergues. 2014. Movement patterns in a partial migrant: a multi-event capture-recapture approach. PLOS One 9:e96478.

Grannemann, N. 2010. Great Lakes and Watersheds Shapefiles. U.S. Geological Survey. <https://www.sciencebase.gov/catalog/item/530f8a0ee4b0e7e46bd300dd>. Accessed 9 Sep 2019.

Guillemain, M., L. Bacon, K. J. Kardynal, A. Olivier, M. Podhrazsky, P. Musil, and K. A. Hobson. 2019. Geographic origin of migratory birds based on stable isotope analysis: the case of the greylag goose (*Anser anser*) wintering in Camargue, southern France. European Journal of Wildlife Research 65:67.

Guillemain, M., S. L. Van Wilgenburg, P. Legagneux, and K. A. Hobson. 2014. Assessing geographic origins of Teal (*Anas crecca*) through stable-hydrogen (δ^{2}H) isotope analyses of feathers and ring-recoveries. Journal of Ornithology 155:165–172.

Gunnarsson, G., N. Latorre-Margalef, K. A. Hobson, S. L. Van Wilgenburg, J. Elmberg, B. Olsen, R. A. M. Fouchier, and J. Waldenström. 2012. Disease dynamics and bird migration — Linking Mallards *Anas platyrhynchos* and subtype diversity of the Influenza A virus in time and space. PLOS One 7:e35679.

Harvey, K. M. 2022. Geographic origins and genetics of banded mallards in the northern Atlantic and Mississippi flyways. MSc Thesis. State University of New York College of Environmental Science and Forestry, Syracuse, NY, USA.

Hijmans, R. J. 2020. raster: geographic data analysis and modeling. R package version 3.3-13. <https://CRAN.R-project.org/package=raster>.

Hijmans, R. J. 2022. geosphere: Spherical Trigonometry. R package version 1.5-18. <https://CRAN.R-project.org/package=geosphere>.

Hijmans, R. J. 2023. terra: spatial data analysis. R package version 1.7-46. <https://CRAN.R-project.org/package=terra>.

Hobson, K. A. 2019. Application of isotopic methods to tracking animal movements. Pages 85–115 *in* K. A. Hobson and L. I. Wassenaar, editors. Tracking Animal Migration with Stable Isotopes. Second Edition. Academic Press, Cambridge, MA, USA.

Hobson, K. A., and R. G. Clark. 1992. Assessing avian diets using stable isotopes I: turnover of ^{13}C in tissues. The Condor 94:181–188.

Hobson, K. A., H. Lormée, S. L. Van Wilgenburg, L. I. Wassenaar, and J. M. Boutin. 2009. Stable isotopes (δD) delineate the origins and migratory connectivity of harvested animals: the case of European woodpigeons. Journal of Applied Ecology 46:572–581.

Hobson, K. A., S. Van Wilgenburg, L. I. Wassenaar, H. Hands, W. P. Johnson, M. O'Meilia, and P. Taylor. 2006. Using stable hydrogen isotope analysis of feathers to delineate origins of harvested Sandhill Cranes in the central flyway of North America. Waterbirds 29:137–147.

Inman, R. L., K. T. Scribner, H. H. Prince, J. A. Warrillow, D. R. Luukkonen, and P. I. Padding. 2003. A novel method for Canada goose harvest derivation using genetic analysis of tail feathers. Wildlife Society Bulletin 1126–1131.

Jiguet, F., A. Robert, R. Lorrillière, K. A. Hobson, K. J. Kardynal, R. Arlettaz, F. Bairlein, V. Belik, P. Bernardy, J. L. Copete, M. A. Czajkowski, S. Dale, V. Dombrovski, D. Ducros, R. Efrat, J. Elts, Y. Ferrand, R. Marja, S. Minkevicius, P. Olsson, M. Pérez, M. Piha, M. Raković, H. Schmaljohann, T. Seimola, G. Selstam, J.-P. Siblet, M. Skierczyǹski, A. Sokolov, J. Sondell, and C. Moussy. 2019. Unravelling migration connectivity reveals unsustainable hunting of the declining ortolan bunting. Science Advances 5:eaau2642.

Klimstra, J. D., and P. I. Padding. 2012. Harvest distribution and derivation of Atlantic flyway Canada Geese. Journal of Fish and Wildlife Management 3:43–55.

Kucia, S. R., M. L. Schummer, J. W. Kusack, K. A. Hobson, and C. A. Nicolai. 2023. Origins of Mallards harvested in the Atlantic flyway of North America: implications for conservation and management. Avian Conservation and Ecology 18:10.

Kusack, J. W., D. C. Tozer, K. M. Harvey, M. L. Schummer, and K. A. Hobson. 2023. Assigning harvested waterfowl to geographic origin using feather δ^2H isoscapes: What is the best analytical approach? PLOS One 18:e0288262.

Kusack, J. W., D. C. Tozer, M. L. Schummer, and K. A. Hobson. 2022. Origins of harvested American black ducks: stable isotopes support the flyover hypothesis. The Journal of Wildlife Management 87:e22324.

Magozzi, S., C. P. Bataille, K. A. Hobson, M. B. Wunder, J. D. Howa, A. Contina, H. B. Vander Zanden, and G. J. Bowen. 2021. Calibration chain transformation improves the comparability of organic hydrogen and oxygen stable isotope data. Methods in Ecology and Evolution 12:732–747.

Munro, R. E., and C. F. Kimball. 1982. Population ecology of the mallard: VII. Distribution and derivation of the harvest. Resource Publication, Report, Washington, D.C. <http://pubs.er.usgs.gov/publication/5230180>.

North American Waterfowl Management Plan. 2018. 2018 North American Waterfowl Management Plan (NAWMP) update: connecting people, waterfowl, and wetlands. <https://nawmp.org/timeline/2018-update >

Palumbo, M. D., J. W. Kusack, D. C. Tozer, S. W. Meyer, C. Roy, and K. A. Hobson. 2020. Source areas of Blue-winged Teal harvested in Ontario and Prairie Canada based on stable isotopes: implications for sustainable management. Journal of Field Ornithology 91:64–76.

Palumbo, M. D., D. C. Tozer, and K. A. Hobson. 2019. Origins of harvested Mallards from Lake St. Clair, Ontario: a stable isotope approach. Avian Conservation and Ecology 14:3.

Patterson, T. A., L. Thomas, C. Wilcox, O. Ovaskainen, and J. Matthiopoulos. 2008. State–space models of individual animal movement. Trends in Ecology & Evolution 23:87–94.

Pebesma, E. 2018. Simple features for R: standardized support for spatial vector data. The R Journal 10:439–446.

Prince, H. H., P. I. Padding, and R. W. Knapton. 1992. Waterfowl use of the Laurentian Great Lakes. Journal of Great Lakes Research 18:673–699.

R Core Team. 2023. R: a language and environment for statistical computing. R Foundation for Statistical Computing, Vienna, AT.

Raftovich, R., K. Fleming, S. Chandler, and C. Cain. 2022. Migratory bird hunting activity and harvest during the 2020-21 and 2021-22 hunting seasons. U.S. Fish and Wildlife Service, Laurel, MD, USA.

Reed, E. T., K. J. Kardynal, J. A. Horrocks, and K. A. Hobson. 2018. Shorebird hunting in Barbados: using stable isotopes to link the harvest at a migratory stopover site with sources of production. The Condor 120:357–370.

Reich, M. S., D. T. T. Flockhart, D. R. Norris, L. Hu, and C. P. Bataille. 2021. Continuous-surface geographic assignment of migratory animals using strontium isotopes: A case study with monarch butterflies. Methods in Ecology and Evolution 12:2445–2457.

Roberts, A., A. L. Scarpignato, A. Huysman, J. A. Hostetler, and E. B. Cohen. 2022. Migratory connectivity of North American waterfowl across administrative flyways. Ecological Applications 33:e2788.

Robinson, O. J., C. P. McGowan, and P. K. Devers. 2016. Updating movement estimates for American black ducks (*Anas rubripes*). PeerJ 4:e1787.

Roy, C., S. G. Cumming, and E. J. B. McIntire. 2015. Spatial and temporal variation in harvest probabilities for American black duck. Ecology and Evolution 5:1992–2004.

Royle, J. A., and D. R. Rubenstein. 2004. The role of species abundance in determining breeding origins of migratory birds with stable isotopes. Ecological Applications 14:1780–1788.

RStudio Team. 2023. RStudio: integrated development for R. RStudio, Inc., Boston, MA, USA.

Ruegg, K. C., E. C. Anderson, R. J. Harrigan, K. L. Paxton, J. F. Kelly, F. Moore, and T. B. Smith. 2017. Genetic assignment with isotopes and habitat suitability (gaiah), a migratory bird case study. Methods in Ecology and Evolution 8:1241–1252.

Scarpignato, A. L., A. E. Huysman, M. F. Jimenez, C. J. Witko, A.-L. Harrison, N. E. Seavy, M. A. Smith, J. L. Deppe, C. B. Wilsey, and P. P. Marra. 2023. Shortfalls in tracking data available to inform North American migratory bird conservation. Biological Conservation 286:110224.

Schummer, M. L., A. D. Afton, S. S. Badzinski, S. A. Petrie, G. H. Olsen, and M. A. Mitchell. 2018. Evaluating the waterfowl breeding population and habitat survey for scaup. The Journal of Wildlife Management 82:1252–1262.

Schummer, M. L., J. Simpson, B. Shirkey, S. R. Kucia, P. Lavretsky, and D. C. Tozer. 2023. Population genetics and geographic origins of mallards harvested in northwestern Ohio. PLOS One 18:e0282874.

Sullins, D. S., W. C. Conway, D. A. Haukos, K. A. Hobson, L. I. Wassenaar, C. E. Comer, and I.-K. Hung. 2016. American woodcock migratory connectivity as indicated by hydrogen isotopes. The Journal of Wildlife Management 80:510–526.

Szymanski, M. L., and J. A. Dubovsky. 2013. Distribution and derivation of the Blue-winged Teal (*Anas discors*) harvest, 1970-2003. United States Department of the Interior, Fish and Wildlife Service, Washington, DC, USA.

Terzer-Wassmuth, S., L. I. Wassenaar, J. M. Welker, and L. J. Araguás. 2021. Improved high-resolution global and regionalized isoscapes of δ^{18}O, δ^2H, and *d*-excess in precipitation. Hydrological Processes 35:e14254.

Thurber, B. G., C. Roy, and J. R. Zimmerling. 2020. Long-term changes in the autumn migration phenology of dabbling ducks in southern Ontario and implications for waterfowl management. Wildlife Biology 2020:wlb.00668.

U.S. Environmental Protection Agency. 2010. North American Ecoregions - Level II. United States Environmental Protection Agency, Washington, DC, USA. <https://www.epa.gov/eco-research/ecoregions-north-america>. Accessed 8 Apr 2024.

U.S. Fish and Wildlife Service. 2017. USFWS Administrative Waterfowl Flyway Boundaries. U.S. Fish and Wildlife Service, Natural Resource Program Center, Fort Collins, CO, USA. <https://ecos.fws.gov/ServCat/Reference/Profile/42276>. Accessed 20 Sep 2019.

U.S. Fish and Wildlife Service. 2021. Adaptive Harvest Management: 2022 hunting season. U.S. Department of the Interior, Washington, DC, USA.

U.S. Fish and Wildlife Service. 2023. Adaptive Harvest Management: 2024 Hunting Season. U.S. Department of the Interior, Washington, DC, USA.

Verheijen, B. H. F., E. B. Webb, M. G. Brasher, and H. M. Hagy. 2023. Spatiotemporal dynamics of duck harvest distributions in the Central and Mississippi flyways, 1960–2019. The Journal of Wildlife Management 88:e22521.

Wassenaar, L. I., and K. A. Hobson. 2003. Comparative equilibration and online technique for determination of non-exchangeable hydrogen of keratins for use in animal migration studies. Isotopes in Environmental and Health Studies 39:211–217.

van Wilgenburg, S. L., and K. A. Hobson. 2011. Combining stable-isotope (δD) and band recovery data to improve probabilistic assignment of migratory birds to origin. Ecological Applications 21:1340–1351.

Wojtaszek, D. 2022. Using Stable Isotope Techniques to Complement Existing Northern Pintail Management. MSc Thesis. Western University, London, ON, CA.

Zuur, A., E. N. Ieno, N. Walker, A. A. Saveliev, and G. M. Smith. 2009. Mixed effects models and extensions in ecology with R. Springer, Berlin, DE.

Chapter 6

6   General Discussion

My dissertation examined the harvest connectivity of waterfowl in North America using multiple intrinsic markers (stable isotopes) and an extrinsic marker (bands) to inform direct connections between harvest and individual bird source areas. I focused on critically assessing and improving current methods to assign waterfowl to origin using stable-isotope measurements of feathers. Below, I summarize my results and discuss recommendations for future research.

6.1   Methodological advancements

Much of my dissertation evaluated current approaches to assign migratory wildlife to likely origins using stable isotopes. In just the past five years, the assignR (Ma et al. 2020) and isocat (Campbell et al. 2020) packages in the R statistical framework have made isotope assignments more user-friendly. With downloadable pre-processed gridded isoscapes (Terzer et al. 2013, Bowen 2021, Terzer-Wassmuth et al. 2021) and laboratories offering continuous-flow isotope ratio mass spectrometry at a relatively low cost (~20–30$ CDN per sample), researchers can collect tissue samples and perform assignments to origin with relative ease. Although the process is more streamlined, the statistics of isotopic assignment have remained fundamentally unchanged since their inception (Hobson and Wassenaar 1997). Recent advancements are undoubtedly positive, but with an ever-advancing field, there are few direct recommendations to follow for best practices when performing isotopic assignments, especially for waterfowl. Although my dissertation is focused entirely on waterfowl in North America, the recommendations and discussion below are relevant to anyone using metabolically inert keratinous tissue (e.g., feathers, hair, claw, chitin) to assign origin to migratory animals.

6.1.1   Isoscapes and calibration

Understanding the relationship between the stable isotopic composition of environmental hydrogen (δ^2H) and δ^2H in animal tissues is essential when predicting tissue-specific isoscapes. Although these isoscapes can be summarized in many different ways (e.g.,

monthly, growing-season, or mean annual δ^2H$_p$ values), growing-season precipitation δ^2H surfaces (i.e., months with average temperatures > 0 °C) are the most widely applied in wildlife in temperate areas compared to mean annual precipitation surfaces. To better understand which isoscape to use for waterfowl, in Chapter 3 I evaluated the strength of the relationships between known-origin δ^2H$_f$ and δ^2H$_p$ values and found a strong positive relationship between δ^2H$_f$ values and both mean growing-season and mean annual δ^2H$_p$ measurements. Neither isoscape presented a calibration relationship with greater model fit and, in practice, neither resulted in markedly better precision or accuracy in assignment. This is a promising result, as it suggests that the use of these calibrations is flexible for waterfowl and either mean growing-season or mean annual δ^2H$_p$ measurements could be justified for use in stable-hydrogen isotopic assignment. This is likely because of the high variability in these calibration relationships, which minimizes the benefit of using isoscapes derived at more specific temporal scales. A similar trade-off is seen when using year-specific isoscapes rather than the long-term averaged surfaces, where these surfaces show significantly lower predictive power due to fewer δ^2H$_p$ sampling points in a given year (Vander Zanden et al. 2014).

Traditionally, the approach to calibrate environmental isoscapes has been to collect known-origin tissue isotope data (e.g., Hobson et al. 1999) or to use published calibration equations (e.g., δ^2H$_{tissue} = \delta^2$H$_p$ * slope + intercept ‰) derived from known-origin tissue isotope data. With the shift towards greater data accessibility in publications, it is becoming considerably easier to calculate relevant calibration equations on a study-by-study basis using open-access known-origin δ^2H$_{tissue}$ data (e.g., assignR 'knownOrig' database; Ma et al. 2020). Using raw known-origin δ^2H values instead of a calibration equation requires the selection of relevant calibration data that matches the context of the study system (e.g., geographic location, timing of tissue growth, taxonomic similarity, diet). Ultimately, this may introduce more user error, but can also allow for a better understanding of the underlying calibration process. With raw calibration data, workflows to convert δ^2H values into different reference scales (Magozzi et al. 2021), such as those in assignR (Ma et al. 2020), can minimize many of the issues with comparing samples analyzed using different laboratory methods. To further this effort, I have made all of the known-origin data obtained in Chapter 3 available (Kusack et al.

2023*a*) and I encourage others to do the same. Adding to these databases allows us to better describe $\delta^2H_f \sim \delta^2H_p$ relationships in a changing world.

Although there are > 60 studies with derived calibration equations (Table B1 and Table 1.1), some of which provide open-access data, these are not the only available known-origin δ^2H_{Tissue} data. Many studies have analyzed known-origin individuals for δ^2H independent of the context of developing calibration equations (e.g., Szymanski et al. 2007, Coulton et al. 2009). Aggregating the data and metadata (e.g., calibration standards) for these studies would be an incredibly valuable undertaking. These data can fill spatial and temporal gaps and allow for additional taxa-specific calibration relationships, where possible. Most importantly, continuing to collect these data allows for better estimation of the variability in these calibration relationships, which can be propagated into assignment likelihoods. Propagating as much of the known error as possible into assignments is the objective of most practitioners and with the adoption of newer assignment algorithms (Campbell et al. 2020, Ma et al. 2020) these sources of error, including spatially explicit estimates of δ^2H_p variability (Bowen 2021), can be incorporated directly into likelihood-based assignment algorithms, to provide the most complete estimates of assignment error.

6.1.2   Recommendation

For waterfowl applications, I recommend the use of the combined foraging-guild-specific calibration datasets (Kusack et al. 2023*b*) paired with a mean annual δ^2H_p surface (Bowen 2021). Compared to the mean growing-season surface, the mean annual δ^2H_p surface is the most parsimonious interpretation of environmental H when considering waterfowl that extensively use surface waters. Considering near identical calibration model fits, the mean annual surface should be used for waterfowl. The foraging-guild approach to calibration is supported by other work in songbirds (Hobson et al. 2012). If a more relevant (species- or geographic-specific) calibration dataset is available, the more specific dataset should be explored, but at this time the only robust datasets are for Mallard (*Anas platyrhynchos*, Hebert and Wassenaar 2005, van Dijk et al. 2014, Kusack et al. 2023*b*) and Lesser Scaup (*Aythya affinis*, Clark et al. 2006). I found that combining species within a foraging-guild increased the variability in the calibration relationship,

leading to lower overall precision but higher accuracy in the resulting assignment. Despite lower precision, I consider these foraging-guild datasets to be the most conservative and realistic relationship that accounts for the best error estimates for those groups.

6.1.3   Prior probabilities of origin

The use of prior probabilities of origin in likelihood-based assignment informs regions of likely origin based on known prior information in the study system (Royle and Rubenstein 2004). Although Bayesian methods allow for broad data sources including genetics (e.g., Ruegg et al. 2017) and relative abundance (e.g., Fournier et al. 2017), the most commonly applied prior probabilities of origin for waterfowl applications are based on band-return data. Using band returns, likely origins have been delineated by the flyway of origin (Asante et al. 2017, Palumbo et al. 2019), directional movement vectors (Gunnarsson et al. 2012, Guillemain et al. 2014), and movement probabilities among regions (Ashley et al. 2010). Despite waterfowl having the most band returns of any wildlife group, the consequences of using band-return priors have received little attention. In Chapter 5, I explored prior probabilities of origin based on band returns in several frameworks (flyway, 5° longitudinal zone, movement direction). Using a multi-species approach, I found flyway and longitudinal zone to be the most promising frameworks, as they take advantage of longitudinal movement information that supplements the latitudinal information gained from δ^2H isoscapes (at least for North America). The number of band returns will dictate what resolution the prior can be estimated at. Still, I recommend initial exploration to explore the use of both flyway and longitudinal-block priors.

When available, the use of published movement probabilities between flyways or other management units can be used as prior probabilities of origin. For Chapter 2, I used movement probabilities between American Black Duck management regions. For Chapter 5, there were no published movement probabilities for the Great Lakes harvest specifically. There are published flyway-level movement probabilities (Roberts et al. 2022), but these are estimated using encounters outside of the Great Lakes area, which also spans two flyways (Mississippi and Atlantic). In Chapter 5, my estimated prior

probabilities of origin did not match these flyway-scale estimates. For example, flyway-scale transition probabilities for American Green-winged Teal (*Anas crecca carolinensis*) showed some movement from the Pacific and Central flyways to the Mississippi and Atlantic flyways (Roberts et al. 2022), but the priors I derived showed the only non-zero probabilities of origin along the border of the Mississippi and Atlantic flyways. If possible, estimating priors at the scale of a given study can and should be explored using available band-return data (Nakash et al. 2023). Taking this concept further, I also found that subdividing the study area and estimating priors separately for each region allowed for a more fine-scale representation of priors within the study area. This necessitates abundant band-return data across the study area, which for the Great Lakes was only possible for Mallard. Unfortunately, not all species will have adequate band returns to allow for this fine-scale prior derivation.

Despite the usefulness of prior probabilities of origin, careful interpretation is needed, as priors can strongly influence these regions of likely origin. Priors cannot provide information on regions where no information is available. Creating more spatially explicit probability surfaces can lead to spurious results when the underlying data is patchy. In these cases, the use of flyway transition probabilities derived at the continental scale may be necessary. At the very least, when depicting origins, I encourage depicting likely origins estimated using all sources of data (i.e., δ^2H + prior) and each source of data separately, to allow for independent evaluation of all data sources.

6.2   Harvest connectivity

Understanding migratory connectivity is key for adaptive harvest management (AHM) because it provides information on zones of production (sources) leading to the recruitment of individuals into the fall harvest. Under AHM in North America, species are managed based on the status of one of three flyway-specific stocks (U.S. Fish and Wildlife Service 2023) under the assumption that the population trends and production zones for the chosen stock represent the species in that flyway. This is complicated as we are currently in a time of unprecedented climatic and anthropogenic change resulting in changes in migratory behaviour of waterfowl (Thurber et al. 2020, Cox et al. 2023, Verheijen et al. 2023, Frei et al. 2024, but see Roberts et al. 2022), necessitating regular

estimation of connectivity to validate the underlying assumptions of AHM and ensure overexploitation does not occur.

6.2.1   Banding-bias and gaps

As stable isotopes are an intrinsic marker, requiring no initial capture to provide information on source origins, they effectively turn every capture point into a recapture (Hobson 2019). This makes stable isotopes extremely useful for species with limited marking efforts, especially those breeding in the far north where banding is logistically difficult. Relying entirely on band returns obtained in the southern portion of breeding ranges to derive parameters for AHM (e.g., survival, age-ratios, sex-ratios, etc.) may also introduce bias. Therefore, in Chapter 5, I determined likely origins of harvested individuals using direct band returns and δ^2H measurements of feathers, directly comparing two different sources of connectivity information. Overlap between the two estimates of origin was low across all species, except for Wood Duck (*Aix sponsa*) which breeds entirely in proximity to human-populated areas. Species with very minimal banding effort, like Bufflehead (*Bucephala albeola*) and Lesser Scaup, showed the lowest overlap. For Greater Scaup (*Aythya marila*), banding on the breeding grounds is practically non-existent. In these cases, stable isotopes are incredibly valuable as they may be one of the only sources of connectivity information available. Although these results are specific to the Great Lakes harvest, they highlight the need to multiple sources of connectivity information to establish source areas.

6.2.2   American Black Duck

Current harvest management of black ducks assumes a single population (U.S. Fish and Wildlife Service 2023), despite evidence of different stocks within the breeding population (Geis et al. 1971, Pendleton and Sauer 1992, Conroy et al. 2002). In Chapter 2, I focused on the American Black Duck (*Anas rubripes*) to test the 'flyover hypothesis', which proposed that ducks produced in the Boreal are less susceptible to harvest by hunters in Atlantic Canada and the northeastern United States, areas that primarily harvest birds produced relatively close to harvest sites (Ashley et al. 2010, Roy et al. 2015, Black Duck Joint Venture 2018). Using feathers from across their range and

incorporating adults for the first time, I was able to more completely test the flyover hypothesis. I found evidence in support of the 'flyover hypothesis', where American Black Duck harvested in Atlantic Canada had more southern origins, indicative of nearby breeding locations with relatively few individuals assigned to breeding regions farther north. This contrasted with all other management regions, which showed origins in the northern boreal areas, well north of harvest areas. I inferred a Mississippi Flyway stock produced in the Boreal Shield and Hudson Plains of Ontario that is harvested in the Great Lakes and interior of Canada and the United States and an Atlantic Flyway stock harvested both as local breeders and with some migrants from northern Quebec and Newfoundland and Labrador in the Boreal Softwood and Taiga Shield. My results combined with the findings of Ashley et al. (2010) and Roy et al. (2015) suggest that regional black duck harvest regulations may improve harvest management.

Although it was not among my major initial objectives, I was also able to test the consequences of using two different calibrations δ^2H_f and δ^2H_p measurements and different prior probabilities to assign American Black Duck in the Great Lakes, as I used different methods in Chapter 2 and 5. In Chapter 2 I used the calibration equation for Mallard moulting in Europe (van Dijk et al. 2014) which at the time was the most recently derived dabbling duck calibration equation. Since then, I aggregated additional known-origin data into a larger and more robust calibration dataset in Chapter 3, which I used to assign the waterfowl to origin in Chapter 5. Directly comparing the results (without priors) for American Black Duck harvest in the Great Lakes, the regions of likely origin were slightly more north when the van Dijk et al. (2014) equation was used. These slight differences were similar to those seen in Chapter 3 where I tested the consequences of using a diving duck calibration on a dabbling duck. Regions of likely origin varied slightly, but at this scale, differences in origin were not enough to suggest different broad-scale origins.

For the prior probabilities of origin, in Chapter 2 I used movement probabilities between management regions, which indicated zero probability of American Black Ducks remaining within southern Ontario after banding (Robinson et al. 2016). My approach in Chapter 5, which used longitudinal or flyway-level regions, mirrored the previous

management estimates of movement within the American Black Duck range where three flyway-like strata (western, central, eastern) were used (Zimpfer and Conroy 2006). Likely origins using these two methods did not match for the Great Lakes birds. As discussed in Chapter 2, stable isotopes indicated origins across much of the Great Lakes and northern Atlantic forests, but movement probabilities indicated a low likelihood of origins in these regions. This disagreement between the band-return and stable-isotope data highlights the importance of considering all sources of information.

6.3   Management implications

Migratory movements of waterfowl require collaborative international strategies to ensure fair allocation of harvested birds among countries (Nichols et al. 2007) and effective conservation efforts (North American Waterfowl Management Plan 2018). Current adaptive harvest management (AHM) frameworks make flyway-level management decisions based on a representative population or populations in that flyway (U.S. Fish and Wildlife Service 2023), with a few species-specific exceptions where species have been highlighted as conservation concerns (e.g., American Black Duck, Northern Pintail *Anas acuta*). AHM models rely on metrics derived from aerial surveys, harvest surveys, and banding to estimate breeding population size and other population parameters to set fall bag limits.

6.3.1   Flyway-level management

Flyways are the fundamental management unit for AHM in North America (U.S. Fish and Wildlife Service 2023). The underlying assumption is that populations in a given flyway follow similar population trends to the chosen candidate species (e.g., Mallard in the midcontinent) and that source areas match. In both Chapter 4 and 5, I explored the natal origins of waterfowl harvest in eastern North America. I found evidence for flyway-specific natal sources, despite northward shifts in natal areas later in the harvest period. At the flyway scale (Chapter 4 - Mississippi and Atlantic flyways) and for a specific harvest area within these flyways (Chapter 5 – Great Lakes), these results were consistent with unit-specific (i.e., midcontinent or Atlantic Flyway) harvest, supporting the assumptions of AHM. The only notable exception to this American Green-winged Teal

harvested in the Mississippi Flyway which did not strictly follow the assumptions of AHM and instead showed natal sources from Alaska to the Atlantic Coast.

In the Mississippi Flyway, which is part of the midcontinent management unit, AHM is based on Mallard breeding primarily in the Prairie Pothole region (U.S. Fish and Wildlife Service 2023). In Chapter 4 I showed that spatiotemporal patterns and geographic location of for Mallard natal sources in the midcontinent matched all other species except American Green-winged Teal. In this case broad natal sources may not pose a significant mismatch between teal population trends and midcontinent Mallard trends, especially for a species of minimal conservation concern, but at the very least, these connectivity metrics should be further explored.

Here I provide an initial look into spatiotemporal dynamics of source areas and connectivity for waterfowl harvested in Eastern North America, but these metrics can be explored in more detail on a species-by-species basis. This research provides a framework to spatiotemporally visualize flyway- and species-specific source areas and derive subsequent connectivity estimates (e.g., Cohen et al. 2018, Roberts et al. 2022).

6.3.2   Future sampling opportunities

The vast majority of feathers collected for my research were sourced from harvest surveys (Parts Collection Survey, Raftovich et al. 2023; Species Composition Survey, Gendron and Smith 2019) and preseason banding. These existing surveys provide a unique opportunity to collect feathers at a continent scale. These surveys already facilitate project-specific sampling, but the suggestions below provide a broader sampling method to collect feathers while ensuring the use of current resources.

For the harvest surveys, wings (> 15,000/year in Canada; Gendron and Smith 2019) are brought to a central location for processing, and unless the wings are needed for research or educational purposes they are destroyed. It is not reasonable or useful to collect feathers from all of these wings every year, but I suggest some potential priorities that could be considered moving forward. The most valuable feather samples are those from species of direct conservation concern (e.g., Greater Scaup), species with few wings

submitted each year, and samples with additional data, such as marked birds. If these marked birds are a direct recovery, they are effectively a known-origin sample, assuming no feather regrowth. From a stable-isotopes perspective, these samples are valuable as additional validation, that can be applied over a greater geographic and temporal scale across many species. Storing feathers requires very minimal space and once cleaned the feathers can be stored at room temperature indefinitely. The same protocol could apply to other harvested species that are processed through these surveys such as American Woodcock (*Scolopax minor*), Mourning Dove (*Zenaida macroura*), and Sandhill Crane (*Grus canadensis*).

These surveys could be leveraged to explore continent-wide estimates of connectivity for harvested species, similar to those done using band-return data (e.g., Szymanski and Dubovsky 2013). Similar continent-wide efforts have been done in songbirds to delineate banding station catchment areas (Wassenaar and Hobson 2001, Hobson et al. 2015), but this would be on a much larger scale as samples are collected wherever hunting occurs. To date, range-wide estimates of connectivity have only been done for American Black Duck (Kusack et al. 2022) and Northern Pintail (Wojtaszek 2022). These connectivity estimates could be paired with band returns, as I did in Chapter 5, to achieve the most robust estimates of source areas.

The other primary source of feathers I took advantage of was from birds caught during preseason banding. In North America, 300,000 individuals are banded each year (Celis-Murillo et al. 2022). Many of these preseason banding stations, especially those in Canada, are targeted close to or on the breeding grounds. Although many are still more south than the core breeding areas, many stations catch locally produced hatch-year birds. Feathers could be collected from local birds during regular banding operations as a supplement to calibration datasets, especially in remote locations. Introducing system-wide sampling protocols would likely face push-back, but if metrics gained from stable-isotope assignment (see below) are incorporated into AHM models, then maintaining a robust calibration dataset is integral.

6.3.3   Supplementing AHM frameworks

Many metrics are incorporated in AHM models, to best predict population size for the fall harvest (Nichols et al. 2007, U.S. Fish and Wildlife Service 2023). For example, in the 2010 Northern Pintail AHM model, average breeding latitude estimated from the aerial survey is included to account for latitudinal changes in productivity (US Fish and Wildlife Service 2010). Similar information could be gained using δ^2H_f measurements. This does come with a cost, per wing, to process samples in the lab. This approach has the benefit of representing the actual harvest, as opposed to the overall breeding population, as the samples are gained directly from harvested birds. Using existing monitoring surveys to collect feathers and derive estimates of origin could supplement annual parameter estimation through AHM frameworks with minimal additional logistics.

6.4   Concluding remarks

Many of the current waterfowl monitoring programs (e.g., preseason banding) are spatially limited due to accessibility, but intrinsic markers provide a complementary method to directly assess harvest source areas and evaluate bias. As I have demonstrated here, intrinsic markers can also be used to derive regions of past occupancy but have yet to receive full support in AHM. Across four data chapters, I used stable isotopes to inform direct connections between harvest and source areas for harvested waterfowl. These contributions address key conservation questions for a species of conservation concern, inform best practices when utilizing stable isotopes, and demonstrate the value of stable isotopes as a tool for waterfowl management.

6.5   References

Asante, C. K., T. D. Jardine, S. L. Van Wilgenburg, and K. A. Hobson. 2017. Tracing origins of waterfowl using the Saskatchewan River Delta: incorporating stable isotope approaches in continent-wide waterfowl management and conservation. The Condor 119:261–274.

Ashley, P., K. A. Hobson, S. L. Van Wilgenburg, N. North, and S. A. Petrie. 2010. Linking Canadian harvested juvenile American Black Ducks to their natal areas using stable isotope (δD, δ^{13}C, and δ^{15}N) methods. Avian Conservation and Ecology 5:7.

Black Duck Joint Venture. 2018. Notice of funding opportunity, Migratory Bird Joint Ventures (Black Duck Joint Venture) Catalog of Federal Domestic Assistance (CFDA) Number 15.637. U.S. Fish and Wildlife Service, Division of Migratory Bird Management. Washington, DC, USA.

Bowen, G. J. 2021. Gridded maps of the isotopic composition of meteoric waters. <http://www.waterisotopes.org.>. Accessed 23 Aug 2021.

Campbell, C. J., M. C. Fitzpatrick, H. B. Vander Zanden, and D. M. Nelson. 2020. Advancing interpretation of stable isotope assignment maps: comparing and summarizing origins of known-provenance migratory bats. Animal Migration 7:27–41.

Celis-Murillo, A., M. Malorodova, and E. Nakash. 2022. North American Bird Banding Dataset 1960–2022 retrieved 2022-07-14. U.S. Geological Survey, Eastern Ecological Science Center at the Patuxent Research Refuge, Laurel, MD, USA.

Clark, R. G., K. A. Hobson, and L. I. Wassenaar. 2006. Geographic variation in the isotopic (δD, δ^{13}C, δ^{15}N, δ^{34}S) composition of feathers and claws from Lesser Scaup and Northern Pintail: implications for studies of migratory connectivity. Canadian Journal of Zoology 84:1395–1401.

Cohen, E. B., J. A. Hostetler, M. T. Hallworth, C. S. Rushing, T. S. Sillett, and P. P. Marra. 2018. Quantifying the strength of migratory connectivity. Methods in Ecology and Evolution 9:513–524.

Conroy, M. J., M. W. Miller, and J. E. Hines. 2002. Identification and synthetic modeling of factors affecting American Black Duck populations. Wildlife Monographs 150:1–64.

Coulton, D. W., R. G. Clark, K. A. Hobson, L. I. Wassenaar, and C. E. Hebert. 2009. Temporal sources of deuterium (δD) variability in waterfowl feathers across a prairie-to-boreal gradient. The Condor 111:255–265.

Cox, A. R., B. Frei, S. E. Gutowsky, F. B. Baldwin, K. Bianchini, and C. Roy. 2023. Sixty-years of community-science data suggest earlier fall migration and short-stopping of waterfowl in North America. Ornithological Applications 125:duad041.

van Dijk, J. G., W. Meissner, and M. Klaassen. 2014. Improving provenance studies in migratory birds when using feather hydrogen stable isotopes. Journal of Avian Biology 45:103–108.

Fournier, A. M. V., A. R. Sullivan, J. K. Bump, M. Perkins, M. C. Shieldcastle, and S. L. King. 2017. Combining citizen science species distribution models and stable isotopes reveals migratory connectivity in the secretive Virginia rail. Journal of Applied Ecology 54:618–627.

Frei, B., A. R. Cox, A. C. Morales, and C. Roy. 2024. Community-science reveals delayed fall migration of waterfowl and spatiotemporal effects of a changing climate. Journal of Animal Ecology 93:377–392.

Geis, A. D., R. I. Smith, and J. P. Rogers. 1971. Black duck distribution, harvest characteristics, and survival. U.S. Department of the Interior, Fish and Wildlife Service, Bureau of Sport Fisheries and Wildlife, Washington, DC, USA.

Gendron, M., and A. Smith. 2019. National Harvest Survey website. Canadian Wildlife Service, Environment and Climate Change Canada, Ottawa, Ontario. <https://wildlife-species.canada.ca/harvest-survey>. Accessed 28 Jan 2020.

Guillemain, M., S. L. Van Wilgenburg, P. Legagneux, and K. A. Hobson. 2014. Assessing geographic origins of Teal (*Anas crecca*) through stable-hydrogen (δ^2H) isotope analyses of feathers and ring-recoveries. Journal of Ornithology 155:165–172.

Gunnarsson, G., N. Latorre-Margalef, K. A. Hobson, S. L. Van Wilgenburg, J. Elmberg, B. Olsen, R. A. M. Fouchier, and J. Waldenström. 2012. Disease dynamics and bird migration — Linking Mallards *Anas platyrhynchos* and subtype diversity of the Influenza A virus in time and space. PLOS One 7:e35679.

Hebert, C. E., and L. I. Wassenaar. 2005. Feather stable isotopes in western North American waterfowl: spatial patterns, underlying factors, and management applications. Wildlife Society Bulletin 33:92–102.

Hobson, K. A. 2019. Application of isotopic methods to tracking animal movements. Pages 85–115 *in* K. A. Hobson and L. I. Wassenaar, editors. Tracking Animal Migration with Stable Isotopes. Second Edition. Academic Press, Cambridge, MA, USA.

Hobson, K. A., S. L. Van Wilgenburg, E. H. Dunn, D. J. T. Hussell, P. D. Taylor, and D. M. Collister. 2015. Predicting origins of passerines migrating through Canadian migration monitoring stations using stable-hydrogen isotope analyses of feathers: a new tool for bird conservation. Avian Conservation and Ecology 10. <http://www.ace-eco.org/vol10/iss1/art3/>.

Hobson, K. A., S. L. Van Wilgenburg, L. I. Wassenaar, and K. Larson. 2012. Linking hydrogen (δ^2H) isotopes in feathers and precipitation: sources of variance and consequences for assignment to isoscapes. PLOS One 7:e35137.

Hobson, K. A., and L. I. Wassenaar. 1997. Linking breeding and wintering grounds of neotropical migrant songbirds using stable hydrogen isotopic analysis of feathers. Oecologia 109:142–148.

Hobson, K. A., L. I. Wassenaar, and O. R. Taylor. 1999. Stable isotopes (δD and δ^{13}C) are geographic indicators of natal origins of monarch butterflies in eastern North America. Oecologia 120:397–404.

Kusack, J. W., D. C. Tozer, K. M. Harvey, M. L. Schummer, and K. A. Hobson. 2023*a*. Data from: Assigning harvested waterfowl to geographic origin using feather δ^2H isoscapes: What is the best analytical approach? Dryad, Dataset. <https://doi.org/10.5061/dryad.9w0vt4bmd>.

Kusack, J. W., D. C. Tozer, K. M. Harvey, M. L. Schummer, and K. A. Hobson. 2023*b*. Assigning harvested waterfowl to geographic origin using feather δ^2H isoscapes: What is the best analytical approach? PLOS One 18:e0288262.

Kusack, J. W., D. C. Tozer, M. L. Schummer, and K. A. Hobson. 2022. Origins of harvested American black ducks: stable isotopes support the flyover hypothesis. The Journal of Wildlife Management 87:e22324.

Ma, C., H. B. Vander Zanden, M. B. Wunder, and G. J. Bowen. 2020. assignR: an R package for isotope-based geographic assignment. Methods in Ecology and Evolution 11:996–1001.

Magozzi, S., C. P. Bataille, K. A. Hobson, M. B. Wunder, J. D. Howa, A. Contina, H. B. Vander Zanden, and G. J. Bowen. 2021. Calibration chain transformation improves the comparability of organic hydrogen and oxygen stable isotope data. Methods in Ecology and Evolution 12:732–747.

Nakash, E., A. Celis-Murillo, M. Malorodova, and L.-A. Howes. 2023. North American Bird Banding Program Dataset 1960–2023 retrieved 2023-07-12. U.S. Geological Survey, Eastern Ecological Science Center at the Leetown Research Laboratory, Kearneysville, WV, USA.

Nichols, J. D., M. C. Runge, F. A. Johnson, and B. K. Williams. 2007. Adaptive harvest management of North American waterfowl populations: a brief history and future prospects. Journal of Ornithology 148:343–349.

North American Waterfowl Management Plan. 2018. 2018 North American Waterfowl Management Plan (NAWMP) update: connecting people, waterfowl, and wetlands. <https://nawmp.org/timeline/2018-update >

Palumbo, M. D., D. C. Tozer, and K. A. Hobson. 2019. Origins of harvested Mallards from Lake St. Clair, Ontario: a stable isotope approach. Avian Conservation and Ecology 14:3.

Pendleton, G. W., and J. R. Sauer. 1992. Black duck population units as determined by patterns of band recovery. Pages 687–695 in D. R. McCullough and R. H. Barrett, editors. Wildlife 2001: Populations. Springer Netherlands, Dordrecht, NL.

Raftovich, R., K. Fleming, S. Chandler, and C. Cain. 2023. Migratory bird hunting activity and harvest during the 2021-22 and 2022-23 hunting seasons. U.S. Fish and Wildlife Service, Laurel, MD, USA.

Roberts, A., A. L. Scarpignato, A. Huysman, J. A. Hostetler, and E. B. Cohen. 2022. Migratory connectivity of North American waterfowl across administrative flyways. Ecological Applications 33:e2788.

Robinson, O. J., C. P. McGowan, and P. K. Devers. 2016. Updating movement estimates for American black ducks (*Anas rubripes*). PeerJ 4:e1787.

Roy, C., S. G. Cumming, and E. J. B. McIntire. 2015. Spatial and temporal variation in harvest probabilities for American black duck. Ecology and Evolution 5:1992–2004.

Royle, J. A., and D. R. Rubenstein. 2004. The role of species abundance in determining breeding origins of migratory birds with stable isotopes. Ecological Applications 14:1780–1788.

Ruegg, K. C., E. C. Anderson, R. J. Harrigan, K. L. Paxton, J. F. Kelly, F. Moore, and T. B. Smith. 2017. Genetic assignment with isotopes and habitat suitability (gaiah), a migratory bird case study. Methods in Ecology and Evolution 8:1241–1252.

Szymanski, M. L., A. D. Afton, and K. A. Hobson. 2007. Use of stable isotope methodology to determine natal origins of Mallards at a fine scale within the Upper Midwest. The Journal of Wildlife Management 71:1317–1324.

Szymanski, M. L., and J. A. Dubovsky. 2013. Distribution and derivation of the Blue-winged Teal (*Anas discors*) harvest, 1970-2003. United States Department of the Interior, Fish and Wildlife Service, Washington, DC, USA.

Terzer, S., L. I. Wassenaar, L. J. Araguás-Araguás, and P. K. Aggarwal. 2013. Global isoscapes for δ^{18}O and δ^2H in precipitation: improved prediction using regionalized climatic regression models. Hydrology and Earth System Sciences 17:4713–4728.

Terzer-Wassmuth, S., L. I. Wassenaar, J. M. Welker, and L. J. Araguás. 2021. Improved high-resolution global and regionalized isoscapes of δ^{18}O, δ^2H, and *d*-excess in precipitation. Hydrological Processes 35:e14254.

Thurber, B. G., C. Roy, and J. R. Zimmerling. 2020. Long-term changes in the autumn migration phenology of dabbling ducks in southern Ontario and implications for waterfowl management. Wildlife Biology 2020:wlb.00668.

US Fish and Wildlife Service. 2010. Northern pintail harvest strategy. US Department of Interior, Washington, DC, USA.

U.S. Fish and Wildlife Service. 2023. Adaptive Harvest Management: 2024 Hunting Season. U.S. Department of the Interior, Washington, DC, USA.

Vander Zanden, H. B., M. B. Wunder, K. A. Hobson, S. L. Van Wilgenburg, L. I. Wassenaar, J. M. Welker, and G. J. Bowen. 2014. Contrasting assignment of migratory organisms to geographic origins using long-term versus year-specific precipitation isotope maps. Methods in Ecology and Evolution 5:891–900.

Verheijen, B. H. F., E. B. Webb, M. G. Brasher, and H. M. Hagy. 2023. Spatiotemporal dynamics of duck harvest distributions in the Central and Mississippi flyways, 1960–2019. The Journal of Wildlife Management 88:e22521.

Wassenaar, L. I., and K. A. Hobson. 2001. A Stable-Isotope Approach to Delineate Geographical Catchment Areas of Avian Migration Monitoring Stations in North America. Environmental Science & Technology 35:1845–1850.

Wojtaszek, D. 2022. Using Stable Isotope Techniques to Complement Existing Northern Pintail Management. MSc Thesis. Western University, London, ON, CA.

Zimpfer, N. L., and M. J. Conroy. 2006. Modeling movement and fidelity of American Black Ducks. The Journal of Wildlife Management 70:1770–1777.

Appendix A

A   Supplementary Information for Chapter 2

Table A1 Age ratios (juveniles/adults) and fall age ratio (R) for black duck harvested in Canada (CA) and the United States (USA) based on harvested parts survey data (harvested juveniles/harvested adults [W_j/W_a]) and band-return data (juvenile band returns/adult band returns [B_j/B_a]; Gendron and Smith 2019, Raftovich et al. 2021), 2000–18.

	CA			USA		
Year	W_j/W_a	B_j/B_a	R	W_j/W_a	B_j/B_a	R
2000	2.69	5.75	0.47	0.76	2.65	0.29
2001	3.87	6.98	0.55	1.09	2.70	0.40
2002	3.53	7.40	0.48	1.06	2.44	0.44
2003	4.93	7.59	0.65	1.11	2.66	0.42
2004	3.34	5.26	0.64	0.97	2.46	0.39
2005	3.56	4.36	0.82	1.58	2.48	0.64
2006	3.74	8.53	0.44	1.47	2.92	0.50
2007	4.27	4.71	0.91	1.22	3.01	0.41
2008	4.20	6.48	0.65	0.98	2.49	0.39
2009	4.43	3.49	1.27	1.27	3.03	0.42
2010	5.02	12.18	0.41	1.58	3.08	0.51
2011	3.02	3.97	0.76	1.27	2.77	0.46
2012	3.27	6.61	0.49	1.47	3.88	0.38
2013	2.58	4.58	0.56	1.56	3.01	0.52
2014	2.00	4.47	0.45	1.12	2.54	0.44
2015	4.10	2.55	1.61	1.55	2.48	0.63
2016	2.56	3.77	0.68	1.46	2.70	0.54
2017	3.26	5.95	0.55	1.02	2.96	0.34
2018	2.63	7.24	0.36	1.11	2.69	0.41

Table A2 Age ratios (juveniles/adults) and fall age ratio (R) for Canadian harvested black duck stratified by province or region (Ontario [ON], Quebec [QC], Atlantic Canada [ATL]), based on harvested parts survey data (harvested juveniles/harvested adults [W_j/W_a]) and band-return data (juvenile band returns/adult band returns [B_j/B_a]), 2000–18 (Gendron and Smith 2019, Raftovich et al. 2021).

	ON			QC			ATL		
Year	W_j/W_a	B_j/B_a	R	W_j/W_a	B_j/B_a	R	W_j/W_a	B_j/B_a	R
2000	2.20	5.22	0.42	2.34	2.60	0.90	2.97	7.38	0.40
2001	4.15	12.25	0.34	4.07	2.16	1.89	3.67	8.27	0.44
2002	2.73	4.80	0.57	3.33	6.58	0.51	3.87	8.59	0.45
2003	7.07	12.00	0.59	3.74	2.78	1.34	5.09	9.31	0.55
2004	2.26	6.11	0.37	2.95	3.95	0.75	4.01	5.84	0.69
2005	3.06	2.75	1.11	3.21	3.70	0.87	4.05	5.92	0.68
2006	3.50	7.57	0.46	3.98	6.52	0.61	3.67	10.80	0.34
2007	2.23	3.50	0.64	3.54	4.76	0.74	5.04	4.95	1.02
2008	3.43	3.83	0.90	4.67	3.74	1.25	4.11	8.21	0.50
2009	3.36	1.78	1.89	6.33	4.07	1.56	3.57	3.67	0.97
2010	5.57	15.50	0.36	5.46	20.83	0.26	4.51	4.52	1.00
2011	2.05	2.29	0.90	3.20	4.82	0.66	3.19	3.89	0.82
2012	4.13	13.00	0.32	4.39	5.07	0.87	2.71	6.04	0.45
2013	3.31	5.33	0.62	3.16	2.85	1.11	2.20	5.03	0.44
2014	1.91	1.57	1.21	2.52	3.32	0.76	1.75	5.86	0.30
2015	2.32	2.38	0.98	3.67	2.89	1.27	4.91	2.44	2.02
2016	2.91	6.20	0.47	3.20	2.61	1.23	2.21	3.71	0.60
2017	1.91	4.25	0.45	2.03	3.89	0.52	4.52	7.88	0.57
2018	1.84	7.67	0.24	2.16	4.07	0.53	3.10	8.72	0.36
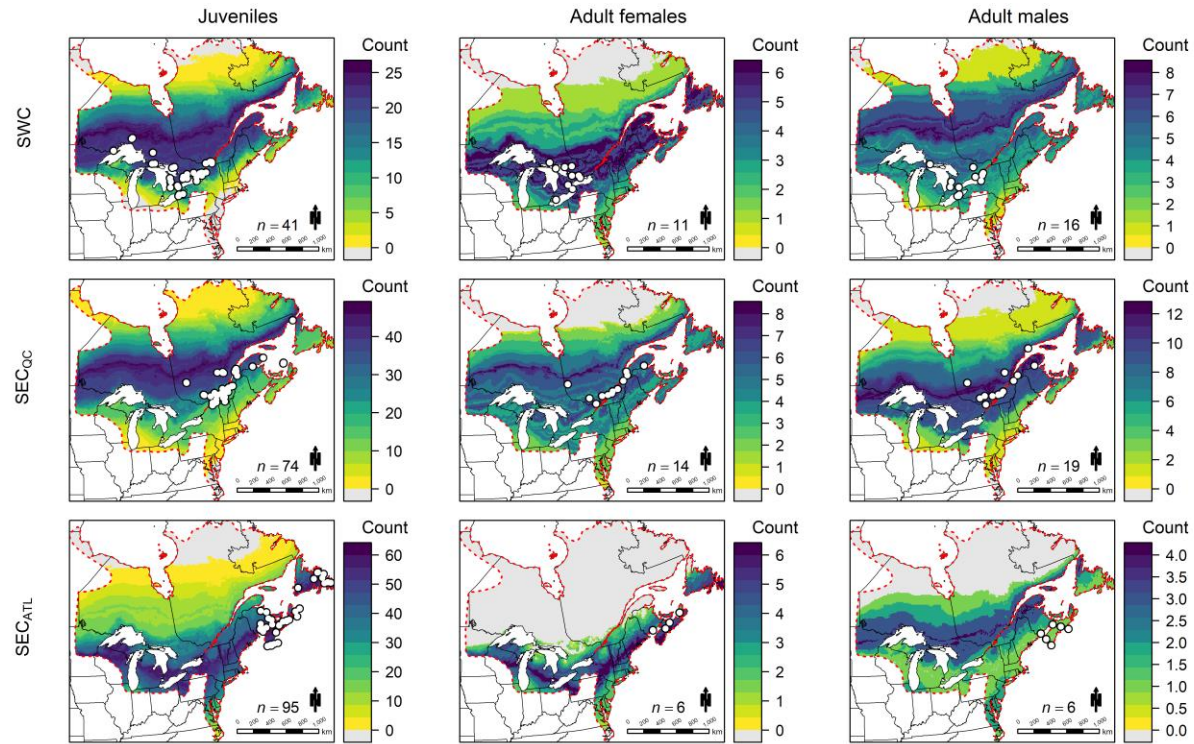
Figure A1 Likely origins of black ducks harvested within Canada from 2017–19. Individuals were grouped by age/sex cohort (columns; juvenile, adult female, adult male) and black duck conservation region of harvest (rows; southwestern Canada [SWC], southeastern Canada-Quebec [SEC_QC], southeastern Canada-Atlantic [SEC_ATL]). Sample sizes show the number of individuals within a given group. Scale represents the number of individuals assigned to a given pixel, under a 2:1 odds ratio.
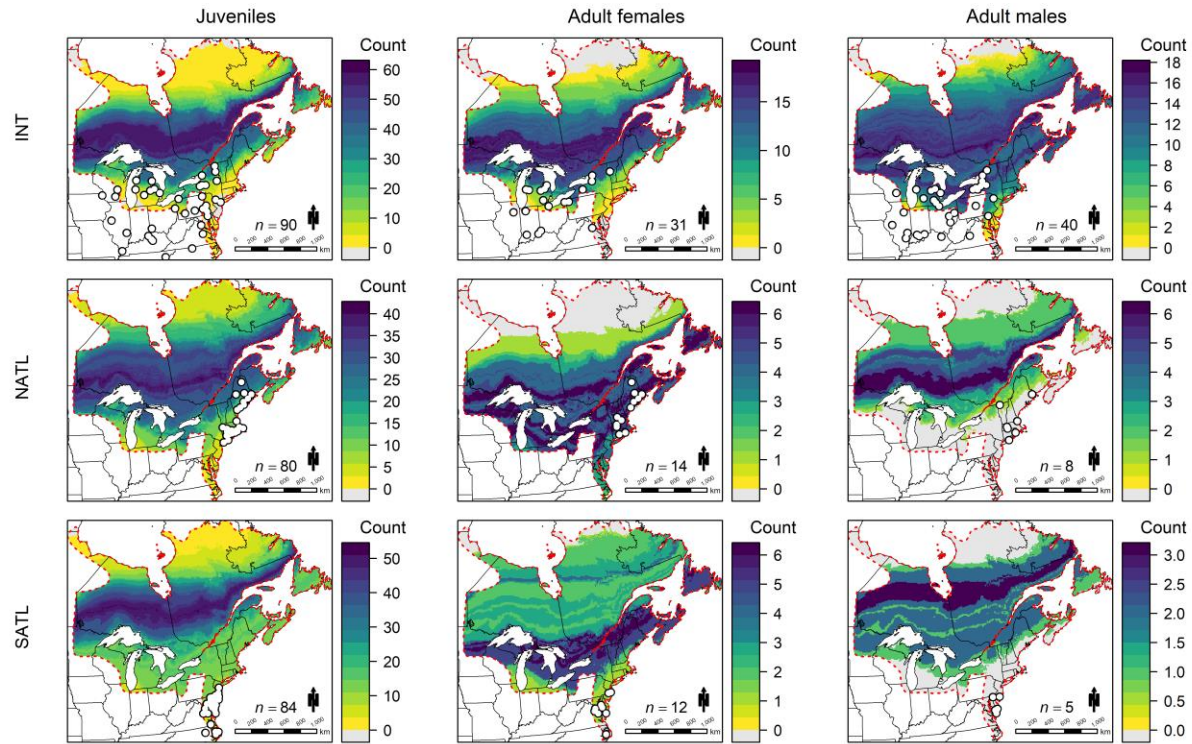
Figure A2 Likely origins of black ducks harvested within the United States from 2017–20. Individuals were grouped by age/sex cohort (columns; juvenile, adult female, adult male) and black duck conservation region of harvest (rows; interior United States [INT], north Atlantic United States [NATL], south Atlantic United States [SATL]). Sample sizes show the number of individuals within a given group. Scale represents the number of individuals assigned to a given pixel, under a 2:1 odds ratio.

Appendix B

B   Supplementary Information for Chapter 3

Table B1 Summary table for published calibration equations and known-origin data. Supplementary table available at:
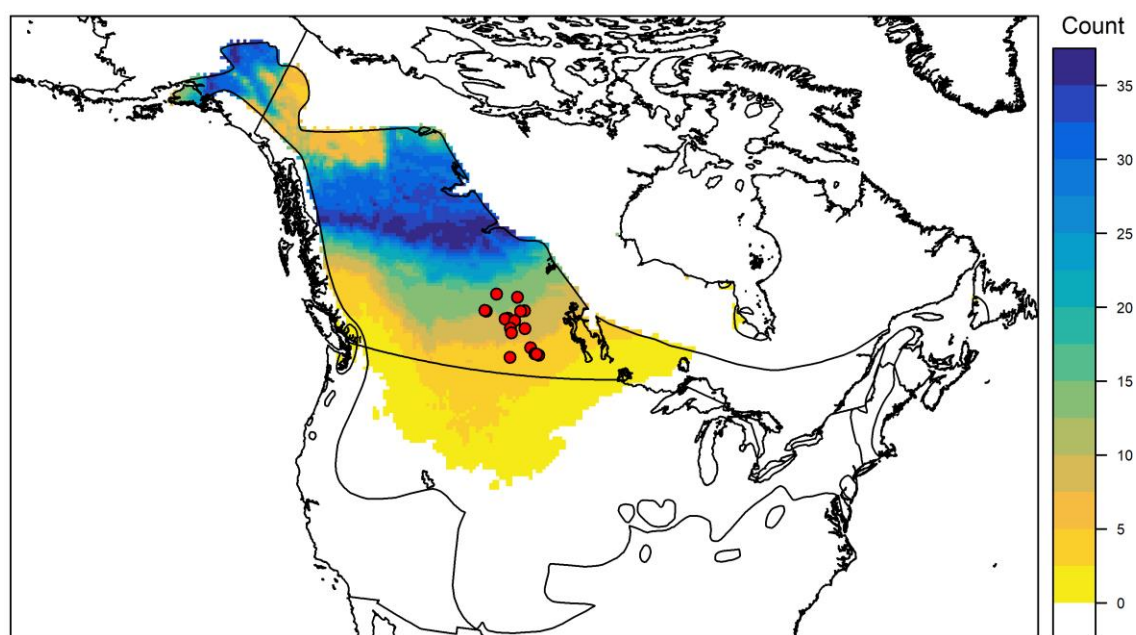
Figure B1 Recreation of original figure from Palumbo et al. (2020). Likely origins of Blue-winged Teal (*Spatula discors*) harvested in southern Saskatchewan (n = 47, 2014–18 (Palumbo et al. 2020)) using the assignment methods from the original publication (calibration: δ^2H_f = -31.6 + 0.93 * δ^2H_p; SD_{resid} = 12.8). The colour indicates the number of individuals that were assigned to a given pixel under a 2:1 odds ratio. Harvest locations for samples are shown as red points.
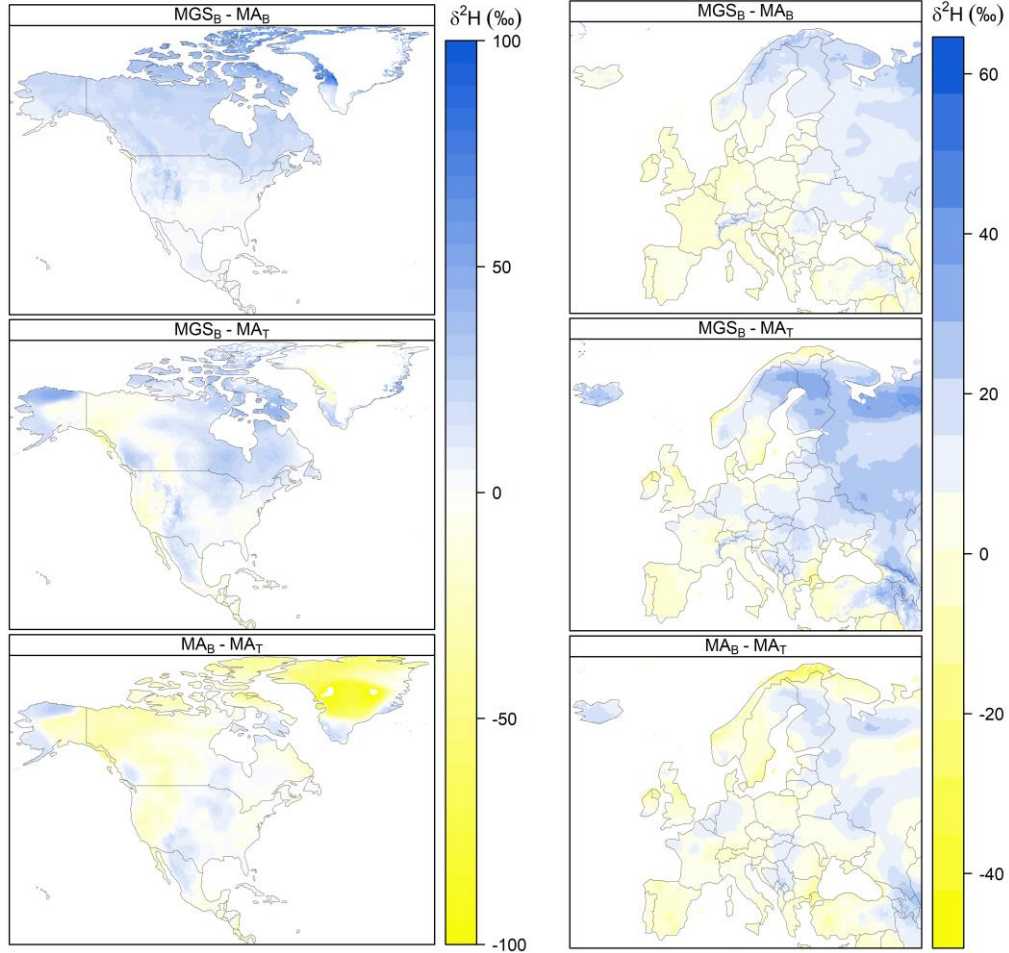
Figure B2 Spatial representation of differences in δ^2H_p between precipitation isoscape methods, for North America and Europe. Each panel shows the difference (first isoscape minus second) between paired isoscapes (MGS_B – MA_B, MGS_B – MA_T, MA_B – MA_T): amount-weighted mean growing-season precipitation (Bowen 2021) (MGS_B) and amount-weighted mean annual precipitation (MA_B, (Bowen 2021); MA_T, (Terzer-Wassmuth et al. 2021)). Blue regions represent areas where the first isoscape is much more positive than the second and yellow regions represent areas where the first isoscape is more negative than the second.

C   Supplementary Information for Chapter 4
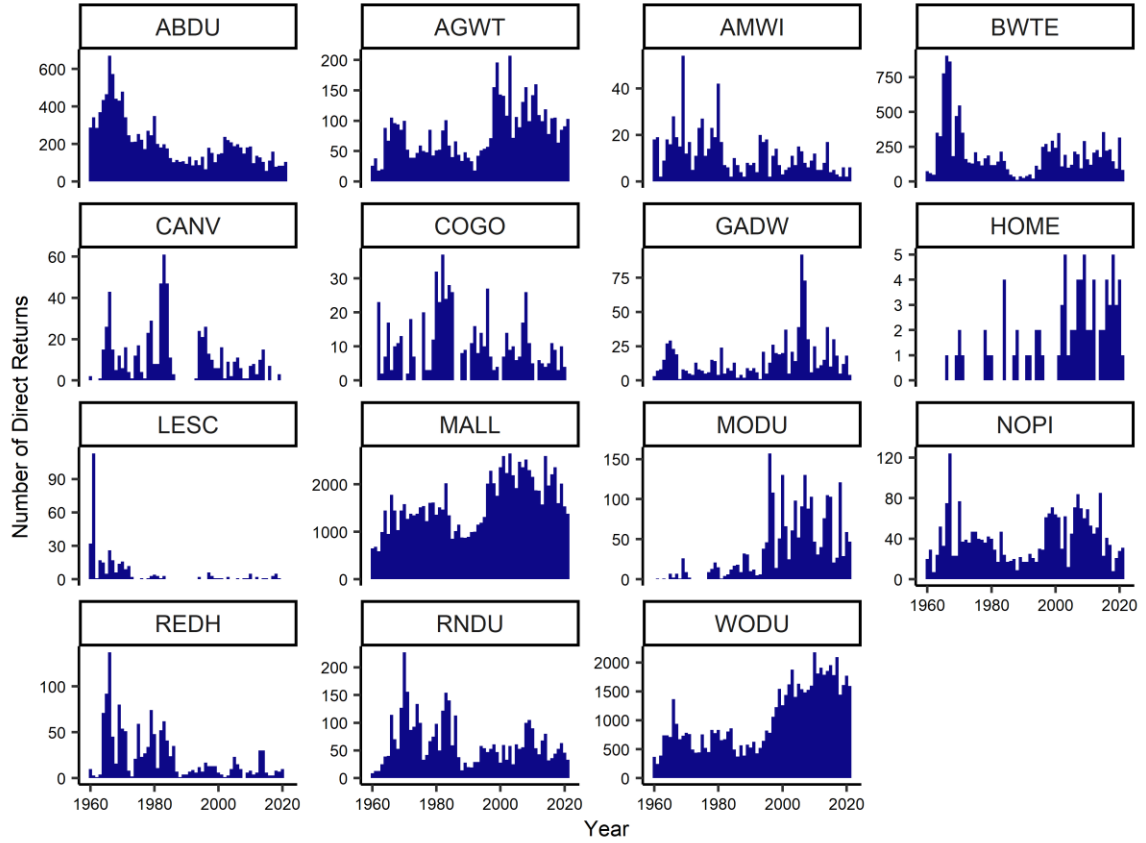
Figure C1 Direct recoveries distributions 1960–2022. Histograms for the number of direct recoveries 1960–2022 by species. See Table 4.1 for species alpha-code definitions.
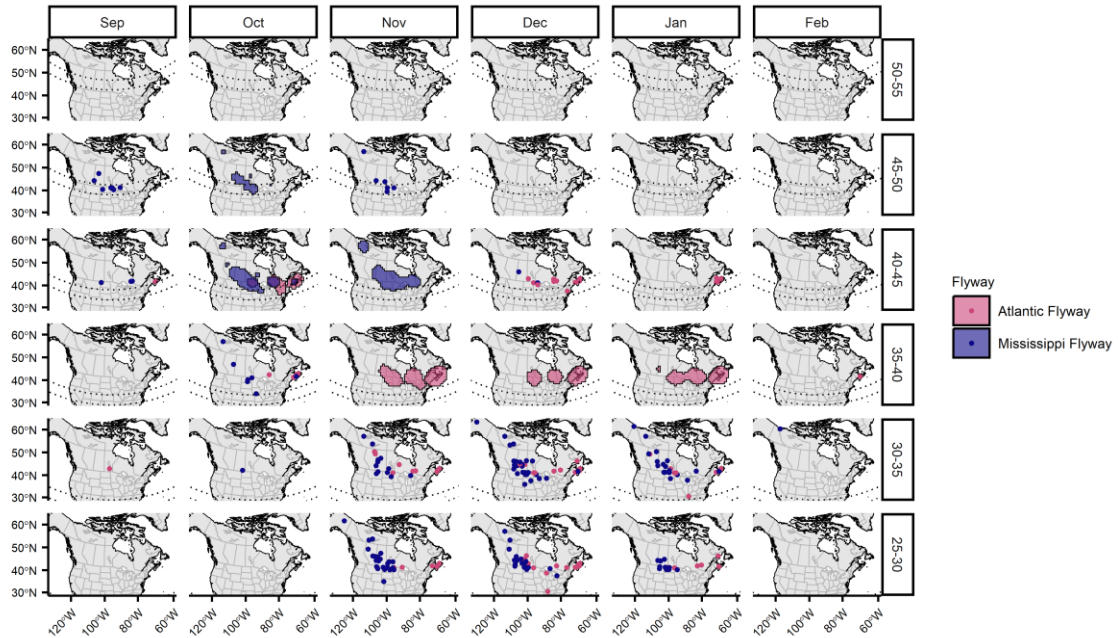
Figure C2 KDE harvest derivation for American Wigeon. Kernel density estimated harvest derivations (90 % density area) for American Wigeon (*Mareca americana*) harvested in the Mississippi (blue; n = 620, 1960–2021) and Atlantic (pink; n = 428, 1960–2022) flyways, separated by month of harvest (September–February) and latitude of harvest (25–55, by 5° bands). Upper and lower limits of harvest area (latitudinal band) are shown with dotted curved lines. Points show banding locations when sample sizes were < 50.
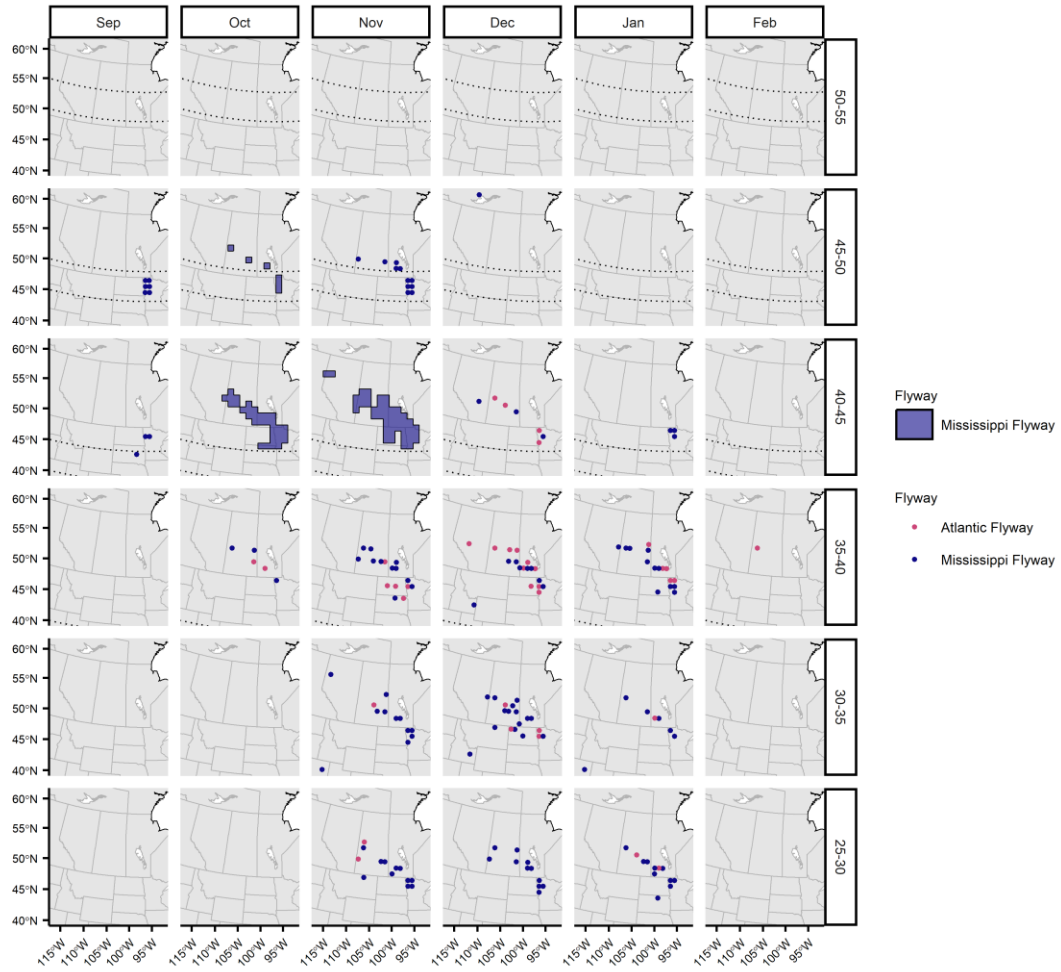
Figure C3 KDE harvest derivation for Canvasback. Kernel density estimated harvest derivations (90 % density area) for Canvasback (*Aythya valisineria*) harvested in the Mississippi (blue; n = 812, 1960–2019) and Atlantic (pink; n = 91, 1960–2019) flyways, separated by month of harvest (September–February) and latitude of harvest (25–55, by 5° bands). Upper and lower limits of harvest area (latitudinal band) are shown with dotted curved lines. Points show banding locations when sample sizes were < 50.
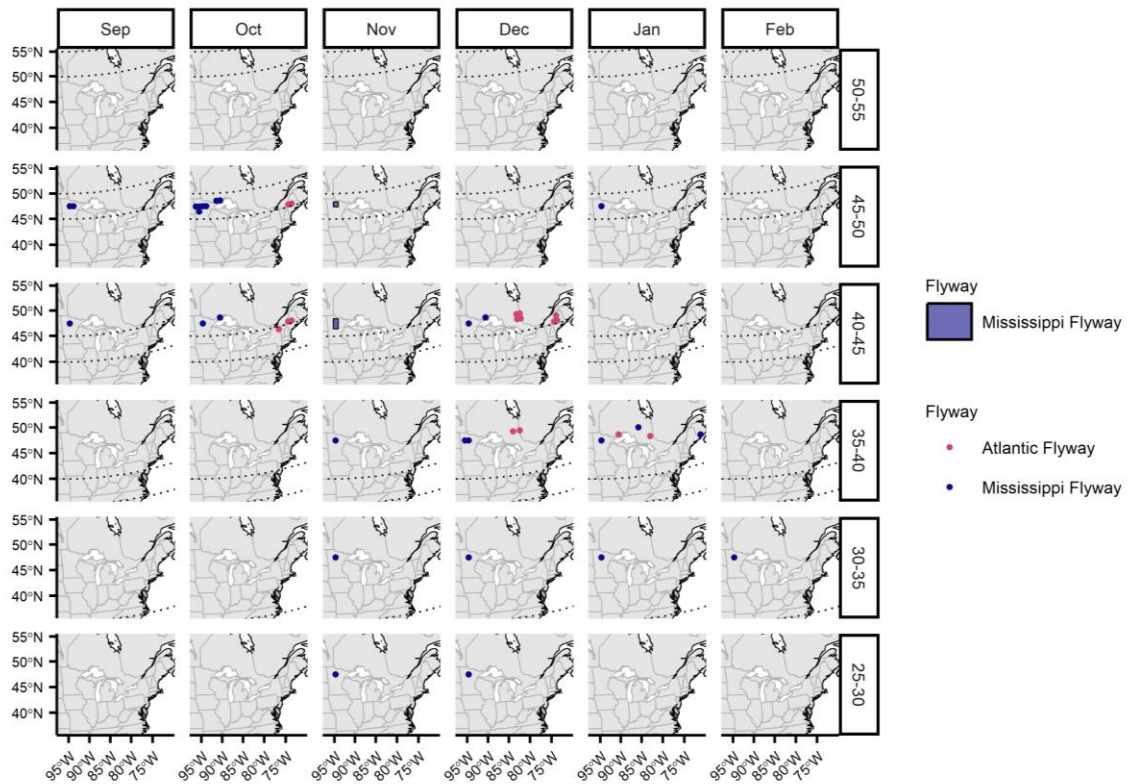
Figure C4 KDE harvest derivation for Common Goldeneye. Kernel density estimated harvest derivations (90 % density area) for Common Goldeneye (*Bucephala clangula*) harvested in the Mississippi (blue; n = 734, 1962–2022) and Atlantic (pink; n = 46, 1960–2021) flyways, separated by month of harvest (September–February) and latitude of harvest (25–55, by 5° bands). Upper and lower limits of harvest area (latitudinal band) are shown with dotted curved lines. Points show banding locations when sample sizes were < 50.
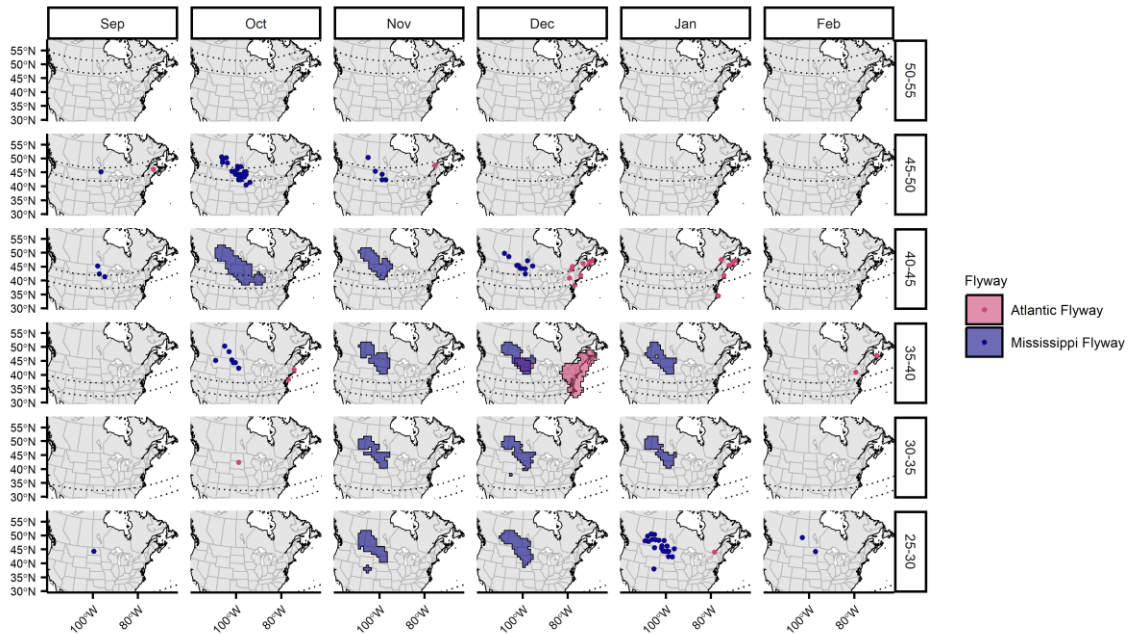
Figure C5 KDE harvest derivation for Gadwall. Kernel density estimated harvest derivations (90 % density area) for Gadwall (*Mareca strepera*) harvested in the Mississippi (blue; n = 832, 1960–2022) and Atlantic (pink; n = 197, 1960–2022) flyways, separated by month of harvest (September–February) and latitude of harvest (25–55, by 5° bands). Upper and lower limits of harvest area (latitudinal band) are shown with dotted curved lines. Points show banding locations when sample sizes were < 50.
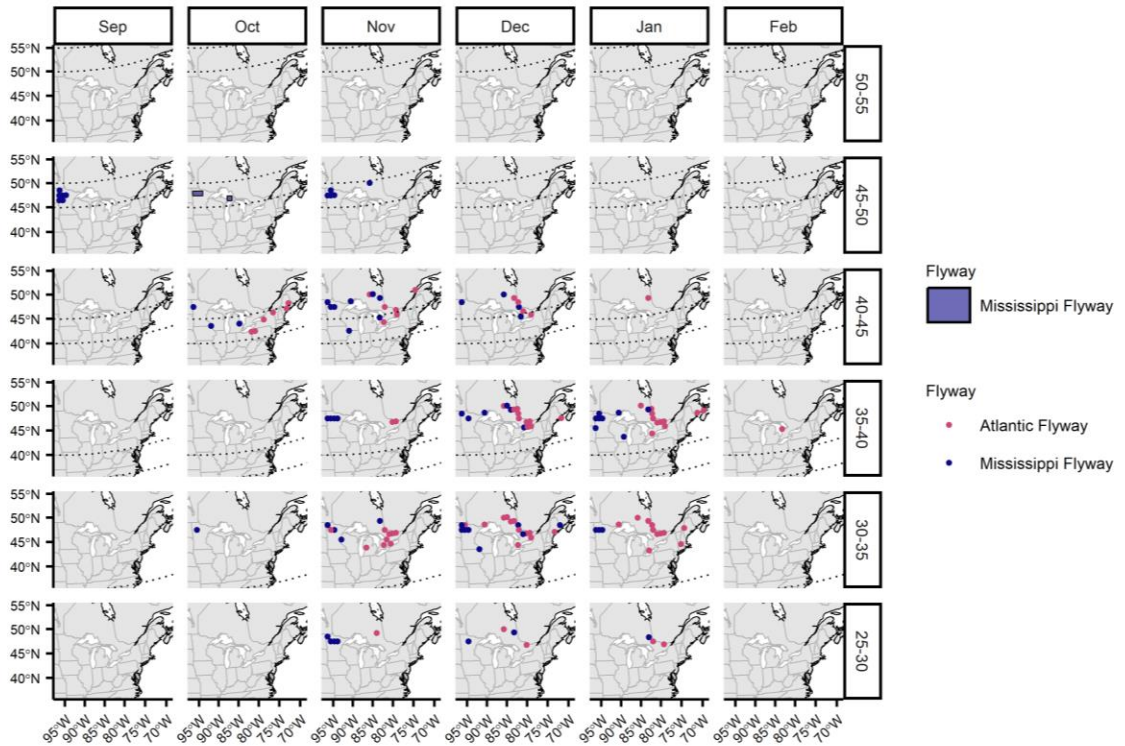
Figure C6 KDE harvest derivation for Hooded Merganser. Kernel density estimated harvest derivations (90 % density area) for Hooded Merganser (*Lophodytes cucullatus*) harvested in the Mississippi (blue; n = 181, 1962–2021) and Atlantic (pink; n = 78, 1964–2022) flyways, separated by month of harvest (September–February) and latitude of harvest (25–55, by 5° bands). Upper and lower limits of harvest area (latitudinal band) are shown with dotted curved lines. Points show banding locations when sample sizes were < 50.
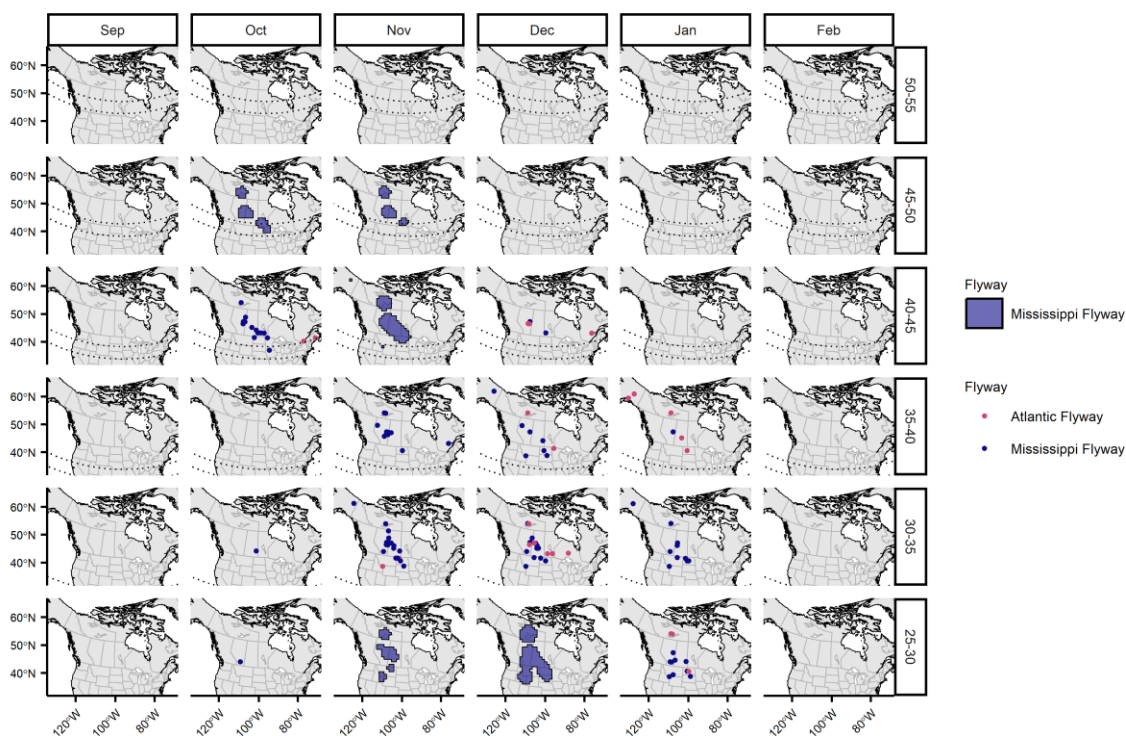
Figure C7 KDE harvest derivation for Lesser Scaup. Kernel density estimated harvest derivations (90 % density area) for Lesser Scaup (*Aythya affinis*) harvested in the Mississippi (blue; n = 469, 1960–2021) and Atlantic (pink; n = 39, 1960–2021) flyways, separated by month of harvest (September–February) and latitude of harvest (25–55, by 5° bands). Upper and lower limits of harvest area (latitudinal band) are shown with dotted curved lines. Points show banding locations when sample sizes were < 50.
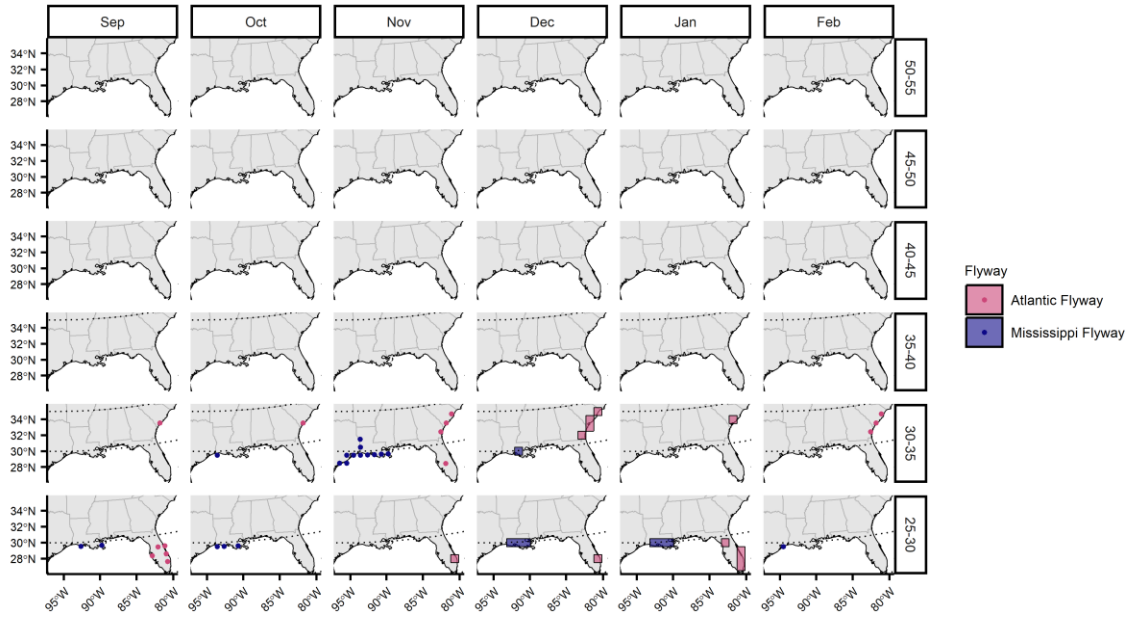
Figure C8 KDE harvest derivation for Mottled Duck. Kernel density estimated harvest derivations (90 % density area) for Mottled Duck (*Anas fulvigula*) harvested in the Mississippi (blue; n = 1,408, 1963–2022) and Atlantic (yellow; n = 458, 1961–2022) flyways, separated by month of harvest (September–February) and latitude of harvest (25–55, by 5° bands). Upper and lower limits of harvest area (latitudinal band) are shown with dotted curved lines. Points show banding locations when sample sizes were < 50.
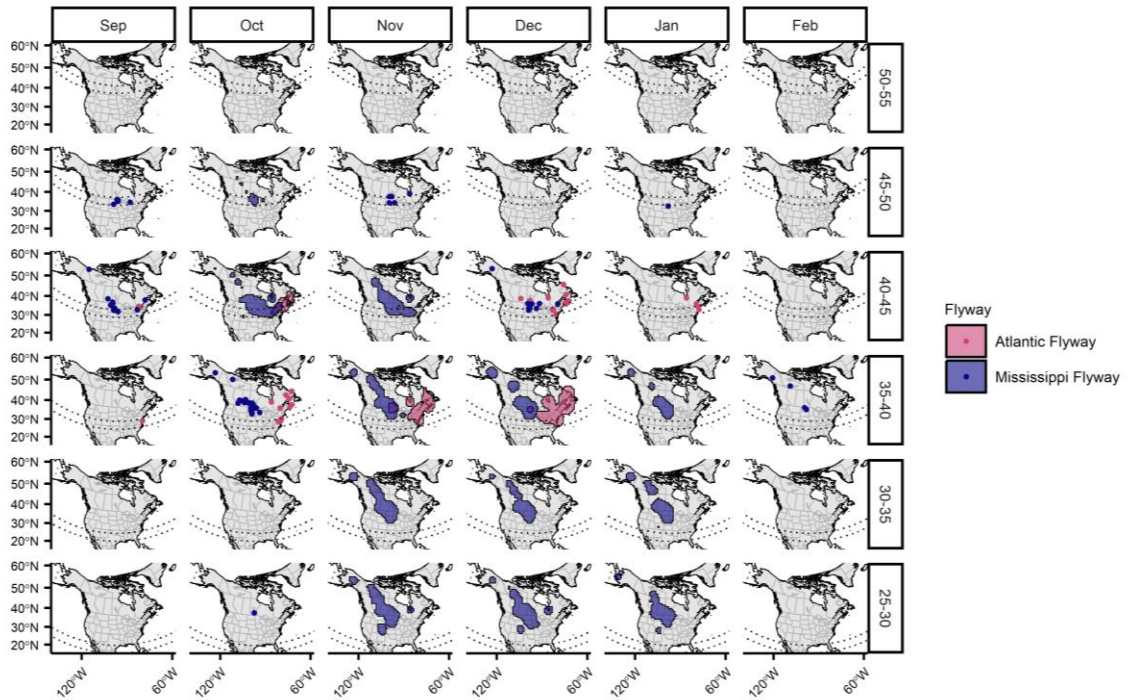
Figure C9 KDE harvest derivation for Northern Pintail. Kernel density estimated harvest derivations (90 % density area) for Northern Pintail (*Anas acuta*) harvested in the Mississippi (blue; n = 1,892, 1960–2022) and Atlantic (pink; n = 354, 1960–2019) flyways, separated by month of harvest (September–February) and latitude of harvest (25–55, by 5° bands). Upper and lower limits of harvest area (latitudinal band) are shown with dotted curved lines. Points show banding locations when sample sizes were < 50.
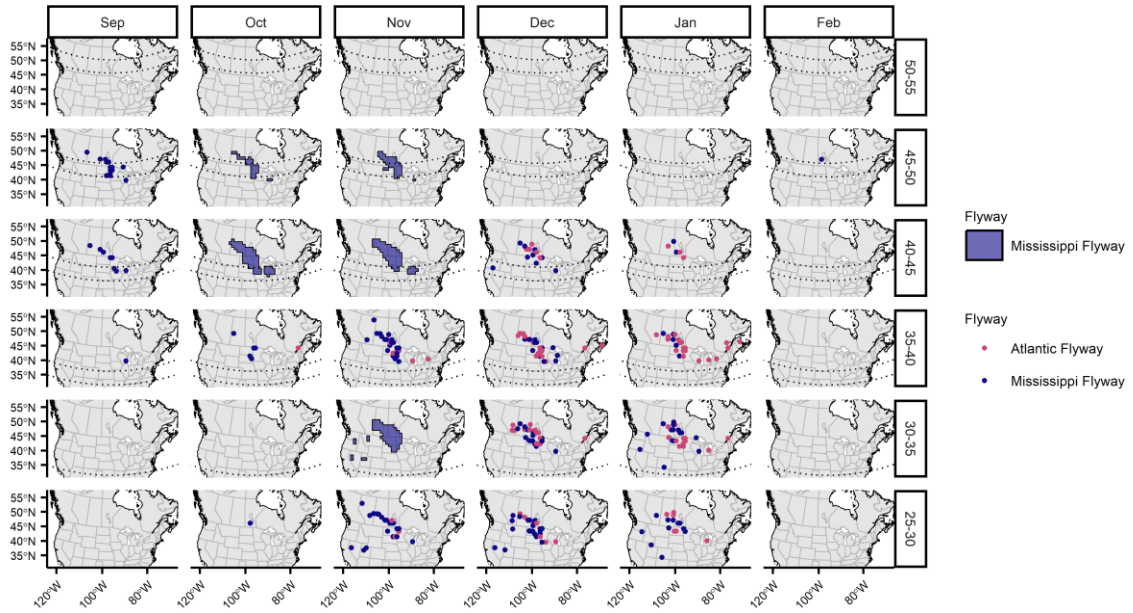
Figure C10 KDE harvest derivation for Redhead. Kernel density estimated harvest derivations (90 % density area) for Redhead (*Aythya americana*) harvested in the Mississippi (blue; n = 1,676, 1960–2022) and Atlantic (pink; n = 578, 1961–2022) flyways, separated by month of harvest (September–February) and latitude of harvest (25–55, by 5° bands). Upper and lower limits of harvest area (latitudinal band) are shown with dotted curved lines. Points show banding locations when sample sizes were < 50.
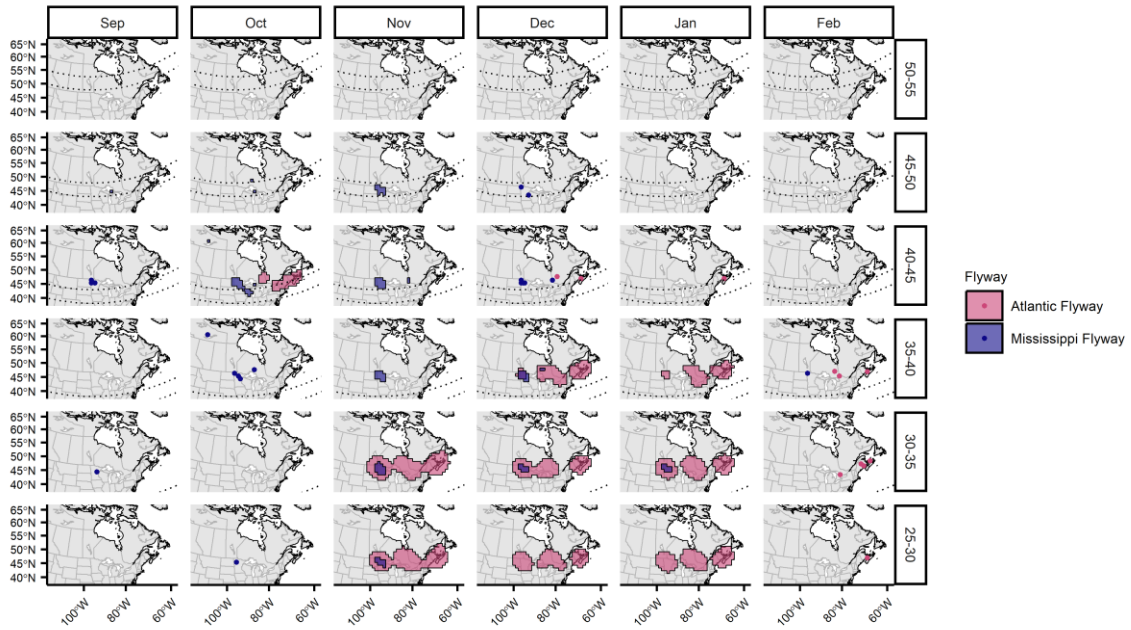
Figure C11 KDE harvest derivation for Ring-necked Duck. Kernel density estimated harvest derivations (90 % density area) for Ring-necked Duck (*Aythya collaris*) harvested in the Mississippi (blue; n = 3,174, 1960–2022) and Atlantic (pink; n = 578, 1960–2022) flyways, separated by month of harvest (September–February) and latitude of harvest (25–55, by 5° bands). Upper and lower limits of harvest area (latitudinal band) are shown with dotted curved lines. Points show banding locations when sample sizes were < 50.
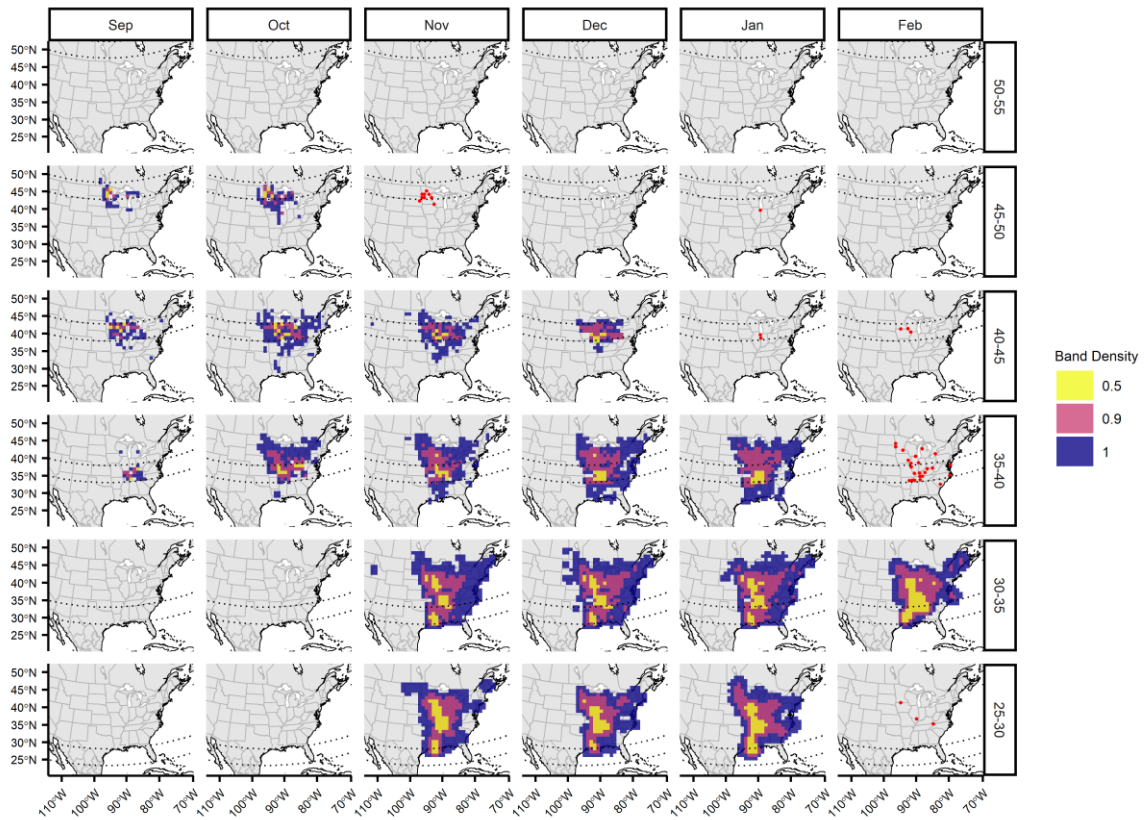
Figure C12 KDE harvest derivation for Wood Duck in Mississippi flyway. Monthly (columns) harvest derivation, based on band returns, for Wood Duck (*Aix sponsa*) harvested in the Mississippi Flyway (n = 40,559, 1960–2022). Derivation limits were derived from kernel density estimates, extracting all cells (i.e., density = 1, in blue) or cells representing the upper 50 % or 90 % of density estimates (i.e., density = 0.5 and 0.9, in yellow and pink). Upper and lower limits of harvest area (latitudinal band — rows) are shown with dotted curved lines. For panels (month × latitudinal band) with less than 50 band recoveries, banding locations are shown with red points.
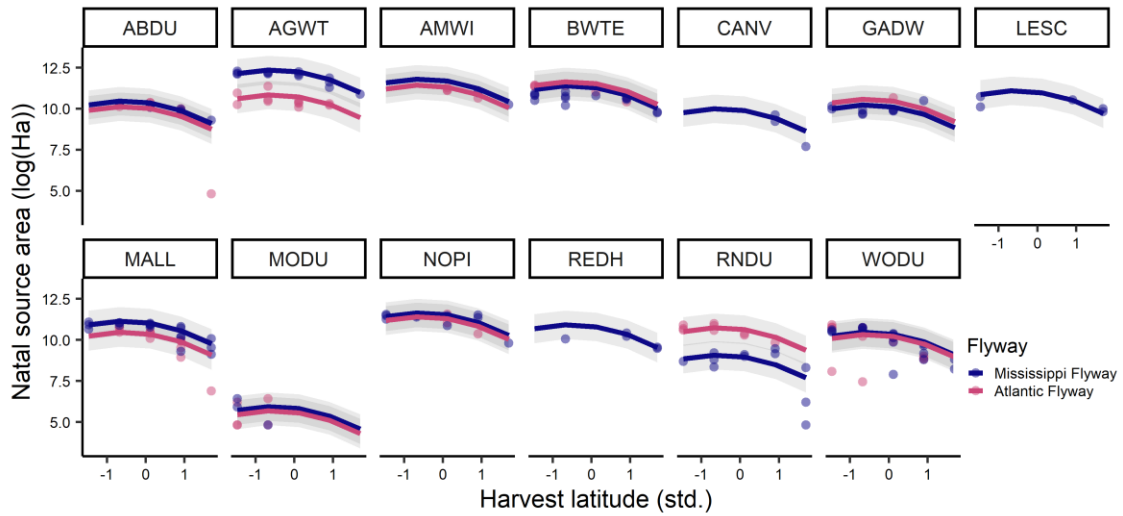
Figure C13 Change in harvest derivation area at different harvest latitudes.
Relationship between natal source area (log(Ha)) and harvest latitude (standardized) for 13 species of waterfowl harvested in the Great Lakes region (n = 206, 1920–2020). Line colour represents the flyway of harvest. Lines are the estimated marginal means from a linear mixed-effect model (fitted with 'ggpredict' from ggeffects package version 1.3.2, Lüdecke 2018), holding the effect of sample size and date constant. The grey region represents the prediction intervals. For species with derivations in only one flyway, marginal means were only shown for that flyway. See Table 4.1 for species alpha-code definitions.
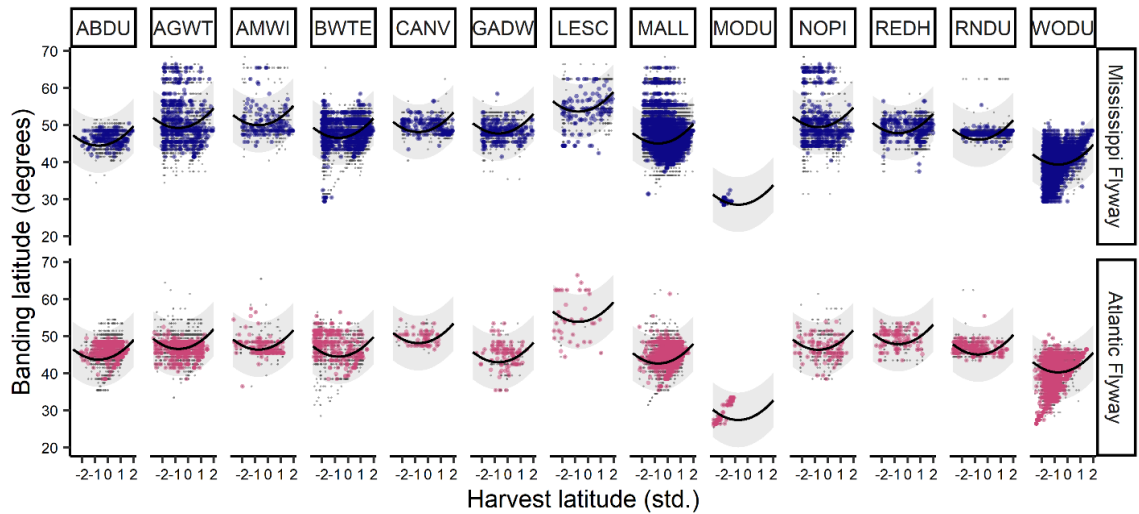
Figure C14 Change in banding latitude at different harvest latitudes. Relationship between banding latitude (°) and harvest latitude (standardized) for 13 species of waterfowl harvested in the Great Lakes region (n = 202,762, 1920–2020). Line colour represents the flyway of harvest. Lines are the estimated marginal means from the multi-species linear mixed-effect model (fitted with 'ggpredict' from ggeffects package version 1.3.2, Lüdecke 2018), holding the effect of sample size and date constant. The grey region represents the prediction intervals. Raw data are shown as grey points. Mean banding latitude for each unique harvest day in a given latitudinal band are shown in colour to give a visual representation of centrality. See Table 4.1 for species alpha-code definitions.
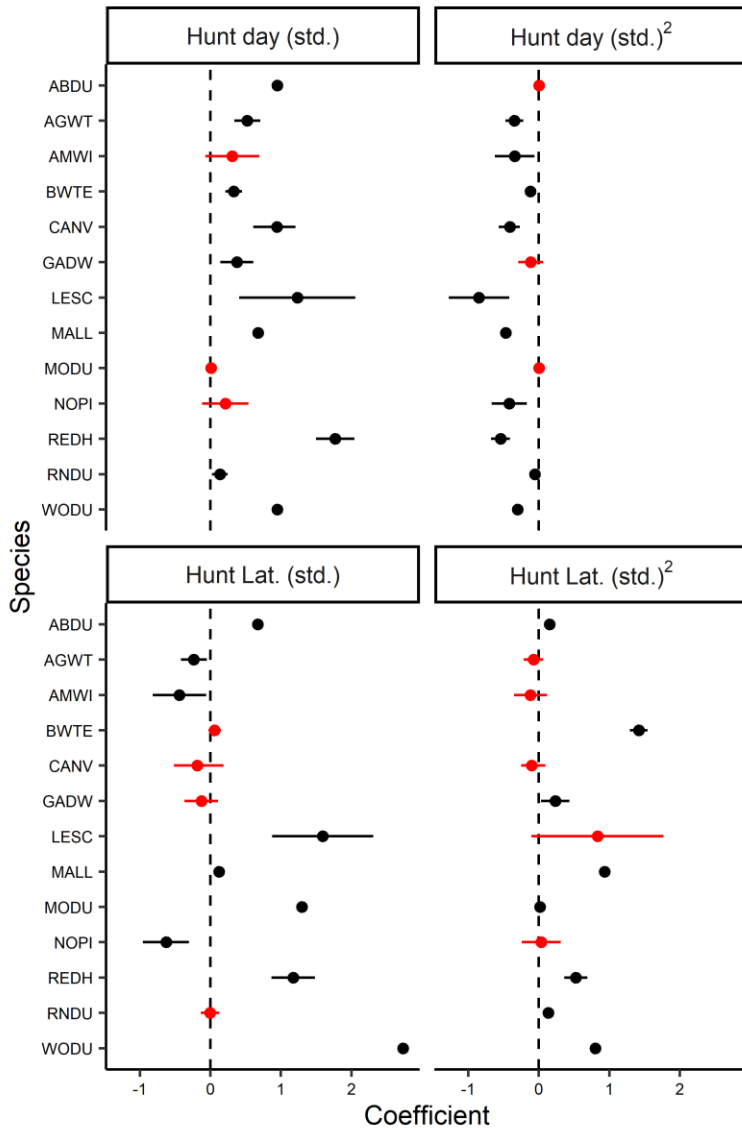
Figure C15 Parameter estimates for species-specific models. Parameter estimates from species-specific linear mixed-effects models evaluating the relationships between both harvest day and harvest latitude (standardized) and banding latitude (response). Points show the parameter coefficients with the 95 % confidence interval. Intervals overlapping zero are shown in red, with those not overlapping zero in black. See Table 4.1 for species alpha-code definitions.

Appendix D

D   Supplementary Information for Chapter 5

Table D1 Sample size for feathers, by species and harvest season of collection.

Species	Season 2017–18	2018–19	2019–20	2020–21
American Black Duck	48	22	0	0
American Green-winged Teal	41	19	0	0
Bufflehead	27	51	0	0
Canvasback	1	14	0	7
Greater Scaup	13	18	0	0
Lesser Scaup	17	25	0	0
Mallard	19	150	0	0
Northern Pintail	14	34	39	19
Redhead	12	51	0	24
Ring-necked Duck	18	33	0	0
Wood Duck	31	0	0	0
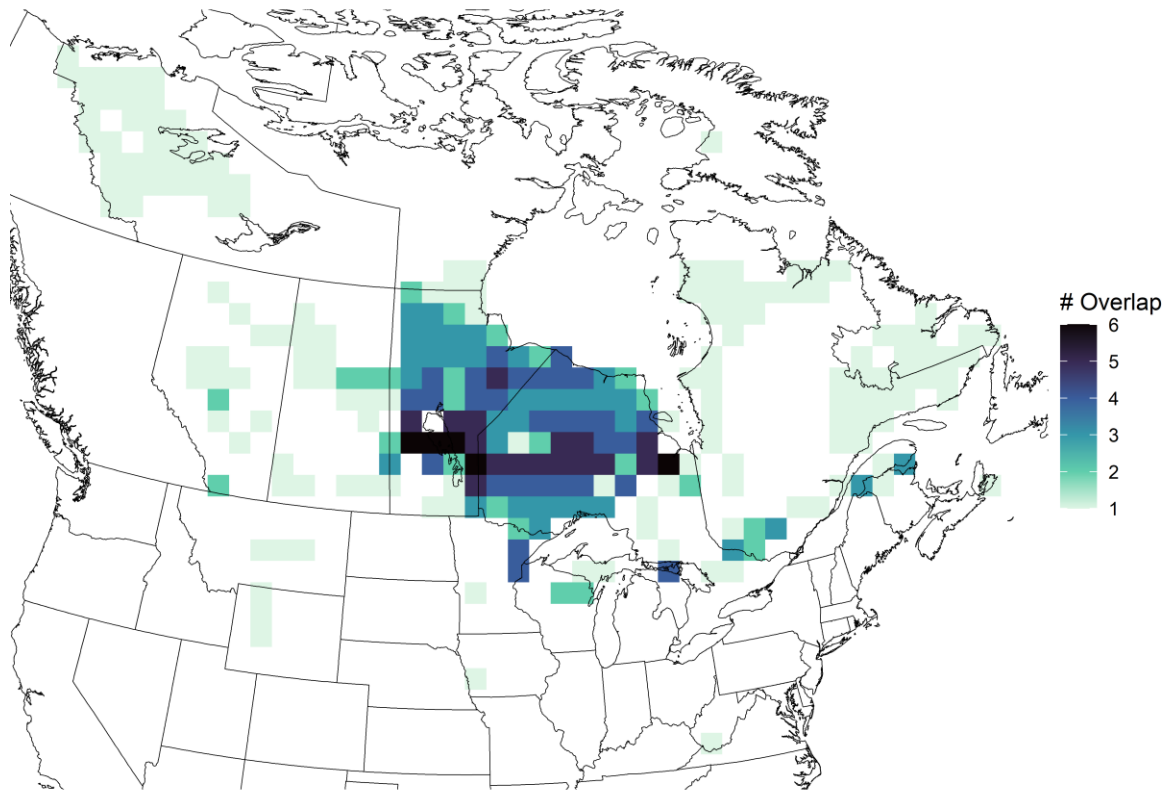
Figure D1 Overlapping target regions for future banding effort (i.e., regions of disagreement between likely origin [δ^2H_f + flyway prior] and banding effort). The scale depicts the number of species overlapping in a given cell.
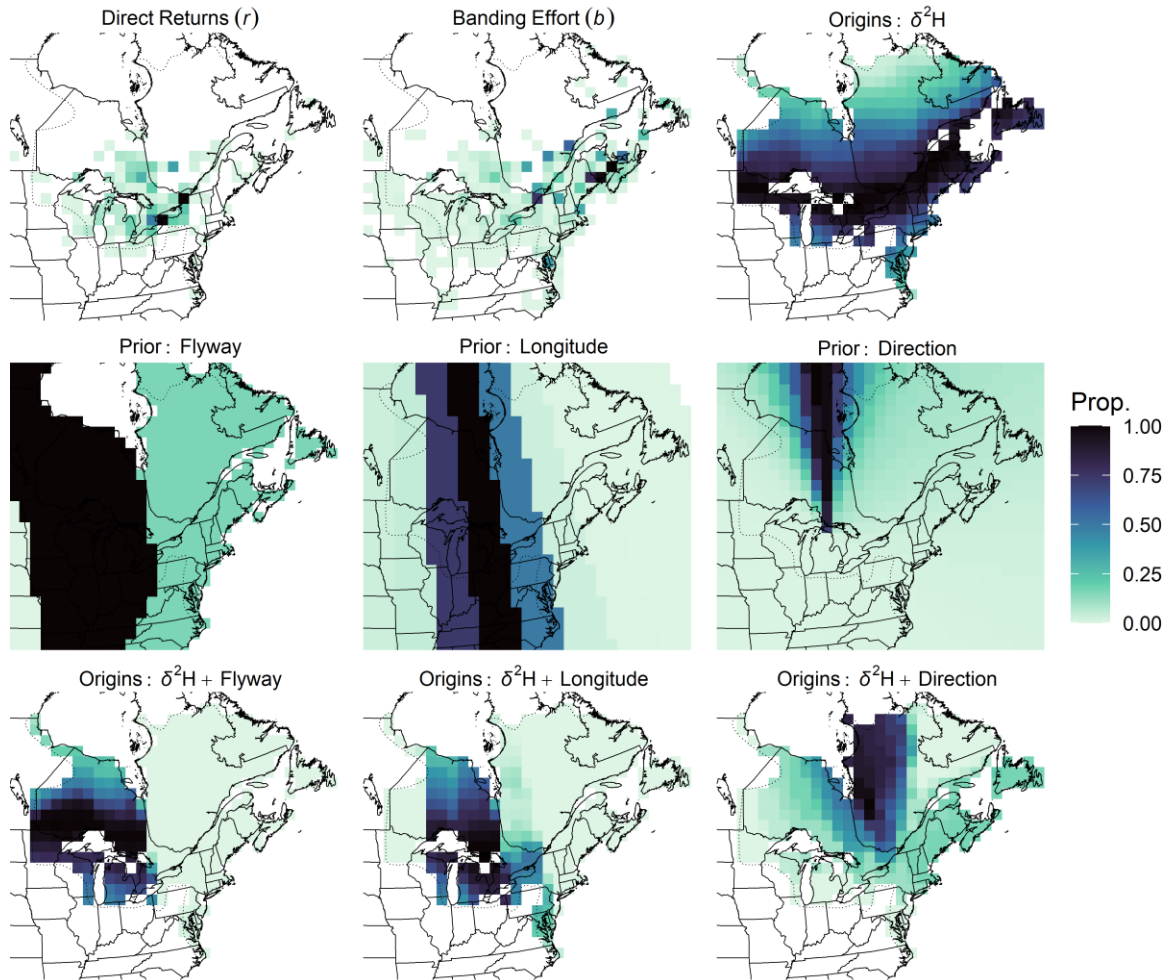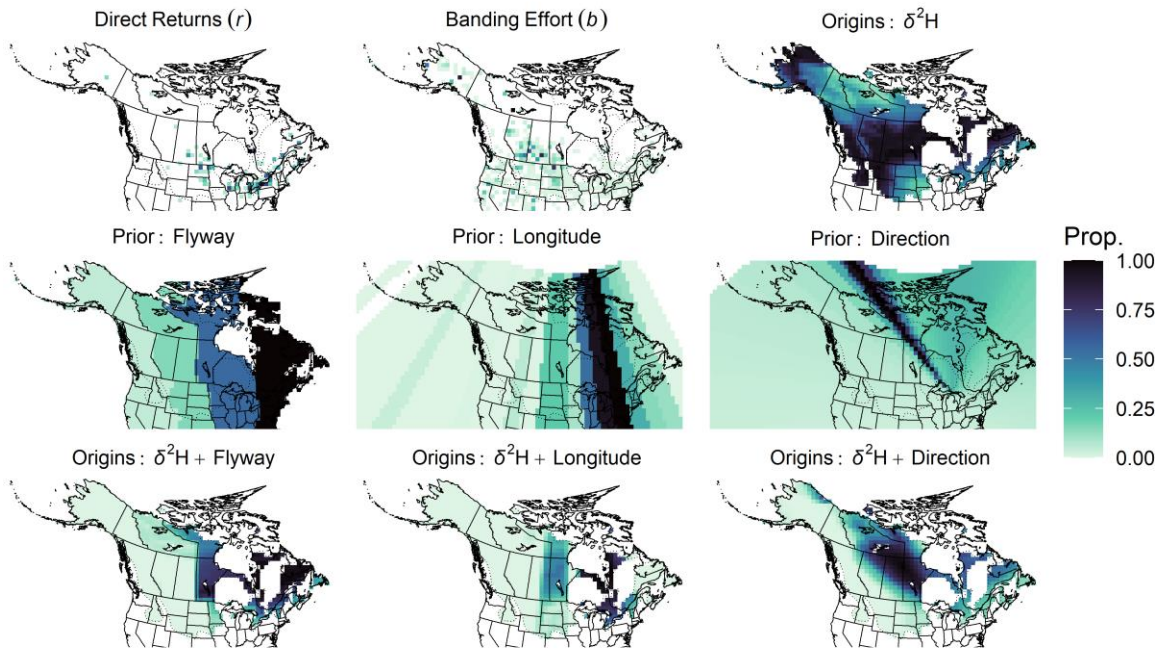
Figure D2 Direct recoveries (*r*), banding effort (*b*), priors (Flyway, 5° longitudinal zone = "Longitude", movement direction = "Direction") and likely origins of juvenile American Black Duck (*Anas rubripes*) harvested in the Great Lakes. Titles for panels specify whether the likely origin is based on stable isotopes (n = 70, 2017–18 and 2018–19) alone (δ^2H) or whether a prior (n = 3,780 and $n_{migrants}$ = 1,122, 1960–2022) is included (δ^2H + prior). Within each panel, the values were rescaled to be a proportion of the maximal value, to better visualize relative differences.
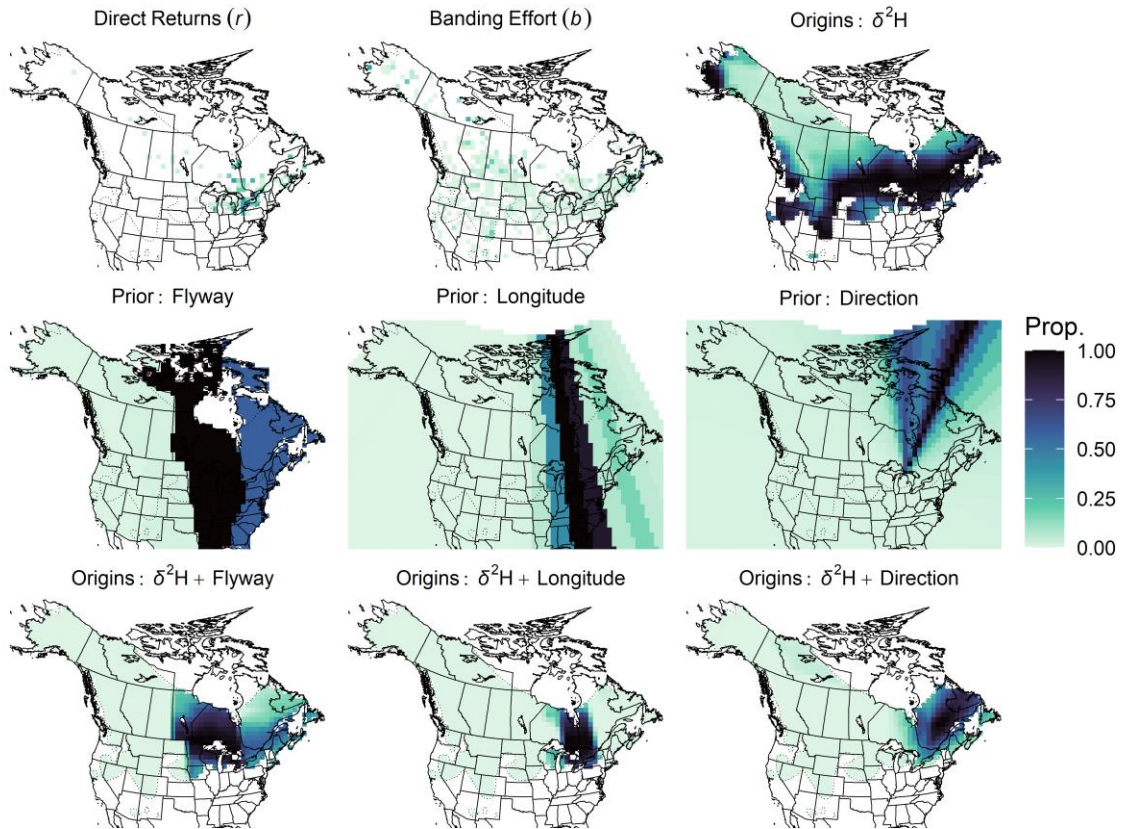
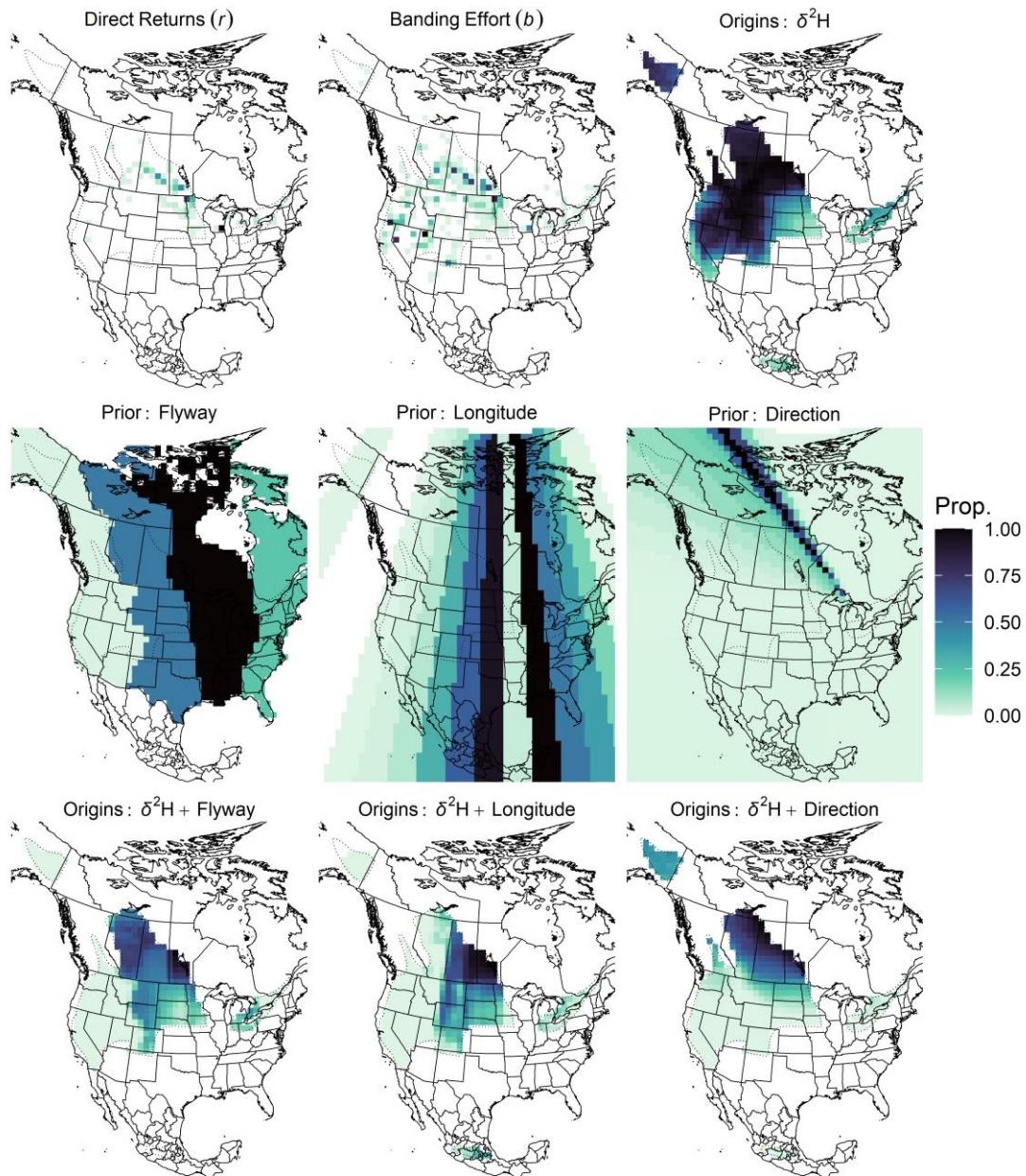**Figure D3 Direct recoveries (*r*), banding effort (*b*), priors (Flyway, 5° longitudinal zone = "Longitude", movement direction = "Direction") and likely origins of juvenile American Green-winged Teal (*Anas crecca carolinensis*) harvested in the Great Lakes.** Titles for panels specify whether the likely origin is based on stable isotopes (n = 60, 2017–18 and 2018–19) alone (δ^2H) or whether a prior (n = 671 and $n_{migrants}$ = 358, 1960–2022) is included (δ^2H + prior). Within each panel, the values were rescaled to be a proportion of the maximal value, to better visualize relative differences.
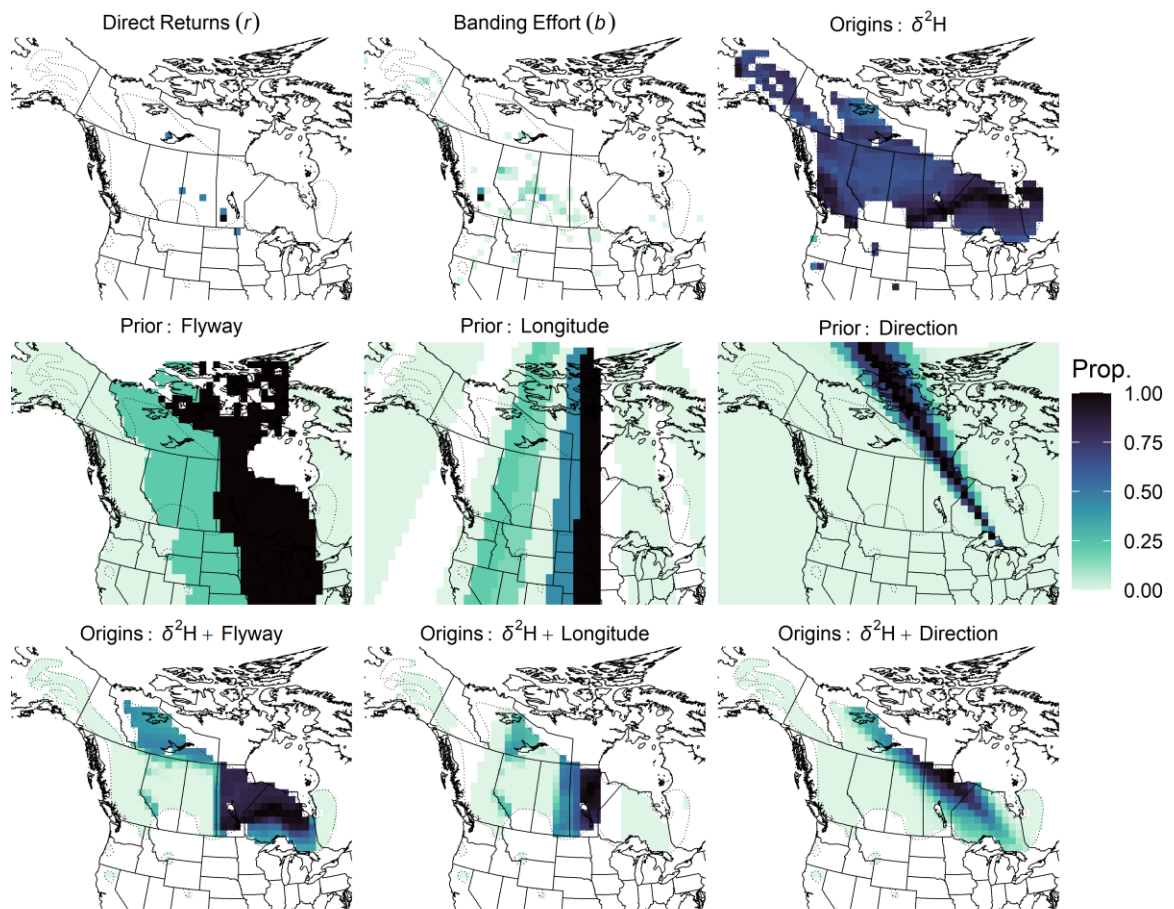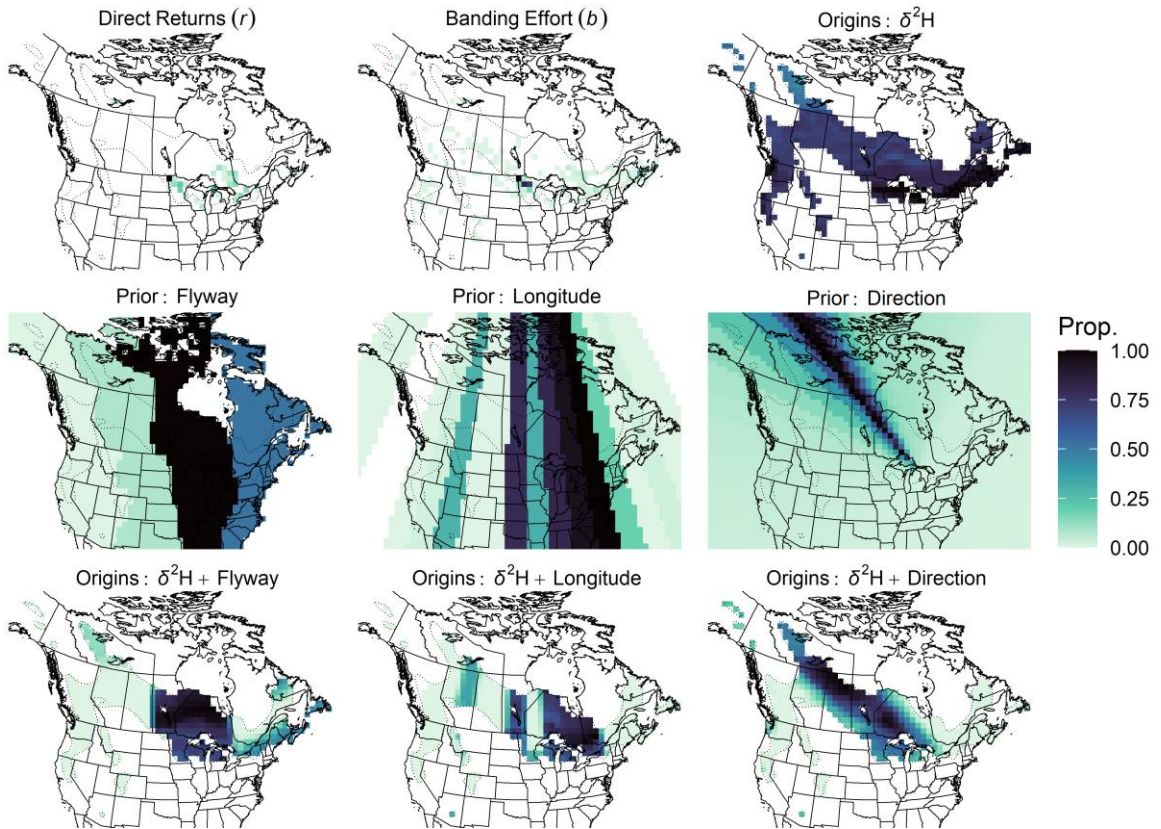
Figure D4 Direct recoveries (*r*), banding effort (*b*), priors (Flyway, 5° longitudinal zone = "Longitude", movement direction = "Direction") and likely origins of juvenile Bufflehead (*Bucephala albeola*) harvested in the Great Lakes. Titles for panels specify whether the likely origin is based on stable isotopes (n = 78, 2017–18 and 2018–19) alone (δ^2H) or whether a prior (n = 7 and $n_{migrants}$ = 7, 1960–2022) is included (δ^2H + prior). Within each panel, the values were rescaled to be a proportion of the maximal value, to better visualize relative differences.
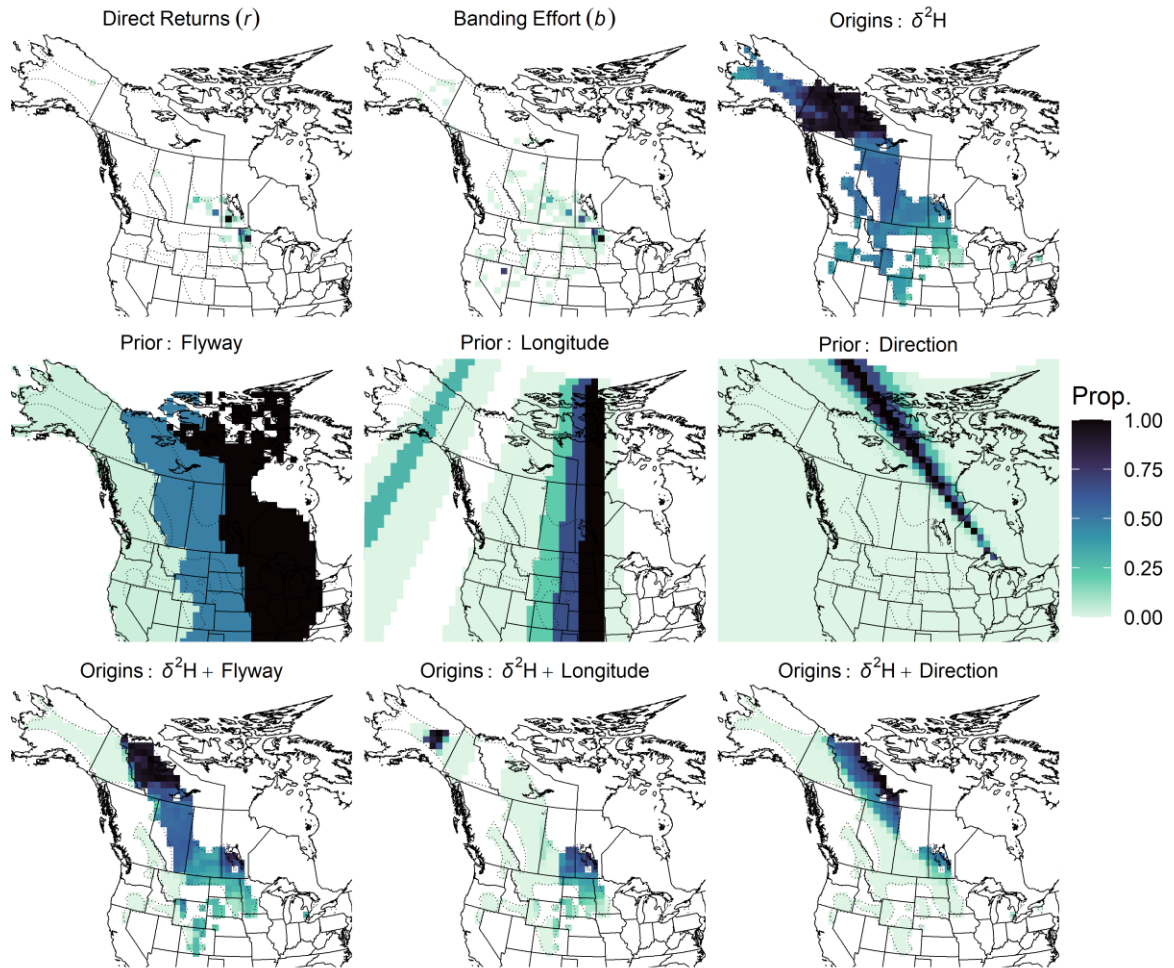
Figure D5 Direct recoveries (*r*), banding effort (*b*), priors (Flyway, 5° longitudinal zone = "Longitude", movement direction = "Direction") and likely origins of juvenile Canvasback (*Aythya valisineria*) harvested in the Great Lakes. Titles for panels specify whether the likely origin is based on stable isotopes (n = 22, 2017–18, 2018–19, and 2020–21) alone (δ^2H) or whether a prior (n = 229 and $n_{migrants}$ = 229, 1960–2022) is included (δ^2H + prior). Within each panel, the values were rescaled to be a proportion of the maximal value, to better visualize relative differences.
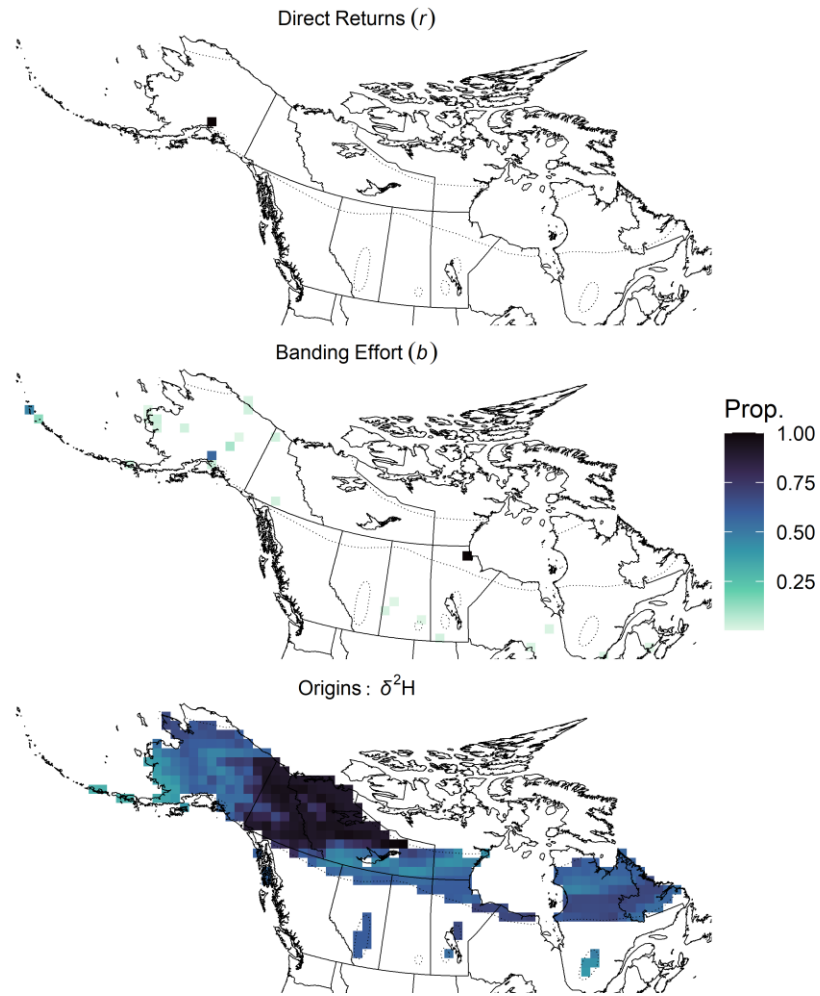
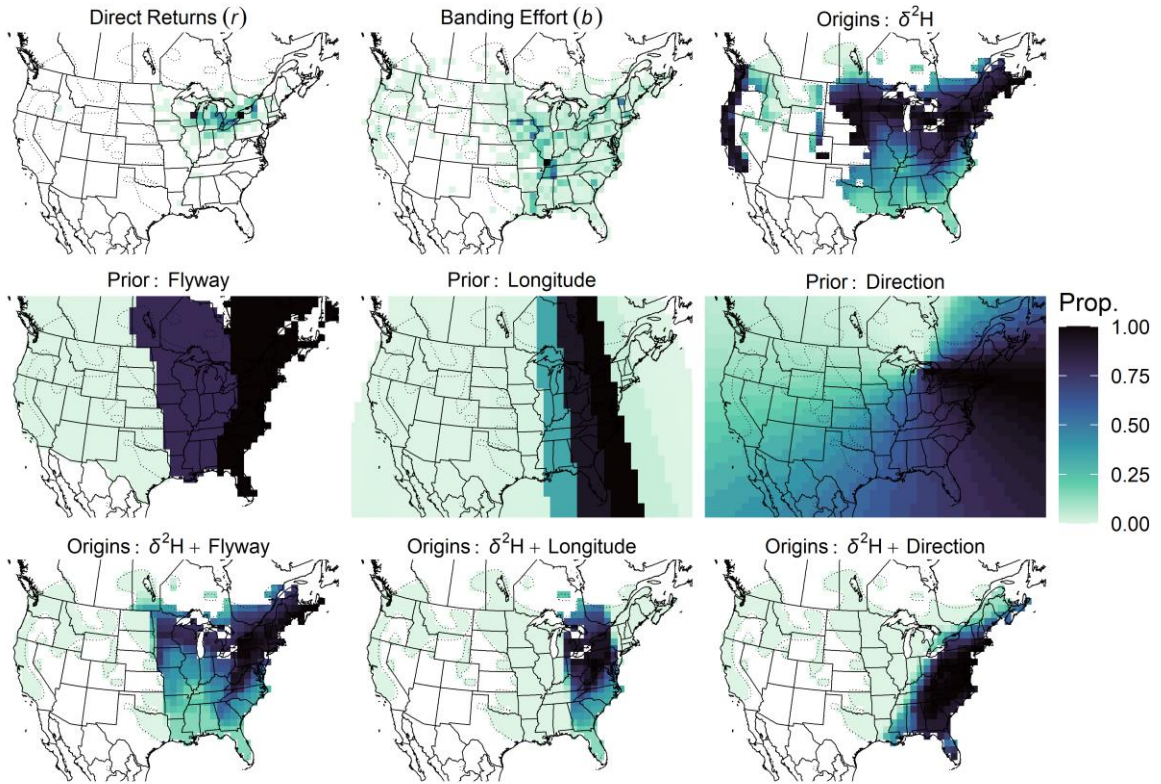**Figure D6 Direct recoveries (*r*), banding effort (*b*), and likely origins of juvenile Greater Scaup (*Aythya affinis*) harvested in the Great Lakes (n = 42, 2017–18 and 2018–19).** Within each panel, the values were rescaled to be a proportion of the maximal value, to better visualize relative differences.
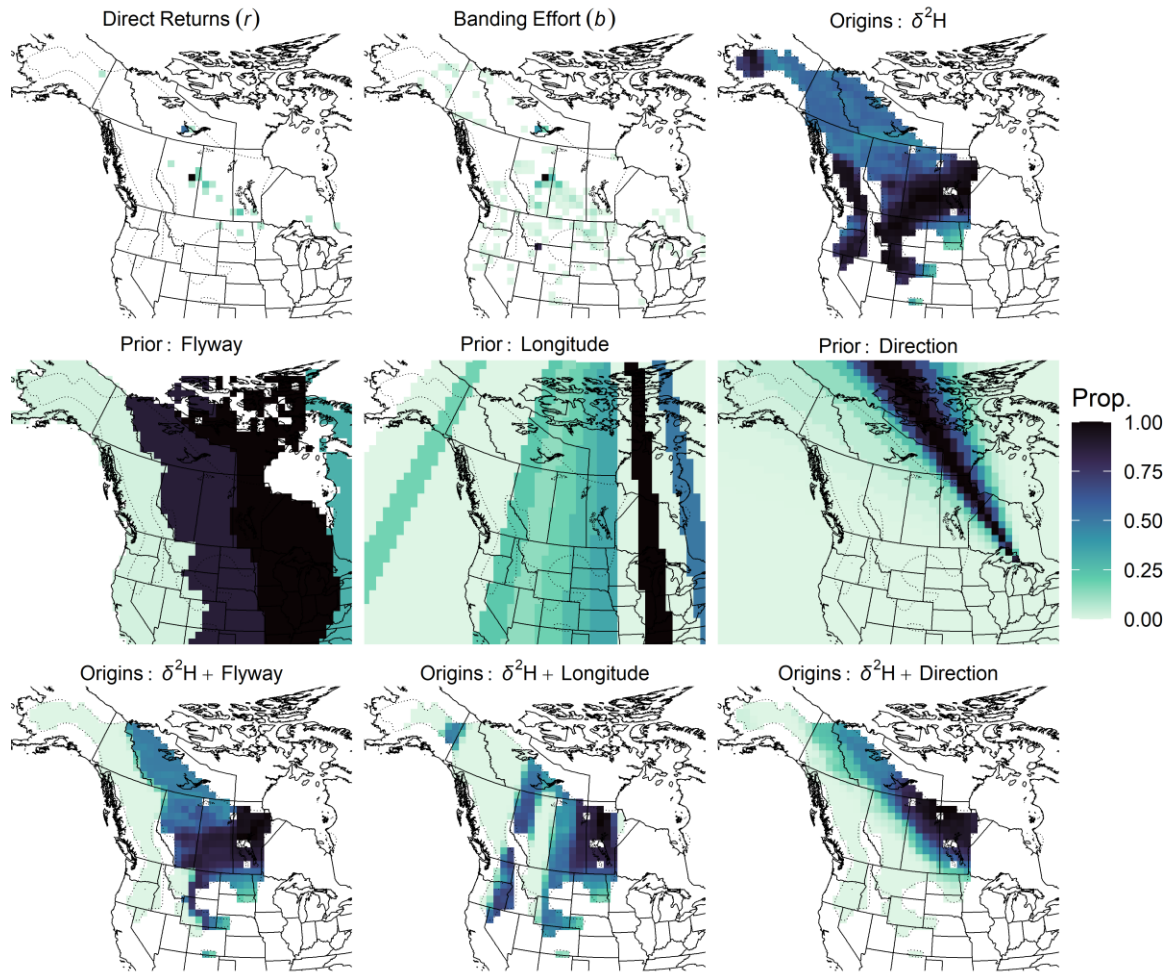
Figure D7 Direct recoveries (*r*), banding effort (*b*), priors (Flyway, 5° longitudinal zone = "Longitude", movement direction = "Direction") and likely origins of juvenile Lesser Scaup (*Aythya affinis*) harvested in the Great Lakes. Titles for panels specify whether the likely origin is based on stable isotopes (n = 42, 2017–18 and 2018–19) alone (δ^2H) or whether a prior (n = 44 and $n_{migrants}$ = 43, 1960–2022) is included (δ^2H + prior). Within each panel, the values were rescaled to be a proportion of the maximal value, to better visualize relative differences.
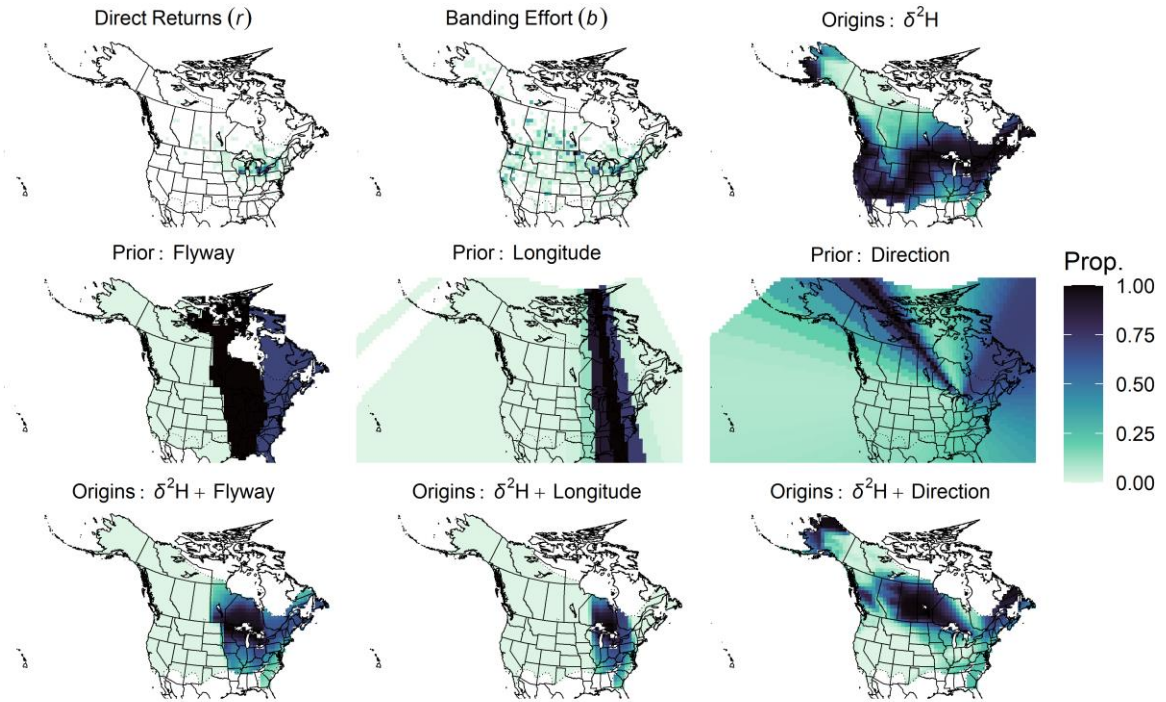
Figure D8 Direct recoveries (*r*), banding effort (*b*), priors (Flyway, 5° longitudinal zone = "Longitude", movement direction = "Direction") and likely origins of juvenile Mallard (*Anas platyrhynchos*) harvested in the Great Lakes. Titles for panels specify whether the likely origin is based on stable isotopes (n = 169, 2017–18 and 2018–19) alone (δ^2H) or whether a prior (n = 36,240 and $n_{migrants}$ = 5,678, 1960–2022) is included (δ^2H + prior). Within each panel, the values were rescaled to be a proportion of the maximal value, to better visualize relative differences.

Figure D9 Direct recoveries (*r*), banding effort (*b*), priors (Flyway, 5° longitudinal zone = "Longitude", movement direction = "Direction") and likely origins of juvenile Northern Pintail (*Anas acuta*) harvested in the Great Lakes. Titles for panels specify whether the likely origin is based on stable isotopes (n = 106, 2017–18, 2018–19, 2019–20, and 2020–21) alone (δ^2H) or whether a prior (n = 235 and n$_{migrants}$ = 133, 1960–2022) is included (δ^2H + prior).Within each panel, the values were rescaled to be a proportion of the maximal value, to better visualize relative differences.

Figure D10 Direct recoveries (*r*), banding effort (*b*), priors (Flyway, 5° longitudinal zone = "Longitude", movement direction = "Direction") and likely origins of juvenile Redhead (*Aythya americana*) harvested in the Great Lakes. Titles for panels specify whether the likely origin is based on stable isotopes (n = 88, 2017–18, 2018–19, and 2020–21) alone (δ^2H) or whether a prior (n = 787 and $n_{migrants}$ = 662, 1960–2022) is included (δ^2H + prior). Within each panel, the values were rescaled to be a proportion of the maximal value, to better visualize relative differences.

Figure D11 Direct recoveries (*r*), banding effort (b), priors (Flyway, 5° longitudinal zone = "Longitude", movement direction = "Direction") and likely origins of juvenile Ring-necked Duck (*Aythya collaris*) harvested in the Great Lakes. Titles for panels specify whether the likely origin is based on stable isotopes (n = 51, 2017–18 and 2018–19) alone (δ^2H) or whether a prior (n = 251 and $n_{migrants}$ = 177, 1960–2022) is included (δ^2H + prior). Within each panel, the values were rescaled to be a proportion of the maximal value, to better visualize relative differences.

Figure D12 Direct recoveries (*r*), banding effort (*b*), priors (Flyway, 5° longitudinal zone = "Longitude", movement direction = "Direction") and likely origins of juvenile Wood Duck (*Aix sponsa*) harvested in the Great Lakes. Titles for panels specify whether the likely origin is based on stable isotopes (n = 31, 2017–18) alone (δ^2H) or whether a prior (n = 4,857 and $n_{migrants}$ = 183, 1960–2022) is included (δ^2H + prior). Within each panel, the values were rescaled to be a proportion of the maximal value, to better visualize relative differences.

Appendix E

E   Permission to reproduce

Institution name	Western University

Expected presentation date	Aug 2024

Requestor Location	Mr. Jackson Kusack 1151 Richmond St London, ON N6A 3K7 Canada Attn: Mr. Jackson Kusack

Publisher Tax ID	EU826007151

Total	0.00 CAD

Terms and Conditions

229

the terms of the license are extended to include subsequent editions and for editions in other languages, provided such editions are for the work as a whole in situ and does not involve the separate exploitation of the permitted figures or extracts, You may not alter, remove or suppress in any manner any copyright, trademark or other notices displayed by the Wiley Materials. You may not license, rent, sell, loan, lease, pledge, offer as security, transfer or assign the Wiley Materials on a stand-alone basis, or any of the rights granted to you hereunder to any other person.

- The Wiley Materials and all of the intellectual property rights therein shall at all times remain the exclusive property of John Wiley & Sons Inc, the Wiley Companies, or their respective licensors, and your interest therein is only that of having possession of and the right to reproduce the Wiley Materials pursuant to Section 2 herein during the continuance of this Agreement. You agree that you own no right, title or interest in or to the Wiley Materials or any of the intellectual property rights therein. You shall have no rights hereunder other than the license as provided for above in Section 2. No right, license or interest to any trademark, trade name, service mark or other branding ("Marks") of WILEY or its licensors is granted hereunder, and you agree that you shall not assert any such right, license or interest with respect thereto

- NEITHER WILEY NOR ITS LICENSORS MAKES ANY WARRANTY OR REPRESENTATION OF ANY KIND TO YOU OR ANY THIRD PARTY, EXPRESS, IMPLIED OR STATUTORY, WITH RESPECT TO THE MATERIALS OR THE ACCURACY OF ANY INFORMATION CONTAINED IN THE MATERIALS, INCLUDING, WITHOUT LIMITATION, ANY IMPLIED WARRANTY OF MERCHANTABILITY, ACCURACY, SATISFACTORY QUALITY, FITNESS FOR A PARTICULAR PURPOSE, USABILITY, INTEGRATION OR NON-INFRINGEMENT AND ALL SUCH WARRANTIES ARE HEREBY EXCLUDED BY WILEY AND ITS LICENSORS AND WAIVED BY YOU.

- WILEY shall have the right to terminate this Agreement immediately upon breach of this Agreement by you.

- You shall indemnify, defend and hold harmless WILEY, its Licensors and their respective directors, officers, agents and employees, from and against any actual or threatened claims, demands, causes of action or proceedings arising from any breach of this Agreement by you.

- IN NO EVENT SHALL WILEY OR ITS LICENSORS BE LIABLE TO YOU OR ANY OTHER PARTY OR ANY OTHER PERSON OR ENTITY FOR ANY SPECIAL, CONSEQUENTIAL, INCIDENTAL, INDIRECT, EXEMPLARY OR PUNITIVE DAMAGES, HOWEVER CAUSED, ARISING OUT OF OR IN CONNECTION WITH THE DOWNLOADING, PROVISIONING, VIEWING OR USE OF THE MATERIALS REGARDLESS OF THE FORM OF ACTION, WHETHER FOR BREACH OF CONTRACT, BREACH OF WARRANTY, TORT, NEGLIGENCE, INFRINGEMENT OR OTHERWISE (INCLUDING, WITHOUT LIMITATION, DAMAGES BASED ON LOSS OF PROFITS, DATA, FILES, USE, BUSINESS OPPORTUNITY OR CLAIMS OF THIRD PARTIES), AND WHETHER OR NOT THE PARTY HAS BEEN ADVISED OF THE POSSIBILITY OF SUCH DAMAGES. THIS LIMITATION SHALL APPLY NOTWITHSTANDING ANY FAILURE OF ESSENTIAL PURPOSE OF ANY LIMITED REMEDY PROVIDED HEREIN.

- Should any provision of this Agreement be held by a court of competent jurisdiction to be illegal, invalid, or unenforceable, that provision shall be deemed amended to achieve as nearly as possible the same economic effect as the original provision, and the legality, validity and enforceability of the remaining provisions of this Agreement shall not be affected or impaired thereby.

- The failure of either party to enforce any term or condition of this Agreement shall not constitute a waiver of either party's right to enforce each and every term and condition of this Agreement. No breach under this agreement shall be deemed waived or excused by either party unless such waiver or consent is in writing signed by the party granting such waiver or consent. The waiver by or consent of a party to a breach of any provision of this Agreement shall not operate or be construed as a

waiver of or consent to any other or subsequent breach by such other party.

- This Agreement may not be assigned (including by operation of law or otherwise) by you without WILEY's prior written consent.

- Any fee required for this permission shall be non-refundable after thirty (30) days from receipt by the CCC.

- These terms and conditions together with CCC's Billing and Payment terms and conditions (which are incorporated herein) form the entire agreement between you and WILEY concerning this licensing transaction and (in the absence of fraud) supersedes all prior agreements and representations of the parties, oral or written. This Agreement may not be amended except in writing signed by both parties. This Agreement shall be binding upon and inure to the benefit of the parties' successors, legal representatives, and authorized assigns.

- In the event of any conflict between your obligations established by these terms and conditions and those established by CCC's Billing and Payment terms and conditions, these terms and conditions shall prevail.

- WILEY expressly reserves all rights not specifically granted in the combination of (i) the license details provided by you and accepted in the course of this licensing transaction, (ii) these terms and conditions and (iii) CCC's Billing and Payment terms and conditions.

- This Agreement will be void if the Type of Use, Format, Circulation, or Requestor Type was misrepresented during the licensing process.

- This Agreement shall be governed by and construed in accordance with the laws of the State of New York, USA, without regards to such state's conflict of law rules. Any legal action, suit or proceeding arising out of or relating to these Terms and Conditions or the breach thereof shall be instituted in a court of competent jurisdiction in New York County in the State of New York in the United States of America and each party hereby consents and submits to the personal jurisdiction of such court, waives any objection to venue in such court and consents to service of process by registered or certified mail, return receipt requested, at the last known address of such party.

WILEY OPEN ACCESS TERMS AND CONDITIONS

Wiley Publishes Open Access Articles in fully Open Access Journals and in Subscription journals offering Online Open. Although most of the fully Open Access journals publish open access articles under the terms of the Creative Commons Attribution (CC BY) License only, the subscription journals and a few of the Open Access Journals offer a choice of Creative Commons Licenses. The license type is clearly identified on the article.

The Creative Commons Attribution License

The Creative Commons Attribution License (CC-BY) allows users to copy, distribute and transmit an article, adapt the article and make commercial use of the article. The CC-BY license permits commercial and non-

Creative Commons Attribution Non-Commercial License

The Creative Commons Attribution Non-Commercial (CC-BY-NC)License permits use, distribution and reproduction in any medium, provided the original work is properly cited and is not used for commercial purposes.(see below)

Creative Commons Attribution-Non-Commercial-NoDerivs License

The Creative Commons Attribution Non-Commercial-NoDerivs License (CC-BY-NC-ND) permits use, distribution and reproduction in any medium, provided the original work is properly cited, is not used for commercial purposes and no modifications or adaptations are made. (see below)

Use by commercial "for-profit" organizations

Use of Wiley Open Access articles for commercial, promotional, or marketing purposes requires further explicit permission from Wiley and will be subject to a fee.

Further details can be found on Wiley Online Library
http://olabout.wiley.com/WileyCDA/Section/id-410895.html

Other Terms and Conditions:

v1.10 Last updated September 2015

Questions? customercare@copyright.com.

Curriculum Vitae

Name: Jackson Kusack

Post-secondary   Thompson Rivers University
Education and   Kamloops, British Columbia, Canada
Degrees: 2011–16 B.Sc.H.

                  The University of Western Ontario
                  London, Ontario, Canada
                  2016–18 M.Sc.

                  The University of Western Ontario
                  London, Ontario, Canada
                  2019–24 Ph.D.

Honours and   Undergraduate Research Experience Award, Thompson Rivers
Awards: University
                  2015

                  Student Travel Award, Society of Canadian Ornithologists /
                  la Société des Ornithologistes du Canada (SCO-SOC)
                  2015, 2018

                  Student Poster Award, Society of Canadian Ornithologists /
                  la Société des Ornithologistes du Canada (SCO-SOC)
                  2015

                  Graduate Teaching Award, Western University
                  2018, 2020

                  Queen Elizabeth II Scholarship in Science and Technology
                  (QEII-GSST)
                  2019–20, 2020–21

                  Student Travel Award, North American Duck Symposium 8
                  2019

                  Dave Ankney & Sandi Johnson Graduate Research Scholarship,
                  Ontario Fishers, Anglers, and Hunters
                  2020

                  Natural Science and Engineering Research Council of Canada

postgraduate scholarship-doctoral (NSERC PGS-D)
2021–24

Related Work   Teaching Assistant
Experience   The University of Western Ontario
2016–24

Publications:

1) **Kusack, J. W.**, D. C. Tozer, K. M. Harvey, M. L. Schummer, and K. A. Hobson. 2023. Assigning harvested waterfowl to geographic origin using feather δ^2H isoscapes: What is the best analytical approach? PLOS One 18:e0288262.

2) **Kusack, J. W.** 2023. Extralimital records of Marsh Sandpiper in North America. Ontario Birds 41:93–99.

3) Kucia, S. R., M. L. Schummer, **J. W. Kusack**, K. A. Hobson, and C. A. Nicolai. 2023. Natal origins of mallards harvested in the Atlantic flyway of North America: Implications for conservation and management. Avian Conservation and Ecology 18:1.

4) **Kusack, J. W.**, D. C. Tozer, M. L. Schummer, and K. A. Hobson. 2022. Origins of harvested American black ducks: stable isotopes support the flyover hypothesis. The Journal of Wildlife Management 87:e22324.

5) Hobson, K. A., **J. W. Kusack**, J. Gootgarts, F. J., Longstaffe, and J. N. McNeil. 2022. Using stable isotopes (δ^2H, δ^{13}C) to identify natal origins and larval host plant use by western bean cutworm, *Striacosta albicosta* (Lepidoptera: Noctuidae) captured in southern Ontario. Ecological Entomology 47:347–356.

6) Zhao, Q., G. W. Mitchell, M. D. Cadman, **J. W. Kusack**, D. R. Evans, K. Bumelis, K. A. Hobson, M. D. Weegman, A. Salvadori, and S. Wilson. 2021. Integrating regional and site-level data to assess drivers of population decline in insectivorous birds. Biological Conservation 265:10924.

7) Put, J. E., G. W. Mitchell, N. A. Mahony, J. Costa, T. L. Imlay, S. Bossuyt, C. K. Boynton, G. Burness, D. R. Evans, K. A. Hobson, **J. W. Kusack**, O. Lansdorp, A. K. Lenske, B. McClenaghan, E. Nol, A. Salvadori, A. C. Smith, T. D. Williams, B. Whittam, and M. D. Cadman. 2021. Regional variability in trajectories of Barn Swallow populations across Canada are not predicted by breeding performance. Avian Conservation and Ecology 16:10.

8) **Kusack**, **J. W.**, G. W. Mitchell, D. R. Evans, M. D. Cadman, J. L. McCune, and K. A. Hobson. 2021. Diet of nestling Barn Swallows in an agroecosystem: insights from fecal DNA barcoding and feather stable isotopes (δ^{13}C, δ^{15}N). Journal of Ornithology 163:137–150.

9) Hobson, K. A., **J. W. Kusack**, and B. X. Mora-Alvarez. 2021. Origins of six species of butterflies migrating through Northeastern Mexico: new insights from stable isotope (δ^2H) analyses and a call for documenting butterfly migrations. Diversity 13:102.

10) Hobson, K. A., H. Jinguji, Y. Ichikawa, **J. W. Kusack**, and R. C. Anderson. 2020. Long-distance migration of the Globe Skimmer Dragonfly through Japan revealed using stable hydrogen (δ^2H) isotopes. Environmental Entomology 50:247–255.

11) Beauchamp, A. T., **J. W. Kusack**, K. A. Hobson, and C. G. Guglielmo. 2020. Testing the utility of condition indices in nestling swallows: a quantitative magnetic resonance approach. Journal of Ornithology 162:1–13.

12) **Kusack**, **J. W.**, G. W. Mitchell, D. R. Evans, M. D. Cadman, and K. A. Hobson,. 2020. Effects of agricultural intensification on condition and fledging success of nestling barn swallows (*Hirundo rustica*). Science of the Total Environment 709:136195.

13) Palumbo, M. D., **J. W. Kusack**, D. C. Tozer, S. W. Meyer, C. Roy, and K. A. Hobson. 2020. Origins of Blue-winged Teal harvested in Ontario relative to Prairie Canada: implications for the management of a sustainable population in Ontario using stable isotopes. Journal of Field Ornithology 91:64–76.

14) Evans, D. R., K. A. Hobson, **J. W. Kusack**, M. D. Cadman, M. J. Falconer, and G. W. Mitchell. 2020. Individual condition but not fledging phenology carries over to affect post fledging survival in a Neotropical migratory songbird. Ibis 162:331–344.

15) LaZerte, S.E., M. W. Reudink, K. A. Otter, **J. Kusack**, J. M. Bailey, A. Woolverton, M. Paetkau, A. de Jong, and D. J. Hill. 2017. feedr and animalnexus.ca: A paired R package and user-friendly Web application for transforming and visualizing animal movement data from static stations. Ecology and Evolution 7:7884–7896.